NEUROINFLAMMATION, TNF, AND CERAMIDE SIGNALING: PUTATIVE PATHWAYS FOR NEUROTOXICITY IN PARKINSON'S DISEASE

APPROVED BY SUPERVISORY COMMITTEE

Malú G. Tansey, Ph.D.

Joyce J. Repa, Ph.D.

Matthew G. Goldberg, Ph.D.

Amelia J. Eisch, Ph.D.

Joel Elmquist, Ph.D., D.V.M.

ACKNOWLEDGEMENTS AND DEDICATION

I would like to thank my family and friends; without their love and support, this journey would not have been possible. I thank my parents for instilling in me a passion for learning. I thank my sister, Sabrina – the best twin ever, and my brother Tres, for his encouragement and comic relief. I thank my mentor Malú Tansey, the best mentor I could have ever asked for.

I dedicate this work in loving memory of my father (September 15, 1937-March 21, 2008). I know that he would have been thrilled to see me complete this journey and embark on another chapter in my life. “Hay te wacho”.

NEUROINFLAMMATION, TNF AND CERAMIDE SIGNALING: PUTATIVE PATHWAYS FOR NEUROTOXICITY IN PARKINSON'S DISEASE

by

TERINA NICHOLE MARTINEZ

DISSERTATION

Presented to the Faculty of the Graduate School of Biomedical Sciences

The University of Texas Southwestern Medical Center at Dallas

In Partial Fulfillment of the Requirements

For the Degree of

DOCTOR OF PHILOSOPHY

The University of Texas Southwestern Medical Center at Dallas

Dallas, Texas

March, 2010

NEUROINFLAMMATION, TNF AND CERAMIDE SIGNALING: PUTATIVE PATHWAYS FOR NEUROTOXICITY IN PARKINSON'S DISEASE

TERINA NICHOLE MARTINEZ, Ph.D.

The University of Texas Southwestern Medical Center at Dallas, 2010

MALU G. TANSEY, Ph.D.

Parkinson's disease is a progressive neurodegenerative disorder that is characterized by the loss of dopaminergic neurons in the substantia nigra that innervate the striatum, and it is the loss of these neurons that causes the motor dysfunction that is associated with the disease. However, the mechanisms that contribute to the induction and perpetuation of dopaminergic neuronal cell death in Parkinson's disease are multi-faceted and poorly understood. Inflammation has been shown to contribute to cytotoxicity in animal models of Parkinson's disease, and increased levels of inflammatory cytokines have been observed in the cerebral spinal fluid and striatum of Parkinson's disease patients. We have previously demonstrated that blocking soluble tumor necrosis factor (TNF) signaling with dominant-negative TNF inhibitors attenuates the loss of dopaminergic neurons in models of Parkinson's disease, but which signaling pathways downstream of TNF mediate this effect remain undetermined. Here, I show that TNF-dependent ceramide signaling contributes to dopamine neuron cytotoxicity by compromising mitochondrial membrane potential, inducing endoplasmic reticulum stress and activating caspase signaling *in vitro*. My data demonstrate that TNF-induced cytotoxicity is partially ceramide-dependent, as TNF-induced cytotoxic effects are attenuated with two different pharmacological inhibitors of sphingomyelinase, an enzyme that hydrolyzes active ceramide from inactive sphingomyelin pools. Collectively, my data support a model whereby low-dose TNF and concomitant low TNF receptor1 occupancy activates downstream ceramide signaling and metabolism, culminating in caspase-dependent cytotoxic cell death of dopaminergic neurons. My data and the data associating ceramide biology and metabolism with Parkinson's disease warrants future studies examining the potential neuroprotective effects of inhibition of sphingomyelinase

in animal models of Parkinson's disease, and may eventually lead to improved therapy for patients who suffer from Parkinson's disease.

TABLE OF CONTENTS

PRIOR PUBLICATIONS

McCoy, MK., Martinez, TN., Meinert, KA., Szymkowski, DE., Smith, CG., Botterman, BR., Tansey, KE., Tansey, MG. (2006) Blocking soluble Tumor Necrosis Factor signaling with dominant negative TNF inhibitor attenuates loss of dopaminergic neurons in models of Parkinson's disease. *J Neurosci* 26(37):9365-75.

McCoy*, M.K., Martinez*, T.N., Ruhn, K.A., Wrage, P.C., Keefer, E.W., Botterman, B.R., Tansey, K.E., Tansey, M.G., (2008) Autologous transplants of Adipose-Derived Adult Stromal (ADAS) cells afford dopaminergic neuroprotection in a model of Parkinson's disease. *Experimental Neurology* 210(1):14-29.
*Equal contribution

Tansey, M.G., Frank-Cannon, T.C., McCoy, M.K., Lee, J.K., Martinez, T.N., McAlpine, F.E., Ruhn, K.A., Tran, T.A. (2008) Neuroinflammation in Parkinson's disease: Is there sufficient evidence for mechanism based interventional therapy? *Frontiers in Bioscience* Review. 13:709-717.

McCoy MK, Ruhn KA, Martinez TN, McAlpine FE, Blesch A, Tansey MG. (2008) Intranigral lentiviral delivery of dominant negative TNF attenuates neurodegeneration and behavioral deficits in hemiparkinsonian rats. *Molecular Therapy,* 16(9):1572-9.

Frank-Cannon, TC, Tran, T, Ruhn, KA, Martinez, TN, Marvin, M, Hong, J, Hartley, M, Treviño, I, Casey, B, Goldberg, MS, Tansey, MG. (2008) Parkin deficiency increases vulnerability to inflammation-related nigral degeneration. *J Neurosci*, 22;28(43):10825-34.

LIST OF FIGURES

LIST OF TABLES

LIST OF APPENDICES

LIST OF ABBREVIATIONS

AB – assay buffer

ALS – autophagy lysosome system

ANOVA – analysis of variance

AP – anterior posterior

ARE – antioxidant response element

AR-JP – autosomal recessive juvenile Parkinsonism

A-SMase – acid sphingomyelinase

ATF6 – activating transcription factor 6

BBB – blood brain barrier

bFGF – basic fibroblast growth factor

BiP – binding protein

BMSCs – bone marrow stormal cells

BSA – bovine serum albumin

C2-DH-cer – C2-dihydroceramide

C2-cer – C2-ceramide

C3R – complement 3 receptor

CCCP – carbonyl cyanide 3-chlorophenyl hydrazone

CHOP – C/EBP homologous protein

cIAPs – cytosolic inhibitor of apoptosis proteins

CMA – chaperone-mediated autophagy

DA – dopamine or dopaminergic

DAT – dopamine transporter

DAB – 3,3-diaminobenzidine

Des - desipramine

DISC – death-inducing signaling complex

DM – differentiation medium

DMSO – dimethyl sulfoxide

DNA – deoxyribonucleic acid

DN-TNF – dominant-negative TNF

DV – dorsal ventral

ESC – embryonic stem cell

ERAD – ER associated degradation

ER – endoplasmic reticulum

EVM – embryonic ventral mesencephalon

FB1 – fumonisin B1

FBS – fetal bovine serum

FDA – federal drug association

GD – Gaucher's disease

GBA – glucocerebrosidase

GNF – Genomics Institute of the Novartis Research Foundation

IOD – integrated optical density

iPS cells – induced-pluripotent stem cells

IR - immunoreactive

IRE1 – inositol-requiring 1

JEBV – Japanese encephalitis B virus

L-dopa - levodopa

LPS – lipopolysaccharide

LRRK2 – leucine-rich repeat kinase 2

MAO-B – monoamine oxidase B

MAP-2 – microtubule-associated protein 2

MFB – medial forebrain bundle

ML – medial lateral

$MPDP^+$ - 1-methyl-4-phenyl-2-3-dihydropyridium

MPP^+ - 1-methyl-4-phenylpyridinium

mRNA – message ribonucleic acid

mtDNA – mitochondrial deoxyribonucleic acid

MPTP – 1-methyl-1-4-phenyl-1,3,5,6-tetrahydropyridum

NADPH - nicotinamide adenine dinucleotide phosphate

NE – nasal epithelium

NMDA – N-methyl-D-aspartate

NRF-2 – nuclear factor erythroid 2-related factor

NSAIDs – non-steroidal anti-inflammatoyr durgs

N-SMase – neutral sphingomyelinase

PBS – phosphate buffered saline

PD – Parkinson's diseas

PERK – PKR-like ER-localized eIF2α kinase

PI3 kinase – phosphatidyl-inositol-3-kinase/protein kinase B

PINK – PTEN-induced kinase 1

PLL – poly-L-lysine

PTEN – phosphatase and homolog of tensin

Q-RT-PCR – quantitative real-time polymerase chain reaction

REM – rapid eye movement

rhTNF – recombinant human TNF

rmTNF – recombinant mouse TNF

RIP – receptor interacting protein

RNS – reactive nitrogen species

ROS – reactive oxygen species

SKPs – skin-derived precursors

SMAse – sphingomyelinase

SM - sphingomyelin

SN – substantia nigra

SNpc – substantia nigra pars compacta

SODD – silencer of death domains

sol TNF – soluble TNF

TACE – TNFα-converting enzyme

TH – tyrosine hydroxylase

TMRM – tetra-methyl rhodamine methyl ester

TNF – tumor necrosis factor

TNFR1 – TNF receptor 1

TNFR2 – TNF receptor 2

tmTNF – transmembrane TNF

TRADD – TNF receptor-associated death domains

TBS – tris buffered saline

TBST – tris buffered saline with triton-x-100

UCHL1 – ubiquitin carboxyl-terminal hudrolase L1

UPS – ubiquitin proteasome system

VM – ventral mesencephalon

VTA – ventral tagmental area

6-OHDA – 6-hydroxydopamine

CHAPTER ONE
Introduction and Review of the Literature

OVERVIEW OF PARKINSON'S DISEASE

Etiology, pathology and symptoms

Etiology

Parkinson's disease (PD) was first formally described almost two centuries ago by the London physician James Parkinson in "An Essay on the Shaking Palsy," which was published in 1817 (J Neuropsychiatry Clin Neurosci, 2002). PD is now known to be the second most common neurodegenerative disorder and most common movement disorder /worldwide, and is associated with an age-related onset such that approximately 1% of the global population at age 65 and approximately 4-5% of people 85 years old are afflicted with PD (Fahn, 2003; Farrer, 2006). Considered to be a non-genetic disease for decades, the etiology of PD remains largely undetermined, despite intensive research efforts and significant insight over the last several years into genetic factors associated with PD. Linkage analysis studies of large-scale PD pedigrees have revealed mutations in several different genes that are associated with heritable PD, but the vast majority of PD cases are considered to have a sporadic etiology, and are believed to result from complex genetic interactions among genes and between genes and environmental factors (Xiromerisiou et al., 2010).

Pathology

Pathologically, PD is characterized by the progressive loss of neuromelanin-containing dopamine (DA) neurons in the Substantia Nigra pars compacta (SNpc) of the midbrain.

DA neurons of the SNpc project to the striatum, which plays a major role in the initiation and modulation of movement. The histopathological hallmark of PD is the intraneuronal presence of Lewy bodies, which are cytoplasmic inclusions of aggregated α-synuclein and ubiquitin proteins, first described by Frederick Henry Lewy in 1912 (Forstl et al., 1993). The progressive nature of PD has long been appreciated (Halliday et al., 2008) and in 2003, Braak and colleagues introduced a staging procedure based on the topographical extent of Lewy body distribution throughout brain tissue and subsequent brain lesion to better elucidate the course of PD pathology in sporadic PD cases (Braak et al., 2003). The concept of histological disease progression in PD suggests an association with clinical disease progression, which was elegantly explored by Halliday and colleagues who studied disease progression in longitudinally followed PD patients from the Sydney Multicentre Study (Halliday et al., 2008). Halliday et al., describe the types of PD pathology observed in numerous PD patients in five year increments over the course of more than twenty years, and report that case selection for typical PD (i.e. levodopa-responsive) identifies three main clinicopathological phenotypes: patients with early dementia-dominant syndrome and severe neocortical disease, patients with younger disease onset with a "typical" clinical course consistent with the Braak staging, and patients with older age disease onset who are more likely to experience a complex disease course with curtailed survival. Halliday and colleagues surmise that their data are not consistent with a unitary concept of the pathogenesis of Lewy body pathology, and advocate further assessment of PD patients with younger age of disease onset and longer disease progression to better elucidate Lewy body pathology in PD progression. While

there is still much progress to be made in better elucidating the progression of PD, the symptoms of PD pathology are more apparent.

Clinical symptoms (motor)

It is the progressive loss of DA tone in the striatum that leads to the insidious onset and gradual progression of the primary motor symptoms associated with PD, namely postural instability, rigidity, bradykinesia, tremor (especially at rest), flexed posture, and the transient freezing phenomenon, where the feet cannot be moved from the ground (Fahn, 2003). The first symptoms to emerge in PD are usually rigidity, bradykinesia, and resting tremor which are directly related to the progressive loss of nigrostriatal DA and are therefore responsive to dopamine replacement or agonist therapy while the development of other motor symptoms associated with PD (diminished postural reflexes, freezing phenomenon, and flexed posture) are usually more protracted in onset and tend to be therapeutically intractable (Fahn, 2003).

The loss of innervation in the nigrostriatal pathway in PD essentially short-circuits the neurological function of the basal ganglia. There are two main neurological pathways through the basal ganglia which oppose each other and are thought to work in balance, the direct pathway, which facilitates movement and the indirect pathway, which is believed to inhibit unwanted movement. Both pathways originate in the cortex and terminate in the internal segment of the globus pallidus. The DeLong model of basal ganglia circuitry maintains that DA depletion (as in PD) elicits a two-fold effect: 1.) increased activity of the indirect striatal pathway and 2.) decreased activity of the direct

striatal pathway (DeLong and Wichmann, 2007). The net effect of nigrostriatal DA depletion can thus be simplified as abnormal hypokinetic movement due to aberrantly increased output via the indirect striatal pathway (i.e. increased inhibition of movement) and consequently, decreased output through the direct pathway (resulting in inefficient initiation of movement).

Clinical symptoms (non-motor)

Many of the non-motor symptoms of PD are thought to precede motor impairment and include: anosmia, rapid eye movement (REM) behavior disorder, anxiety, depression, excessive daytime somnolence, and constipation (Park and Stacy, 2009). Additionally, it has been hypothesized that aberrant function of autonomic neurons in the spinal cord, gastrointestinal and genitourinary tracts may be early components of PD (Braak et al., 2003). Furthermore, it is believed that in addition to aberrant dopamine system function, PD pathology may also involve abnormal noradrenergic, serotonergic and cholinergic neurotransmitter systems (Boeve et al., 2007; Bohnen et al., 2003) which may contribute to symptoms of cognitive, neuropsychiatric and sleep abnormalities in PD patients. When considering the non-motor symptoms of PD, it is important to distinguish, as much as possible, symptoms that are primary to PD pathology from symptoms that are secondary to PD therapy (such as dopamine replacement treatment). It may be possible to achieve earlier diagnosis and treatment in PD by screening patients for primary non-motor PD symptoms that occur prior to onset of motor symptoms.

THE IMPACT OF GENETIC AND ENVIRONMENTAL FACTORS ON PARKINSON'S DISEASE ONSET AND PROGRESSION

Contribution of genetic factors to PD

The conviction that Parkinson's disease had no genetic component persisted until the last couple of decades when several genes were described to be associated with Mendelian inheritance patterns for PD. The number of PD cases that are considered to be idiopathic, or sporadic (i.e. exhibiting no known PD-causing genetic mutation) far outnumber genetic PD cases, rendering the overall contribution of genetics to PD extremely difficult to define or appreciate. However, much has been learned from studying PD genetics in terms of elucidation of pathogenic mechanisms and pathways in PD as well as from the development of PD animal models in which to develop and test novel therapeutics. An overview of the most significant genes that have been recently genetically linked to familial PD is provided below. Furthermore, it is quite likely that there are yet to be discovered additional genetic mutations that lead to PD, and it is equally likely that there are multiple genes that lead to increased susceptibility when combined with environmental factors.

Dominant "PARK" loci (α-synuclein, LRRK2, and UCHL1)

Dominant alleles can cause aberrant gene function in many ways, such as gain of endogenous function that leads to abnormal gene or protein action, gain of a novel toxic function, simple loss of genetic or protein function, or loss of function through a

dominant negative mechanism. The PARK nomenclature system is assigned to genetic loci linked to a monogenic form of PD or a related disorder.

α-synuclein (PARK1/4)

The first gene to be genetically linked to PD was α-synuclein (SCNA), which was designated PARK1/4 and was initially described in a large Greek/Italian kindred that exhibited autosomal PD with a mean onset of approximately fifty years old (Polymeropoulos et al., 1997). Soon thereafter, wild type α-synuclein was determined to be a component of Lewy bodies (Spillantini et al., 1997). Subsequently, a total of three point mutations (A53T, A30P and E46K) have been described for α-synuclein, and disease-associated gene duplications and triplications have also been described (Fuchs et al., 2007; Singleton et al., 2003). Because α-synuclein-associated PD exhibits dominant inheritance and can be caused both by point mutations and duplications of SCNA, it is likely that a mechanism of α-synuclein-induced cytotoxicity is attributable to its inherent propensity to aggregate (Hardy et al., 2009). Significantly, α-synuclein is ubiquitously expressed and its endogenous function has not yet been fully delineated. It is hypothesized however, that aberrant α-synuclein may be pathologically correlated to idiopathic PD by age-related dysfunction of and impingement on the ubiquitin proteosome system (UPS) (reviewed by (Bedford et al., 2008)) and the autophagy lysosome system (ALS) (Cuervo et al., 2004).

LRRK2 (PARK8)

Another gene with mutations linked to dominantly inherited PD is leucine-rich repeat kinase-2 (LRRK2), which is designated as PARK8. LRRK2 mutations were first discovered in Japanese families (Funayama et al., 2002) and was later validated as a PD gene by positional cloning in families from Spain and England (Paisan-Ruiz et al., 2004). Subsequently, numerous missense mutations in LRRK2 have been described (Paisan-Ruiz et al., 2009) and some insight into the function of LRRK2 and therefore its potential role in PD pathology has been made. The protein encoded by the LRRK2 gene has been shown to be largely localized to the cytoplasm but also associates with the mitochondrial outer membrane, potentially implicating LRRK2 in mitochondrial function. LRRK2 also interacts with the gene *parkin* and expression of mutant LRRK2 induces neuronal apoptosis in neuroblastoma and murine primary cortical neurons (Smith et al., 2005b). LRRK2 is a large kinase protein with multiple domains, suggesting that it may have numerous distinct functions, and mutations can occur in many of these domains, potentially affecting the kinase function of LRRK2 if mutations occur in the kinase domain or its interaction with other proteins if mutations occur outside of the kinase domain. Complicating the elucidation of direct mechanisms of LRRK2 toxicity in PD, neither the upstream activators nor the immediate downstream targets of LRRK2 have been identified (Hardy et al., 2009).

UCHL1 (PARK5)

Ubiquitin carboxyl-terminal hydrolase L1 (UCHL1), designated as PARK5, has been identified as a deubiquitinating enzyme and was linked to autosomal dominant PD in a German family in 1998 (Leroy et al., 1998) but subsequent epidemiological and genetic

studies have yielded conflicting results and interpretations regarding the classification of UCHL1 as a PD-linked gene (Healy et al., 2006; Maraganore et al., 2004). However, UCHL1 is abundantly expressed in brain, is enriched in brain areas relevant to PD (Wilkinson et al., 1992; Wilkinson et al., 1989) is present in Lewy bodies and has putative function in the UPS pathway (Lowe et al., 1990), a cellular pathway that has been implicated in PD pathogenicity. Potentially further connecting UCHL1 function with PD pathology, transgenic mice expressing the UCHL1 I93M mutation were observed to have mild DA neuron cell loss (decreased by approximately 30%) *in vivo* at twenty weeks of age (Setsuie et al., 2007). However, further large-scale genetic studies and rigorous meta analyses of previously conducted familial studies focusing on association of UCHL1 with PD are warranted to clarify what role, if any, UCHL1 may play in familial PD.

Recessive "PARK" loci (parkin, PINK and DJ-1)

Understanding the genetic component of PD is inherently mired with difficulty. Further complicating the understanding of the genetic etiology of PD is the issue that recessive mutations of genes linked to familial PD often have variable penetrance. Additionally, many of the genes associated with recessive inheritance of PD harbor multiple, distinct mutations and it is possible that more than one different recessive PD gene mutation can combine with other recessive mutations or other susceptibility factors to elicit complex gene interactions.

Parkin (PARK2)

The PARK2 gene encodes the protein Parkin. Mutations in parkin were initially described in the mid to late 1990's in multiple Japanese families who suffered from the syndrome referred to as autosomal recessive juvenile Parkinsonism (AR-JP) (Ishikawa and Tsuji, 1996; Kitada et al., 1998). Subsequent analysis of parkin has clearly associated PARKIN mutations with early onset familial PD and has revealed that Parkin is a RING-finger-containing protein that functions as an E3 ubiquitin ligase (Shimura et al., 2000); however, identifying putative substrates of Parkin has proven to be elusive and has yielded disparate results.

Approximately sixty different point mutations in *parkin* have been described (Mata et al., 2004). Patients with homozygous exonic deletions that nullify Parkin protein function exhibit selective loss of DA neurons in the SN and locus coeruleus but do not manifest either Lewy body or neurofibrillary tangle pathology, in remarkable contrast to patients who have compound heterozygous mutations in PARKIN and have been observed to have concomitant neurofibrillary tangle or Lewy body pathology (Pramstaller et al., 2005).These divergent outcomes to different *parkin* mutations may be mutation specific, as the localization of the mutation likely affects the degree of endogenous *parkin* function and may also affect the interaction of Parkin with other proteins.

Parkin has been shown to interact with PINK1 and LRRK 2, the products of two different PD-linked genes (Ng et al., 2009; Thomas and Cookson, 2009) and over-expression of Parkin is protective against the effects of over-expressed mutant α-synuclein in DA neurons (Lo Bianco et al., 2004). Additionally, Parkin has been shown

to interact with different pathways that have been associated with PD pathology such as mitochondrial dysfunction (Berger et al., 2009), and mitophagy (Geisler et al., 2010). A wide array of oxidative stressors, including MPP^+, paraquat, rotenone, 6-hydroxydopamine (6OHDA), nitric oxide and dopamine have been determined to modify the solubility of Parkin, leading to Parkin protein aggregation (Wang et al., 2005) thus suggesting a potential mechanism for Parkin dysfunction in sporadic PD. Furthermore, we have demonstrated that *parkin* deficiency increases vulnerability to inflammation-related nigral degeneration (Frank-Cannon et al., 2008) supporting the hypothesis that inflammatory pathways triggered by a variety of ailments can impinge on wild-type or mutant Parkin to modify predisposition to onset and progression of PD.

PINK (PARK6)

Loss of function mutations in the gene PTEN-induced kinase 1 (PINK), which is designated as PARK6, were determined to be the cause of early onset familial PD from linkage studies of consanguineous families. The PINK1 transcript is ubiquitously expressed and encodes a mitochondrial serine-threonine kinase similar to the Ca^{2+}/calmodulin family of kinases (Valente et al., 2004). Single point mutations and compound heterozygous mutations in PINK1 have been reported (Hedrich et al., 2006). Mutations in PINK1 have diverse effects on protein stability, localization, and kinase activity (Beilina et al., 2005). Studies examining the WT function of PINK1 have revealed that PINK1 seems to be protective against stress-induced mitochondrial dysfunction and apoptosis in neurons (Deng et al., 2005; Petit et al., 2005) and PINK1 and Parkin have a cooperative mitochondrial function (with PINK1 apparently

functioning upstream of Parkin) in drosophila models (Clark et al., 2006). While these and similar studies of wild type PINK1 have imparted valuable information regarding its endogenous function, much remains unknown about the pathological effects of mutant PINK1 in DA neurons, as neither its direct activators/repressors nor downstream targets are known. To date, no patients with homozygous mutations in PINK1 have been pathologically examined at autopsy (Farrer, 2006; Hardy et al., 2006), but the histopathological analysis of patients with heterozygous PINK1 mutations reveals the presence of Lewy bodies (Gandhi et al., 2006; Stayner et al., 2006).

DJ-1 (PARK7)

Initially cloned as an oncogene, (Nagakubo et al., 1997) DJ-1 (designated as PARK7) was first identified by family linkage analysis in a Dutch population and has been shown to cause early onset familial PD with a phenotype similar to AR-JP (Bonifati et al., 2003). The DJ-1 protein exists primarily as a dimer localized to the mitochondria and is a putative molecular chaperone that is induced under conditions of oxidative stress (Tao and Tong, 2003; Zhang et al., 2005). Several mutagenic sequence variants of DJ-1 have been described, and some point mutations have been shown to disrupt DJ-1 dimerization, leading to rapid degradation of the protein via the UPS (Miller et al., 2003). In addition to its apparent function as a chaperone protein, other experiments examining the function of DJ-1 strongly support its role in oxidative stress responses. The isoelectric point of DJ-1 shifts to more oxidized forms under conditions of oxidative stress (Canet-Aviles et al., 2004) and these oxidized forms of DJ-1 have been observed in brain samples from PD patients ((Bandopadhyay et al., 2004). Additionally, over-expression of

DJ-1 is protective from a variety of stimuli that induce oxidative stress (Aleyasin et al., 2010; Taira et al., 2004). One possible mechanism of DJ-1-induced antioxidant capacity is its function as a transcriptional inducer of glutamate cysteine ligase, which is the rate-limiting enzyme of glutathione biosynthesis (Zhou and Freed, 2005) and as an indirect transcriptional stabilizer for nuclear factor erythroid 2-related factor 2 (NRF2) which itself is an antioxidant transcriptional master regulator (Clements et al., 2006).

DJ-1 null mice have been generated, and while they exhibit no overt nigrostriatal degeneration, (Goldberg et al., 2005; Yamaguchi and Shen, 2007) they do exhibit hypokinesia and age-dependent motor deficits and dopaminergic dysfunction, and have heightened sensitivity to the dopaminergic neurotoxin MPTP (Goldberg et al., 2005; Yamaguchi and Shen, 2007). The lack of overt DA neuron loss in DJ-1 null mice implies that environmental or epigenetic factors may converge with loss of DJ-1 gene/protein function, to culminate in increased succeptibility to PD.

Contribution of Environmental Factors to PD

Familial Parkinson's disease is quite rare, and the vast majority of PD cases are considered to be sporadic or idiopathic. Additionally, among families who harbor the same genetic mutation for PD, disease onset is often quite variable, futher implicating environmental factors in PD onset and pathology. In addition to the overall rarity of genetic or familial PD, one of the most compelling indications of an environmental component to PD were the results of a large twin study published in 1999. Assuming an integral contribution of genetic factors, the concordance rate of PD would be expected to

be greater in monozygotic twins relative to dizygotic twins; however data from Bronstein and colleagues reported similar concordance for PD in either monozygotic or dizygotic (Bronstein et al., 2009) twin pairs, indicating that identification of environmental contributions to PD is requisite for a better comprehension of PD etiology and patholgy.

Increasing age

The most incontrovertible risk factor for PD is increasing age, as incidence of PD is extremely rare prior to age 50 and its incidence increases from age 50 onward (Di Monte et al., 2002). The molecular mechanisms that render the aging brain more susceptible to nigrostriatal degeneration remain quite elusive, although recent data indicate that redox homeostasis and cellular stress response mechanisms are compromised with aging and in neurodegenerative disease (Calabrese et al., 2010). Additionally, age-dependent changes in inflammatory responses in the brain, have been associated with neurodegeneration. Age-related changes in microglia cells (brain resident inflammatory cells of macrophage lineage) have been hypothesized to contribute to the onset of neurodegenerative diseases by inducing cytotoxicity instead of neuroprotection (Sawada et al., 2008; von Bernhardi et al., 2010). Furthermore, there is an age-associated decline in the function and homeostasis of several cellular pathways that have been associated with PD, such as the UPS and the ALS as well as accumulation of mitochondrial DNA mutations, all of which will be discussed later in further detail. A major hurdle in deciphering the effects of environmental insults and aging in PD is compounded by a very vague understanding of the so called “latent phase” of PD, which is the pre-clinical disease phase that preceeds acute symptomatic onset (Tanner et al., 2001) and is likely to be significantly variable

depending on environmental interactions. Many different environmental factors that are proposed to contribute to PD are discussed below.

Pesticide exposure

Epidemiological studies over the years have consistently proposed an association between PD and exposure to agricultural chemicals (Brown et al., 2006). Brown and colleagues investigated 38 different case studies on environmental exposures and incidence of PD, across North and South America, Europe, Asia, Australia and Africa and found an association with farming and professional pesticide use and PD (Brown et al., 2006). These studies suggest that PD risk increases proportionally with both increased duration of exposure as well as exposure to high dose of pesticides. The types of pesticides that have been associated with PD are numerous and varied and include: insecticides (e.g., organophosphates, carbamates, rotenone); herbicides (e.g., bipridyls and paraquat); fungicides (e.g. maneb); and organochlorines (e.g. DDT and dieldran) (Brown et al., 2006).

Many of these pesticides are quite dissimilar in chemical nature, so it is likely that their adverse association with PD result from several divergent mechanisms. Some of these pesticides are overtly neurotoxic both *in vivo* and *in vitro* (Betarbet et al., 2000; Bove et al., 2005; Karen et al., 2001) and many pesticides are capable of inducing or inhibiting enzymes that function in zenobiotic pathways (Le Couteur et al., 1999) which may impact metabolism of endogenous or exogenous neurotoxins. These and similar studies have implicated numerous potential mechanisms of pesticide-induced dopaminergic neurotoxicity, including oxidative stress, mitochondrial toxicity, and

aberrant interactions with α-synuclein. Potential limitations to these *in vivo* and *in vitro* studies of the mechanisms of pesticide-mediated toxicity is that they tend to be acute and short-term in nature, (importantly, data from human case studies analyzed by Brown and colleagues, discussed above, was most correlative to PD over the duration of ten to twenty years), involve doses and routes of exposure that may not be environmentally relevant, and few studies using multiple or mixed pesticides have been attempted (Elbaz et al., 1999). Thus continued studies are warranted to further elucidate the mechanisms of pesticide-indued nigrostriatal toxicity, especially since professional pesticide exposure is a preventable exposure.

1-methyl-4-phenyl-1,2,5,6-tetrahydropyridine (MPTP)

If environmental agents like pesticides are likely to impact the etiology of PD, it is essential to demonstrate that toxicant exposure can recapitulate many aspects of the disease; the neurotoxin 1-Methyl-4-phenyl-1,2,5,6-tetrahydropyridine (MPTP) largly achieves this requirement (Di Monte et al., 2002). Although there were occasional early reports of MPTP-induced neurotoxicity, the potential role of MPTP in parkinsonism was not fully appreciated until the early 1980's after several young heroin users in the San Francisco Bay area presented at emergency rooms with symptoms that were indistinguishable from those of PD (Langston, 1985; Langston et al., 1983). The symptoms of the MPTP-induced parkinsonsim responded to dopamine replacement therapy, strongly implicating the nigrostriatal pathway in symptom onset. Interestingly, the case of MPTP is one of the rare instances where the effects of a neurotoxin were discovered first in humans.

Subsequent development of non-human primate (Burns et al., 1983) and rodent (Heikkila et al., 1984) models of MPTP have fostered a wealth of information on the mechanisms of MPTP-induced dopaminergic neurotoxicity and have provided models in which to test potential PD therapeutics. After repeated systemic injection of MPTP, the MPTP crosses the blood brain barier (BBB) and is then metabolized by the enzyme monoamine oxidase B (MAO-B), which is enriched in endothelial cells of the BBB microvasculature and in glial cells (astrocytes and microglia) into the metabolite 1-methyl-4-phenyl-2,3-dihydropyridium ($MPDP^+$). $MPDP^+$ is then deprotonated to generate MPP^+. Once converted to the MPP^+ species within glia, MPP^+ robustly stimulates inflammatory responses, inducing upregulation of TNF, IL-1β, and IL-6 (Teismann et al., 2003; Youdim et al., 2002) which in turn generate inducible nitric oxide synthase (iNOS) (Hunot et al., 1999). The MPP^+ that is released into the extracellular space is then readily taken up by neighboring cells, primarily via the dopamine transporter (DAT). MPP^+ is a potent mitochondrial toxin that binds to complex 1 of the mitochondrial transport chain, inhibiting electron flow and inducing reactive oxygen species (ROS) and other mediators of oxidative stress, such as hemeoxygenase-1 (Rossetti et al., 1988). Additionally, MPTP toxicity has been shown to induce the redistribution and aggregation of α-synuclein within degenerating DA neurons *in vivo* in non-human primates, likely modeling the early stages of Lewy body formation (Kowall et al., 2000).

Infection, Inflammation and Autoimmunity

Viral encephalitis, which is literally brain inflammation due to viral infection, is one environmental trigger that has long been associated with delayed or secondary PD onset. Over a dozen different viruses have been associated with viral encephalitis-related PD, including influenza Type A, Measles, Epstein-Barr, Cytomegalovirus, West Nile virus, and Japanese encephalitis B virus (JEBV) (reviewed by (Jang et al., 2009)). Influenza virus has been implicated as a causative factor of PD (both directly and indirectly) based on epidemiological studies and clinical description. Most famously, the 1918 influenza pandemic, caused by an influenza H1N1 Type A virus, led to an eruption of subsequent postencephalic parkinsonism. Studies have shown that several type A influenza viruses are neurotropic (Klopfleisch et al., 2006) and one hypothesis proposed to explain the mechanism of ensuing PD following postviral encephalitis is the "hit and run" mechanism, whereby the initial transient insult induces a chronic immune response in the brain that persists long after the original insult is cleared (Langston et al., 1999). Experimental evidence associating viral encephalitis and PD has been generated from animal studies using JEBV, which is the most common cause of viral encephalitis in Asia. Rats experimentally infected with JEBV exhibited significant gliosis in the SNpc as well as bradykinesia that was tractable with levodopa administration (Ogata et al., 1997).

Recently, to account for a portion of PD cases, an autoimmune hypothesis has emerged (reviewed by (Monahan et al., 2008)), postulating that autoimmunity and peripheral inflammation contribute to PD etiology. A proposed mechanism to explain this association is that BBB dysfunction is prevalent in some animal models of PD, allowing peripheral vascular factors and immune cells to freely enter the brain and potentially

facilitate a progressive degenerative process (reviewed by (Monahan et al., 2008)). Important principles of this hypothesis question some long-standing CNS paradigms, including the assumption of an inpenetrable BBB, the brain existing as an immune privleged area, and dissociation between a pathogenic insult and disease progression, suggesting different mechansms for neurodegenerative disease progression. Future studies in this field are crucial to clarify these questions and many others that confound the association between inflammation and PD.

Cellular protein handling systems: the ubiquitin proteasome system and the autophagy lysosome system

The mammalian cell has two primary systems for maintaining protein homeostasis and cellular quality control, the ubiquitin proteasome system (UPS) and the autophagy lysosome system (ALS). Altered protein handling has been associated with a number of neurodegenerative diseases (which are alternatively referred to as proteinopathies) including PD, in which protein aggregation is correlated with disease pathology. Under conditions of cellular stress resulting in protein damage, the protein handling systems work cooperatively to refold (if possible) or degrade damaged proteins. Importantly, the efficiency of the UPS and ALS seems to generally decrease with age (Massey et al., 2006). A brief synopsis describing how the UPS and ALS may relate to PD is provided below.

Function of the ubiquitin proteasome system in Parkinson's disease

The evidence for UPS impairment in PD is mounting; however, whether UPS function is a cause or consequence of PD (or plays a role in both) remains ambiguious. One piece of evidence liking UPS function to PD comes from post-mortem studies of the SN of PD patients. Using immunoblotting and histological analysis, subunits of the 20S proteasome and PA700/19S complex were found to be reduced in the SN of PD patients, but were unaltered in non-nigral brain regions (McNaught et al., 2002; McNaught and Jenner, 2001). Another link between the UPS and pathogenesis of PD is that use of lactacystin, an ihibitor of the UPS, leads to neuronal degeneratation and formation of α-synuclean and ubiqutin positive inculsions in rat primary ventral mesencephalon cultures (Rideout et al., 2005). Further linking sporadic PD to the UPS is the observation that UPS function is compromised following exposure to the pesticides rotenone, paraquat, and maneb (Betarbet et al., 2006). Additionally, some of the genes with mutations linked to familial PD have been shown to impact UPS function. For example, aggregated α-synuclein impairs the UPS to a greater extent that monomeric non-aggregated α-synuclein and recent data has shown that mutant (but not wild type) LRRK2 binds to the heat shock protein hsp90. In order for mutant LRRK2 to be degraded by the UPS, the UPS must be functioning normally and the mutant LRRK2-hsp90 complex must dissociate (Wang et al., 2008). Thus dysregulated UPS function could lead to accumulation of mutant LRRK2. Furthermore, there is an assumed general link between UPS function and Lewy body formation as Lewy bodies contain ubiquitin, aggregated α-synuclein, and occasionally PINK1, which localizes to aggresomes along with Parkin under conditions of UPS stress (Gandhi et al., 2006; Muqit et al., 2006).

Functions of the autophagy lysosome system (ALS) in Parkinson's disease

Autophagy is a highly conserved process across species and in addition to being a regulated pathway for degrading long-lived proteins, it is the only pathway involved in organelle turnover. The two main steps in autophagy are the delivery of substrates to the lysosomal lumen followed by the degradation of the substrates inside lysosomes by resident enzymes. The degradation step is universal, but different types of autophagy have been described in mammalian cells depending on the mechanisms that engage in delivery of cargo to the lysosome: macroautophagy, microautophagy, and chaperone-mediated autophagy (CMA). Macroautophagy is an inducible autophagic vesicle mediated pathway that is upregulated in response to stress and involves *de novo* formation of a double membrane referred to as an autophagosome or autophagic vacuole, and is the only cellular mechanism that engages in organelle turnover. Microautophagy involves the budding of the autophagosome membranes to engulf small cytoplasmic areas (Ohsumi and Mizushima, 2004). CMA has only been defined in mammals (Massey et al., 2004), and only selective cytosolic proteins (but not organelles) are targeted (via a unique amino acid motif on substrate proteins) for degradation by individual translocation into the lysosomal lumen without engagement of vesicular trafficking (Cuervo and Dice, 1998).

Recently, there has been growing interest in deciphering the role of the ALS in neurodegeneration (reviewed by (Martinez-Vicente and Cuervo, 2007; Rubinsztein, 2006)) as defects in the ALS pathway have been linked to neurodegenerative diseases (Bandyopadhyay and Cuervo, 2007; Ravikumar et al., 2004). Alpha-synuclein is a CMA

substrate protein, and more than any other gene product associated with PD, α-synuclein has been implicated in ALS dysfunction. Dopamine-modified α-synuclein has been shown to impair the CMA pathway (Martinez-Vicente et al., 2008) and there is likewise impaired degradation of mutant α-synuclein by the CMA pathway due to aberrant interactions between mutant α-synuclein and the CMA lysosomal receptor LAMP-2A (Cuervo et al., 2004). Additionally, the UCHL1 I93M mutant protein, which is linked to familial PD, also interacts with LAMP-2A as well as with the heat shock chaperone proteins Hsc70 and Hsc90, which are components of the CMA pathway, and expression of mutant UCHL1 I93M induces a CMA inhibition-associated increase in the amount of α-synuclein (Kabuta et al., 2008).

Furthermore, mutations in the gene that encodes glucocerebrosidase (GBA), a lysosomal enzyme in the ceramide metabolism pathway, have been associated with PD. Homozygous mutations in GBA cause a lysomal storage disorder called Gaucher's disease (GD). Epidemiological studies suggest that heterozygous carriers of GBA mutations are at increased risk of developing PD (Aharon-Peretz et al., 2004; Gan-Or et al., 2008), potentially due to disruption of CMA-mediated degradion of α-synuclein. The connection between PD and GBA and the ceramide pathway will be discussed in further detail below.

Mitophagy, the autophagic degradation of mitochondria, has been proposed as a cellular compensatory mechanism engaged during the progression of PD. The PD-associated proteins Parkin and PINK1 are believed to function in maintenance of

mitochondrial integrity (Cherra et al., 2009; Narendra et al., 2009; Whitworth and Pallanck, 2009). The PINK1/Parkin pathway has been proposed to regulate mitochondrial dynamics by promoting mitophagic turnover of damaged mitochondria; therefore, the absence or mutant/aberrant function of Parkin/PINK1 may disrupt the turnover of damaged mitochondria, contributing to pathogenesis in PD.

Organelles and pathways implicated in PD: mitochondrial dysfunction, oxidative stress, endoplasmic reticulum stress, and ceramide metabolism

Recent data from studies of genetic and sporadic forms of PD have revealed several common molecular pathways believed to be involved in pathogenesis. These pathways include mitochondrial dysfunction, oxidative stress, endoplasmic reticulum (ER) stress, and ceramide metabolism. Below is a brief discussion of these pathways and how they interact with genetic and sporadic PD.

Mitochondrial dysfunction in Parkinson's disease

The exclusive degeneration of dopaminergic neurons following systemic exposure to mitochondrial toxicants such as MPTP and rotenone strongly supports a role for mitochondrial dysfunction in PD. In general mitochondria are key regulators of cellular bioenergetics and are effectors of cell death. Mutations in mitochondrial DNA and the mitochondrial release of reactive oxygen species (ROS) contribute to aging, and aging is the greatest risk factor associated with PD and neurodegenerative diseases. The brain is acutely sensitive to oxidative damage due to its high content of easily peroxidized unsaturated fatty acids, high oxygen consumption rate, and relative paucity of antioxidant

enzymes compared to other organs (Nunomura et al., 2006). Disrupted mitochondrial energy metabolism leads to decreased ATP production, impaired Ca^{2+} homeostasis, and increased generation of ROS (Beal, 2005). Additionally, mitochondrial DNA (mtDNA) is especially vulnerable to oxidative damage because of its close vicinity to the electron transport chain (which is a potent source of ROS), it is not protected by histones like genomic DNA, and employs an inefficient repair mechanism, all of which combine to lead to a high mtDNA mutation rate (Lin and Beal, 2006).

Mitochondrial involvement in the pathogenesis of idiopathic PD is further supported by post-mortem biochemical studies wherein a disease-specific and drug-independent defect of the mitochondrial respiratory complex 1 (an approximate 25-30% inhibition) was found in SN tissue from patients with idiopathic PD (Hattori et al., 1991). Additionally, MPTP and many pesticides also impinge on mitochondrial function. Connecting mitochondria and familial PD, a remarkable number of PD-specific proteins interact with mitochondria and mounting experimental evidence suggests that mitochondrial dysfunction occurs early and acts causally in PD pathogenesis (reviewed by (Lin and Beal, 2006)).

Although there is no direct evidence for mitochondrial localization, dysfunction of α-synuclein has been shown to indirectly but robustly impinge on mitochondrial function in neurons (Abou-Sleiman et al., 2006). Additionally, recent *in vitro* data indicate that knockdown of α-synuclein attenuates MPP^+-induced mitochondrial dysfunction in SH-SY5Y cells (Wu et al., 2009).

Compared to α-synuclein, there is a more direct association between Parkin and mitochondria in PD. Parkin has been shown to be requisite for mitochondrial function in drosophila, as *parkin* null mutants exhibit severe mitochondrial pathology, flight muscle degeneration, apoptosis and shortened lifespan (Greene et al., 2003). While mammalian *parkin* null models do not exhibit as severe of a phenotype as the drosophila *parkin* null model, there is still strong evidence to support a role for Parkin protein in mammalian mitochondria function. From *in vitro* experiments using differentiated PC12 cells, Parkin protein has been shown to localize to the outer mitochondrial membrane where it has a crucial role in maintaining mitochondrial morphology by preventing swelling and rupture secondary to ceramide toxicity (Darios et al., 2003a). Additionally, Parkin has been experimentally placed in a linear pathway with PINK1 as a mitochondrial quality control system (Whitworth and Pallanck, 2009). PINK1 and Parkin seem to promote neuroprotection through a cooperative role in mitophagy. PINK1 and Parkin have been linked to mitochondrial fission, which promotes the segregation of terminally dysfunctional mitochondria for degradation by the lysosome through mitophagy (Whitworth and Pallanck, 2009). Additionally, PINK1 interacts with mitochondrial pathways independent of Parkin. The kinase PINK1 harbors a mitochondrial localization sequence and has been shown to mediate mitochondrial functions. From overexpression studies using G309D mutant PINK1, PINK1 is surmised to play a role in maintaining mitochondrial membrane potential in response to cellular stress, as cells expressing G309D mutant PINK1 had disrupted mitochondrial membrane potential in response to the proteasome inhibitor MG-132 but were unaffected at baseline. Moreover, cells that

over-expressed wild type PINK1 had higher mitochondrial membrane potential and subsequently less cell death due to MG-132-induced toxicity (Valente et al., 2004).

Oxidative Stress in Parkinson's disease

Oxidative stress is the general term used to describe the steady state level of oxidative damage (redox state) in cells, tissue, organs etc., caused by an intracellular accumulation of reactive oxygen and nitrogen species (ROS and RNS, respectively). Perturbation of the normal redox state of a cell can elicit toxic damage of many cellular components, including proteins, lipids and DNA by peroxides and free radicals.

Overall, ROS and RNS can be linked to nearly every pathogenic mechanism posited to play a role in PD, including protein aggregation, mitochondrial dysfunction, inflammation, ER stress, and pesticides; ROS can also significantly amplify cell death pathways (Levy et al., 2009). Numerous studies have reported augmented levels of multiple markers of oxidative damage in the SN of PD patients: DNA damage, protein oxidation, lipid peroxidation, reduced glutathione and increased deposition of iron (Jenner and Olanow, 2006). ROS is generated in a number of ways, including leakage of electrons from the electron transport chain leading to partial reduction of O_2 to superoxide species (reviewed by (Lin and Beal, 2006)), peroxide formation from dopamine catabolism by monoamine oxidase (Chen et al., 2002) and through inflammatory signaling in glia (Tansey et al., 2007). In inflammatory signaling, microglia cells become activated through the action of nicotinamide adenine dinucleotide phosphate (NADPH) oxidase which generates ROS (reviewed by (Dringen, 2005). Interestingly,

NADPH oxidase is more highly expressed in SNpc microglia from sporadic PD patients relative to SNpc microglia from unaffected controls (Wu et al., 2003). RNS can be generated by entry of Ca^{2+} through N-methyl-D-aspartate (NMDA) receptors, stimulating nitric oxide synthase activity by binding calmodulin, a cofactor for NOS (Bredt and Snyder, 1990).

Endoplasmic reticulum (ER) stress in Parkinson's disease

Endoplasmic reticulum (ER) stress describes the imbalance between the cellular demand for ER function and ER capacity and is induced upon accumulation of unfolded and/or misfolded proteins in the lumen of the ER. To cope with ER stress, numerous pathways of the unfolded protein response (UPR) are activated. The purpose of the UPR is to remove aberrant substrates and restore ER homeostasis, which is achieved through a tripartite signal that 1.) inhibits general translation to attenuate the load of proteins to the ER, 2.) induces transcriptional activation of chaperone proteins to increase folding capacity, and 3.) activates ER-associated degradation (ERAD) to promote degradation of misfolded proteins (reviewed by (Wang and Takahashi, 2007)). If the ER stress is severe or prolonged however, eventually apoptotic signaling is activated, leading to programmed cell death. The inhibition of general translation is regulated by the PKR-like ER-localized eIF2α kinase (PERK) pathway, increased transcription of chaperone proteins is mediated by activating transcription factor 6 (ATF6), inositol-requiring 1 (IRE1), and PERK, ERAD is regulated by IRE1 and ATF6, and cell death is activated by CIEBP homologous protein (CHOP), JNKs and the ER-resident caspase 12 (reviewed by (Wang and Takahashi, 2007)). ER stress has been determined to be an important pathway

in PD (Yamamuro et al., 2006), but it is not fully clear if ER stress is a cause, result, or epiphenomenon in PD.

ER stress has been observed in models of familial PD. In PC12 cells, inducible overexpression of A53T mutant α-synuclein induces ER stress as evidenced by elevated protein expression of CHOP, increased phosphorylation of PERK and activation of caspase 12 (Smith et al., 2005a). Furthermore, in these experiments ER stress was shown to contribute to cell death, as use of a selective inhibitor of cellular phosphatase complexes that dephosphorylate PERK and inhibition of caspase 12 each attenuated A53T mutant α-synuclein-induced cell death.

There is also compelling evidence for the function of Parkin in the ER stress pathway. Parkin is an E3 ubiquitin ligase that interacts with cognate E2 (ubiquitin conjugating enzyme) partners Ubc6 and Ubc7, which are ER-associated E2 enzymes involved in ERAD, thereby stationing Parkin in the ERAD machinery (Wang and Takahashi, 2007). Additionally, cells from AR-JP patients over-expressing wild type but not mutant Parkin were found to be resistant to cell death induced by unfolded proteins (Imai et al., 2000), presumably due to collaboration between Parkin and Ubc6/Ubc7 in ERAD.

Additionally, experimental data support a role for ER stress in toxin-induced models of PD. Ryu and colleagues used a functional genomics approach to identify transcriptional changes in genes associated with the UPR in a PC12 cellular model of PD and discovered that CHOP, PERK and JNK were dramatically upregulated in response to

rotenone, MPP^+ and 6-OHDA, but were unchanged in response to apoptotic stimuli (Ryu et al., 2002). It is possible that ER stress is induced by these toxins upon accumulation of damaged oxidized proteins or that oxidative stress can directly impact ER stress. Furthermore primary sympathetic neuronal cultures from *perk*$^{+/-}$ mice, which are defective in their ER stress response were found to be significantly more sensitive to 6-OHDA-induced cell death relative to control neurons (Ryu et al., 2002), indicating that ER stress contributes to 6-OHDA-induced cytotoxic cell death.

Finally, ER stress can be directly or indirectly triggered by oxidative stress (Friedlander et al., 2000; Malhotra and Kaufman, 2007) and Holtz and colleagues demonstrated that oxidative stress-induced UPR is upstream of intrinsic apoptotic cell death evoked by 6-OHDA (Holtz et al., 2006). As oxidative stress is a pathway that is common to all models of PD, it is thus likely that ER stress is likewise a common pathogenic pathway in PD due to oxidative stress-induced ER stress.

Ceramide signaling and metabolism in Parkinson's disease

Ceramide is a sphingolipid composed of a sphingoid base and a single fatty acid attached at C1 via N-acetylation. Ceramide is the backbone of all complex sphingolipids, which are formed by attachment of different head groups at C1. Sphingolipids are one of the three lipid components of the plasma membrane and have a well-established role in cell membrane homeostasis (Goni and Alonso, 2006). In its structural capacity ceramide has been shown to increase lipid order, contribute to lateral phase separation, facilitate transmembrane (flip-flop) lipid motion, and increase membrane permeability (reviewed

by (Morales et al., 2007)). However, what is becoming more appreciated is a role for ceramide as a second messenger sphingolipid that regulates many diverse cellular functions, such as differentiation, proliferation and apoptosis, and is crucial in the cellular response to a variety of stresses (reviewed by (Hannun and Obeid, 2008)).

Ceramide signaling has been shown to induce caspase-dependent and caspase-independent cell death (Lock et al., 2007). Proposed mechanisms of ceramide-induced neurotoxicity include increased intracellular Ca^{2+} (Colina et al., 2005), mitochondrial dysregulation (Darios et al., 2003b), ER stress (Xue et al., 2005) and inhibition of the neuronal survival pathway regulated by phosphatidyl-inositol-3-kinase/protein kinase B (PI3K)/Akt (Arboleda et al., 2009). Additionally, experimental data indicate that ceramide is neurotoxic (Willaime et al., 2001) but the mechanisms of ceramide-induced neurotoxicity in DA neurons have not been fully delineated.

Recently, a connection has been drawn between ceramide signaling/metabolism and PD. In an effort to identify pathways of Lewy body pathogenicity by examination and identification of common pathology as opposed to examination of common clinical characteristics, Bras and colleagues suggest that ceramide metabolism is a general theme for pathogenesis in Lewy body disease (Bras et al., 2008). Notably, PD is considered a Lewy body disease, and mutations in many PARK loci are associated with Lewy body disease as well. In the last few years, heterozygous mutations in the gene that encodes the lysosomal enzyme glucocerebrosidase (GBA) have been associated with early onset PD (Aharon-Peretz et al., 2004; Gan-Or et al., 2008), and while it has not been assigned a

PARK locus, GBA is the gene with the strongest association to PD in the PDGene database (Alzheimer Research Forum. Available at: http://www.pdgene.org/. Accessed February 2009). Notably, the lysosomes of patients with heterozygous mutations of GBA display normal levels of GBA and its associated substrates, implying that general ceramide metabolism, rather than acute loss of GBA function, may be causative in early onset PD.

Interaction between genetics and environment in the onset and pathogenesis of Parkinson's disease

In addition to the aforementioned genetic and environmental susceptibilities associated with PD, it is likely that there are several yet-to-be elucidated genes with potential PD-associated mutations and additional predisposing environmental factors, but their identification is complicated by incomplete penetrance, subtle effects, and otherwise intangible interactions between genetic predispositions and etiologic heterogeneity. It is assumed that in most cases, PD results from a complex interaction of multiple genetic susceptibilities and environmental factors on the background of an aging brain (reviewed by (Gasser, 2009)). One clue to the complex interaction between genetics and environment in PD is its notably worldwide prevalence among different ethnic groups and geographical locations (Benmoyal-Segal and Soreq, 2006). Various countries have reported on their prevalence of PD, with the lowest prevalence occurring in the Far East, specifically China. The relatively large representation of PD in the global population (estimated to be approximately 1%) and its variable etiology support the ideology of environmental/genetic interaction in PD.

Due to the presumed complex interaction between genes and environment in PD, a so called "second-hit" hypothesis has been developed (reviewed by (Sulzer, 2007)). In support of this hypothesis, the common PD pathways, protein aggregation, mitochondrial dysfunction, and oxidative stress, coincide with the "clustered" functions of PD susceptibility genes which can generally be segregated into the following categories: 1.) proteins affecting mitochondria (e.g., PINK, DJ-1); 2.) proteins involved in vesicular trafficking (e.g., α-synuclein); 3.) proteins involved in macromolecular degradation pathways, (e.g. Parkin and DJ-1 in the UPS, and GBA and α-synuclein in the ALS); 4.) proteins that modify oxidative stress or antioxidant function (e.g., DJ-1) (reviewed by (Sulzer, 2007)). According to Sulzer, a primary hit might lead to neuronal stress within the SN, and secondary hits, by loss or inhibition of stress-induced protective pathways, may combine with primary hits in a manner that may elicit significant DA neuron loss in the SNpc (Sulzer, 2007). Thus future studies aimed at elucidating the complex milieu of genetics and environment in PD, as well as development of "second hit" models of PD are warranted and necessary to provide a better understanding of PD onset and progression and to rationally identify putative therapeutic targets.

INFLAMMATION AND PARKINSON'S DISEASE

Evidence of Neuroinflammation in Parkinson's Disease

Inflammation has been cited as a common pathway in PD (reviewed by (Sulzer, 2007) and impinges on many other pathways common to PD such as ER stress (Ryu et al., 2002), and oxidative stress (reviewed by (Jenner and Olanow, 2006)). Increased levels of

pro-inflammatory cytokines have been detected in the CSF and striatum of PD patients relative to healthy age-matched controls (Mogi et al., 2000; Muller et al., 1998). Additionally, levels of inflammatory cytokines are likewise elevated in the MPTP and 6-OHDA animal models of PD (Mogi et al., 1999; Nagatsu and Sawada, 2005) and neuroinflammation has a general role in transgenic PD mouse models (Schwab et al., 2009). Furthermore, activated glial cells expressing inflammatory cytokines and iNOS have been observed in the SN of PD (Hirsch et al., 1998; Hunot et al., 1996). Moreover, polymorphisms in genes for the inflammatory cytokines TNF and IL-1β confer risk of developing PD (Wahner et al., 2007). Conversely, use of non-steroidal anti-inflammatory drugs (NSAIDs) reduce the risk of developing PD (reviewed by (Esposito et al., 2007)).

Characteristics of Neuroinflammation

The four classic signs of inflammation in the periphery, *rubor* (redness), *color* (heat), *dolor* (pain) and *tumor* (swelling) are not present in the CNS largely due to the physical restriction of the skull. The brain was formerly considered to be an immune privileged organ and it was presumed that the blood brain barrier (BBB) was inpenetrable. It is now appreciated that the brain possesses an inflammatory repertoire, referred to as neuroinflammation, that is distinct from peripheral inflammation and that under certain developmental and pathological conditions, the BBB can be breached. Moreover, the role of neuroinflammation in aging and neurodegenerative disease is becoming more appreciated.

Microglia: mediators of neuroinflammation

Microglia cells are derived from the macrophage lineage and are brain resident immune cells obligate for proper immune function in the brain. Microglia represent 10% of the total cell population in the brain and perform crucial functions in normal physiological conditions and as well as in injury and disease (Streit et al., 2004). In their resting state, microglia exhibit a ramified morphology, characterized by long branching processes and a small cellular body, and have low expression of membrane receptors (Whitton, 2007). Under normal physiological conditions, microglia are maintained in their quiescent state by expression of the glycoprotein CD200 on the surface of neurons (Hoek et al., 2000). Non-activated microglia provide trophic support for neurons and perform a phagocytic surveillance function to remove cellular debris. Microglia are a dynamic cell type capable of diverse functions and respond rapidly to their changing microenvironment and are involved in inflammation, trauma, ischemia and neuronal death (reviewed by (Kraft et al., 2009)). To perform these latter functions, microglia become activated and undergo a morphological change with a widening of the cell body and concomitant retraction of processes (Whitton, 2007). Upon activation, microglia upregulate cell surface glycoproteins such as CD40, CD80 and CD86, which provide powerful stimulus for immune cell activation, and if sustained, promote microglial proliferation and migration to sites of injury (Aloisi, 1999, 2001; Whitton, 2007). Thus microglia have been described as a double-edged sword in neuroinflammation, with an innate role in immune regulation that can lead to cell loss and tissue damage if chronically sustained (Tansey et al., 2007; Wyss-Coray and Mucke, 2002).

Cytokines and chemokines

When activated, microglia (and to a lesser extent astrocytes) produce and secrete many substances including growth factors, cytokines (e.g. TNF, IL-1, IL-6, IFNγ and TGF-β), chemokines (which are chemotactic cytokines), prostaglandins, and RNS/ROS (reviewed by (Tansey et al., 2008)). Some of these substances provide trophic support for neurons, but others can lead to cell loss and tissue damage (Aloisi et al., 2000). Cytokines can be neuroprotective independent of their inflammatory capacity and depending on cellular cues, cytokines and chemokines can promote apoptosis of neurons, oligodendrocytes, and astrocytes. The overall outcome of cytokine signaling in the brain is very dynamic, depending on the pathophysiological context, cellular source and compartmentalization of cytokine release and the presence of cofactors (reviewed by (Tansey et al., 2008)). Importantly, activated microglia in the SN are found in several models of PD (reviewed by (Miller and Streit, 2007)) and cytokines and the inflammatory processes they mediated play an important role in PD (Sawada et al., 2006).

Tumor Necrosis Factor (TNF) signaling in Parkinson's disease

TNF signaling

TNF is a pro-inflammatory cytokine; TNF signaling has been implicated in diverse cellular functions, from proliferation and differentiation to inflammation and apoptosis. To mediate its diverse signaling functions, the TNF homotrimer ligand can be membrane bound (tmTNF) or cleaved by the metalloprotease TNF-α-converting enzyme (TACE) into a soluble fragment (solTNF). Both species of TNF are biologically active and the TNF ligand signals through two receptors, TNF receptor 1 (TNFR1) and TNF receptor 2 (TNFR2) (Aggarwal et al., 1985; Aggarwal, 2000). Through engagement and

concomitant activation TNF receptors, TNF utilizes numerous downstream effectors including ceramide, NFκB, P38, MAPK, and JNK; TNF signaling through these downstream mediators leads to activation of proteases, caspases, and ROS (reviewed by (MacEwan, 2002).

SolTNF preferentially signals through TNFR1, which is a canonical transmembrane death receptor, to potently transduce inflammatory stimuli (Ruuls et al., 2001; Tartaglia et al., 1993). Importantly, TNFR1 is constitutively expressed by most cell types (Grell, 1995; McGuire et al., 2001). SolTNF signaling through TNFR1 leads to a membrane signaling complex facilitated by dissociation of silencer of death domains (SODD), binding to TNF receptor-associated death domain (TRADD) and subsequent recruitment of adaptor proteins such as receptor interacting protein (RIP) (Hsu et al., 1996a; Hsu et al., 1996b). This membrane associated complex can then activate ERK, JNK, p38 MAP kinase, and ceramide/sphingomyelinase pathways (Dressler et al., 1992; Lee et al., 2003; Mathias et al., 1991; Winston et al., 1995). TNFR1 can also be internalized after engagement with the solTNF ligand, leading to dissociation of the TRADD/TRAF2/RIP complex and eventual caspase signaling via association of the Fas-associated death domain (FADD) and subsequent recruitment of pro-caspase 8 and assembly of the death-inducing signaling complex (DISC), further activating executioner caspase cascades (McCoy and Tansey, 2008; Micheau and Tschopp, 2003; Schneider-Brachert et al., 2004).

TNFR2 is inducible, is expressed primarily on endothelial and hematopoietic cells and preferentially binds tmTNF, although solTNF can also bind TNFR2 but with much lower affinity (Grell, 1995). Activation of TNFR2 leads to TNF-dependent inflammatory and pro-survival signal pathways via recruitment of TRAF1 and TRAF2 adaptor proteins and subsequent activation of cytosolic inhibitor of apoptosis proteins (cIAPs), and the NFκB pathway (McCoy and Tansey, 2008; Rao et al., 1995; Rothe et al., 1995; Rothe et al., 1994). Additionally, TNFR2 can also activate PI3K-independent signaling which has been shown to promote neuron survival (Fontaine et al., 2002; Marchetti et al., 2004). Moreover, TNFR2 does not contain a death domain and cannot lead directly to caspase activation as TNFR1 can. Overall, TNFR2 activation is considered to initiate predominately pro-inflammatory and pro-survival signaling (McCoy and Tansey, 2008).

Thus TNF binding and concomitant activation of signaling through its obligate receptors can lead to diverse cellular outcomes, and is regulated by the overall ratio of TNFR1 to TNFR2 on the cell surface and cell and context-specific cofactors. TNF-mediated inflammatory signaling has been implicated in the progression of numerous diseases, such as Chron's disease, rheumatoid arthritis, and neurodegenerative diseases.

Evidence of TNF signaling in Parkinson's disease

There is mounting evidence supporting a role for TNF signaling in PD. Increased levels of TNF have been observed in the CSF and post-mortem brains of PD patients, with the highest levels of TNF found in brain regions important in PD pathology (Boka et al.,

1994; Mogi et al., 1994; Mogi et al., 2000). Additionally, elevated TNF mRNA and protein levels have been detected within the midbrain of 6-hydroxydopamine (6-OHDA), MPTP and lipopolysaccharide (LPS) rodent models of PD (Gao et al., 2002; Mogi et al., 1999; Rousselet et al., 2002; Sriram et al., 2002) and DA neurons have been shown to be acutely sensitive to TNF *in vitro* and *in vivo* (Carvey et al., 2005; McCoy et al., 2006; McGuire et al., 2001). Moreover, high frequency of a single nucleotide polymorphism in the TNF promoter (TNF-308) resulting in overproduction of TNF has been associated with early onset PD (Nishimura et al., 2001) establishing a potential genetic association between TNF and PD in addition to the presumed role for TNF-mediated inflammation as a modifying factor in sporadic PD progression.

ANIMAL MODELS OF PARKINSON'S DISEASE

Animal models of human disease can play critical roles in the elucidation of pathogenic pathways, enabling identification of putative therapeutic targets, and providing disease-appropriate contexts in which to test and optimize novel drug therapies. Animal models of neurodegenerative diseases are invaluable as most neurodegenerative diseases exhibit an age-related onset, thus the shorter life-spans of rodents and murine transgenic technology provide valuable model systems. Additionally, as human PD patients are often not diagnosed until after significant progression through the latent /non-symptomatic phase of the disease, the use of animal models may enlighten a better understanding of early disease pathology that could not otherwise be afforded.

However, the usefulness of a given animal model resides in the degree to which the model is translatable to the human condition. As reviewed by Cicchetti and colleagues, animals are ultimately limited in their ability to mimic the human PD state due to the following potential shortcomings: inadequate characterization of the disease state being modeled, inadequate comprehension of the effect of the route of exposure on disease pathogenesis, and biochemical or anatomical differences between animals and humans (Cicchetti et al., 2009). Following is a brief synopsis of some non-genetic PD models, elaborating on their apparent strengths and limitations as well as an opinioned evaluation on how well they model the human PD condition.

The 6-hydroxydopamine (6-OHDA) rat model of Parkinson's disease

The earliest models established for PD research were developed by using specific neurotoxic agents, namely 6-OHDA and MPTP that selectively destroyed chatecholaminergic systems (Dauer and Przedborski, 2003). 6-OHDA is a hydroxylated analog of dopamine (Blum et al., 2001) and is preferentially taken up by the DA transporter (DAT) and accumulates in the cytosol to induce specific non-apoptotic cell death of catecholaminergic neurons (Jeon et al., 1995; Luthman et al., 1989). Collectively, the pathogenic mechanisms of 6-OHDA are respiratory inhibition, and oxidative stress induced by free radical formation, and these mechanisms appear to act synergistically to induce DA neurotoxicity (Schober, 2004b). Importantly, 6-OHDA does not cross the BBB, and therefore has to be stereotaxically injected directly into the brain. The magnitude of the nigrostriatal lesion induced by 6-OHDA depends on the site of the injection, the amount of 6-OHDA injected, and the species used, as rats are more

sensitive to 6-OHDA than are mice (Betarbet et al., 2002). The severity of the 6-OHDA lesion and the degree to which motor behavior is affected depends on the injections site(s) and number of injections used, with more pronounced deficits observed in animals where the total dose of 6-OHDA was distributed over multiple sites along the rostro-caudal extent of the lateral striatum or where the injections were made in close proximity to the junction of the globus pallidus (reviewed by (Kirik et al., 1998)).

In summary, 6-OHDA induces selective degeneration of DA neurons, sparing other neuron populations. Importantly, the 6-OHDA model does not mimic all pathological and clinical features of human parkinsonism, as other brain regions that are affected in PD, such as locus coeruleus and anterior olfactory regions, are unaltered by 6-OHDA and Lewy body formation is not generally observed (Schober, 2004a). Additionally, 6-OHDA is rather acute in action, with DA neuron degeneration occurring within hours and appreciable striatal dopamine depletion occurring on the order of days (Faull and Laverty, 1969).

The lipopolysaccharide (LPS) rat model of Parkinson's disease

Lipopolysaccharide (LPS) is a bacterial endotoxin found on the protein coat of certain Gram-negative bacteria. LPS is recognized by the toll-like 4 receptor (which is expressed on microglia and other immune cells) which is important in pathogen recognition and innate immune response (Raetz and Whitfield, 2002). The LPS model was initially developed to study the role of inflammation in PD and involved a single intranigral injection of (2µg LPS in 2µl volume of PBS) into either the medial forebrain bundle

(MFB), SN, or striatum (Castano et al., 1998; Herrera et al., 2000). Using this model, the authors reported that the SN was acutely sensitive to an LPS stimulus, as death was selective to DA neurons, sparing GABAergic and serotonergic neurons. Additionally, the authors observed initial, robust microglial activation in the SN (within days) that waned to near baseline levels one week later. The DA neuron loss was permanent, however and was observed up to one year after LPS injection (Herrera et al., 2000).

Gao and colleagues then developed a more progressive version of the LPS model by infusion of LPS into the nigral region (5ng/hr, 1.68μg total) over the course of two weeks. In this less acute LPS model, microglial activation was observed to initiate quickly, persist and plateau at two weeks, but remain elevated for an additional 8 weeks after infusion onset. The authors observed DA neuron loss at four to six weeks following initiation of LPS infusion, culminating in an approximately 70% loss of DA neurons at 10 weeks post the onset of infusion (Gao et al., 2002).

Additionally, subtle changes to the LPS model have been used to study the role of neuroinflammation in PD revealing that prenatal exposure to LPS induces loss of neurons in postnatal mice. A single injection of LPS was intraperitoneally administered to timed-pregnant female rats at embryonic day 10.5. The pups were sacrificed at postnatal day 21 and exhibited reduced DA (29%), increased levels of TNF (101%) and cell death (27%) in the mesencephalon (Ling et al., 2002). In other studies of rats prenatally exposed to LPS, glutathione homeostasis was altered (Zhu et al., 2007).

Moreover, when a single systemic LPS injection (5mg/kg) was administered to adult mice, it led to microglial activation, increased expression of several pro-inflammatory factors (including TNF) and decreased DA neurons in the SN by 23% at 7 months after LPS injection that progressed to 47% at 10 months post LPS treatment. Importantly, these effects were observed in wild type but not TNFR1/R2$^{-/-}$ mice (Qin et al., 2007). Finally, the LPS model has recently been used in mice on the C57Bl/6 background; intrastriatal LPS injection induced a Parkinson's-like phenotype, recapitulating results observed in rat LPS models (Hunter et al., 2009).

While the LPS model does not perfectly recapitulate human PD (there is no Lewy body pathology and motor symptoms are mild) there are many advantages to the LPS model, including its progressive nature, relative to neurotoxin PD models, and its recapitulation of a ubiquitous environmental insult, as numerous disorders exhibit chronic inflammation (e.g., Chron's disease, Rheumatoid Arthritis, Metabolic Syndrome, etc.,). Additionally, the single injection LPS models may model a common PD phenotype that is secondary to brain inflammation induced by divergent triggers like post-viral encephalitis or traumatic brain injury. Furthermore, the above and other studies using the LPS rodent model of PD support a general role for inflammation in onset, progression and even causation of PD. Lastly, progressive models such as the LPS model are well suited for combination with other PD-relevant environmental factors/models and warrant future study.

"Second-hit" models of Parkinson's disease

Due to the heterogeneous etiology of PD, perhaps "second hit" models of PD will enlighten further understanding of the complicated interaction of multiple susceptibility factors in PD. As described by Sulzer and outlined above, a primary hit might be an insult that leads to neuronal stress in the SN (such as dopamine oxidation or mitochondrial dysfunction, perhaps even aging) and secondary hits may synergize with primary hits to elicit significant DA neuron loss in the SNpc (Sulzer, 2007). Candidate secondary hits might be inhibition of a protective cellular mechanism, such as loss of Parkin or stress-induced loss of UPS or ALS function. At its simplest, a multiple hit model would synergistically combine more than one potential PD gene or trigger with another trigger or environmental susceptibility.

We recently published a second hit model of inflammation-induced nigral degeneration on the background of *parkin*$^{-/-}$ mice (Frank-Cannon et al., 2008). Importantly, *parkin*$^{-/-}$ mice do not exhibit overt/spontaneous nigral degeneration, but when we induced chronic systemic inflammation via intraperitoneally administered LPS to wild type and parkin$^{-/-}$ mice over the course of three or six months, we observed selective loss of DA neurons in the SN, as determined by stereological estimates. Notably, our analysis indicated that inflammation was induced in both wild type and parkin$^{-/-}$ mice, but only parkin$^{-/-}$ mice exhibited nigral degeneration secondary to inflammation. From this study we conclude that loss of parkin function increases vulnerability of nigral DA neurons to inflammation-related degeneration.

Other groups have also examined multiple hit models for PD. The combination of LPS and the neurotoxin MPTP was found to induce synergistic dopaminergic neurotoxicity (Gao HM, Liu B, Zhang W, Hong JS, FASEB J, 2003; Byler SL, Boem GW, Karp JD, et al., Brian Res 2009). Other groups have administered MPTP to alpha-synuclein, parkin and DJ-1 transgenic mice (reviewed by (Manning-Bog and Langston, 2007)). Additionally, Boger and colleagues describe an age-related dual hit model to investigate progressive parkinsonism. The authors sought to investigate combined factors that would exacerbate the age-related inherent decline in the DA system. Therefore the authors investigated the effects of methamphetamine or MPTP in aged *Gfrα*$^{+/-}$ and wild type mice and found that the *Gfrα*$^{+/-}$ mice were more susceptible to methamphetamine and MPTP. *Gfrα* is the high affinity receptor for GDNF, and *Gfrα*$^{+/-}$ mice exhibit progressive motor deficits, and DA neurons loss in the SN, similar to *Gdnf*$^{+/-}$ mice (Boger et al., 2010). Therefore, future studies of "multiple hits" will be fundamental for better elucidation of complex interactions between genetic and environmental susceptibilities in PD and will assist in the development of better animal models in which to explore novel therapies.

CURRENT AND PROSPECTIVE THERAPIES FOR PARKINSON'S DISEASE

Although much has been learned about the potential pathological mechanisms of PD, there remains a paucity of disease modifying/curative therapies and preventative measures in PD. Pharmacologic treatment of motor symptoms remains the primary treatment for PD and has been the therapeutic approach for decades.

Current therapies for Parkinson's disease

Dopamine replacement therapy

The motor symptoms of PD exhibit as a direct result due to loss of dopamine producing neurons in the SNpc, leading to aberrant motor signaling in the striatum. Therefore, the mainstay in PD symptom treatment is dopamine replacement therapy, which has dominated PD therapeutics since the 1960's. Levodopa (L-dopa) is the precursor to dopamine and is competent to cross the BBB (dopamine is not). Thus systematic administration of L-dopa leads to its conversion to dopamine in the brain. While it can cross the BBB, L-dopa is subject to significant first-pass clearance and only approximately 1% of an orally administered dose will reach its target in the brain (Nutt and Fellman, 1984). To address this problem of bioavailability, L-dopa is administered along with a dopa decarboxylase inhibitor (DDCI) which does not cross the BBB and imparts a 10-fold improvement in L-dopa delivery to its target (Pletscher and DaPrada, 1993). Importantly, DDCIs block DA metabolism only in the periphery, as they do not cross the BBB. While it is still the most effective symptomatic therapy for PD, L-dopa is associated with adverse side effects including dyskinesia, and its effectiveness declines over time. In addition to L-dopa therapy, dopamine agonists have been developed to increase DA levels in the brain, but they possess similar limitations to L-dopa in terms of effectiveness and are while they have less impact on untoward motor complications, they are associated with other adverse side effects including psychiatric disorders (reviewed by (Grosset, 2008)).

Deep brain stimulation (DBS)

A surgical therapy for Parkinson's disease is deep brain stimulation (DBS). DBS utilizes electrical stimulation to ablate aberrant neurological activity related to parkinsonian tremor. DBS can be targeted to the thalamus or the ventral intermediate of the thalamus to reduce tremors, but the most efficacious application of DBS is to the subthalamic nucleus, which results in reduced tremor, rigidity and dyskinesia (Yu and Neimat, 2008). Multiple criteria are used to screen candidates for DBS, and preoperative L-dopa responsiveness is the best indicator of successful DBS response (Hughes et al., 1991). Contraindications to DBS include dementia, extensive brain atrophy, and co-morbid health conditions that preclude safe surgery (Yu and Neimat, 2008) so many PD patients are not candidates for DBS.

Monoamine oxidase B (MAO-B) inhibitors

Monoamine oxidase B (MAO-B) enzymatically degrades dopamine within the brain. Selective inhibitors for MAO-B thus increase DA and have been shown to improve motor symptoms in both early and late disease stages, are well tolerated and are associated with good patient compliance. Conversely, drawbacks to MAO-B inhibitors include a disappointingly mild efficacy and potential cognitive effects (Schapira et al., 2006).

Prospective therapies for Parkinson's disease

Cell replacement therapy

The prospect of cell replacement therapy potentially provides the most disease modifying potential in Parkinson's disease therapy, as it may be able to replace DA neurons and restore function to the dopamine system. One advantage to cell replacement strategies in PD relative to other CNS disorders, is the small, well-defined target area of the SNpc (reviewed by (Hedlund and Perlmann, 2009)).

Successful transplantation of fetal dopaminergic cells into animals was reported in 1979; importantly therapeutic benefit was only observed with graft placement in the striatum, presumably because the grafted cells could not extend processes far enough to terminate in the striatum if transplanted in the SN (Bjorklund and Stenevi, 1979; Perlow et al., 1979). Following this success, two open-label clinical trials were carried out in Mexico and Sweden, with both trials using embryonic ventral mesencephalon (VM) tissue transplanted into the striatum (Lindvall et al., 1989; Madrazo et al., 1988). The results of these trials were met with minimum success, but paved the way for improved techniques and provided proof-of-principal to further pursue similar trials. The results of these latter trials indicated that grafts of VM tissue could survive the host environment, and become sufficiently integrated enough to afford sustained clinical benefits (Hauser et al., 1999; Kordower et al., 1996; Piccini et al., 2000). However, the outcomes of these trials were quite variable and a complication of graft induced dyskinesias was observed (Ma et al., 2002). These confounding issues, technical hurdles of harvesting and preparing a large number of cells and ethical concerns motivated a search for alternative cell sources.

Embryonic stem cells (ESCs) likewise encounter many hurdles to widespread use, similar to embryonic tissue grafts, prompting intensive research into generating pluripotent ESC-like cells from adult somatic cells using the technology of reprogramming adult cell populations. Utilizing viral vector technology, Takahashi and Yamanaka demonstrated that ESC like cells could be derived from adult fibroblasts via over-expression of four transcription factors: Oct3/4, Sox2, c-Myc, and Klf4 (Takahashi and Yamanaka, 2006). These reprogrammed adult cells, referred to as induced pluripotent stem cells (iPS cells), exhibited several common properties with ESCs, including differentiation into distinct cell types, but lacked other important characteristics to ESCs, having a slightly divergent gene expression profile (Rodolfa and Eggan, 2006). Takahashi and colleagues used a similar approach to successfully generate iPS cells from human fibroblasts (Takahashi et al., 2007). Upon withdrawal of other factors, the majority of the cells were Tuj-1 positive and approximately 5% of the Tuj-1 positive cells were also TH positive. After transplanting 100,000-300,000 of these cells into the striatum of 6-OHDA lesioned rats, the authors observed functional recovery in four out of five rats, although they later had to modify their method of cell sorting prior to transplantation in order to avoid tumorigenesis (Wernig et al., 2008).

Of interest, a number of adult cell populations have been shown to be capable of expressing neuronal markers, including bone marrow stromal cells (BMSCs) (Bonilla et al., 2005; Bossolasco et al., 2005) skin-derived precursors (SKPs) (Amoh et al., 2005; Fernandes et al., 2004) and adipose-derived adult stromal (ADAS) cells (Safford et al., 2002; Safford et al., 2004).

Recent interest in transplantation of adult progenitor cells into PD models has expanded. Instriatal transplantation of mouse BMSCs was found to improve motor behavior deficit in 6-OHDA lesioned mice (Offen et al., 2007). Additionally, regenerative effects were observed after transplantation of neural-induced human mesenchymal stromal cells in 6-OHDA-lesioned rats (Levy et al., 2008). We recently published a study demonstrating that adipose-derived adult stromal (ADAS) cells afford dopaminergic neuroprotection in the 6-OHDA rat model of Parkinson's disease (see Appendix A). In this study, we show that while the ADAS cells do not maintain a phenotypically stable neuronal phenotype *in vivo*, they afford protection from 6-OHDA-induced dopaminergic neurotoxicity when transplanted into the rat striatum one week after 6-OHDA-lesion. The apparent mechanisms by which ADAS cells afford neuroprotection from 6-OHDA are through generation of trophic factors and modulation of inflammation.

Other potential therapies for Parkinson's disease

Mounting evidence supports a complex interaction between genetics and environment in Parkinosn's disease. Although no current PD drug therapy has proven to be disease modifying or neuroprotective, development of novel drugs guided by selective targeting of specific mediators in common pathogenic pathways in PD shows promise in this regard. Based on our studies and the data of others, putative therapeutic targets for PD include: inflammation, oxidative stress, aberrant calcium homeostasis, ER stress and

apoptosis. Therefore, potential modulation of these pathways via pharmacological agents or gene therapy may provide much needed disease modifying therapies for PD.

REFERENCES

Abou-Sleiman, P.M., Muqit, M.M., and Wood, N.W. (2006). Expanding insights of mitochondrial dysfunction in Parkinson's disease. Nat Rev Neurosci *7*, 207-219.

Aggarwal, B.B., Eessalu, T.E., and Hass, P.E. (1985). Characterization of receptors for human tumour necrosis factor and their regulation by gamma-interferon. Nature *318*, 665-667.

Aggarwal, B.B., Samanta, A., and Feldmann, M. (2000). TNF Receptors. In Cytokine Reference, J.J.a.F. Oppenheim, M., ed. (London, Academic Press), pp. pp. 1620-1632.

Aharon-Peretz, J., Rosenbaum, H., and Gershoni-Baruch, R. (2004). Mutations in the glucocerebrosidase gene and Parkinson's disease in Ashkenazi Jews. N Engl J Med *351*, 1972-1977.

Aleyasin, H., Rousseaux, M.W., Marcogliese, P.C., Hewitt, S.J., Irrcher, I., Joselin, A.P., Parsanejad, M., Kim, R.H., Rizzu, P., Callaghan, S.M.*, et al.* (2010). DJ-1 protects the nigrostriatal axis from the neurotoxin MPTP by modulation of the AKT pathway. Proc Natl Acad Sci U S A *107*, 3186-3191.

Aloisi, F. (1999). The role of microglia and astrocytes in CNS immune surveillance and immunopathology. Adv Exp Med Biol *468*, 123-133.

Aloisi, F. (2001). Immune function of microglia. Glia *36*, 165-179.

Aloisi, F., Ria, F., and Adorini, L. (2000). Regulation of T-cell responses by CNS antigen-presenting cells: different roles for microglia and astrocytes. Immunol Today *21*, 141-147.

Amoh, Y., Li, L., Katsuoka, K., Penman, S., and Hoffman, R.M. (2005). Multipotent nestin-positive, keratin-negative hair-follicle bulge stem cells can form neurons. Proc Natl Acad Sci U S A *102*, 5530-5534.

Arboleda, G., Morales, L.C., Benitez, B., and Arboleda, H. (2009). Regulation of ceramide-induced neuronal death: cell metabolism meets neurodegeneration. Brain Res Rev *59*, 333-346.

Bandopadhyay, R., Kingsbury, A.E., Cookson, M.R., Reid, A.R., Evans, I.M., Hope, A.D., Pittman, A.M., Lashley, T., Canet-Aviles, R., Miller, D.W.*, et al.* (2004). The expression of DJ-1 (PARK7) in normal human CNS and idiopathic Parkinson's disease. Brain *127*, 420-430.

Bandyopadhyay, U., and Cuervo, A.M. (2007). Chaperone-mediated autophagy in aging and neurodegeneration: lessons from alpha-synuclein. Exp Gerontol *42*, 120-128.

Beal, M.F. (2005). Mitochondria take center stage in aging and neurodegeneration. Ann Neurol *58*, 495-505.

Bedford, L., Hay, D., Paine, S., Rezvani, N., Mee, M., Lowe, J., and Mayer, R.J. (2008). Is malfunction of the ubiquitin proteasome system the primary cause of alpha-synucleinopathies and other chronic human neurodegenerative disease? Biochim Biophys Acta *1782*, 683-690.

Beilina, A., Van Der Brug, M., Ahmad, R., Kesavapany, S., Miller, D.W., Petsko, G.A., and Cookson, M.R. (2005). Mutations in PTEN-induced putative kinase 1 associated with recessive parkinsonism have differential effects on protein stability. Proc Natl Acad Sci U S A *102*, 5703-5708.

Benmoyal-Segal, L., and Soreq, H. (2006). Gene-environment interactions in sporadic Parkinson's disease. J Neurochem *97*, 1740-1755.

Berger, A.K., Cortese, G.P., Amodeo, K.D., Weihofen, A., Letai, A., and LaVoie, M.J. (2009). Parkin selectively alters the intrinsic threshold for mitochondrial cytochrome c release. Hum Mol Genet *18*, 4317-4328.

Betarbet, R., Canet-Aviles, R.M., Sherer, T.B., Mastroberardino, P.G., McLendon, C., Kim, J.H., Lund, S., Na, H.M., Taylor, G., Bence, N.F*., et al.* (2006). Intersecting pathways to neurodegeneration in Parkinson's disease: effects of the pesticide rotenone on DJ-1, alpha-synuclein, and the ubiquitin-proteasome system. Neurobiol Dis *22*, 404-420.

Betarbet, R., Sherer, T.B., and Greenamyre, J.T. (2002). Animal models of Parkinson's disease. Bioessays *24*, 308-318.

Betarbet, R., Sherer, T.B., MacKenzie, G., Garcia-Osuna, M., Panov, A.V., and Greenamyre, J.T. (2000). Chronic systemic pesticide exposure reproduces features of Parkinson's disease. Nat Neurosci *3*, 1301-1306.

Bjorklund, A., and Stenevi, U. (1979). Reconstruction of the nigrostriatal dopamine pathway by intracerebral nigral transplants. Brain Res *177*, 555-560.

Blum, D., Torch, S., Lambeng, N., Nissou, M., Benabid, A.L., Sadoul, R., and Verna, J.M. (2001). Molecular pathways involved in the neurotoxicity of 6-OHDA, dopamine and MPTP: contribution to the apoptotic theory in Parkinson's disease. Prog Neurobiol *65*, 135-172.

Boeve, B.F., Dickson, D.W., Olson, E.J., Shepard, J.W., Silber, M.H., Ferman, T.J., Ahlskog, J.E., and Benarroch, E.E. (2007). Insights into REM sleep behavior disorder pathophysiology in brainstem-predominant Lewy body disease. Sleep Med *8*, 60-64.

Boger, H.A., Granholm, A.C., McGinty, J.F., and Middaugh, L.D. (2010). A dual-hit animal model for age-related parkinsonism. Prog Neurobiol *90*, 217-229.

Bohnen, N.I., Kaufer, D.I., Ivanco, L.S., Lopresti, B., Koeppe, R.A., Davis, J.G., Mathis, C.A., Moore, R.Y., and DeKosky, S.T. (2003). Cortical cholinergic function is more severely affected in parkinsonian dementia than in Alzheimer disease: an in vivo positron emission tomographic study. Arch Neurol *60*, 1745-1748.

Boka, G., Anglade, P., Wallach, D., Javoy-Agid, F., Agid, Y., and Hirsch, E.C. (1994). Immunocytochemical analysis of tumor necrosis factor and its receptors in Parkinson's disease. Neurosci Lett *172*, 151-154.

Bonifati, V., Rizzu, P., van Baren, M.J., Schaap, O., Breedveld, G.J., Krieger, E., Dekker, M.C., Squitieri, F., Ibanez, P., Joosse, M.*, et al.* (2003). Mutations in the DJ-1 gene associated with autosomal recessive early-onset parkinsonism. Science *299*, 256-259.

Bonilla, S., Silva, A., Valdes, L., Geijo, E., Garcia-Verdugo, J.M., and Martinez, S. (2005). Functional neural stem cells derived from adult bone marrow. Neuroscience *133*, 85-95.

Bossolasco, P., Cova, L., Calzarossa, C., Rimoldi, S.G., Borsotti, C., Deliliers, G.L., Silani, V., Soligo, D., and Polli, E. (2005). Neuro-glial differentiation of human bone marrow stem cells in vitro. Exp Neurol *193*, 312-325.

Bove, J., Prou, D., Perier, C., and Przedborski, S. (2005). Toxin-induced models of Parkinson's disease. NeuroRx *2*, 484-494.

Braak, H., Del Tredici, K., Rub, U., de Vos, R.A., Jansen Steur, E.N., and Braak, E. (2003). Staging of brain pathology related to sporadic Parkinson's disease. Neurobiol Aging *24*, 197-211.

Bras, J., Singleton, A., Cookson, M.R., and Hardy, J. (2008). Emerging pathways in genetic Parkinson's disease: Potential role of ceramide metabolism in Lewy body disease. FEBS J *275*, 5767-5773.

Bredt, D.S., and Snyder, S.H. (1990). Isolation of nitric oxide synthetase, a calmodulin-requiring enzyme. Proc Natl Acad Sci U S A *87*, 682-685.

Bronstein, J., Carvey, P., Chen, H., Cory-Slechta, D., DiMonte, D., Duda, J., English, P., Goldman, S., Grate, S., Hansen, J.*, et al.* (2009). Meeting report: consensus statement-Parkinson's disease and the environment: collaborative on health and the environment and Parkinson's Action Network (CHE PAN) conference 26-28 June 2007. Environ Health Perspect *117*, 117-121.

Brown, T.P., Rumsby, P.C., Capleton, A.C., Rushton, L., and Levy, L.S. (2006). Pesticides and Parkinson's disease--is there a link? Environ Health Perspect *114*, 156-164.

Burns, R.S., Chiueh, C.C., Markey, S.P., Ebert, M.H., Jacobowitz, D.M., and Kopin, I.J. (1983). A primate model of parkinsonism: selective destruction of dopaminergic neurons in the pars compacta of the substantia nigra by N-methyl-4-phenyl-1,2,3,6-tetrahydropyridine. Proc Natl Acad Sci U S A *80*, 4546-4550.

Calabrese, V., Cornelius, C., Mancuso, C., Lentile, R., Stella, A.M., and Butterfield, D.A. (2010). Redox homeostasis and cellular stress response in aging and neurodegeneration. Methods Mol Biol *610*, 285-308.

Canet-Aviles, R.M., Wilson, M.A., Miller, D.W., Ahmad, R., McLendon, C., Bandyopadhyay, S., Baptista, M.J., Ringe, D., Petsko, G.A., and Cookson, M.R. (2004). The Parkinson's disease protein DJ-1 is neuroprotective due to cysteine-sulfinic acid-driven mitochondrial localization. Proc Natl Acad Sci U S A *101*, 9103-9108.

Carvey, P.M., Chen, E.Y., Lipton, J.W., Tong, C.W., Chang, Q.A., and Ling, Z.D. (2005). Intra-parenchymal injection of tumor necrosis factor-alpha and interleukin 1-beta produces dopamine neuron loss in the rat. J Neural Transm *112*, 601-612.

Castano, A., Herrera, A.J., Cano, J., and Machado, A. (1998). Lipopolysaccharide intranigral injection induces inflammatory reaction and damage in nigrostriatal dopaminergic system. J Neurochem *70*, 1584-1592.

Chen, B.T., Avshalumov, M.V., and Rice, M.E. (2002). Modulation of somatodendritic dopamine release by endogenous H(2)O(2): susceptibility in substantia nigra but resistance in VTA. J Neurophysiol *87*, 1155-1158.

Cherra, S.J., 3rd, Dagda, R.K., Tandon, A., and Chu, C.T. (2009). Mitochondrial autophagy as a compensatory response to PINK1 deficiency. Autophagy *5*, 1213-1214.

Cicchetti, F., Drouin-Ouellet, J., and Gross, R.E. (2009). Environmental toxins and Parkinson's disease: what have we learned from pesticide-induced animal models? Trends Pharmacol Sci *30*, 475-483.

Clark, I.E., Dodson, M.W., Jiang, C., Cao, J.H., Huh, J.R., Seol, J.H., Yoo, S.J., Hay, B.A., and Guo, M. (2006). Drosophila pink1 is required for mitochondrial function and interacts genetically with parkin. Nature *441*, 1162-1166.

Clements, C.M., McNally, R.S., Conti, B.J., Mak, T.W., and Ting, J.P. (2006). DJ-1, a cancer- and Parkinson's disease-associated protein, stabilizes the antioxidant transcriptional master regulator Nrf2. Proc Natl Acad Sci U S A *103*, 15091-15096.

Colina, C., Flores, A., Rojas, H., Acosta, A., Castillo, C., Garrido Mdel, R., Israel, A., DiPolo, R., and Benaim, G. (2005). Ceramide increase cytoplasmic Ca2+ concentration in Jurkat T cells by liberation of calcium from intracellular stores and activation of a store-operated calcium channel. Arch Biochem Biophys *436*, 333-345.

Cuervo, A.M., and Dice, J.F. (1998). Lysosomes, a meeting point of proteins, chaperones, and proteases. J Mol Med *76*, 6-12.

Cuervo, A.M., Stefanis, L., Fredenburg, R., Lansbury, P.T., and Sulzer, D. (2004). Impaired degradation of mutant alpha-synuclein by chaperone-mediated autophagy. Science *305*, 1292-1295.

Darios, F., Corti, O., Lucking, C.B., Hampe, C., Muriel, M.P., Abbas, N., Gu, W.J., Hirsch, E.C., Rooney, T., Ruberg, M*., et al.* (2003a). Parkin prevents mitochondrial swelling and cytochrome c release in mitochondria-dependent cell death. Hum Mol Genet *12*, 517-526.

Darios, F., Lambeng, N., Troadec, J.D., Michel, P.P., and Ruberg, M. (2003b). Ceramide increases mitochondrial free calcium levels via caspase 8 and Bid: role in initiation of cell death. J Neurochem *84*, 643-654.

Dauer, W., and Przedborski, S. (2003). Parkinson's disease: mechanisms and models. Neuron *39*, 889-909.

DeLong, M.R., and Wichmann, T. (2007). Circuits and circuit disorders of the basal ganglia. Arch Neurol *64*, 20-24.

Deng, H., Jankovic, J., Guo, Y., Xie, W., and Le, W. (2005). Small interfering RNA targeting the PINK1 induces apoptosis in dopaminergic cells SH-SY5Y. Biochem Biophys Res Commun *337*, 1133-1138.

Di Monte, D.A., Lavasani, M., and Manning-Bog, A.B. (2002). Environmental factors in Parkinson's disease. Neurotoxicology *23*, 487-502.

Dressler, K.A., Mathias, S., and Kolesnick, R.N. (1992). Tumor necrosis factor-alpha activates the sphingomyelin signal transduction pathway in a cell-free system. Science *255*, 1715-1718.

Dringen, R. (2005). Oxidative and antioxidative potential of brain microglial cells. Antioxid Redox Signal *7*, 1223-1233.

Elbaz, A., Grigoletto, F., Baldereschi, M., Breteler, M.M., Manubens-Bertran, J.M., Lopez-Pousa, S., Dartigues, J.F., Alperovitch, A., Tzourio, C., and Rocca, W.A. (1999). Familial aggregation of Parkinson's disease: a population-based case-control study in Europe. EUROPARKINSON Study Group. Neurology *52*, 1876-1882.

Esposito, E., Di Matteo, V., Benigno, A., Pierucci, M., Crescimanno, G., and Di Giovanni, G. (2007). Non-steroidal anti-inflammatory drugs in Parkinson's disease. Exp Neurol *205*, 295-312.

Fahn, S. (2003). Description of Parkinson's disease as a clinical syndrome. Ann N Y Acad Sci *991*, 1-14.

Farrer, M.J. (2006). Genetics of Parkinson disease: paradigm shifts and future prospects. Nat Rev Genet *7*, 306-318.

Faull, R.L., and Laverty, R. (1969). Changes in dopamine levels in the corpus striatum following lesions in the substantia nigra. Exp Neurol *23*, 332-340.

Fernandes, K.J., McKenzie, I.A., Mill, P., Smith, K.M., Akhavan, M., Barnabe-Heider, F., Biernaskie, J., Junek, A., Kobayashi, N.R., Toma, J.G.*, et al.* (2004). A dermal niche for multipotent adult skin-derived precursor cells. Nat Cell Biol *6*, 1082-1093.

Fontaine, V., Mohand-Said, S., Hanoteau, N., Fuchs, C., Pfizenmaier, K., and Eisel, U. (2002). Neurodegenerative and neuroprotective effects of tumor Necrosis factor (TNF) in retinal ischemia: opposite roles of TNF receptor 1 and TNF receptor 2. J Neurosci *22*, RC216.

Forstl, H., Burns, A., Luthert, P., Cairns, N., and Levy, R. (1993). The Lewy-body variant of Alzheimer's disease. Clinical and pathological findings. Br J Psychiatry *162*, 385-392.

Frank-Cannon, T.C., Tran, T., Ruhn, K.A., Martinez, T.N., Hong, J., Marvin, M., Hartley, M., Trevino, I., O'Brien, D.E., Casey, B.*, et al.* (2008). Parkin deficiency increases vulnerability to inflammation-related nigral degeneration. J Neurosci *28*, 10825-10834.

Friedlander, R., Jarosch, E., Urban, J., Volkwein, C., and Sommer, T. (2000). A regulatory link between ER-associated protein degradation and the unfolded-protein response. Nat Cell Biol *2*, 379-384.

Fuchs, J., Nilsson, C., Kachergus, J., Munz, M., Larsson, E.M., Schule, B., Langston, J.W., Middleton, F.A., Ross, O.A., Hulihan, M.*, et al.* (2007). Phenotypic variation in a large Swedish pedigree due to SNCA duplication and triplication. Neurology *68*, 916-922.

Funayama, M., Hasegawa, K., Kowa, H., Saito, M., Tsuji, S., and Obata, F. (2002). A new locus for Parkinson's disease (PARK8) maps to chromosome 12p11.2-q13.1. Ann Neurol *51*, 296-301.

Gan-Or, Z., Giladi, N., Rozovski, U., Shifrin, C., Rosner, S., Gurevich, T., Bar-Shira, A., and Orr-Urtreger, A. (2008). Genotype-phenotype correlations between GBA mutations and Parkinson disease risk and onset. Neurology *70*, 2277-2283.

Gandhi, S., Muqit, M.M., Stanyer, L., Healy, D.G., Abou-Sleiman, P.M., Hargreaves, I., Heales, S., Ganguly, M., Parsons, L., Lees, A.J.*, et al.* (2006). PINK1 protein in normal human brain and Parkinson's disease. Brain *129*, 1720-1731.

Gao, H.M., Jiang, J., Wilson, B., Zhang, W., Hong, J.S., and Liu, B. (2002). Microglial activation-mediated delayed and progressive degeneration of rat nigral dopaminergic neurons: relevance to Parkinson's disease. J Neurochem *81*, 1285-1297.

Gasser, T. (2009). Molecular pathogenesis of Parkinson disease: insights from genetic studies. Expert Rev Mol Med *11*, e22.

Geisler, S., Holmstrom, K.M., Skujat, D., Fiesel, F.C., Rothfuss, O.C., Kahle, P.J., and Springer, W. (2010). PINK1/Parkin-mediated mitophagy is dependent on VDAC1 and p62/SQSTM1. Nat Cell Biol *12*, 119-131.

Goldberg, M.S., Pisani, A., Haburcak, M., Vortherms, T.A., Kitada, T., Costa, C., Tong, Y., Martella, G., Tscherter, A., Martins, A.*, et al.* (2005). Nigrostriatal dopaminergic deficits and hypokinesia caused by inactivation of the familial Parkinsonism-linked gene DJ-1. Neuron *45*, 489-496.

Goni, F.M., and Alonso, A. (2006). Biophysics of sphingolipids I. Membrane properties of sphingosine, ceramides and other simple sphingolipids. Biochim Biophys Acta *1758*, 1902-1921.

Greene, J.C., Whitworth, A.J., Kuo, I., Andrews, L.A., Feany, M.B., and Pallanck, L.J. (2003). Mitochondrial pathology and apoptotic muscle degeneration in Drosophila parkin mutants. Proc Natl Acad Sci U S A *100*, 4078-4083.

Grell, M. (1995). Tumor necrosis factor (TNF) receptors in cellular signaling of soluble and membrane-expressed TNF. J Inflamm *47*, 8-17.

Grosset, D. (2008). Dopamine agonists and therapy compliance. Neurol Sci *29 Suppl 5*, S375-376.

Halliday, G., Hely, M., Reid, W., and Morris, J. (2008). The progression of pathology in longitudinally followed patients with Parkinson's disease. Acta Neuropathol *115*, 409-415.

Hannun, Y.A., and Obeid, L.M. (2008). Principles of bioactive lipid signalling: lessons from sphingolipids. Nat Rev Mol Cell Biol *9*, 139-150.

Hardy, J., Cai, H., Cookson, M.R., Gwinn-Hardy, K., and Singleton, A. (2006). Genetics of Parkinson's disease and parkinsonism. Ann Neurol *60*, 389-398.

Hardy, J., Lewis, P., Revesz, T., Lees, A., and Paisan-Ruiz, C. (2009). The genetics of Parkinson's syndromes: a critical review. Curr Opin Genet Dev *19*, 254-265.

Hattori, N., Tanaka, M., Ozawa, T., and Mizuno, Y. (1991). Immunohistochemical studies on complexes I, II, III, and IV of mitochondria in Parkinson's disease. Ann Neurol *30*, 563-571.

Hauser, R.A., Freeman, T.B., Snow, B.J., Nauert, M., Gauger, L., Kordower, J.H., and Olanow, C.W. (1999). Long-term evaluation of bilateral fetal nigral transplantation in Parkinson disease. Arch Neurol *56*, 179-187.

Healy, D.G., Abou-Sleiman, P.M., Casas, J.P., Ahmadi, K.R., Lynch, T., Gandhi, S., Muqit, M.M., Foltynie, T., Barker, R., Bhatia, K.P*., et al.* (2006). UCHL-1 is not a Parkinson's disease susceptibility gene. Ann Neurol *59*, 627-633.

Hedlund, E., and Perlmann, T. (2009). Neuronal cell replacement in Parkinson's disease. J Intern Med *266*, 358-371.

Hedrich, K., Hagenah, J., Djarmati, A., Hiller, A., Lohnau, T., Lasek, K., Grunewald, A., Hilker, R., Steinlechner, S., Boston, H*., et al.* (2006). Clinical spectrum of homozygous and heterozygous PINK1 mutations in a large German family with Parkinson disease: role of a single hit? Arch Neurol *63*, 833-838.

Heikkila, R.E., Hess, A., and Duvoisin, R.C. (1984). Dopaminergic neurotoxicity of 1-methyl-4-phenyl-1,2,5,6-tetrahydropyridine in mice. Science *224*, 1451-1453.

Herrera, A.J., Castano, A., Venero, J.L., Cano, J., and Machado, A. (2000). The single intranigral injection of LPS as a new model for studying the selective effects of inflammatory reactions on dopaminergic system. Neurobiol Dis *7*, 429-447.

Hirsch, E.C., Hunot, S., Damier, P., and Faucheux, B. (1998). Glial cells and inflammation in Parkinson's disease: a role in neurodegeneration? Ann Neurol *44*, S115-120.

Hoek, R.M., Ruuls, S.R., Murphy, C.A., Wright, G.J., Goddard, R., Zurawski, S.M., Blom, B., Homola, M.E., Streit, W.J., Brown, M.H*., et al.* (2000). Down-regulation of the macrophage lineage through interaction with OX2 (CD200). Science *290*, 1768-1771.

Holtz, W.A., Turetzky, J.M., Jong, Y.J., and O'Malley, K.L. (2006). Oxidative stress-triggered unfolded protein response is upstream of intrinsic cell death evoked by parkinsonian mimetics. J Neurochem *99*, 54-69.

Hsu, H., Huang, J., Shu, H.B., Baichwal, V., and Goeddel, D.V. (1996a). TNF-dependent recruitment of the protein kinase RIP to the TNF receptor-1 signaling complex. Immunity *4*, 387-396.

Hsu, H., Shu, H.B., Pan, M.G., and Goeddel, D.V. (1996b). TRADD-TRAF2 and TRADD-FADD interactions define two distinct TNF receptor 1 signal transduction pathways. Cell *84*, 299-308.

Hughes, A.J., Lees, A.J., and Stern, G.M. (1991). Challenge tests to predict the dopaminergic response in untreated Parkinson's disease. Neurology *41*, 1723-1725.

Hunot, S., Boissiere, F., Faucheux, B., Brugg, B., Mouatt-Prigent, A., Agid, Y., and Hirsch, E.C. (1996). Nitric oxide synthase and neuronal vulnerability in Parkinson's disease. Neuroscience *72*, 355-363.

Hunot, S., Dugas, N., Faucheux, B., Hartmann, A., Tardieu, M., Debre, P., Agid, Y., Dugas, B., and Hirsch, E.C. (1999). FcepsilonRII/CD23 is expressed in Parkinson's disease and induces, in vitro, production of nitric oxide and tumor necrosis factor-alpha in glial cells. J Neurosci *19*, 3440-3447.

Hunter, R.L., Cheng, B., Choi, D.Y., Liu, M., Liu, S., Cass, W.A., and Bing, G. (2009). Intrastriatal lipopolysaccharide injection induces parkinsonism in C57/B6 mice. J Neurosci Res *87*, 1913-1921.

Imai, Y., Soda, M., and Takahashi, R. (2000). Parkin suppresses unfolded protein stress-induced cell death through its E3 ubiquitin-protein ligase activity. J Biol Chem *275*, 35661-35664.

Ishikawa, A., and Tsuji, S. (1996). Clinical analysis of 17 patients in 12 Japanese families with autosomal-recessive type juvenile parkinsonism. Neurology *47*, 160-166.

Jang, H., Boltz, D.A., Webster, R.G., and Smeyne, R.J. (2009). Viral parkinsonism. Biochim Biophys Acta *1792*, 714-721.

Jenner, P., and Olanow, C.W. (2006). The pathogenesis of cell death in Parkinson's disease. Neurology *66*, S24-36.

Jeon, B.S., Jackson-Lewis, V., and Burke, R.E. (1995). 6-Hydroxydopamine lesion of the rat substantia nigra: time course and morphology of cell death. Neurodegeneration *4*, 131-137.

Kabuta, T., Furuta, A., Aoki, S., Furuta, K., and Wada, K. (2008). Aberrant interaction between Parkinson disease-associated mutant UCH-L1 and the lysosomal receptor for chaperone-mediated autophagy. J Biol Chem *283*, 23731-23738.

Karen, D.J., Li, W., Harp, P.R., Gillette, J.S., and Bloomquist, J.R. (2001). Striatal dopaminergic pathways as a target for the insecticides permethrin and chlorpyrifos. Neurotoxicology *22*, 811-817.

Kirik, D., Rosenblad, C., and Bjorklund, A. (1998). Characterization of behavioral and neurodegenerative changes following partial lesions of the nigrostriatal dopamine system induced by intrastriatal 6-hydroxydopamine in the rat. Exp Neurol *152*, 259-277.

Kitada, T., Asakawa, S., Hattori, N., Matsumine, H., Yamamura, Y., Minoshima, S., Yokochi, M., Mizuno, Y., and Shimizu, N. (1998). Mutations in the parkin gene cause autosomal recessive juvenile parkinsonism. Nature *392*, 605-608.

Klopfleisch, R., Werner, O., Mundt, E., Harder, T., and Teifke, J.P. (2006). Neurotropism of highly pathogenic avian influenza virus A/chicken/Indonesia/2003 (H5N1) in experimentally infected pigeons (Columbia livia f. domestica). Vet Pathol *43*, 463-470.

Kordower, J.H., Rosenstein, J.M., Collier, T.J., Burke, M.A., Chen, E.Y., Li, J.M., Martel, L., Levey, A.E., Mufson, E.J., Freeman, T.B.*, et al.* (1996). Functional fetal nigral grafts in a patient with Parkinson's disease: chemoanatomic, ultrastructural, and metabolic studies. J Comp Neurol *370*, 203-230.

Kowall, N.W., Hantraye, P., Brouillet, E., Beal, M.F., McKee, A.C., and Ferrante, R.J. (2000). MPTP induces alpha-synuclein aggregation in the substantia nigra of baboons. Neuroreport *11*, 211-213.

Kraft, A.D., McPherson, C.A., and Harry, G.J. (2009). Heterogeneity of microglia and TNF signaling as determinants for neuronal death or survival. Neurotoxicology *30*, 785-793.

Langston, J.W. (1985). MPTP neurotoxicity: an overview and characterization of phases of toxicity. Life Sci *36*, 201-206.

Langston, J.W., Ballard, P., Tetrud, J.W., and Irwin, I. (1983). Chronic Parkinsonism in humans due to a product of meperidine-analog synthesis. Science *219*, 979-980.

Langston, J.W., Forno, L.S., Tetrud, J., Reeves, A.G., Kaplan, J.A., and Karluk, D. (1999). Evidence of active nerve cell degeneration in the substantia nigra of

humans years after 1-methyl-4-phenyl-1,2,3,6-tetrahydropyridine exposure. Ann Neurol *46*, 598-605.

Le Couteur, D.G., McLean, A.J., Taylor, M.C., Woodham, B.L., and Board, P.G. (1999). Pesticides and Parkinson's disease. Biomed Pharmacother *53*, 122-130.

Lee, T.H., Huang, Q., Oikemus, S., Shank, J., Ventura, J.J., Cusson, N., Vaillancourt, R.R., Su, B., Davis, R.J., and Kelliher, M.A. (2003). The death domain kinase RIP1 is essential for tumor necrosis factor alpha signaling to p38 mitogen-activated protein kinase. Mol Cell Biol *23*, 8377-8385.

Leroy, E., Boyer, R., Auburger, G., Leube, B., Ulm, G., Mezey, E., Harta, G., Brownstein, M.J., Jonnalagada, S., Chernova, T.*, et al.* (1998). The ubiquitin pathway in Parkinson's disease. Nature *395*, 451-452.

Levy, O.A., Malagelada, C., and Greene, L.A. (2009). Cell death pathways in Parkinson's disease: proximal triggers, distal effectors, and final steps. Apoptosis *14*, 478-500.

Levy, Y.S., Bahat-Stroomza, M., Barzilay, R., Burshtein, A., Bulvik, S., Barhum, Y., Panet, H., Melamed, E., and Offen, D. (2008). Regenerative effect of neural-induced human mesenchymal stromal cells in rat models of Parkinson's disease. Cytotherapy *10*, 340-352.

Lin, M.T., and Beal, M.F. (2006). Mitochondrial dysfunction and oxidative stress in neurodegenerative diseases. Nature *443*, 787-795.

Lindvall, O., Rehncrona, S., Brundin, P., Gustavii, B., Astedt, B., Widner, H., Lindholm, T., Bjorklund, A., Leenders, K.L., Rothwell, J.C.*, et al.* (1989). Human fetal dopamine neurons grafted into the striatum in two patients with severe Parkinson's disease. A detailed account of methodology and a 6-month follow-up. Arch Neurol *46*, 615-631.

Ling, Z., Gayle, D.A., Ma, S.Y., Lipton, J.W., Tong, C.W., Hong, J.S., and Carvey, P.M. (2002). In utero bacterial endotoxin exposure causes loss of tyrosine hydroxylase neurons in the postnatal rat midbrain. Mov Disord *17*, 116-124.

Lo Bianco, C., Schneider, B.L., Bauer, M., Sajadi, A., Brice, A., Iwatsubo, T., and Aebischer, P. (2004). Lentiviral vector delivery of parkin prevents dopaminergic degeneration in an alpha-synuclein rat model of Parkinson's disease. Proc Natl Acad Sci U S A *101*, 17510-17515.

Lock, E.A., Reed, C.J., Kinsey, G.R., and Schnellmann, R.G. (2007). Caspase-dependent and -independent induction of phosphatidylserine externalization during apoptosis in human renal carcinoma Cak(1)-1 and A-498 cells. Toxicology *229*, 79-90.

Lowe, J., McDermott, H., Landon, M., Mayer, R.J., and Wilkinson, K.D. (1990). Ubiquitin carboxyl-terminal hydrolase (PGP 9.5) is selectively present in ubiquitinated inclusion bodies characteristic of human neurodegenerative diseases. J Pathol *161*, 153-160.

Luthman, J., Fredriksson, A., Sundstrom, E., Jonsson, G., and Archer, T. (1989). Selective lesion of central dopamine or noradrenaline neuron systems in the neonatal rat: motor behavior and monoamine alterations at adult stage. Behav Brain Res *33*, 267-277.

Ma, Y., Feigin, A., Dhawan, V., Fukuda, M., Shi, Q., Greene, P., Breeze, R., Fahn, S., Freed, C., and Eidelberg, D. (2002). Dyskinesia after fetal cell transplantation for parkinsonism: a PET study. Ann Neurol *52*, 628-634.

MacEwan, D.J. (2002). TNF receptor subtype signalling: differences and cellular consequences. Cell Signal *14*, 477-492.

Madrazo, I., Leon, V., Torres, C., Aguilera, M.C., Varela, G., Alvarez, F., Fraga, A., Drucker-Colin, R., Ostrosky, F., Skurovich, M.*, et al.* (1988). Transplantation of fetal substantia nigra and adrenal medulla to the caudate nucleus in two patients with Parkinson's disease. N Engl J Med *318*, 51.

Malhotra, J.D., and Kaufman, R.J. (2007). Endoplasmic reticulum stress and oxidative stress: a vicious cycle or a double-edged sword? Antioxid Redox Signal *9*, 2277-2293.

Manning-Bog, A.B., and Langston, J.W. (2007). Model fusion, the next phase in developing animal models for Parkinson's disease. Neurotox Res *11*, 219-240.

Maraganore, D.M., Lesnick, T.G., Elbaz, A., Chartier-Harlin, M.C., Gasser, T., Kruger, R., Hattori, N., Mellick, G.D., Quattrone, A., Satoh, J.*, et al.* (2004). UCHL1 is a Parkinson's disease susceptibility gene. Ann Neurol *55*, 512-521.

Marchetti, L., Klein, M., Schlett, K., Pfizenmaier, K., and Eisel, U.L. (2004). Tumor necrosis factor (TNF)-mediated neuroprotection against glutamate-induced excitotoxicity is enhanced by N-methyl-D-aspartate receptor activation. Essential role of a TNF receptor 2-mediated phosphatidylinositol 3-kinase-dependent NF-kappa B pathway. J Biol Chem *279*, 32869-32881.

Martinez-Vicente, M., and Cuervo, A.M. (2007). Autophagy and neurodegeneration: when the cleaning crew goes on strike. Lancet Neurol *6*, 352-361.

Martinez-Vicente, M., Talloczy, Z., Kaushik, S., Massey, A.C., Mazzulli, J., Mosharov, E.V., Hodara, R., Fredenburg, R., Wu, D.C., Follenzi, A.*, et al.* (2008). Dopamine-modified alpha-synuclein blocks chaperone-mediated autophagy. J Clin Invest *118*, 777-788.

Massey, A., Kiffin, R., and Cuervo, A.M. (2004). Pathophysiology of chaperone-mediated autophagy. Int J Biochem Cell Biol *36*, 2420-2434.

Massey, A.C., Kiffin, R., and Cuervo, A.M. (2006). Autophagic defects in aging: looking for an "emergency exit"? Cell Cycle *5*, 1292-1296.

Mata, I.F., Lockhart, P.J., and Farrer, M.J. (2004). Parkin genetics: one model for Parkinson's disease. Hum Mol Genet *13 Spec No 1*, R127-133.

Mathias, S., Dressler, K.A., and Kolesnick, R.N. (1991). Characterization of a ceramide-activated protein kinase: stimulation by tumor necrosis factor alpha. Proc Natl Acad Sci U S A *88*, 10009-10013.

McCoy, M.K., Martinez, T.N., Ruhn, K.A., Szymkowski, D.E., Smith, C.G., Botterman, B.R., Tansey, K.E., and Tansey, M.G. (2006). Blocking soluble tumor necrosis factor signaling with dominant-negative tumor necrosis factor inhibitor attenuates loss of dopaminergic neurons in models of Parkinson's disease. J Neurosci *26*, 9365-9375.

McCoy, M.K., and Tansey, M.G. (2008). TNF signaling inhibition in the CNS: implications for normal brain function and neurodegenerative disease. J Neuroinflammation *5*, 45.

McGuire, S.O., Ling, Z.D., Lipton, J.W., Sortwell, C.E., Collier, T.J., and Carvey, P.M. (2001). Tumor necrosis factor alpha is toxic to embryonic mesencephalic dopamine neurons. Exp Neurol *169*, 219-230.

McNaught, K.S., Belizaire, R., Jenner, P., Olanow, C.W., and Isacson, O. (2002). Selective loss of 20S proteasome alpha-subunits in the substantia nigra pars compacta in Parkinson's disease. Neurosci Lett *326*, 155-158.

McNaught, K.S., and Jenner, P. (2001). Proteasomal function is impaired in substantia nigra in Parkinson's disease. Neurosci Lett *297*, 191-194.

Micheau, O., and Tschopp, J. (2003). Induction of TNF receptor I-mediated apoptosis via two sequential signaling complexes. Cell *114*, 181-190.

Miller, D.W., Ahmad, R., Hague, S., Baptista, M.J., Canet-Aviles, R., McLendon, C., Carter, D.M., Zhu, P.P., Stadler, J., Chandran, J.*, et al.* (2003). L166P mutant DJ-1, causative for recessive Parkinson's disease, is degraded through the ubiquitin-proteasome system. J Biol Chem *278*, 36588-36595.

Miller, K.R., and Streit, W.J. (2007). The effects of aging, injury and disease on microglial function: a case for cellular senescence. Neuron Glia Biol *3*, 245-253.

Mogi, M., Harada, M., Riederer, P., Narabayashi, H., Fujita, K., and Nagatsu, T. (1994). Tumor necrosis factor-alpha (TNF-alpha) increases both in the brain and in the cerebrospinal fluid from parkinsonian patients. Neurosci Lett *165*, 208-210.

Mogi, M., Togari, A., Kondo, T., Mizuno, Y., Komure, O., Kuno, S., Ichinose, H., and Nagatsu, T. (2000). Caspase activities and tumor necrosis factor receptor R1 (p55) level are elevated in the substantia nigra from parkinsonian brain. J Neural Transm *107*, 335-341.

Mogi, M., Togari, A., Tanaka, K., Ogawa, N., Ichinose, H., and Nagatsu, T. (1999). Increase in level of tumor necrosis factor (TNF)-alpha in 6-hydroxydopamine-lesioned striatum in rats without influence of systemic L-DOPA on the TNF-alpha induction. Neurosci Lett *268*, 101-104.

Monahan, A.J., Warren, M., and Carvey, P.M. (2008). Neuroinflammation and peripheral immune infiltration in Parkinson's disease: an autoimmune hypothesis. Cell Transplant *17*, 363-372.

Morales, A., Lee, H., Goni, F.M., Kolesnick, R., and Fernandez-Checa, J.C. (2007). Sphingolipids and cell death. Apoptosis *12*, 923-939.

Muller, T., Blum-Degen, D., Przuntek, H., and Kuhn, W. (1998). Interleukin-6 levels in cerebrospinal fluid inversely correlate to severity of Parkinson's disease. Acta Neurol Scand *98*, 142-144.

Muqit, M.M., Abou-Sleiman, P.M., Saurin, A.T., Harvey, K., Gandhi, S., Deas, E., Eaton, S., Payne Smith, M.D., Venner, K., Matilla, A.*, et al.* (2006). Altered cleavage and localization of PINK1 to aggresomes in the presence of proteasomal stress. J Neurochem *98*, 156-169.

Nagakubo, D., Taira, T., Kitaura, H., Ikeda, M., Tamai, K., Iguchi-Ariga, S.M., and Ariga, H. (1997). DJ-1, a novel oncogene which transforms mouse NIH3T3 cells in cooperation with ras. Biochem Biophys Res Commun *231*, 509-513.

Nagatsu, T., and Sawada, M. (2005). Inflammatory process in Parkinson's disease: role for cytokines. Curr Pharm Des *11*, 999-1016.

Narendra, D., Tanaka, A., Suen, D.F., and Youle, R.J. (2009). Parkin-induced mitophagy in the pathogenesis of Parkinson disease. Autophagy *5*, 706-708.

Ng, C.H., Mok, S.Z., Koh, C., Ouyang, X., Fivaz, M.L., Tan, E.K., Dawson, V.L., Dawson, T.M., Yu, F., and Lim, K.L. (2009). Parkin protects against LRRK2 G2019S mutant-induced dopaminergic neurodegeneration in Drosophila. J Neurosci *29*, 11257-11262.

Nishimura, M., Mizuta, I., Mizuta, E., Yamasaki, S., Ohta, M., Kaji, R., and Kuno, S. (2001). Tumor necrosis factor gene polymorphisms in patients with sporadic Parkinson's disease. Neurosci Lett *311*, 1-4.

Nunomura, A., Honda, K., Takeda, A., Hirai, K., Zhu, X., Smith, M.A., and Perry, G. (2006). Oxidative damage to RNA in neurodegenerative diseases. J Biomed Biotechnol *2006*, 82323.

Nutt, J.G., and Fellman, J.H. (1984). Pharmacokinetics of levodopa. Clin Neuropharmacol *7*, 35-49.

Offen, D., Barhum, Y., Levy, Y.S., Burshtein, A., Panet, H., Cherlow, T., and Melamed, E. (2007). Intrastriatal transplantation of mouse bone marrow-derived stem cells improves motor behavior in a mouse model of Parkinson's disease. J Neural Transm Suppl, 133-143.

Ogata, A., Tashiro, K., Nukuzuma, S., Nagashima, K., and Hall, W.W. (1997). A rat model of Parkinson's disease induced by Japanese encephalitis virus. J Neurovirol *3*, 141-147.

Ohsumi, Y., and Mizushima, N. (2004). Two ubiquitin-like conjugation systems essential for autophagy. Semin Cell Dev Biol *15*, 231-236.

Paisan-Ruiz, C., Jain, S., Evans, E.W., Gilks, W.P., Simon, J., van der Brug, M., Lopez de Munain, A., Aparicio, S., Gil, A.M., Khan, N.*, et al.* (2004). Cloning of the gene containing mutations that cause PARK8-linked Parkinson's disease. Neuron *44*, 595-600.

Paisan-Ruiz, C., Washecka, N., Nath, P., Singleton, A.B., and Corder, E.H. (2009). Parkinson's disease and low frequency alleles found together throughout LRRK2. Ann Hum Genet *73*, 391-403.

Park, A., and Stacy, M. (2009). Non-motor symptoms in Parkinson's disease. J Neurol *256 Suppl 3*, 293-298.

Perlow, M.J., Freed, W.J., Hoffer, B.J., Seiger, A., Olson, L., and Wyatt, R.J. (1979). Brain grafts reduce motor abnormalities produced by destruction of nigrostriatal dopamine system. Science *204*, 643-647.

Petit, A., Kawarai, T., Paitel, E., Sanjo, N., Maj, M., Scheid, M., Chen, F., Gu, Y., Hasegawa, H., Salehi-Rad, S.*, et al.* (2005). Wild-type PINK1 prevents basal and induced neuronal apoptosis, a protective effect abrogated by Parkinson disease-related mutations. J Biol Chem *280*, 34025-34032.

Piccini, P., Lindvall, O., Bjorklund, A., Brundin, P., Hagell, P., Ceravolo, R., Oertel, W., Quinn, N., Samuel, M., Rehncrona, S.*, et al.* (2000). Delayed recovery of movement-related cortical function in Parkinson's disease after striatal dopaminergic grafts. Ann Neurol *48*, 689-695.

Pletscher, A., and DaPrada, M. (1993). Pharmacotherapy of Parkinson's disease: research from 1960 to 1991. Acta Neurol Scand Suppl *146*, 26-31.

Polymeropoulos, M.H., Lavedan, C., Leroy, E., Ide, S.E., Dehejia, A., Dutra, A., Pike, B., Root, H., Rubenstein, J., Boyer, R.*, et al.* (1997). Mutation in the alpha-synuclein gene identified in families with Parkinson's disease. Science *276*, 2045-2047.

Pramstaller, P.P., Schlossmacher, M.G., Jacques, T.S., Scaravilli, F., Eskelson, C., Pepivani, I., Hedrich, K., Adel, S., Gonzales-McNeal, M., Hilker, R.*, et al.* (2005). Lewy body Parkinson's disease in a large pedigree with 77 Parkin mutation carriers. Ann Neurol *58*, 411-422.

Qin, L., Wu, X., Block, M.L., Liu, Y., Breese, G.R., Hong, J.S., Knapp, D.J., and Crews, F.T. (2007). Systemic LPS causes chronic neuroinflammation and progressive neurodegeneration. Glia *55*, 453-462.

Raetz, C.R., and Whitfield, C. (2002). Lipopolysaccharide endotoxins. Annu Rev Biochem *71*, 635-700.

Rao, P., Hsu, K.C., and Chao, M.V. (1995). Upregulation of NF-kappa B-dependent gene expression mediated by the p75 tumor necrosis factor receptor. J Interferon Cytokine Res *15*, 171-177.

Ravikumar, B., Vacher, C., Berger, Z., Davies, J.E., Luo, S., Oroz, L.G., Scaravilli, F., Easton, D.F., Duden, R., O'Kane, C.J.*, et al.* (2004). Inhibition of mTOR induces autophagy and reduces toxicity of polyglutamine expansions in fly and mouse models of Huntington disease. Nat Genet *36*, 585-595.

Rideout, H.J., Lang-Rollin, I.C., Savalle, M., and Stefanis, L. (2005). Dopaminergic neurons in rat ventral midbrain cultures undergo selective apoptosis and form inclusions, but do not up-regulate iHSP70, following proteasomal inhibition. J Neurochem *93*, 1304-1313.

Rodolfa, K.T., and Eggan, K. (2006). A transcriptional logic for nuclear reprogramming. Cell *126*, 652-655.

Rossetti, Z.L., Sotgiu, A., Sharp, D.E., Hadjiconstantinou, M., and Neff, N.H. (1988). 1-Methyl-4-phenyl-1,2,3,6-tetrahydropyridine (MPTP) and free radicals in vitro. Biochem Pharmacol *37*, 4573-4574.

Rothe, M., Pan, M.G., Henzel, W.J., Ayres, T.M., and Goeddel, D.V. (1995). The TNFR2-TRAF signaling complex contains two novel proteins related to baculoviral inhibitor of apoptosis proteins. Cell *83*, 1243-1252.

Rothe, M., Wong, S.C., Henzel, W.J., and Goeddel, D.V. (1994). A novel family of putative signal transducers associated with the cytoplasmic domain of the 75 kDa tumor necrosis factor receptor. Cell *78*, 681-692.

Rousselet, E., Callebert, J., Parain, K., Joubert, C., Hunot, S., Hartmann, A., Jacque, C., Perez-Diaz, F., Cohen-Salmon, C., Launay, J.M.*, et al.* (2002). Role of TNF-alpha receptors in mice intoxicated with the parkinsonian toxin MPTP. Exp Neurol *177*, 183-192.

Rubinsztein, D.C. (2006). The roles of intracellular protein-degradation pathways in neurodegeneration. Nature *443*, 780-786.

Ruuls, S.R., Hoek, R.M., Ngo, V.N., McNeil, T., Lucian, L.A., Janatpour, M.J., Korner, H., Scheerens, H., Hessel, E.M., Cyster, J.G.*, et al.* (2001). Membrane-bound TNF supports secondary lymphoid organ structure but is subservient to secreted TNF in driving autoimmune inflammation. Immunity *15*, 533-543.

Ryu, E.J., Harding, H.P., Angelastro, J.M., Vitolo, O.V., Ron, D., and Greene, L.A. (2002). Endoplasmic reticulum stress and the unfolded protein response in cellular models of Parkinson's disease. J Neurosci *22*, 10690-10698.

Safford, K.M., Hicok, K.C., Safford, S.D., Halvorsen, Y.D., Wilkison, W.O., Gimble, J.M., and Rice, H.E. (2002). Neurogenic differentiation of murine and human adipose-derived stromal cells. Biochem Biophys Res Commun *294*, 371-379.

Safford, K.M., Safford, S.D., Gimble, J.M., Shetty, A.K., and Rice, H.E. (2004). Characterization of neuronal/glial differentiation of murine adipose-derived adult stromal cells. Exp Neurol *187*, 319-328.

Sawada, M., Imamura, K., and Nagatsu, T. (2006). Role of cytokines in inflammatory process in Parkinson's disease. J Neural Transm Suppl, 373-381.

Sawada, M., Sawada, H., and Nagatsu, T. (2008). Effects of aging on neuroprotective and neurotoxic properties of microglia in neurodegenerative diseases. Neurodegener Dis *5*, 254-256.

Schapira, A.H., Bezard, E., Brotchie, J., Calon, F., Collingridge, G.L., Ferger, B., Hengerer, B., Hirsch, E., Jenner, P., Le Novere, N.*, et al.* (2006). Novel pharmacological targets for the treatment of Parkinson's disease. Nat Rev Drug Discov *5*, 845-854.

Schneider-Brachert, W., Tchikov, V., Neumeyer, J., Jakob, M., Winoto-Morbach, S., Held-Feindt, J., Heinrich, M., Merkel, O., Ehrenschwender, M., Adam, D.*, et al.* (2004). Compartmentalization of TNF receptor 1 signaling: internalized TNF receptosomes as death signaling vesicles. Immunity *21*, 415-428.

Schober, A. (2004a). Classic toxin-induced animal models of Parkinson's disease: 6-OHDA and MPTP. Cell Tissue Res.

Schober, A. (2004b). Classic toxin-induced animal models of Parkinson's disease: 6-OHDA and MPTP. Cell Tissue Res *318*, 215-224.

Schwab, C., Klegeris, A., and McGeer, P.L. (2009). Inflammation in transgenic mouse models of neurodegenerative disorders. Biochim Biophys Acta.

Setsuie, R., Wang, Y.L., Mochizuki, H., Osaka, H., Hayakawa, H., Ichihara, N., Li, H., Furuta, A., Sano, Y., Sun, Y.J.*, et al.* (2007). Dopaminergic neuronal loss in transgenic mice expressing the Parkinson's disease-associated UCH-L1 I93M mutant. Neurochem Int *50*, 119-129.

Shimura, H., Hattori, N., Kubo, S., Mizuno, Y., Asakawa, S., Minoshima, S., Shimizu, N., Iwai, K., Chiba, T., Tanaka, K.*, et al.* (2000). Familial Parkinson disease gene product, parkin, is a ubiquitin-protein ligase. Nat Genet *25*, 302-305.

Singleton, A.B., Farrer, M., Johnson, J., Singleton, A., Hague, S., Kachergus, J., Hulihan, M., Peuralinna, T., Dutra, A., Nussbaum, R.*, et al.* (2003). alpha-Synuclein locus triplication causes Parkinson's disease. Science *302*, 841.

Smith, W.W., Jiang, H., Pei, Z., Tanaka, Y., Morita, H., Sawa, A., Dawson, V.L., Dawson, T.M., and Ross, C.A. (2005a). Endoplasmic reticulum stress and mitochondrial cell death pathways mediate A53T mutant alpha-synuclein-induced toxicity. Hum Mol Genet *14*, 3801-3811.

Smith, W.W., Pei, Z., Jiang, H., Moore, D.J., Liang, Y., West, A.B., Dawson, V.L., Dawson, T.M., and Ross, C.A. (2005b). Leucine-rich repeat kinase 2 (LRRK2)

interacts with parkin, and mutant LRRK2 induces neuronal degeneration. Proc Natl Acad Sci U S A *102*, 18676-18681.

Spillantini, M.G., Schmidt, M.L., Lee, V.M., Trojanowski, J.Q., Jakes, R., and Goedert, M. (1997). Alpha-synuclein in Lewy bodies. Nature *388*, 839-840.

Sriram, K., Matheson, J.M., Benkovic, S.A., Miller, D.B., Luster, M.I., and O'Callaghan, J.P. (2002). Mice deficient in TNF receptors are protected against dopaminergic neurotoxicity: implications for Parkinson's disease. Faseb J *16*, 1474-1476.

Stayner, C., Iglesias, D.M., Goodyer, P.R., Ellis, L., Germino, G., Zhou, J., and Eccles, M.R. (2006). Pax2 gene dosage influences cystogenesis in autosomal dominant polycystic kidney disease. Hum Mol Genet *15*, 3520-3528.

Streit, W.J., Mrak, R.E., and Griffin, W.S. (2004). Microglia and neuroinflammation: a pathological perspective. J Neuroinflammation *1*, 14.

Sulzer, D. (2007). Multiple hit hypotheses for dopamine neuron loss in Parkinson's disease. Trends Neurosci *30*, 244-250.

Taira, T., Saito, Y., Niki, T., Iguchi-Ariga, S.M., Takahashi, K., and Ariga, H. (2004). DJ-1 has a role in antioxidative stress to prevent cell death. EMBO Rep *5*, 213-218.

Takahashi, K., Tanabe, K., Ohnuki, M., Narita, M., Ichisaka, T., Tomoda, K., and Yamanaka, S. (2007). Induction of pluripotent stem cells from adult human fibroblasts by defined factors. Cell *131*, 861-872.

Takahashi, K., and Yamanaka, S. (2006). Induction of pluripotent stem cells from mouse embryonic and adult fibroblast cultures by defined factors. Cell *126*, 663-676.

Tanner, C.M., Goldman, S.M., Lyons, K.E., Aston, D.A., Tetrud, J.W., Welsh, M.D., Langston, J.W., and Koller, W.C. (2001). Essential tremor in twins: an assessment of genetic vs environmental determinants of etiology. Neurology *57*, 1389-1391.

Tansey, M.G., Frank-Cannon, T.C., McCoy, M.K., Lee, J.K., Martinez, T.N., McAlpine, F.E., Ruhn, K.A., and Tran, T.A. (2008). Neuroinflammation in Parkinson's disease: is there sufficient evidence for mechanism-based interventional therapy? Front Biosci *13*, 709-717.

Tansey, M.G., McCoy, M.K., and Frank-Cannon, T.C. (2007). Neuroinflammatory mechanisms in Parkinson's disease: potential environmental triggers, pathways, and targets for early therapeutic intervention. Exp Neurol *208*, 1-25.

Tao, X., and Tong, L. (2003). Crystal structure of human DJ-1, a protein associated with early onset Parkinson's disease. J Biol Chem *278*, 31372-31379.

Tartaglia, L.A., Rothe, M., Hu, Y.F., and Goeddel, D.V. (1993). Tumor necrosis factor's cytotoxic activity is signaled by the p55 TNF receptor. Cell *73*, 213-216.

Teismann, P., Tieu, K., Cohen, O., Choi, D.K., Wu, D.C., Marks, D., Vila, M., Jackson-Lewis, V., and Przedborski, S. (2003). Pathogenic role of glial cells in Parkinson's disease. Mov Disord *18*, 121-129.

Thomas, K.J., and Cookson, M.R. (2009). The role of PTEN-induced kinase 1 in mitochondrial dysfunction and dynamics. Int J Biochem Cell Biol *41*, 2025-2035.

Valente, E.M., Abou-Sleiman, P.M., Caputo, V., Muqit, M.M., Harvey, K., Gispert, S., Ali, Z., Del Turco, D., Bentivoglio, A.R., Healy, D.G.*, et al.* (2004). Hereditary

early-onset Parkinson's disease caused by mutations in PINK1. Science *304*, 1158-1160.

von Bernhardi, R., Tichauer, J.E., and Eugenin, J. (2010). Aging-dependent changes of microglial cells and their relevance for neurodegenerative disorders. J Neurochem *112*, 1099-1114.

Wahner, A.D., Sinsheimer, J.S., Bronstein, J.M., and Ritz, B. (2007). Inflammatory cytokine gene polymorphisms and increased risk of Parkinson disease. Arch Neurol *64*, 836-840.

Wang, C., Ko, H.S., Thomas, B., Tsang, F., Chew, K.C., Tay, S.P., Ho, M.W., Lim, T.M., Soong, T.W., Pletnikova, O.*, et al.* (2005). Stress-induced alterations in parkin solubility promote parkin aggregation and compromise parkin's protective function. Hum Mol Genet *14*, 3885-3897.

Wang, H.Q., and Takahashi, R. (2007). Expanding insights on the involvement of endoplasmic reticulum stress in Parkinson's disease. Antioxid Redox Signal *9*, 553-561.

Wang, L., Xie, C., Greggio, E., Parisiadou, L., Shim, H., Sun, L., Chandran, J., Lin, X., Lai, C., Yang, W.J.*, et al.* (2008). The chaperone activity of heat shock protein 90 is critical for maintaining the stability of leucine-rich repeat kinase 2. J Neurosci *28*, 3384-3391.

Wernig, M., Zhao, J.P., Pruszak, J., Hedlund, E., Fu, D., Soldner, F., Broccoli, V., Constantine-Paton, M., Isacson, O., and Jaenisch, R. (2008). Neurons derived from reprogrammed fibroblasts functionally integrate into the fetal brain and improve symptoms of rats with Parkinson's disease. Proc Natl Acad Sci U S A *105*, 5856-5861.

Whitton, P.S. (2007). Inflammation as a causative factor in the aetiology of Parkinson's disease. Br J Pharmacol *150*, 963-976.

Whitworth, A.J., and Pallanck, L.J. (2009). The PINK1/Parkin pathway: a mitochondrial quality control system? J Bioenerg Biomembr *41*, 499-503.

Wilkinson, K.D., Deshpande, S., and Larsen, C.N. (1992). Comparisons of neuronal (PGP 9.5) and non-neuronal ubiquitin C-terminal hydrolases. Biochem Soc Trans *20*, 631-637.

Wilkinson, K.D., Lee, K.M., Deshpande, S., Duerksen-Hughes, P., Boss, J.M., and Pohl, J. (1989). The neuron-specific protein PGP 9.5 is a ubiquitin carboxyl-terminal hydrolase. Science *246*, 670-673.

Willaime, S., Vanhoutte, P., Caboche, J., Lemaigre-Dubreuil, Y., Mariani, J., and Brugg, B. (2001). Ceramide-induced apoptosis in cortical neurons is mediated by an increase in p38 phosphorylation and not by the decrease in ERK phosphorylation. Eur J Neurosci *13*, 2037-2046.

Winston, B.W., Lange-Carter, C.A., Gardner, A.M., Johnson, G.L., and Riches, D.W. (1995). Tumor necrosis factor alpha rapidly activates the mitogen-activated protein kinase (MAPK) cascade in a MAPK kinase kinase-dependent, c-Raf-1-independent fashion in mouse macrophages. Proc Natl Acad Sci U S A *92*, 1614-1618.

Wu, D.C., Teismann, P., Tieu, K., Vila, M., Jackson-Lewis, V., Ischiropoulos, H., and Przedborski, S. (2003). NADPH oxidase mediates oxidative stress in the 1-

methyl-4-phenyl-1,2,3,6-tetrahydropyridine model of Parkinson's disease. Proc Natl Acad Sci U S A *100*, 6145-6150.

Wu, F., Poon, W.S., Lu, G., Wang, A., Meng, H., Feng, L., Li, Z., and Liu, S. (2009). Alpha-synuclein knockdown attenuates MPP+ induced mitochondrial dysfunction of SH-SY5Y cells. Brain Res *1292*, 173-179.

Wyss-Coray, T., and Mucke, L. (2002). Inflammation in neurodegenerative disease--a double-edged sword. Neuron *35*, 419-432.

Xiromerisiou, G., Dardiotis, E., Tsimourtou, V., Kountra, P.M., Paterakis, K.N., Kapsalaki, E.Z., Fountas, K.N., and Hadjigeorgiou, G.M. (2010). Genetic basis of Parkinson disease. Neurosurg Focus *28*, E7.

Xue, X., Piao, J.H., Nakajima, A., Sakon-Komazawa, S., Kojima, Y., Mori, K., Yagita, H., Okumura, K., Harding, H., and Nakano, H. (2005). Tumor necrosis factor alpha (TNFalpha) induces the unfolded protein response (UPR) in a reactive oxygen species (ROS)-dependent fashion, and the UPR counteracts ROS accumulation by TNFalpha. J Biol Chem *280*, 33917-33925.

Yamaguchi, H., and Shen, J. (2007). Absence of dopaminergic neuronal degeneration and oxidative damage in aged DJ-1-deficient mice. Mol Neurodegener *2*, 10.

Yamamuro, A., Yoshioka, Y., Ogita, K., and Maeda, S. (2006). Involvement of endoplasmic reticulum stress on the cell death induced by 6-hydroxydopamine in human neuroblastoma SH-SY5Y cells. Neurochem Res *31*, 657-664.

Youdim, M.B., Grunblatt, E., Levites, Y., Maor, G., and Mandel, S. (2002). Early and late molecular events in neurodegeneration and neuroprotection in Parkinson's disease MPTP model as assessed by cDNA microarray; the role of iron. Neurotox Res *4*, 679-689.

Yu, H., and Neimat, J.S. (2008). The treatment of movement disorders by deep brain stimulation. Neurotherapeutics *5*, 26-36.

Zhang, L., Shimoji, M., Thomas, B., Moore, D.J., Yu, S.W., Marupudi, N.I., Torp, R., Torgner, I.A., Ottersen, O.P., Dawson, T.M.*, et al.* (2005). Mitochondrial localization of the Parkinson's disease related protein DJ-1: implications for pathogenesis. Hum Mol Genet *14*, 2063-2073.

Zhou, W., and Freed, C.R. (2005). DJ-1 up-regulates glutathione synthesis during oxidative stress and inhibits A53T alpha-synuclein toxicity. J Biol Chem *280*, 43150-43158.

Zhu, Y., Carvey, P.M., and Ling, Z. (2007). Altered glutathione homeostasis in animals prenatally exposed to lipopolysaccharide. Neurochem Int *50*, 671-680.

CHAPTER TWO

BLOCKING SOLUBLE TUMOR NECROSIS FACTOR SIGNALING WITH DOMINANT-NEGATIVE TUMOR NECROSIS FACTOR INHIBITOR ATTENUATES LOSS OF DOPAMINERGIC NEURONS IN MODELS OF PARKINSON'S DISEASE

The contents of this chapter were previously published:

McCoy MK, Martinez TN, Ruhn KA, Szymkowski DE, Smith CG, Botterman BR, Tansey KE, Tansey MG (2006) Blocking soluble tumor necrosis factor signaling with dominant-negative tumor necrosis factor inhibitor attenuates loss of dopaminergic neurons in models of Parkinson's disease. J Neurosci 26:9365-9375.

ABSTRACT

The mechanisms that trigger or contribute to loss of dopaminergic (DA) neurons in Parkinson's Disease (PD) remain unclear and controversial. Elevated levels of Tumor Necrosis Factor (TNF) in cerebrospinal fluid and postmortem brains of PD patients and animal models of PD implicate this pro-inflammatory cytokine in the pathophysiology of the disease; but a role for TNF in mediating loss of DA neurons in PD has not been clearly demonstrated. Here we report that neutralization of soluble Tumor Necrosis Factor (solTNF) *in vivo* with the engineered dominant-negative TNF (DN-TNF) compound XENP345 reduced by 50% the retrograde nigral degeneration induced by a striatal injection of the oxidative neurotoxin 6-hydroxydopamine (6-OHDA). XENP345 was neuroprotective only when infused into the nigra, not the striatum. XENP345/6-OHDA rats displayed attenuated amphetamine-induced rotational behavior indicating

preservation of striatal dopamine levels. Similar protective effects were observed with chronic *in vivo* co-infusion of XENP345 with bacterial lipopolysaccharide (LPS) into the substantia nigra, confirming a role for solTNF-dependent neuroinflammation in nigral degeneration. In embryonic rat midbrain neuron/glia cell cultures exposed to LPS even delayed administration of XENP345 prevented selective degeneration of DA neurons despite sustained microglia activation and secretion of solTNF. XENP345 also attenuated 6-OHDA-induced DA neuron toxicity *in vitro*. Collectively, our data demonstrate a role for TNF *in vitro* and *in vivo* in two models of PD, and raise the possibility that delaying the progressive degeneration of the nigrostriatal pathway in humans is therapeutically feasible with agents capable of blocking solTNF in early stages of PD.

INTRODUCTION

Parkinson's Disease (PD) is the second most prevalent neurodegenerative disease in the U.S. with a 5% incidence in individuals over 65 (Moore, 2005). Its clinical manifestations result from selective loss of dopaminergic (DA) neurons in the ventral mesencephalon substantia nigra pars compacta (SNpc), with a resulting decrease in striatal dopamine. The critical molecular mediators and mechanisms that elicit death of nigral DA neurons have yet to be identified; but a wealth of studies implicate microglia and inflammatory processes in the pathophysiology of PD (Hald and Lotharius, 2005; Hirsch et al., 2005; McGeer et al., 1988; Vawter et al., 1996), and chronic use of non-steroidal anti-inflammatory drugs can lower risks for development of PD in humans by 46% (Chen et al., 2003).

Cerebrospinal fluid and post-mortem brains of PD patients display elevated levels of the pro-inflammatory cytokine Tumor Necrosis Factor (TNF) as do animals treated with the dopaminergic neurotoxins 1-methyl-4-phenyl-1,2,3,6-tetrahydropyridine (MPTP) and 6-hydroxydopamine (6-OHDA) used to model nigral degeneration in non-human primates and rodents (Barcia et al., 2005; Boka et al., 1994; Hunot et al., 1999; Mogi et al., 2000; Nagatsu and Sawada, 2005; Sriram et al., 2002). TNF is synthesized as a type II transmembrane trimeric protein cleaved by the TACE metalloprotease to a soluble form (Aggarwal, 2000; MacEwan, 2002); both forms are biologically active, but their relative roles in mediating DA neuron survival are unknown. Soluble TNF (solTNF) transduces inflammatory stimuli through the canonical death receptor TNFR1 (Tartaglia et al., 1993) which is highly expressed in nigrostriatal DA neurons rendering them vulnerable to TNF-induced toxicity (Aloe and Fiore, 1997; Carvey et al., 2005; Gayle et al., 2002; McGuire et al., 2001). The role of transmembrane (tm) TNF is less well understood, but it can mediate pro-survival effects through TNFR2 in cortical (Marchetti et al., 2004) and hippocampal (Heldmann et al., 2005) neurons.

We hypothesized that solTNF is a major mediator of neurotoxic mechanisms contributing to degeneration of nigral DA neurons *in vivo*; therefore blocking its activity should yield neuroprotection in animal models of PD. To test our hypothesis, we employed TNF variants engineered to disrupt binding of the solTNF trimer to its receptors by forming dominant-negative TNF (DN-TNF) heterotrimers that eliminate solTNF homotrimers, and thus inhibit its signaling (Steed et al., 2003). To elucidate the cellular mechanisms by which TNF promotes DA neuron death, we utilized rat

embryonic ventral mesencephalon (EVM) neuron/glia cultures. Our findings that solTNF, but not tmTNF, contributes significantly to the progressive loss of DA neurons induced by bacterial and oxidative neurotoxins in cellular and animal models of PD are relevant for the design and testing of novel therapeutic strategies for PD.

MATERIALS AND METHODS

Materials

Rabbit anti-tyrosine hydroxylase (TH), guinea pig anti-GABA, mouse anti-MAP2b, and mouse anti-NeuN (neuron specific nuclear protein) antibodies were obtained from Chemicon (Temecula, CA). Mouse anti-rat complement 3 receptor (C3R) antibody Ox-42 was obtained from Santa Cruz and mouse anti-CD45 antibody was obtained from Serotec. FITC conjugated isolectin-B4, LPS (from *E. coli* 0111:B4, Lot # 114K4133 1.5 x 10^6 EU/mg), 6-OHDA, poly D-lysine, and D-amphetamine were obtained from Sigma-Aldrich Corporation (St. Louis, MO) and a single stock of each was used for all experiments. Cell culture reagents were purchased from Invitrogen Corporation (Carlsbad, CA). Laminin was obtained from BD Biosciences (San Jose, CA). The recombinant dominant-negative TNF XENP345, a PEGylated version of the TNF variant A145R/I97T (Steed et al., 2003), was bacterially produced and formulated by Xencor Inc. to contain less than 0.1 EU/mL. Recombinant mouse TNF was obtained from R&D systems (Minneapolis, MN). Antibodies for quantitative TNF ELISA were obtained from Biosource/Invitrogen Corporation (Carlsbad, CA). Osmotic pumps were purchased from

Alzet Corporation (Cupertino, CA), cannulae and tubing from Plastics One Corp. (Roanoke, VA). All other reagents were obtained from Sigma-Aldrich.

Animal studies

Young adult and timed-pregnant Sprague Dawley SASCO and CDF/Fischer 344 rats were purchased from Charles River Laboratories (Wilmington, MA) and housed in pathogen-free climate-controlled facilities at the Animal Resources Center at The University of Texas Southwestern Medical Center. All animal studies were approved by the Institutional Animal Care and Use Committee at UT Southwestern Medical Center at Dallas.

Methods

Intrastriatal 6-OHDA injection and XENP345 infusions

Young adult female Sprague Dawley SASCO rats (200-225 g) (n= 6 per group, total of 30) were anesthetized with halothane (2%) and placed in a stereotaxic frame. Their eyes were protected with ophthalmic ointment and body temperature was monitored with a rectal probe and maintained with radiant heat under feedback control. The scalp was prepped under sterile conditions and the skull exposed and incised. We chose a previously published regimen of 6-OHDA to induce a mild-to-moderate retrograde lesion in the nigrostriatal pathway (Kirik et al., 1998). Burr holes were drilled to permit unilateral injection of 20 μg 6-OHDA (4 μL of 5 μg/μL) at a rate of 1 μL/min into the striatum on the right hemisphere (stereotaxic coordinates: anteroposterior (AP): -1.2 mm

from bregma, mediolateral (ML): -3.9 mm; and dorsoventral (DV): -5 mm below surface of dura) (Paxinos et al., 1985). Cannulae (gauge 28, Plastics One) connected via polyethylene tubing to a subcutaneously implanted osmotic minipump (Alzet 2002) preloaded with vehicle (sterile saline) or the treatment agent XENP345 (0.08 mg/kg/day) were then stereotaxically inserted through the burr holes into the same site as the 6-OHDA lesion or into an area just above the substantia nigra pars compacta (stereotaxic coordinates from bregma: AP: -4.8mm from bregma, ML: -1.7 mm, and DV: -8 mm below surface of dura) through another burr hole and were left in position for 3 weeks. Cannulae were secured to the skull with surgical glue (Plastics One).

Intranigral LPS or LPS/XENP345 infusions

The low-dose chronic LPS infusion model published previously was used to induce selective, delayed and progressive death of DA neurons *in vivo* (Gao et al., 2002). LPS (5 ng/hr) was unilaterally infused for 2 wk via a 28 gauge cannula into the SNpc (coordinates from bregma AP: -4.8 mm, ML: -1.7 mm, and DV: -8 mm) (Paxinos et al., 1985) of young adult male CDF rats (200-240g) (n=6 per group, 3 sets of experiments) under the same surgical procedures described above. Cannulae were connected via polyethylene tubing (Plastics One) to a subcutaneously implanted osmotic minipump (Alzet 2002) preloaded with the treatment agent. Vehicle (sterile saline) or XENP345 (0.03 mg/kg/day, representing a 5:1 ratio XENP345:LPS) was preloaded along with LPS into the pump and infused for 2 wk (n= 6 per group).

Rotational behavior analyses

At 1, 2 and 3 wk post 6-OHDA lesion, amphetamine-induced rotational behavior was monitored in a glass cylinder (diameter 24.5 cm). Animals received 2.5 mg/kg D-amphetamine prepared in sterile saline (Sigma, St. Louis) i.p. and 60 min after the injection, rotational asymmetry was monitored for 20 min. Rotation towards the lesion (ipsilateral) was scored as positive and net rotational asymmetry score was expressed as full body turns/min.

Perfusion and tissue processing for histology

At 3 wk post 6-OHDA lesion or 8 wk post start of LPS infusion, animals were deeply anesthetized with pentobarbital and intracardially perfused with 300 ml of heparinized PBS pH 7.4, followed by 500 mL of 4% paraformaldehyde in PBS, pH 7.4. Brains were postfixed for 24 h in the same solution and cryoprotected in 20% sucrose in PBS for 18-24 hr. Coronal sections (40 μm-thickness) were cut through the striatum and substantia nigra pars compacta on a Leica cryostat and mounted on glass slides (SuperFrost Plus, Fisher) for immunohistological analyses and stereological estimate of DA neuron number in a fixed 200 μm area in SNpc.

Immunohistochemistry of brain sections

Sections on glass slides were fixed for an additional 15 min in 4% paraformaldehyde, followed by a PBS rinse (pH 7.4). Mounted sections (rather than the standard free-floating sections) were chosen because of the critical importance of maintaining right/left hemisphere orientation at all times for comparison of ipsilateral (lesioned) to contralateral (unlesioned) side in both the unilateral 6-OHDA and LPS lesion models. Even with the

use of standard brain notching techniques, re-establishing correct R/L orientation prior to mounting free-floating sections would have been technically laborious and prone to error. Prior to immunohistochemistry, sections were incubated in 0.2 M glycine (pH 7.4) for 30 min to minimize tissue autofluorescence due to the aldehyde fixative. Pilot experiments were conducted using 40µm brain sections from control (unlesioned rats) to establish the optimum blocking and antibody incubation times to completely penetrate the section all the way to the 2µm bottom guard zone used in the stereological analyses of neuron number. Sections were permeabilized for 35 min in TBS containing 0.3% Triton-X-100 and 1% normal goat serum (NGS), followed by blocking for 60 min in TBS containing 1% NGS. Primary antibody incubations were done for 48 hr at 4˚C in TBS containing 0.1% Triton-X-100 and 1% NGS. Secondary antibody incubations were performed for 4 hr at room temperature in the same dilution buffer. Nuclei were counterstained with 0.5 µg/mL Hoechst 33258. Sections were coverslipped with aqueous-based mounting media with anti-fade reagent (Biomeda).

Nigral DA neuron counts

StereoInvestigator analyses software (Micro Bright Field Inc., Williston, VT) was used to perform unbiased stereological counts of NeuN/TH-immunoreactive (NeuN/TH-IR) cell bodies in the SNpc using the optical fractionator method (West et al., 1991) for both LPS and 6-OHDA studies. The boundary of SNpc was defined according to previous anatomical demarcation in the rat (German and Manaye, 1993). For analysis, the treatment of the various brain sections was blinded to the observer. Cells were counted with a 100X oil immersion objective (1.3 NA) using an Olympus BX61 microscope.

Random and systematic counting frames (each 50 x 50 x 5 μm with 2 μm upper and lower guard zones) on cryosections (40μm serial sections placed 4 per slide) obtained from over 40 rats through the extent of SNpc (from AP:-3.3mm to -5.3mm behind bregma) were sampled using a 20 μ optical dissector. We systematically chose to stain every other slide for TH/NeuN and the intervening slide for complement 3 receptor (OX-42 antibody). A dopaminergic neuron was defined as a NeuN/TH immunoreactive cell body with a clearly visible unstained nucleus. For estimating total neuron number (number of NeuN-positive cell), a cell was defined as a soma with a nucleolus in focus within the counting frame. A microglial cell was defined as an OX-42-immunoreactive cell with processes (ramified) or without processes (ameboid-shape).

Striatal TH fiber density

Fluorescence intensity of TH-immunoreactive fibers above a fixed threshold using entorhinal cortex for background subtraction was used to estimate striatal TH-fiber density. For this analysis, cryosections were taken from a region 1mm anterior to olfactory bulb, through the CPu complex, an ending 1mm posterior to SNpc. Areas at the striatal lesion site (AP: -1.2 mm from bregma, ML: -3.9 mm from midline in right hemisphere; and DV: -5 mm below surface of dura (Paxinos et al., 1985) devoid of cellular material were excluded from the analysis and normalized for comparison to the contralateral (unlesioned side) according to standard practice.

Mesencephalic mixed neuron/glia cultures

Primary rat ventral mesencephalic neuron/glia cultures were prepared by modification of a published protocol (Liu et al., 2000). Briefly, ventral mesencephalic tissues were dissected from embryonic day 14 Fischer 344 rats into Hank's balanced salt solution and dissociated with mild, mechanical trituration in cold media containing 10% FBS. Following trituration, cells were centrifuged at 1200g for 5 minutes, resuspended in 3-4mL complete media for counting, and plated into 4-well chamber slides (two 25 μL-microislands per well at a density of 7.5×10^5 cells/mL) according to the method of (Takeshima et al., 1994) or in 96 well culture plates (100 μL/well at a density of 2×10^5 cells/mL) precoated with poly-D-lysine (0.1 mg/mL) and laminin (20 μg/mL) in DMEM/F12 supplemented with 10% fetal bovine serum (FBS), 1 g/L glucose, 2 mM L-glutamine, 1 mM sodium pyruvate, 100 μM nonessential amino acids, 50 U/mL penicillin, 50 μg/mL streptomycin, and 10 ng/mL basic Fibroblast Growth Factor (bFGF). Cultures were maintained at 37°C in a humidified atmosphere of 5% CO_2/95% air. Cultures were replenished two days later with 0.5 mL/well (chamber slides) or 0.1 mL/well (96-well plate) fresh media lacking bFGF and were used for treatment five days later. For treatment (in duplicate or triplicate) with LPS or 6-OHDA the cultures were maintained in 0.5 mL/well (chamber slides) or 0.1 mL/well (96-well plate) of media supplemented with 2.5% FBS and lacking bFGF.

Quantitative TNF ELISA

The culture medium was collected after treatment of cells with LPS or 6-OHDA as indicated. The quantities of TNF-α were measured with a mouse TNF-α ELISA kit from Biosource/Invitrogen Corporation (Carlsbad, CA) as per manufacturer's instructions.

Immunocytochemistry in EVM cultures

Neurons were stained with anti-MAP2b antibody to detect both somata and neurites or anti-Neuronal antigen N (NeuN) antibody to detect somata only. Dopaminergic neurons were detected with anti-TH antibody. GABAergic neurons were identified with anti-GABA antibody. Microglia were detected with an anti-complement type 3 receptor antibody (OX-42), CD-45 antibody, or FITC-BS-1 isolectin B4. Cells were fixed with 4% paraformaldehyde, permeabilized with TBS containing 3% gelatin from cold water fish skin (Sigma), 1% BSA, and 0.3% Triton-X-100, blocked with TBS containing 3% gelatin from cold water fish skin and 1% BSA. Primary antibody incubations were done for 2 hr at room temperature with primary antibodies diluted in TBS containing antibody diluent (TBS containing 3% gelatin from cold water fish skin, 1% BSA, and 0.1% Triton-X-100) anti-MAP2b, 1:400; anti-Neu-N, 1:400; anti-TH, 1:250; OX-42 1:60; anti-CD-45 1:600; anti-GABA 1:1500; FITC-BS-1 isolectin B4, 0.1 mg/mL; or anti-GFAP, 1:1000). Except for FITC-isolectin B4, the bound primary antibody was visualized on an Olympus BX61 fluorescence microscope after incubation with an appropriate Molecular Probes/Invitrogen Alexa-conjugated secondary antibody (1:1000). Images were captured with either a CoolSnap CCD ES monochromatic or CF color camera and analyzed with MetaMorph software (Universal Imaging Systems, West Chester, PA). For analysis, the treatment of the various cultures was blinded to the observer. Counts were performed in a minimum of 6 fields per well per treatment condition. To obtain average cell counts per well, 20X images were taken throughout the extent of each microisland. The number of

cells per 20X field were averaged and multiplied by the number of fields to obtain the averages per well. Each experimental set was repeated two to three times.

Uptake assays for tritiated DA or GABA

Neurotransmitter uptake was measured using published protocols (Gao et al., 2002). Mixed neuron/glia cultures grown in 96 well plates were washed two times with 100 μL Krebs-Ringer buffer (containing 16 mM sodium phosphate, 119 mM sodium chloride, 4.7 mM potassium chloride, 1.8 mM calcium chloride, 1.2 mM magnesium sulfate, 1.3 mM EDTA, and 5.6 mM glucose; pH 7.4). For DA and GABA uptake the cultures were incubated for 15 min at 37°C with 50 μL of 10 μM [^{3}H]DA (30 Ci/mmol) and 50 μM [^{3}H]GABA (90 Ci/mmol) in Krebs-Ringer buffer, respectively. After being washed three times with 100 μL ice-cold Krebs-Ringer buffer, the cells were collected in 50 μL 1N sodium hydroxide, combined with 1 mL scintillation fluid, and radioactivity was counted with a liquid scintillation counter. Nonspecific uptake was determined in parallel wells that received both the tritiated tracer and 10 μM mazindol (to block specific DA uptake) or 2 mM β-alanine (to block glial GABA uptake) (Mabjeesh et al., 1992). Each treatment condition was done in triplicate. Each experimental set was repeated at least two times.

Statistical Analyses

Differences among means were analyzed using one-way analysis of variance (ANOVA). When ANOVA showed significant differences, comparisons between means were tested by the Tukey-Kramer Multiple Comparisons post-hoc test. Left versus right differences

from the same animals were analyzed using two-tailed paired Student's t test. Values expressed are the group mean ± SEM. For culture experiments, differences in TH cell number among the different groups were analyzed by ANOVA followed by the Newman-Keuls post-hoc test for *p* values significance. Values expressed are the mean ± SD; **p* values < 0.05, ***p* values < 0.01, *** *p* values < 0.001.

RESULTS

Blocking soluble TNF signaling *in vivo* provides protection to dopamine neurons from 6-OHDA-induced death and attenuates rotational behavior.

TNF levels have been reported to increase in striatum and substantia nigra of 6-OHDA injected rats (Mogi et al., 1999). To determine if TNF signaling has a critical role in nigral DA neuron loss *in vivo*, we tested the ability of a DN-TNF inhibitor (XENP345), to provide neuroprotection from 6-OHDA-induced lesions in rats. 6-OHDA neurotoxin rodent models of PD are characterized by increased oxidative stress and striatal terminal die-back followed by loss of DA cell bodies within the SN (Przedborski, 2005; Przedborski and Ischiropoulos, 2005). In these experiments a lesion was induced by a unilateral intrastriatal pre-terminal injection of 6-OHDA into rats (Kirik et al., 1998). Immediately following administration of 6-OHDA (or vehicle) into the striatum, a cannula connected to an osmotic minipump preloaded with XENP345 or saline was stereotaxically positioned into the ipsilateral striatum or ipsilateral SNpc. Using unbiased design-based stereology, the number of TH/MAP2b-positive soma was estimated within

the substantia nigra 3 weeks after administration of the 6-OHDA striatal injection. We found that administration of the XENP345 into the nigra rescued about 50% of the nigral DA neurons from 6-OHDA-induced death and prevented the decrease in TH fiber density (**Figure 2.1 a-e**). In contrast, no statistically significant difference was detected between groups when rats were implanted with striatal pumps pre-loaded with vehicle or XENP345. These findings suggest that the key TNF signaling events mediating neurodegeneration of DA neurons occur at the cell somata in the region of the substantia nigra pars compacta.

As a physiological measure of 6-OHDA-induced striatal DA depletion, we tested amphetamine-induced rotational behavior weekly for 3 weeks following the 6-OHDA lesion. We found that the protection of DA neurons in SNpc achieved with nigral delivery of XENP345 correlated with attenuated ipsiversive circling behavior induced by D-amphetamine (2.5 mg/kg i.p.) (**Figure 2.1 f**). These data suggest that TNF may be crucial for the progressive phase of 6-OHDA induced dopaminergic cell loss, and support a role for TNF signaling in DA neuron loss induced by oxidative neurotoxins.

Blocking soluble TNF signaling *in vivo* during a chronic neuroinflammatory stimulus protects DA neurons from death.

Since inhibition of solTNF signaling was efficacious in protecting DA neurons from death induced by the oxidative neurotoxin 6-OHDA, we hypothesized that a TNF-dependent neuroinflammatory or neurotoxic component is required for robust killing of

nigral DA neurons. To test this, we used a purely neuroinflammatory *in vivo* model of PD and compared survival of TH+ neurons in SNpc after infusion of LPS alone or LPS and XENP345. Previous studies by (Gao et al., 2002) reported that a 2-week supra-nigral infusion of LPS (5 ng/hr) increased the number of complement 3 receptor (Ox-42 antibody) immunoreactive microglia with rod-like morphology as early as three days after the start of LPS infusion which subsequently peaked at 2 weeks and persisted for 8 weeks. This microglial activation profile is consistent with this being a chronic neuroinflammatory model. We have confirmed the persistent presence of Ox-42-positive ameboid-shaped microglia at week 8 after a 2-week chronic LPS infusion into SNpc (**Figure 2.2**). We reasoned that since TNF is a potent activator of microglia (Aggarwal, 2000; Hinkerohe et al., 2005) and a known mediator of LPS action in peripheral tissues (Beutler, 2005), chronic infusion of DN-TNFs to block solTNF signaling during an inflammatory stimulus might prevent TH-positive cell loss in the SNpc of LPS-infused rats. Unbiased stereological measurements of TH-IR/NeuN neuron soma and fluorescence densitometry of TH-positive fiber density revealed that co-infusion of XENP345 (70 ng/hr) with LPS (5 ng/hr) for 14 days into rat substantia nigra rescued about 50% of the LPS-induced nigrostriatal degeneration measured 8 weeks after the start of infusion (**Figure 2.2c**). In addition, rescue of DA neurons was accompanied by a decreased number of C3R-immunoreactive (IR) microglia in SNpc (**Figure 2.2a**). Infusion of XENP345 alone, chronically or in a single bolus (20 µg), did not induce microgliosis and was not associated with any tissue damage (**Figure 2.2a**) consistent with a lack of TNF-like agonistic activity of DN-TNFs published in previous work (Steed et al., 2003). Together with our findings in the 6-OHDA model, these data indicate that

solTNF signaling is a primary mediator of DA neuron loss *in vivo* induced by either neuroinflammatory agents or oxidative neurotoxins, and that inhibition of solTNF can reduce neuroinflammation and subsequent neurodegeneration.

Soluble TNF is a critical mediator of LPS- and 6-OHDA-induced dopaminergic neuron loss *in vitro*.

Given the fact that *in vivo* administration of TNF inhibitors selective for solTNF signaling rescued only 50% of DA neurons from LPS- or 6-OHDA-induced degeneration, it was important to determine whether additional rescue of DA neurons could be achieved by also blocking signaling by tmTNF. To determine the contribution from each form of the ligand to the death of DA neurons in LPS-treated embryonic (E14) rat ventral mesencephalon (EVM) cultures, we compared sparing of TH neurons by two inhibitors with different modes of action. We first measured LPS-induced solTNF production in the media by quantitative ELISA to determine the doses of TNF inhibitors needed to block TNF signaling during an LPS stimulus. We found that treatment of EVM cultures with 10 ng/mL LPS led to rapid release of solTNF which peaked at around 500pg/mL (**Figure 2.3 a**). In pilot experiments, we next confirmed the lack of toxic effects of DN-TNFs alone (XENP345 and others) or etanercept alone and determined the optimal dosing of TNF inhibitors necessary to completely block DA neuron death induced by exogenous solTNF (data not shown). Next we treated EVM neuron/glia cultures with 10 ng/mL LPS (Figure 2.3 b) in the presence of either XENP345 (3 or 200 ng/mL) to block solTNF exclusively (Steed et al., 2003) or with the soluble decoy receptor etanercept (Fc-TNFR2, 100

ng/mL) to block both solTNF and tmTNF signaling (Agnholt et al., 2003; Mitoma et al., 2005; Scallon et al., 2002). Four days after LPS stimulation, DA neuron survival was measured by counting tyrosine hydroxylase and MAP-2b co-labeled neurons (**Figure 2.3 b**). We found that blocking TNF signaling with either inhibitor during an LPS stimulus attenuated LPS-induced loss of DA neuron number (**Figure 2.3 c**) and their neurites (**Figure 2.3 b**) equally well and by approximately half, indicating that the gradual loss of TH positive neurons induced by LPS treatment and dependent on TNF signaling is mediated exclusively by solTNF, since blocking of both tmTNF and solTNF with etanercept yielded no further rescue compared to XENP345. The slight differences between XENP345 and etanercept in ability to rescue DA neurons *in vitro* may be related to pharmacokinetic differences since the doses of both TNF inhibitors used *in vitro* were in excess of that needed to neutralize the amount of secreted solTNF measured by ELISA in response to the LPS challenge (Steed et al., 2003). Given that solTNF and tmTNF bind TNFR1 and TNFR2 with different affinities, and the normal biological role of TNF and its receptors in the nigrostriatal pathway is not at all clear, our findings that XENP345 significantly attenuated the death of DA neurons induced by 6-OHDA or LPS *in vivo* support a direct and neurotoxic role for solTNF as the relevant microglial-derived neuroinflammatory mediator of nigral degeneration. To determine if the rescued neurons retained function, we measured tritiated dopamine uptake in these cultures. Rescue of TH positive neurons correlated with increased DA uptake (**Figure 2.3 d**). Nonspecific dopamine uptake was measured (and subtracted as background) in these cultures using the specific dopamine transport inhibitor mazindol. In agreement with published

observations (Gao et al., 2002), GABAergic neurons were unaffected by LPS treatment (**Figure 2.3 e**).

Based on our findings that *in vivo* inhibition of TNF signaling with XENP345 attenuated 6-OHDA-induced loss of DA neurons and decreased amphetamine-induced ipsiversive circling behavior, we predicted that 6-OHDA-induced neurotoxicity of DA neurons and rescue by XENP345 could also be reproduced *in vitro,* thus allowing identification of the TNF-dependent mechanisms mediating 6-OHDA-induced neurodegeneration. Therefore, we treated EVM cultures with a concentration range of 6-OHDA (5-100 μM) for 24 hr and assayed solTNF release as well as DA uptake in the surviving DA neurons at 4 days after initial exposure to 6-OHDA in the presence or absence of TNF inhibitors. We found that 20 μM 6-OHDA induced neurotoxicity and death in DA neurons comparable to 10 ng/mL LPS (**Figure 2.4**) under the same media conditions and time-course of the experiment. Lower concentrations of 6-OHDA did not induce significant DA neuron death (due to the protective effects of 2.5% FBS) and higher concentrations induced excessive death of both DA and GABA neurons (data not shown). As expected, the level of solTNF release (~ 50pg/mL) evoked by this amount of 6-OHDA (**Figure 2.4 a**) was lower than that evoked by the inflammogen LPS; however, the robust rescue with XENP345 and etanercept indicated this level of solTNF was sufficient to account for a significant fraction (>50%) of the 6-OHDA-induced neurotoxicity (**Figure 2.4 c**). Together, these studies are the first to demonstrate a critical role for solTNF signaling in mediating death of DA neurons *in vitro* and *in vivo* induced by two different neurotoxins used in rodent models of PD.

TNF-dependent potentiation of microglia activation is not the primary mechanism mediating DA neuron degeneration.

Given that microglial-derived oxidative stress has been proposed to be involved in the loss of DA neurons in the LPS model (Gao et al., 2002), we investigated the extent to which rescue of DA neurons by inhibition of TNF signaling correlated with attenuated microglia activation (measured using antibodies against the microglial markers complement 3 receptor, isolectin B4, and CD45). EVM cultures were treated with LPS (10 ng/mL) or with LPS plus XENP345 (200 ng/mL co-added, 100 ng/mL re-added every 24 hr) to measure microglia activation at 12, 24, 48 and 96 hr after addition of LPS. Blocking solTNF signaling with XENP345 did not completely abolish LPS-induced microglia activation, but had its greatest attenuating effects in the early time points (<24 hr) after LPS stimulation (**Figure 2.5 a,b**). In a control experiment, we found that robust induction of microglia activation by 4 ng/mL solTNF can be inhibited completely by a ratio of XENP345 to solTNF of 50:1 (**Figure 2.5 c**), suggesting that partial inhibition of LPS-induced microglia activation with XENP345 was not due to incomplete neutralization of solTNF. From these data we conclude that solTNF is required for potentiation of early LPS-induced microglia activation, yet only partially mediates the neuroinflammatory response elicited by LPS. Therefore, we conclude that the critical microglial-derived mediator responsible for DA neuron loss is solTNF, and attenuation of TNF-mediated effects is sufficient to provide significant rescue of DA neurons, since neuroprotection can be achieved with XENP345 despite persistent microglia activation.

Experiments to identify the cellular and signaling mechanisms mediated by TNF and necessary for 6-OHDA-induced neurodegeneration are in progress. It is well known that the action of the oxidative neurotoxin 6-OHDA involves formation of 6-OHDA-paraquinones and leads to glutathione (GSH)-depletion of mitochondria (Przedborski, 2005; Przedborski and Ischiropoulos, 2005). Such depletion sensitizes many cells to the toxic actions of TNF via mitochondrial targeting of glycosphingolipids and potentiation of intracellular ROS accumulation (Garcia-Ruiz et al., 2003; Garcia-Ruiz et al., 1997). Therefore, these TNF-dependent signaling cascades may have important roles in triggering the death of DA neurons and are therefore under investigation.

Delayed inhibition of TNF signaling also rescues DA neurons from LPS-induced death.

We reasoned that since low-dose LPS exposure results in delayed, progressive and selective death of DA neurons, delayed administration of XENP345 after an LPS insult may still be capable of preventing a substantial portion of DA neuron loss. In these experiments, we treated EVM cultures with LPS and then added XENP345 after delays of 12-72 hr (and re-adding inhibitor every 24 hr). Microglial activation and DA neuron survival were measured 4 days after the initial LPS stimulus. XENP345 was still efficacious in attenuating DA neuron loss (**Figure 2.6 a**) even when added several days after the LPS insult. Despite the ability of delayed addition of XENP345 to block DA neuron loss, we found that delayed inhibition of TNF was unable to block sustained LPS-induced microglia activation, as measured by three immunocytochemical markers of

microglial activation (**Figure 2.6 b**). These data suggest that direct neurotoxicity of microglial-derived TNF on DA neurons, presumably through TNFR1 receptors present on these neurons (McGuire et al., 2001), is likely to be the primary mechanism eliciting delayed death of DA neurons in LPS-treated neuron/glia cultures. However, a second mechanism by which TNF may mediate dopaminergic cell loss is by perpetuating microglial-derived extracellular ROS and RNS production, thus increasing oxidative stress on DA neurons and leading to degeneration**.**

DISCUSSION

This is the first comprehensive study to employ TNF-selective pharmacological inhibitors in two different models of PD to investigate the direct contribution of the two biologically active forms of TNF in mediating degeneration and death of DA neurons in wild-type rodents. Although it has been known that PD brains possess increased gliosis, cytokine levels, and reactive oxygen and nitrogen species, the mechanisms underlying neuroinflammation-mediated DA neuron death have remained unclear. We hypothesized that, independent of the trigger that elicits its production or its cellular source, solTNF might act at two different cellular sites: directly on DA neurons to exert neurotoxic effects and indirectly on microglia to potentiate microglial-derived oxidative stress, and that activation of both routes results in progressive degeneration and loss of DA neurons. Our results that nigral delivery of the soluble TNF inhibitor XENP345 attenuated loss of rat DA neurons, independent of whether this loss is induced by the bacteriotoxin LPS or

by the oxidative neurotoxin 6-OHDA, confirm that solTNF is a critical neuroinflammatory mediator involved in the neurodegenerative actions of both LPS and 6-OHDA *in vivo*. The neuroprotective effects of the immunosuppressant FK-506 in 6-OHDA lesioned rats has been ascribed to inhibition of microglial-derived TNF (Mogi et al., 1999) since FK-506 has been shown to inhibit secretion of pro-inflammatory cytokines by macrophages (Keicho et al., 1991). Mechanistically, our results further indicate that TNF drives late signaling events in eliciting neurotoxicity and triggering DA neuron death, since delayed (up to 72 hr) addition of XENP345 in a 4-day low-dose LPS treatment regimen can markedly attenuate DA neuron death independent of persistent microglial activation as assessed by several microglial markers. Given that clinical diagnosis of PD in humans occurs only after a significant loss (>80%) of nigral DA neuron has occurred, most interventions are in essence 'delayed' so these findings have potential clinical relevance; there may be a therapeutic window during which inhibition of TNF signaling could slow disease progression. Consistent with a role of TNF in the pathophysiology of PD, a cohort of Early Onset PD patients in Japan have an increased frequency of a polymorphic allele (-1031C) in the TNF gene promoter that results in higher transcriptional activity (Nishimura et al., 2001) and causes them to be high TNF producers. A recent prospective study indicating that regular use of non-steroidal anti-inflammatory drugs (NSAIDs) lowers the risk of developing PD by 46% (Chen et al., 2003) also supports a role for chronic inflammation in triggering or accelerating development of PD in humans. There are several possible explanations as to why co-infusion of a solTNF inhibitor into the SNpc did not completely abrogate loss of nigral NeuN/TH-positive neurons. We can rule out a role for tmTNF since etanercept did not

yield greater neuroprotection compared to XENP345 *in vitro*. We can also rule out technical problems with immunohistological detection as a reason for the apparent partial rescue. Specifically, the protocol used for staining and detection of NeuN/TH-positive cells throughout the extent of the 40μm sections required for performing stereology using a 20μm optical fractionator was optimized in pilot experiments to ensure complete penetration of primary and secondary antibodies to the bottom guard zone used in the stereology parameters (See Methods). One possible explanation for the partial rescue that is currently being investigated relates to the potential for limited diffusion of XENP345 away from the delivery site during the chronic infusion. Second, in these experiments, TNF signaling was blocked only in a small region of SNpc for 2 weeks coincident with the chronic LPS infusion or immediately following induction of the intrastriatal 6-OHDA lesion; yet the cascade of neurotoxic and neuroinflammatory events that occurs in these less acute animal models of PD is known to extend beyond the 2-week interval during which TNF signaling was pharmacologically inhibited (Sanchez-Pernaute et al., 2004). Third, partial neuroprotection may be indicative of a component of DA neuron loss that is TNF-independent and might involve the action of other pro-inflammatory cytokines, including IL-1β or IL-6 (Allan and Rothwell, 2001; Hald and Lotharius, 2005; Nagatsu and Sawada, 2005). To distinguish between these three possibilities, experiments are in progress to determine whether longer or continuous solTNF signaling inhibition across a larger volume of SNpc affords greater neuroprotection to nigral DA neurons, and whether continuous TNF signaling inhibition blocks the progressive phase of 6-OHDA-induced DA neuron death shown to be attenuated by selective COX-2 inhibition (Sanchez-Pernaute et al., 2004) Nonetheless, a reduction of nigral DA neuron death by 50% with

delivery of DN-TNF biologics into the CNS would have a significant and positive impact on delaying progression of DA neuron loss in individuals with PD should these *in vivo* results in animal models be realized in clinical trials. Because of their size (~51 kD trimers), XENP345 would not be expected to cross the blood-brain barrier but this possibility is being investigated. Clinically, anti-TNF biologics presently used to treat patients with rheumatoid arthritis (etanercept and infliximab) have been linked to increases in demyelinating disease due to their ability to block tmTNF function (Arnett et al., 2001; Sukal et al., 2006); therefore, a tmTNF-sparing TNF inhibitor for use in PD may be a safer therapy in humans.

To date, evaluation of the role of TNF in mediating DA neuron death in mature animals has only been investigated using acute MPTP intoxication in mice deficient in TNF pathway genes (Ferger et al., 2004; Leng et al., 2005; Rousselet et al., 2002; Sriram et al., 2002), and in wild-type mice treated with thalidomide (Ferger et al., 2004), which inhibits synthesis of TNF and many other genes. However, although these early studies implicated TNF signaling in DA neuron death, these null mice are not ideal models in which to critically address the direct role of TNF in nigral degeneration in adult animals. The brain proteome of TNFR double knockout mice indicates significant changes in expression of numerous genes (Pejovic et al., 2004), including the redox sensor DJ-1 which itself has been shown to be important in protecting DA neurons from oxidative stress (Goldberg et al., 2005; Kim et al., 2005). Moreover, mice that develop without any TNF signaling display arrested dendritic cell development and blunted systemic inflammatory responses (Pasparakis et al., 1996; Ritter et al., 2003; Sriram et al., 2006).

Our own unpublished observations that treatment of neuron/glia cultures from TNF KO mice with TNF or LPS elicits blunted microglial activation and attenuated DA neuron death compared to treatment of cultures from WT mice.

Therefore, it is impossible to discern whether resistance (or lack thereof) to MPTP injury in adult mice that developed without TNF signaling is a direct result of no TNF production (i.e., in TNF KO) or inability to bind TNF (i.e., in TNFR1/R2 double knockout) and/or from modifications in the function of downstream TNF-dependent targets (including microglia). In summary, although studies with genetic models suggested that pharmacological manipulation of the TNF pathway may offer neuroprotection, our study is the first to directly demonstrate the feasibility and efficacy of this approach; plus the translational value of studies in adult rats with the soluble TNF-selective pharmacological inhibitor XENP345 makes our direct approach biologically and clinically relevant to humans.

Our data demonstrate that solTNF significantly contributes to toxicity and degeneration of DA neurons, independent of the trigger that elicits its production. This raises the exciting possibility that anti-TNF therapy specifically targeted against solTNF may be an effective treatment for prevention or attenuation of PD progression without interfering with important tmTNF functions such as maintenance of immune function and resistance to infection (Olleros et al., 2005). Lastly, we posit that our findings regarding a critical role of TNF signaling in death of DA neurons may be applicable to other neurodegenerative diseases in which the role of neuroinflammation is being intensely

investigated both as a contributing factor, and as the basis for development of new vaccination therapies. For example, levels of TNF were found to be elevated in entorhinal cortex coincident with the earliest appearance of pathology (Janelsins et al., 2005) in a triple transgenic Alzheimer's Disease mouse model harboring mutations in presenilin 1, amyloid precursor protein, and tau (Oddo et al., 2003), and chronic exposure to systemic LPS accelerated development of amyloid and tau pathology in these mice (Kitazawa et al., 2005). Given its role as a major effector of LPS action, we hypothesize that TNF is a key mediator of LPS-enhanced neuropathology in these mice perhaps by promoting mitochondrial dysfunction and activation of apoptotic death cascades. Investigations of TNF-dependent neuroinflammatory mechanisms that exacerbate neuropathology and hasten neuron loss may unveil opportunities for development of new anti-inflammatory therapeutics to treat human neurodegenerative diseases like PD and Alzheimer's disease.

FIGURES

Figure 2.1

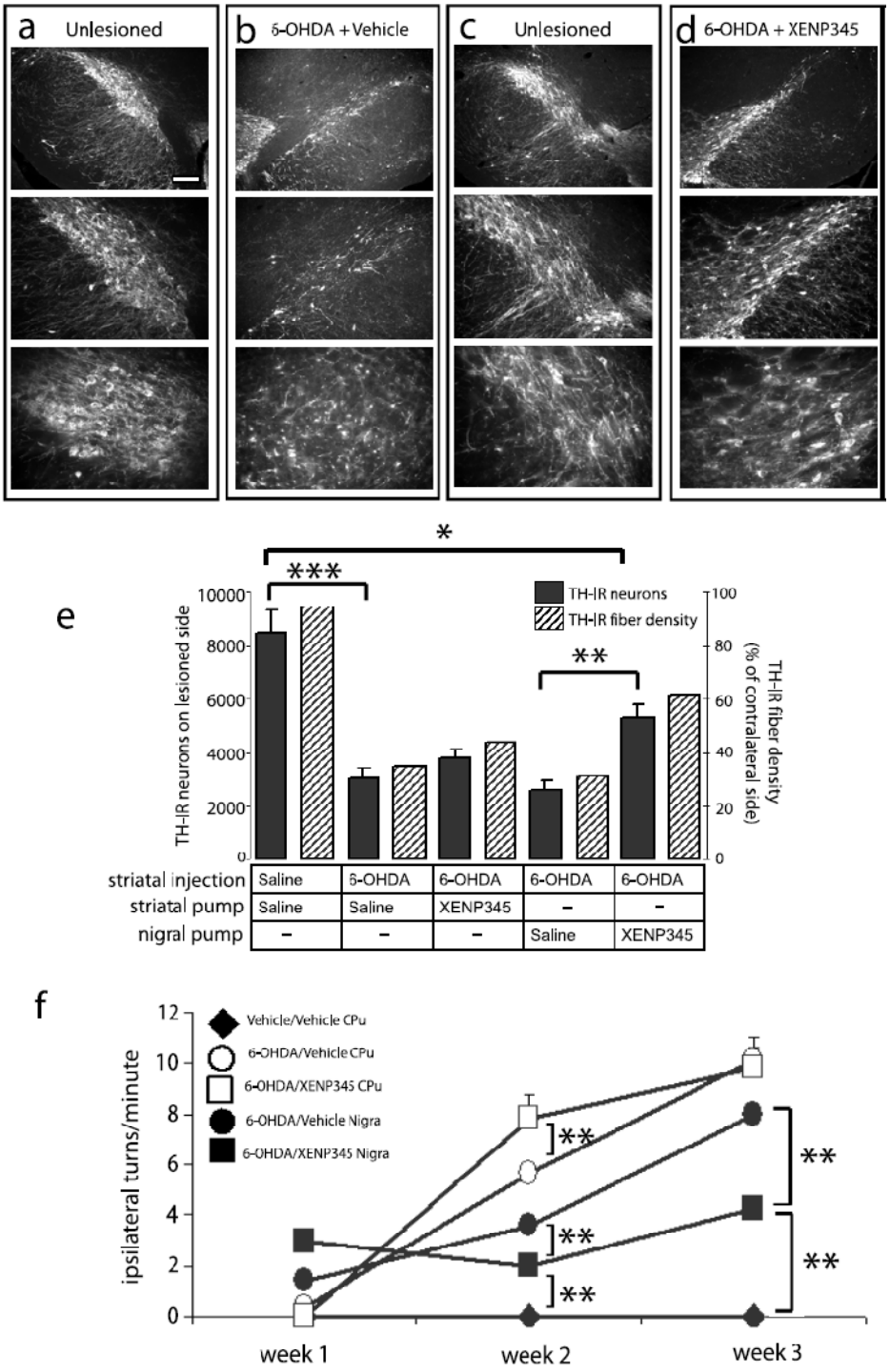

Figure 2.1. Blocking TNF signaling in the nigra attenuates striatal 6-OHDA-induced loss of nigral DA neurons and drug-induced rotational behavior.

A unilateral striatal lesion was induced by injecting 6-OHDA (20 μg) into the caudate-putamen complex of young adult rats; mock-lesioned animals received an injection of saline. Animals were stereotaxically implanted with an ipsilateral striatal or nigral indwelling cannula connected to an osmotic pump to deliver saline vehicle or XENP345 (0.08 mg/kg/day) over a two-week period. Animals were anesthetized and brains were fixed for IHC analyses of TH/NeuN-IR neurons by intracardiac perfusion three weeks after the lesion. Panels from top to bottom represent increasing magnification of representative brain sections used to obtain stereological estimates of nigral DA neuron number in 6-OHDA lesioned animals implanted with pump preloaded with saline (a, contralateral unlesioned side; b, lesioned/pump side) or implanted with nigral pump preloaded with XENP345 (c, contralateral unlesioned side; d, lesioned/pump side). Scale bar top panel = 100μm, middle panel = 50μm and bottom panel = 10μm. (e) Stereological estimate of DA neuron number (TH/NeuN-IR cells) in SNpc expressed as a percentage of the contralateral side (solid bars). Statistical significance was evaluated by ANOVA followed by post-hoc comparison test between groups and to unlesioned control group. Values expressed are group mean + SEM. * $p < 0.05$, ** $p < 0.01$, *** $p < 0.001$. Fluorescence intensity of TH-immunoreactive fibers was used to estimate striatal TH-fiber density (hatched bars) on the lesioned side, expressed as a percentage of the unlesioned contralateral side. (f) As a physiological measure of striatal DA depletion in mock- or 6-OHDA-lesioned animals, rotational behavior induced by an i.p. injection of 2.5 mg/kg amphetamine was measured weekly in all animals and expressed as the number of ipsilateral turns/min. Values expressed are group mean ± SEM; ** $p < 0.01$.

Figure 2.2

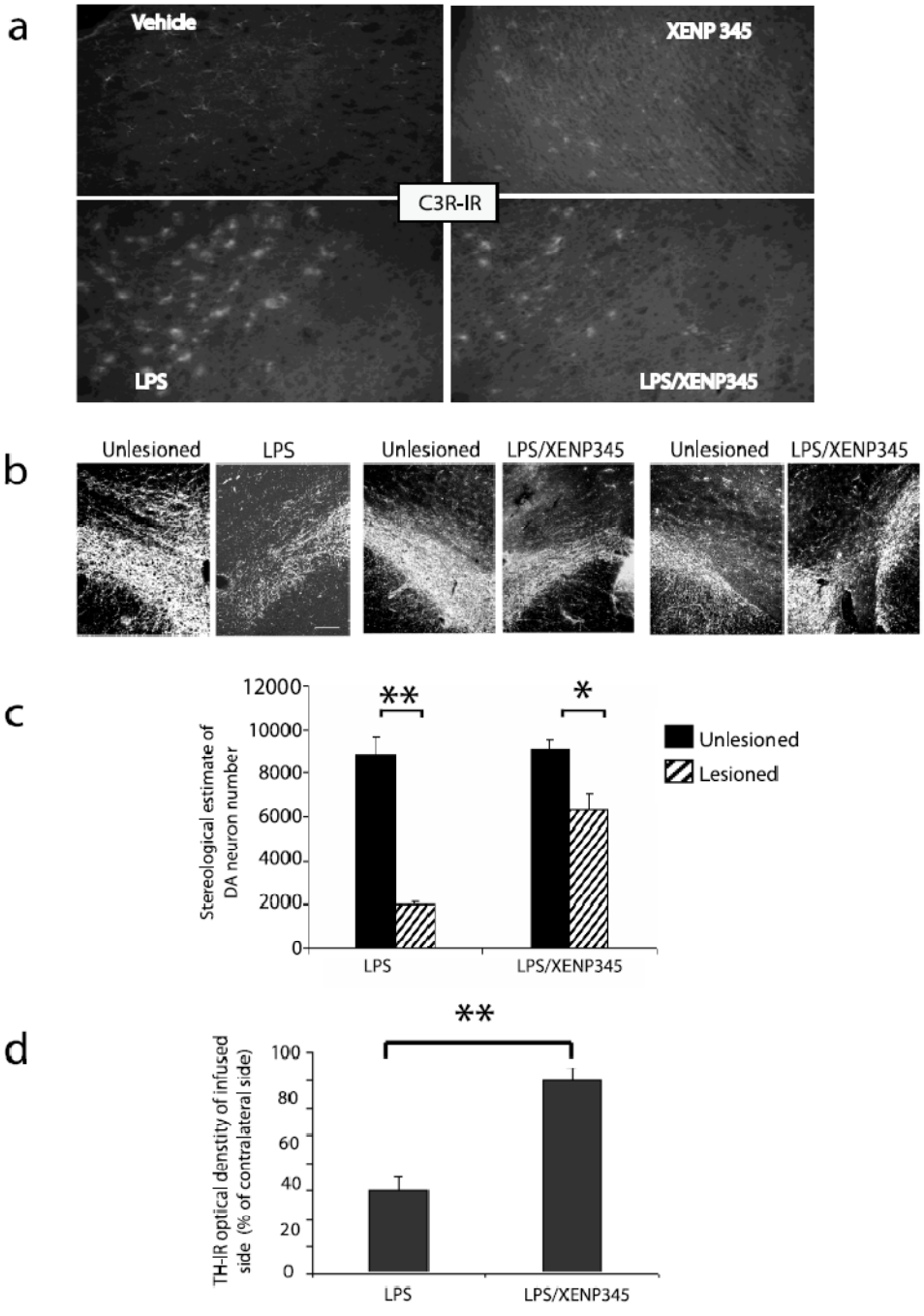
a
Vehicle
XENP 345
C3R-IR
LPS
LPS/XENP345
b
Unlesioned
LPS
Unlesioned
LPS/XENP345
Unlesioned
LPS/XENP345
c
Stereological estimate of DA neuron number
12000
10000
8000
6000
4000
2000
0
**
*
Unlesioned
Lesioned
LPS
LPS/XENP345
d
TH-IR optical denstity of infused side (% of contralateral side)
100
80
60
40
20
0
**
LPS
LPS/XENP345

Figure 2.2. Inhibition of soluble TNF signaling *in vivo* with XENP345 protects DA neurons from LPS-induced death.

Low-dose LPS (5 ng/hr in normal saline) was infused chronically for 2 weeks into the substantia nigra of CDF/Fischer 344 rats with or without XENP345 (70 ng/hr in normal saline). (a) Representative sections of microglia activation detected by complement 3 receptor (C3R)-positive cells in nigral sections from rat SNpc chronically infused with vehicle, LPS, LPS plus XENP345, or a single bolus of XENP345 (20 μg) scale bar = 10 μm. A ramified (resting) morphology is evident in vehicle and XENP345 alone brains. LPS/XENP345 co-infused SNpc displayed fewer ameboid (activated) microglia compared to LPS alone. (b) Representative sections of TH-IR from an animal infused with LPS and two different animals co-infused with LPS/XENP345 (B, scale bar = 100 μm). (c) Stereological estimates of nigral DA neuron number (TH/NeuN co-immunoreactive neurons) after LPS or LPS/XENP345 infusion in SNpc on the unlesioned (contralateral) side in solid bars and lesioned (ipsilateral) side shown in gray hatched bars. Left versus right differences from the same animals were analyzed using two-tailed paired Student's t test. Values were expressed as the group mean ± SEM; *$p<$ 0.05, **$p < 0.01$ significantly different from unlesioned side. (d) Striatal TH-IR optical density on infused side (expressed as a percentage of contralateral side). Values expressed are the mean ± SEM; **p< 0.01 significantly different from LPS only infused group.

Figure 2.3

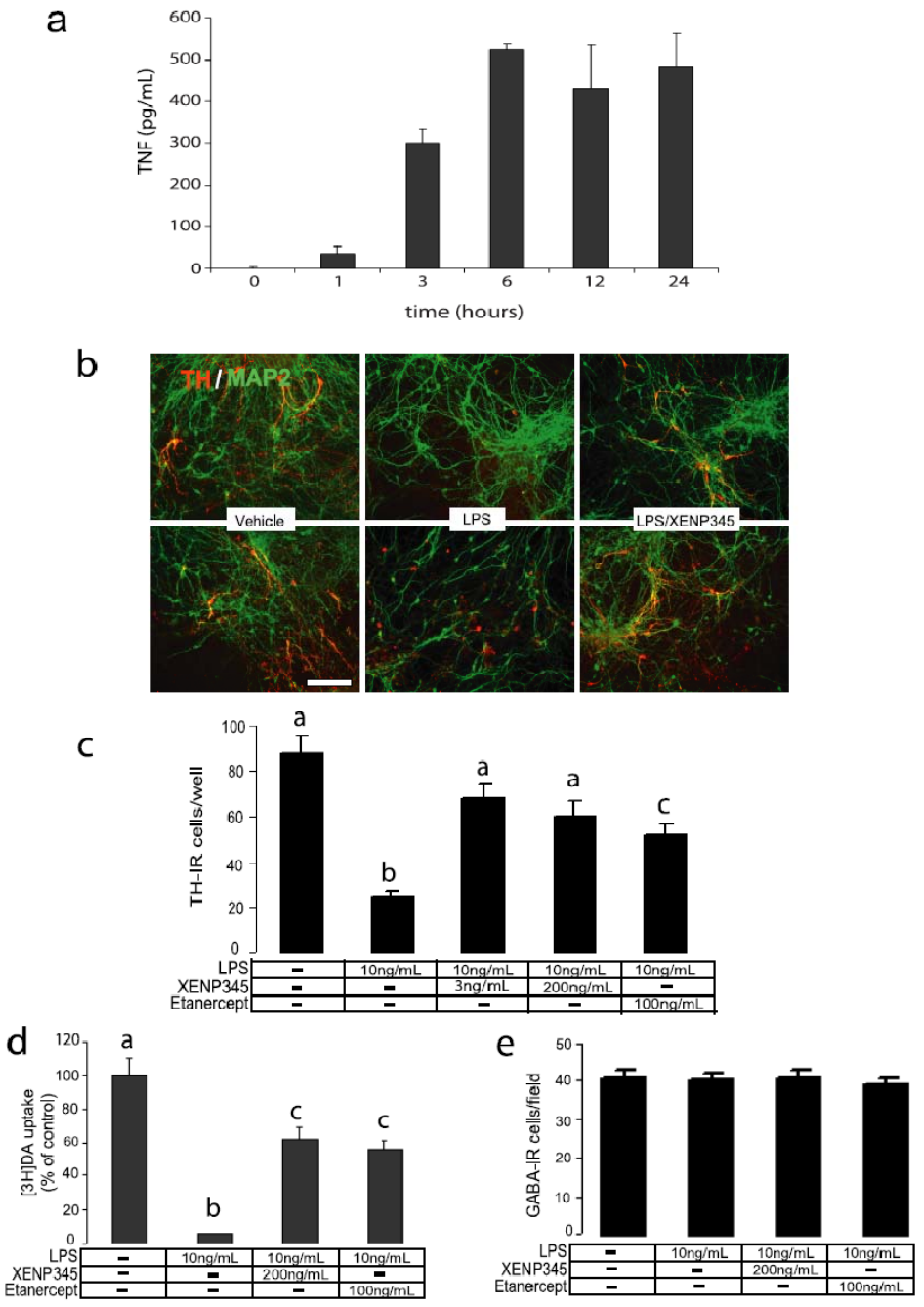
a
TNF (pg/mL)
600
500
400
300
200
100
0
0
1
3
6
12
24
time (hours)
b
TH / MAP2
Vehicle
LPS
LPS/XENP345
c
TH-IR cells/well
100
80
60
40
20
0
a
b
a
a
c
LPS
XENP345
Etanercept
10ng/mL
3ng/mL
200ng/mL
100ng/mL
d
[3-H]DA uptake (% of control)
120
100
80
60
40
20
0
a
b
c
c
LPS
XENP345
Etanercept
10ng/mL
200ng/mL
100ng/mL
e
GABA-IR cells/field
50
40
30
20
10
0
LPS
XENP345
Etanercept
10ng/mL
200ng/mL
100ng/mL

Figure 2.3. Inhibition of TNF signaling by anti-TNF biologics attenuates LPS-induced neurotoxicity and death of dopaminergic (DA) neurons in EVM cultures.

(a) Production of solTNF into culture media elicited by LPS (10 ng/mL) in rat embryonic day 14 (E14) ventral mesencephalon (EVM) neuron/glia cultures was measured by quantitative ELISA. (b) EVM cultures were treated with LPS (10 ng/mL) in media supplemented with 2.5% FBS (see Methods) for 4 d in the presence or absence of solTNF-selective XENP345 or etanercept, a soluble decoy human Fc-TNFR2 receptor that inhibits both tmTNF and solTNF. DA neurons were identified as double-labeled TH/MAP2b cells. Two representative panels are shown for vehicle-, LPS- or LPS plus XENP345-treated cultures. Similar results were obtained in a minimum of three independent experiments. (c) Quantification of DA neuron survival in EVM cultures treated with LPS (10 ng/mL) for 4 days in the presence or absence of TNF inhibitors. Similar results were obtained in a minimum of three independent experiments. Values shown are mean $\pm$ SEM; histogram bars with different letters are significantly different ($p < 0.05$). (d) Uptake of [^{3}H]-dopamine was measured in LPS-treated EVM cultures in the presence or absence of TNF inhibitors. Values shown are background-corrected for non-specific uptake measured by including mazindol during incubation with the tritiated neurotransmitter. Values shown are mean + SEM; histogram bars with different letters are significantly different ($p < 0.05$). Similar results were obtained in three independent experiments. (e) GABAergic neuron survival, assessed by counting number of GABA/NeuN double-labeled cells, was unaffected by LPS treatment. No statistical significant difference was found between groups. Similar results were obtained in two independent experiments.

Figure 2.4

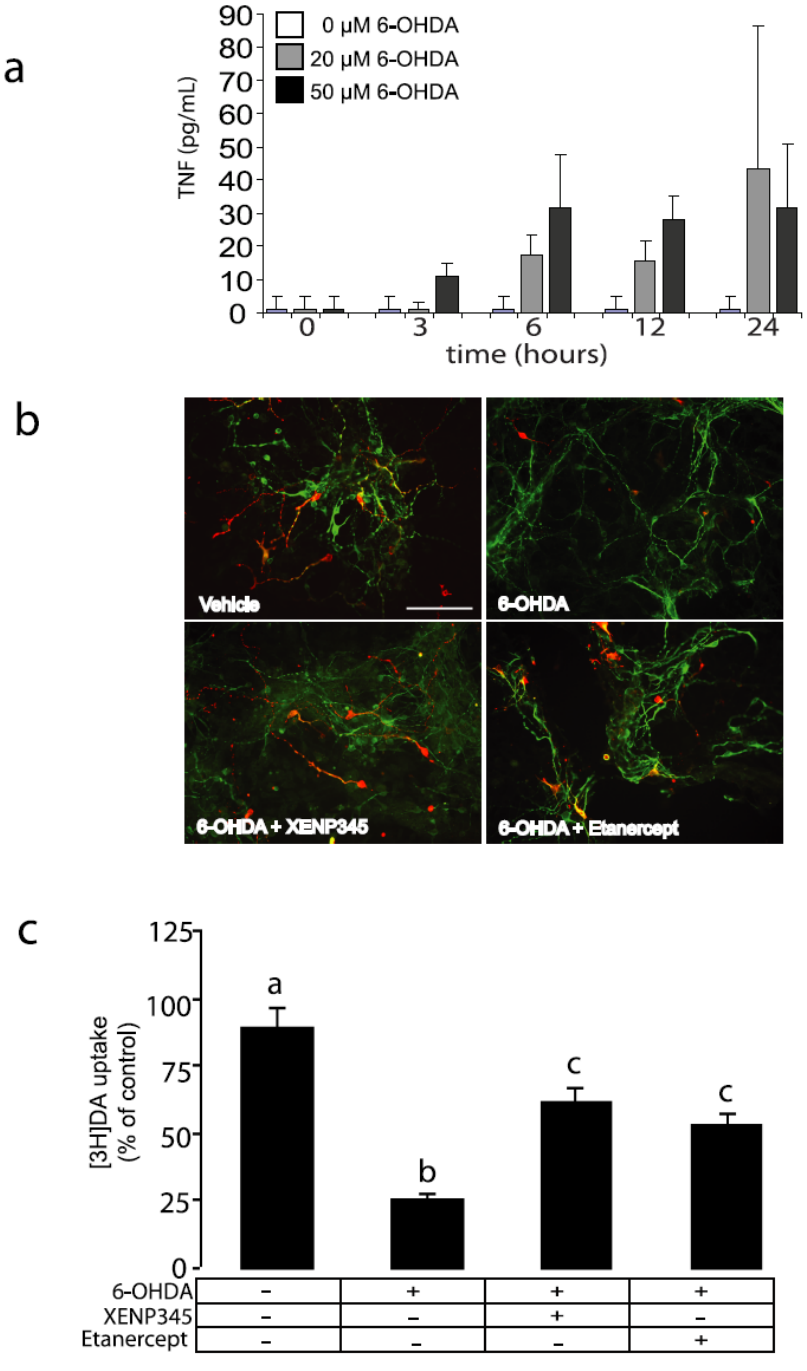
a
0 μM 6-OHDA
20 μM 6-OHDA
50 μM 6-OHDA
TNF (pg/mL)
90
80
70
60
50
40
30
20
10
0
0
3
6
12
24
time (hours)
b
Vehicle
6-OHDA
6-OHDA + XENP345
6-OHDA + Etanercept
c
[3H]DA uptake
(% of control)
125
100
75
50
25
0
a
b
c
c
6-OHDA
XENP345
Etanercept

Figure 2.4. Inhibition of soluble TNF signaling attenuates 6-OHDA-induced death of dopaminergic (DA) neurons in EVM cultures.

(a) Production of solTNF into culture media elicited by 6-OHDA (0μM (white), 20μM (gray), or 50μM (black)) in rat embryonic day 14 (E14) ventral mesencephalon (EVM) neuron/glia cultures was measured by quantitative ELISA. (b) EVM cultures were treated with 6-hydroxydopamine (20 μM) for 24 hr in media supplemented with 2.5% FBS (see Methods) in the presence or absence of the solTNF-selective XENP345 (200 ng/mL) or etanercept (200 ng/mL). DA neuron survival was assessed 96 hr after exposure to 6-OHDA. DA neurons were identified as double-labeled TH/MAP2b cells. Representative panels are shown for vehicle-, 6-OHDA-, 6-OHDA/XENP345-, or 6-OHDA/etanercept-treated cultures (scale bar = 100 μm). (c) Uptake of [^{3}H]-dopamine was measured in 6-OHDA-treated EVM cultures in the presence or absence of TNF inhibitors. Values shown are background-corrected for non-specific uptake measured by including mazindol during incubation with the tritiated neurotransmitter. Values shown are mean $\pm$ SEM; histogram bars with different letters are significantly different ($p < 0.05$).

Figure 2.5

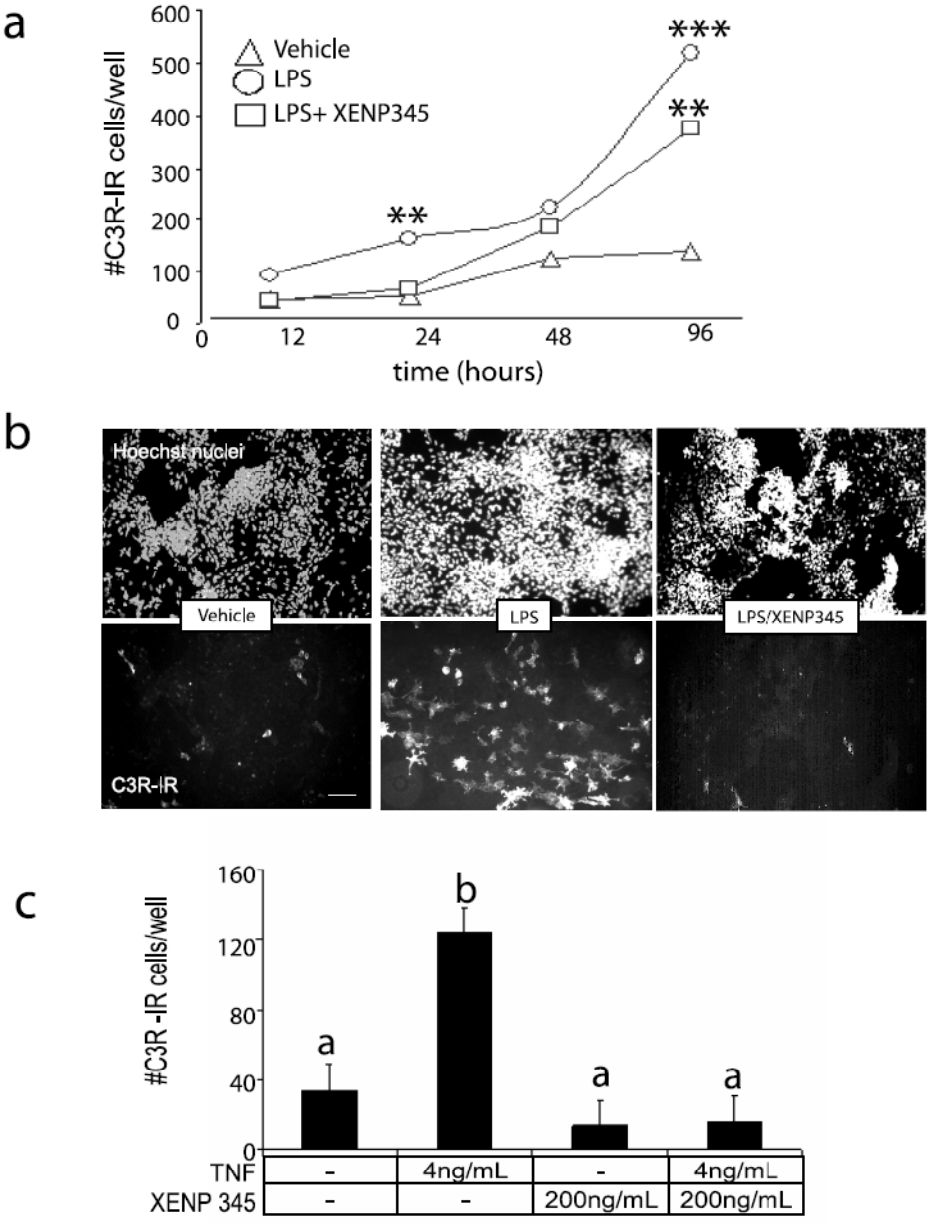
a
#C3R-IR cells/well
600
500
400
300
200
100
0
Vehicle
LPS
LPS+ XENP345
***
**
**
0
12
24
48
96
time (hours)
b
Hoechst nuclei
Vehicle
LPS
LPS/XENP345
C3R-IR
c
#C3R -IR cells/well
160
120
80
40
0
a
b
a
a
TNF
XENP 345
-
4ng/mL
-
4ng/mL
-
-
200ng/mL
200ng/mL

Figure 2.5. Soluble TNF is a primary mediator of LPS-induced microglia activation and death of DA neurons in ventral mesencephalon neuron/glia cultures.

(a) Quantification of microglia activation (measured by C3R immunoreactivity) induced by LPS treatment for 12, 24, 48, or 96 hr in the presence (squares) or absence (circles) of XENP345. Vehicle treated cultures are indicated by triangles. Values are expressed as the mean ± SEM; error bars are smaller than the symbols; $^{**}p < 0.01$, $^{**}p < 0.001$. Similar results were obtained in at least three independent experiments. (b) Representative images of microglia activation measured after 24 hr of LPS stimulation in the presence or absence of XENP345 (scale bar = 50 μm) is indicated by number of ameboid-shaped CR3-immunoreactive microglia in the neuron/glia cell cultures. Similar results were obtained in three independent experiments. (c) Control experiment showing neutralization of solTNF-induced microglia activation by XENP345 and absence of TNF-like activity when used alone. EVM cultures were treated with TNF (4 ng/mL) in the presence or absence of XENP345. After 24 hr stimulation, cells were fixed and stained with an antibody specific for complement 3 receptor (C3R) to quantify extent of microglia activation. Values shown are mean $\pm$ SEM; histogram bars with different letters are significantly different ($p < 0.05$).

Figure 2.6

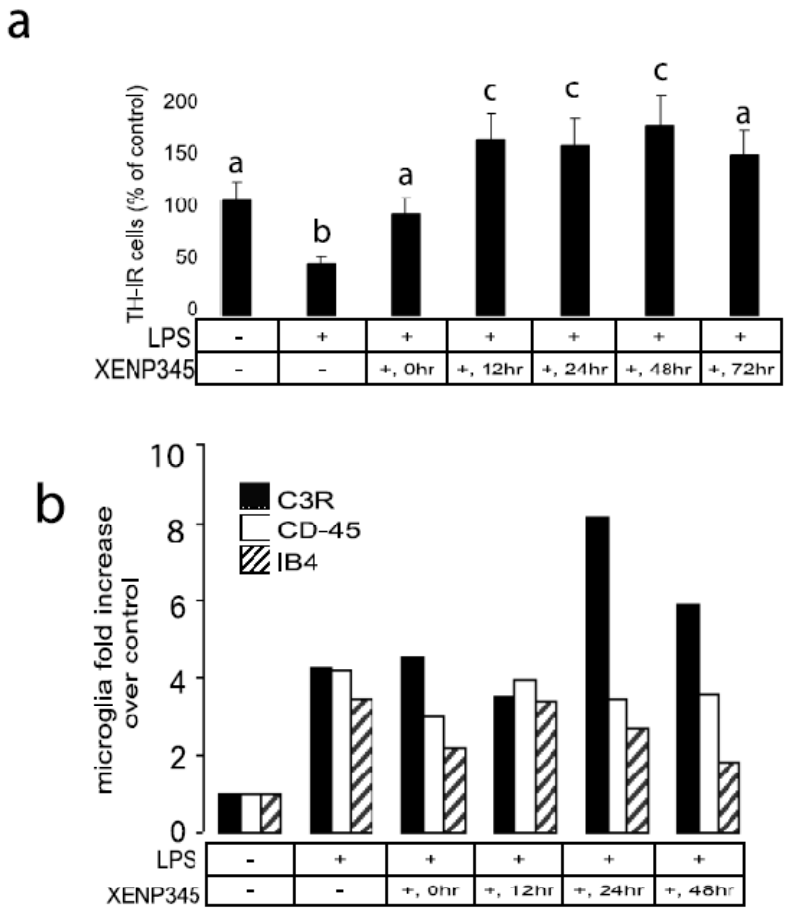
a
TH-IR cells (% of control)
200
150
100
50
0
a
b
a
c
c
c
a
LPS
XENP345
-
+
+
+
+
+
+
-
-
+, 0hr
+, 12hr
+, 24hr
+, 48hr
+, 72hr
b
microglia fold increase over control
10
8
6
4
2
0
C3R
CD-45
IB4
LPS
XENP345
-
+
+
+
+
+
-
-
+, 0hr
+, 12hr
+, 24hr
+, 48hr

Figure 2.6. Delayed addition of XENP345 provides robust rescue of DA neurons despite sustained microglia activation.

(a) Quantification of DA neuron survival after co-addition or delayed addition of XENP345 (200 ng/mL) following LPS (10 ng/mL) treatment. Values shown are mean + SEM; histogram bars with different letters are significantly different ($p < 0.05$). Similar results were obtained in two independent experiments. (b) Quantification of microglia activation in response to LPS (10 ng/mL) in the presence or absence of XENP345 (200 ng/mL) using three different immunocytochemical microglial markers (C3R, CD45, IB4). Similar results were obtained in two independent experiments. Values shown are mean $\pm$ SEM; histogram bars with different letters are significantly different ($p < 0.05$).

ACKNOWLEDEMENTS

Drs. Mark West, Steven Evans, Lutz Slomianka, and Geoff Greene of MicroBrightField for guidance and advice on stereological analyses; Don Copper in the Department of Psychiatry for allowing access to his MicroBrightField Stereo-Investigator equipment; and Joyce Repa and members of the Tansey laboratory, especially Tamy Frank-Cannon for critical discussions and review of this manuscript and Sabrina Martinez-Anz for technical support.

REFERENCES

Aggarwal, B. B., Samanta, A., Feldmann, M., TNFα. In: J. J. a. F. Oppenheim, M., (Ed.), Cytokine Reference. Academic Press, London, 2000, pp. pp. 414-434.

Agnholt, J., Dahlerup, J. F., Kaltoft, K., 2003. The effect of etanercept and infliximab on the production of tumour necrosis factor alpha, interferon-gamma and GM-CSF in in vivo activated intestinal T lymphocyte cultures. Cytokine. 23**,** 76-85.

Allan, S. M., Rothwell, N. J., 2001. Cytokines and acute neurodegeneration. Nat Rev Neurosci. 2**,** 734-44.

Aloe, L., Fiore, M., 1997. TNF-alpha expressed in the brain of transgenic mice lowers central tyroxine hydroxylase immunoreactivity and alters grooming behavior. Neurosci Lett. 238**,** 65-8.

Arnett, H. A., Mason, J., Marino, M., Suzuki, K., Matsushima, G. K., Ting, J. P., 2001. TNF alpha promotes proliferation of oligodendrocyte progenitors and remyelination. Nat Neurosci. 4**,** 1116-22.

Barcia, C., de Pablos, V., Bautista-Hernandez, V., Sanchez-Bahillo, A., Bernal, I., Fernandez-Villalba, E., Martin, J., Banon, R., Fernandez-Barreiro, A., Herrero, M. T., 2005. Increased plasma levels of TNF-alpha but not of IL1-beta in MPTP-treated monkeys one year after the MPTP administration. Parkinsonism Relat Disord. 11**,** 435-9.

Beutler, B., 2005. The Toll-like receptors: analysis by forward genetic methods. Immunogenetics. 57**,** 385-92.

Boka, G., Anglade, P., Wallach, D., Javoy-Agid, F., Agid, Y., Hirsch, E. C., 1994. Immunocytochemical analysis of tumor necrosis factor and its receptors in Parkinson's disease. Neurosci Lett. 172**,** 151-4.

Carvey, P. M., Chen, E. Y., Lipton, J. W., Tong, C. W., Chang, Q. A., Ling, Z. D., 2005. Intra-parenchymal injection of tumor necrosis factor-alpha and interleukin 1-beta produces dopamine neuron loss in the rat. J Neural Transm. 112**,** 601-12.

Chen, H., Zhang, S. M., Hernan, M. A., Schwarzschild, M. A., Willett, W. C., Colditz, G. A., Speizer, F. E., Ascherio, A., 2003. Nonsteroidal anti-inflammatory drugs and the risk of Parkinson disease. Arch Neurol. 60**,** 1059-64.

Ferger, B., Leng, A., Mura, A., Hengerer, B., Feldon, J., 2004. Genetic ablation of tumor necrosis factor-alpha (TNF-alpha) and pharmacological inhibition of TNF-synthesis attenuates MPTP toxicity in mouse striatum. J Neurochem. 89**,** 822-33.

Gao, H. M., Jiang, J., Wilson, B., Zhang, W., Hong, J. S., Liu, B., 2002. Microglial activation-mediated delayed and progressive degeneration of rat nigral dopaminergic neurons: relevance to Parkinson's disease. J Neurochem. 81**,** 1285-97.

Garcia-Ruiz, C., Colell, A., Mari, M., Morales, A., Calvo, M., Enrich, C., Fernandez-Checa, J. C., 2003. Defective TNF-alpha-mediated hepatocellular apoptosis and liver damage in acidic sphingomyelinase knockout mice. J Clin Invest. 111**,** 197-208.

Garcia-Ruiz, C., Colell, A., Mari, M., Morales, A., Fernandez-Checa, J. C., 1997. Direct effect of ceramide on the mitochondrial electron transport chain leads to

generation of reactive oxygen species. Role of mitochondrial glutathione. J Biol Chem. 272**,** 11369-77.

Gayle, D. A., Ling, Z., Tong, C., Landers, T., Lipton, J. W., Carvey, P. M., 2002. Lipopolysaccharide (LPS)-induced dopamine cell loss in culture: roles of tumor necrosis factor-alpha, interleukin-1beta, and nitric oxide. Brain Res Dev Brain Res. 133**,** 27-35.

German, D. C., Manaye, K. F., 1993. Midbrain dopaminergic neurons (nuclei A8, A9, and A10): three-dimensional reconstruction in the rat. J Comp Neurol. 331**,** 297-309.

Goldberg, M. S., Pisani, A., Haburcak, M., Vortherms, T. A., Kitada, T., Costa, C., Tong, Y., Martella, G., Tscherter, A., Martins, A., Bernardi, G., Roth, B. L., Pothos, E. N., Calabresi, P., Shen, J., 2005. Nigrostriatal dopaminergic deficits and hypokinesia caused by inactivation of the familial Parkinsonism-linked gene DJ-1. Neuron. 45**,** 489-96.

Hald, A., Lotharius, J., 2005. Oxidative stress and inflammation in Parkinson's disease: is there a causal link? Exp Neurol. 193**,** 279-90.

Heldmann, U., Thored, P., Claasen, J. H., Arvidsson, A., Kokaia, Z., Lindvall, O., 2005. TNF-alpha antibody infusion impairs survival of stroke-generated neuroblasts in adult rat brain. Exp Neurol. 196**,** 204-8.

Hinkerohe, D., Smikalla, D., Haghikia, A., Heupel, K., Haase, C. G., Dermietzel, R., Faustmann, P. M., 2005. Effects of cytokines on microglial phenotypes and astroglial coupling in an inflammatory coculture model. Glia. 52**,** 85-97.

Hirsch, E. C., Hunot, S., Hartmann, A., 2005. Neuroinflammatory processes in Parkinson's disease. Parkinsonism Relat Disord. 11 Suppl 1**,** S9-S15.

Hunot, S., Dugas, N., Faucheux, B., Hartmann, A., Tardieu, M., Debre, P., Agid, Y., Dugas, B., Hirsch, E. C., 1999. FcepsilonRII/CD23 is expressed in Parkinson's disease and induces, in vitro, production of nitric oxide and tumor necrosis factor-alpha in glial cells. J Neurosci. 19**,** 3440-7.

Janelsins, M. C., Mastrangelo, M. A., Oddo, S., LaFerla, F. M., Federoff, H. J., Bowers, W. J., 2005. Early correlation of microglial activation with enhanced tumor necrosis factor-alpha and monocyte chemoattractant protein-1 expression specifically within the entorhinal cortex of triple transgenic Alzheimer's disease mice. J Neuroinflammation. 2**,** 23.

Keicho, N., Sawada, S., Kitamura, K., Yotsumoto, H., Takaku, F., 1991. Effects of an immunosuppressant, FK506, on interleukin 1 alpha production by human macrophages and a macrophage-like cell line, U937. Cell Immunol. 132**,** 285-94.

Kim, R. H., Smith, P. D., Aleyasin, H., Hayley, S., Mount, M. P., Pownall, S., Wakeham, A., You-Ten, A. J., Kalia, S. K., Horne, P., Westaway, D., Lozano, A. M., Anisman, H., Park, D. S., Mak, T. W., 2005. Hypersensitivity of DJ-1-deficient mice to 1-methyl-4-phenyl-1,2,3,6-tetrahydropyrindine (MPTP) and oxidative stress. Proc Natl Acad Sci U S A. 102**,** 5215-20.

Kirik, D., Rosenblad, C., Bjorklund, A., 1998. Characterization of behavioral and neurodegenerative changes following partial lesions of the nigrostriatal dopamine system induced by intrastriatal 6-hydroxydopamine in the rat. Exp Neurol. 152**,** 259-77.

Kitazawa, M., Oddo, S., Yamasaki, T. R., Green, K. N., LaFerla, F. M., 2005. Lipopolysaccharide-Induced Inflammation Exacerbates Tau Pathology by a Cyclin-Dependent Kinase 5-Mediated Pathway in a Transgenic Model of Alzheimer's Disease. J. Neurosci. 25**,** 8843-8853.

Leng, A., Mura, A., Feldon, J., Ferger, B., 2005. Tumor necrosis factor-alpha receptor ablation in a chronic MPTP mouse model of Parkinson's disease. Neurosci Lett. 375**,** 107-11.

Liu, B., Du, L., Hong, J. S., 2000. Naloxone protects rat dopaminergic neurons against inflammatory damage through inhibition of microglia activation and superoxide generation. J Pharmacol Exp Ther. 293**,** 607-17.

Mabjeesh, N. J., Frese, M., Rauen, T., Jeserich, G., Kanner, B. I., 1992. Neuronal and glial gamma-aminobutyric acid+ transporters are distinct proteins. FEBS Lett. 299**,** 99-102.

MacEwan, D. J., 2002. TNF receptor subtype signalling: differences and cellular consequences. Cell Signal. 14**,** 477-92.

Marchetti, L., Klein, M., Schlett, K., Pfizenmaier, K., Eisel, U. L., 2004. Tumor necrosis factor (TNF)-mediated neuroprotection against glutamate-induced excitotoxicity is enhanced by N-methyl-D-aspartate receptor activation. Essential role of a TNF receptor 2-mediated phosphatidylinositol 3-kinase-dependent NF-kappa B pathway. J Biol Chem. 279**,** 32869-81.

McGeer, P. L., Itagaki, S., Boyes, B. E., McGeer, E. G., 1988. Reactive microglia are positive for HLA-DR in the substantia nigra of Parkinson's and Alzheimer's disease brains. Neurology. 38**,** 1285-91.

McGuire, S. O., Ling, Z. D., Lipton, J. W., Sortwell, C. E., Collier, T. J., Carvey, P. M., 2001. Tumor necrosis factor alpha is toxic to embryonic mesencephalic dopamine neurons. Exp Neurol. 169**,** 219-30.

Mitoma, H., Horiuchi, T., Hatta, N., Tsukamoto, H., Harashima, S., Kikuchi, Y., Otsuka, J., Okamura, S., Fujita, S., Harada, M., 2005. Infliximab induces potent anti-inflammatory responses by outside-to-inside signals through transmembrane TNF-alpha. Gastroenterology. 128**,** 376-92.

Mogi, M., Togari, A., Kondo, T., Mizuno, Y., Komure, O., Kuno, S., Ichinose, H., Nagatsu, T., 2000. Caspase activities and tumor necrosis factor receptor R1 (p55) level are elevated in the substantia nigra from parkinsonian brain. J Neural Transm. 107**,** 335-41.

Mogi, M., Togari, A., Tanaka, K., Ogawa, N., Ichinose, H., Nagatsu, T., 1999. Increase in level of tumor necrosis factor (TNF)-alpha in 6-hydroxydopamine-lesioned striatum in rats without influence of systemic L-DOPA on the TNF-alpha induction. Neurosci Lett. 268**,** 101-4.

Moore, D. J., West, A. B., Dawson, V. L., Dawson, T. M., 2005. Molecular pathophysiology of Parkinson's Disease. Annu Rev Neurosci. 28**,** 57-87.

Nagatsu, T., Sawada, M., 2005. Inflammatory process in Parkinson's disease: role for cytokines. Curr Pharm Des. 11**,** 999-1016.

Nishimura, M., Mizuta, I., Mizuta, E., Yamasaki, S., Ohta, M., Kaji, R., Kuno, S., 2001. Tumor necrosis factor gene polymorphisms in patients with sporadic Parkinson's disease. Neurosci Lett. 311**,** 1-4.

Oddo, S., Caccamo, A., Shepherd, J. D., Murphy, M. P., Golde, T. E., Kayed, R., Metherate, R., Mattson, M. P., Akbari, Y., LaFerla, F. M., 2003. Triple-transgenic model of Alzheimer's disease with plaques and tangles: intracellular Abeta and synaptic dysfunction. Neuron. 39**,** 409-21.

Olleros, M. L., Guler, R., Vesin, D., Parapanov, R., Marchal, G., Martinez-Soria, E., Corazza, N., Pache, J. C., Mueller, C., Garcia, I., 2005. Contribution of transmembrane tumor necrosis factor to host defense against Mycobacterium bovis bacillus Calmette-guerin and Mycobacterium tuberculosis infections. Am J Pathol. 166**,** 1109-20.

Pasparakis, M., Alexopoulou, L., Episkopou, V., Kollias, G., 1996. Immune and inflammatory responses in TNF alpha-deficient mice: a critical requirement for TNF alpha in the formation of primary B cell follicles, follicular dendritic cell networks and germinal centers, and in the maturation of the humoral immune response. J. Exp. Med. 184**,** 1397-1411.

Paxinos, G., Watson, C., Pennisi, M., Topple, A., 1985. Bregma, lambda and the interaural midpoint in stereotaxic surgery with rats of different sex, strain and weight. J Neurosci Methods. 13**,** 139-43.

Pejovic, V., Soskic, V., Pan, W., Kastin, A. J., 2004. Brain proteome of mice lacking the receptors for tumor necrosis factor alpha. Proteomics. 4**,** 1461-4.

Przedborski, S., 2005. Pathogenesis of nigral cell death in Parkinson's disease. Parkinsonism Relat Disord. 11 Suppl 1**,** S3-7.

Przedborski, S., Ischiropoulos, H., 2005. Reactive oxygen and nitrogen species: weapons of neuronal destruction in models of Parkinson's disease. Antioxid Redox Signal. 7**,** 685-93.

Ritter, U., Meissner, A., Ott, J., Korner, H., 2003. Analysis of the maturation process of dendritic cells deficient for TNF and lymphotoxin-alpha reveals an essential role for TNF. J Leukoc Biol. 74**,** 216-22.

Rousselet, E., Callebert, J., Parain, K., Joubert, C., Hunot, S., Hartmann, A., Jacque, C., Perez-Diaz, F., Cohen-Salmon, C., Launay, J. M., Hirsch, E. C., 2002. Role of TNF-alpha receptors in mice intoxicated with the parkinsonian toxin MPTP. Exp Neurol. 177**,** 183-92.

Sanchez-Pernaute, R., Ferree, A., Cooper, O., Yu, M., Brownell, A. L., Isacson, O., 2004. Selective COX-2 inhibition prevents progressive dopamine neuron degeneration in a rat model of Parkinson's disease. J Neuroinflammation. 1**,** 6.

Scallon, B., Cai, A., Solowski, N., Rosenberg, A., Song, X. Y., Shealy, D., Wagner, C., 2002. Binding and functional comparisons of two types of tumor necrosis factor antagonists. J Pharmacol Exp Ther. 301**,** 418-26.

Sriram, K., Matheson, J. M., Benkovic, S. A., Miller, D. B., Luster, M. I., O'Callaghan, J. P., 2002. Mice deficient in TNF receptors are protected against dopaminergic neurotoxicity: implications for Parkinson's disease. Faseb J. 16**,** 1474-6.

Sriram, K., Matheson, J. M., Benkovic, S. A., Miller, D. B., Luster, M. I., O'Callaghan, J. P., 2006. Deficiency of TNF receptors suppresses microglial activation and alters the susceptibility of brain regions to MPTP-induced neurotoxicity: role of TNF-alpha. Faseb J. 20**,** 670-82.

Steed, P. M., Tansey, M. G., Zalevsky, J., Zhukovsky, E. A., Desjarlais, J. R., Szymkowski, D. E., Abbott, C., Carmichael, D., Chan, C., Cherry, L., Cheung, P., Chirino, A. J., Chung, H. H., Doberstein, S. K., Eivazi, A., Filikov, A. V., Gao, S. X., Hubert, R. S., Hwang, M., Hyun, L., Kashi, S., Kim, A., Kim, E., Kung, J., Martinez, S. P., Muchhal, U. S., Nguyen, D. H., O'Brien, C., O'Keefe, D., Singer, K., Vafa, O., Vielmetter, J., Yoder, S. C., Dahiyat, B. I., 2003. Inactivation of TNF signaling by rationally designed dominant-negative TNF variants. Science. 301**,** 1895-8.

Sukal, S. A., Nadiminti, L., Granstein, R. D., 2006. Etanercept and demyelinating disease in a patient with psoriasis. J Am Acad Dermatol. 54**,** 160-4.

Takeshima, T., Johnston, J. M., Commissiong, J. W., 1994. Mesencephalic type 1 astrocytes rescue dopaminergic neurons from death induced by serum deprivation. J Neurosci. 14**,** 4769-79.

Tartaglia, L. A., Rothe, M., Hu, Y. F., Goeddel, D. V., 1993. Tumor necrosis factor's cytotoxic activity is signaled by the p55 TNF receptor. Cell. 73**,** 213-6.

Vawter, M. P., Dillon-Carter, O., Tourtellotte, W. W., Carvey, P., Freed, W. J., 1996. TGFbeta1 and TGFbeta2 concentrations are elevated in Parkinson's disease in ventricular cerebrospinal fluid. Exp Neurol. 142**,** 313-22.

West, M. J., Slomianka, L., Gundersen, H. J., 1991. Unbiased stereological estimation of the total number of neurons in thesubdivisions of the rat hippocampus using the optical fractionator. Anat Rec. 231**,** 482-97.

CHAPTER THREE

TNF-DEPENDENT CERAMIDE SIGNALING IN NEUROTOXICITY IN PARKINSON'S DISEASE

ABSTRACT

The mechanisms that contribute to the induction and perpetuation of dopaminergic neuronal cell death in Parkinson's disease (PD) are multi-faceted and poorly understood. Inflammation has been shown to contribute to cytotoxicity in animal models of PD, and increased levels of inflammatory cytokines have been observed in the cerebral spinal fluid and striatum of PD patients. We have previously demonstrated that blocking soluble tumor necrosis factor (TNF) signaling with dominant-negative TNF inhibitors attenuates the loss of dopaminergic neurons in models of PD, but which signaling pathways downstream of TNF mediate this effect remain undetermined. In this study, we report that TNF-dependent ceramide signaling contributes to dopamine (DA) neuron cytotoxicity by compromising mitochondrial membrane potential, inducing ER stress and activating caspase signaling *in vitro*. Our data demonstrate that TNF-induced cytotoxicity is partially ceramide-dependent, as TNF-induced cytotoxic effects are attenuated with two different pharmacological inhibitors of sphingomyelinase, an enzyme that hydrolyzes active ceramide from inactive sphingomyelin pools. Collectively, our data support a model whereby low-dose TNF and concomitant low TNF receptor 1occupancy activates downstream ceramide signaling and metabolism, culminating in caspase-dependent cytotoxic cell death of DA neurons.

INTRODUCTION

The exact molecular mechanisms that contribute to pathogenesis in Parkinson's disease (PD) have not been well delineated, and many different cellular processes have been implicated in PD, including diminished function of the ubiquitin proteasome system, generation of reactive oxygen species, compromised mitochondrial function and protein aggregation (Thomas 2009). Additionally, inflammation and activated microglia have been generally implicated in PD pathology (McGeer, Itagaki et al. 1988; McGeer, Itagaki et al. 1988; Hunot and Hirsch 2003; Hunot, Vila et al. 2004; Tansey, Frank-Cannon et al. 2008) and increased levels of pro-inflammatory cytokines such as TNF, IL-1β and IL-6, have been observed in the CSF and striatum of PD patients relative to healthy age-matched controls (Nagatsu, Mogi et al. 2000). Furthermore, inflammatory gene polymorphisms (TNF-308 and IL-1β-511) have been associated with an increased risk of developing PD (Wahner, Sinsheimer et al. 2007).

We have previously reported that blocking soluble TNF (solTNF) signaling with novel dominant-negative TNF inhibitors attenuates loss of dopaminergic neurons both *in vitro* and *in vivo* (McCoy, Martinez et al. 2006). Soluble TNF signals through the canonical transmembrane death receptor TNF receptor 1 (TNFR1) to potently transduce inflammatory stimuli (Tartaglia, Rothe et al. 1993; Grell, Wajant et al. 1998). TNFR1 is constitutively expressed by most cell types, and DA neurons are acutely sensitive to TNF-induced toxicity (Grell 1995; McGuire, Ling et al. 2001; Carvey, Chen et al. 2005). However, TNFR1 elicits signaling through numerous down-stream effectors, including p38, JNK, MAPK, and ceramide (Reviewed by (MacEwan 2002)) and the specific

regulators that mediate TNF-induced cytotoxicity in DA neurons have not yet been elucidated.

In this study, we tested the hypothesis that TNF-mediated cytotoxicity of DA neurons is ceramide-dependent. Ceramide is a sphingolipid with a well-established role in cell membrane homeostasis (Goni and Alonso 2006). However, a wealth of data over the past decade have established ceramide as a second messenger sphingolipid due to its rapid and transient generation (Kolesnick and Kronke 1998) that modulates a variety of physiologic and stress responses. Ceramide has been implicated in the cell death pathway activated by the death domain receptor ligands TNF and Fas-L (Obeid, Linardic et al. 1993; Kolesnick 1994; Kolesnick and Golde 1994). Additionally, ceramide has been shown to activate apoptosis in primary cortical neurons (Willaime, Vanhoutte et al. 2001) and in primary neuronal cultures from embryonic mesencephalon (Brugg, Michel et al. 1996), but the mechanisms of ceramide-induced apoptosis in DA neurons have not been fully delineated.

To explore the role of TNF and ceramide signaling in the cytotoxicity of DA neurons, we used the MN9D dopamine neuron-like cell line (Choi, Won et al. 1992). MN9D cells are a hybridoma line derived from fusion of murine embryonic ventral mesencephalon and N18TG2 neuroblastoma cells. MN9D cells are a reasonably good cellular PD model in that they express high levels of tyrosine hydroxylase (TH), the rate limiting enzyme in dopamine biosynthesis, and efficiently synthesize, store and release dopamine (Tang, Todd et al. 1994).

Here, we report that TNF-induced cytotoxicity is partially ceramide-dependent, as TNF-induced cytotoxic effects in differentiated MN9D (diff-MN9D) cells are attenuated with two different pharmacological inhibitors of the enzyme sphingomyelinase, which hydrolyzes active ceramide from inactive sphingomyelin pools. Having established a role for TNF-dependent ceramide signaling in the cytotoxic cell death of diff-MN9D cells, we next sought to examine different pathways and mechanisms associated with TNF or ceramide signaling to determine which and to what extent they contribute to cytotoxicity in DA neurons. Our data indicate that TNF-dependent ceramide signaling contributes to DA neuron cytotoxicity *in vitro* by compromising mitochondrial membrane potential, inducing endoplasmic reticulum (ER) stress and activating caspase signaling, providing rationale for therapeutic targeting of the sphingomyelinase/ceramide pathway in PD.

MATERIALS AND METHODS

Cell culture of the MN9D dopamine neuron-like cell line

The MN9D cell line was developed by Dr. Alfred Heller (Choi, Won et al. 1992), and was a generous gift from Dr. Michael Zigmond, at the University of Pittsburgh Medical Center. MN9D cells were cultured in sterile complete media (CM) which consisted of: high glucose (4,500 mg/L) Dulbecco's Modified Eagle Medium (DMEM, Sigma, D5648) dissolved in sterile tissue culture tested water (Sigma) supplemented with 10% fetal bovine serum (FBS, Hyclone Fetal Clone III), sodium bicarbonate (3.7g/L, Sigma), 25mM HEPES (Sigma), and 1% Penicillin/Streptomycin (Sigma) at a final pH of 7.3 at

37°C in a humidified 5% CO_2 incubator. MN9D cells were seeded forward in 75 cm^2 tissue culture flasks (Costar) and were seeded at a density of 7,500 cells per well for 96-well plates (100µl CM per well), 35,000 cells per well (500 µl CM per well) for 24-well plates, and 50,000 cells per well (2ml CM per well) for 6-well plates. After plating and allowing overnight attachment of cells in CM, MN9D cells were differentiated for 72 hrs via a complete media change to differentiation media (DM) which contained serum free DMEM (same CM as above, except FBS was excluded) supplemented with 5mM 2-Propylpentanoic acid (valproic acid, Sigma, P6273) and 1X N2 supplement (Invitrogen).

Treatment of differentiated MN9D cells with TNF or C2-ceramide

After incubation in DM for 72 hours, diff-MN9D cells cultured in 96-well plates were treated in triplicate or quadruplicate by a 50% media change with DM that contained 2X TNF (recombinant mouse, Roche, MT-410), C2-ceramide (C2-cer, N-acetyl-D-Sphingosine, Sigma A7191) or C2-dihydroceramide (C2-DH-Cer, Sigma, C7980) as a negative control for C2-ceramide because it lacks the 4-5 *trans* bond in the sphingosine moiety and cannot activate downstream ceramide signaling (Bielawska et al., JBC 1993; Obeid et al., Science, 1993). The TNF was dissolved in sterile Phosphate Buffered Saline (PBS, Sigma) and C2-cer and C2-DH-cer were dissolved in DMSO (Sigma) and aliquotted and stored under argon gas. As a control in parallel treatments, a DMSO vehicle condition equivalent to the amount of DMSO in the highest concentration of C2-cer/C2-DH-cer was used. TNF, C2-cer or C2-DH-cer-treated diff-MN9D cells were incubated at 37°C, 5% CO_2 for 72 or 48 hrs respectively, prior to being evaluated for overall viability using the MTS assay (described below). TNF, C2-cer or C2-DH-cer

treatments of diff-MN9D cells in 24-well or 6-well plates were done in duplicate or triplicate by a complete media change from CM to DM containing 1X TNF, C2-cer or C2-DH-cer.

MTS assay for cell viability

Treated diff-MN9D cells in 96-well plates were evaluated for overall viability using the MTS assay (Promega, CellTiter 96 AQueous One Solution Cell Proliferation Assay) according to the manufacturer's instructions. Twenty microliters (20µl) of the MTS reagent was added to DM-containing treatments and/or inhibitors. The cells were incubated with the MTS reagent at 37°C, 5% CO_2 for 2 hrs prior to colorimetric quantification of MTS reduction into a blue formazan by-product by metabolically active cells. The absorbance of blue formazan was measured at 492 nm wavelength using a Multiskan Ascent absorbance plate reader (Thermo Labsystems).

Pre-treatment of differentiated MN9D cells with inhibitors for ceramide

Diff-MN9D cells in 96-well plates were pre-treated in triplicate or quadruplicate with one of four different pharmacological inhibitors of ceramide: the A-SMase inhibitor desipramine HCl, used at 1 µM and 5 µM, (Sigma, D3900, dissolved in sterile H_2O), the N-SMase inhibitor GW4869, used at 10 µM, and 20 µM, (Calbiochem, No. 567715, dissolved in DMSO, aliquotted and stored under argon gas) the serine palmitoyltransferase inhibitor myriocin (a generous gift from Dr. Philip Scherer, UT Southwestern Medical Center at Dallas), dissolved in ethanol and used at 10 µM or the ceramide synthase inhibitor Fumonisin B1, used at 50 µM (Axorra LLC, No.: 350-017-

M001, dissolved in sterile H_2O). Diff-MN9D cells were pre-treated with ceramide inhibitors or control diluents for 30 minutes via a 50% media change with DM that contained a 2X concentration of the respective inhibitor or control diluent (i.e. 50µl of the initial 100 µl DM was removed and replaced with 50µl of DM containing a 2X concentration of a ceramide inhibitor for a final volume of 100 µl). After pre-treatment with ceramide inhibitors for 30 minutes, TNF was added by a 1:100 dilution of a TNF stock concentration (1µl of 100X TNF was added to 100µl DM) that contained ceramide inhibitors. In the case of GW4869, which declines in effective N-SMase-inhibition over time (Luberto, Hassler et al. 2002) the GW4869 reagent was re-added 24 hrs after initial GW4869 pre-treatment by addition of a 1:100 dilution of a GW4869 stock concentration (1µl of 100X GW + 100 µl DM) into DM already containing TNF treatments. Diff-MN9D cells were incubated at 37°C, 5% CO_2 for 48 hrs post TNF treatment prior to being evaluated for viability using the MTS assay.

C2-ceramide treatment of non-differentiated MN9D cells and determination of cell cytotoxicity using the alamarBlue assay

MN9D cells were seeded in 96-well plates at 10,000 cells per well (100µl CM per well) and were incubated overnight then treated with C2-cer in CM for 24 hrs in triplicate or quadruplicate as described above. Cellular cytotoxicity was determined by the alamarBlue assay according to the manufacturer's instructions. Reduction of alamarBlue requires cellular uptake and is characterized by a colorimetric shift from blue (oxidized) to red (reduced). Ten microliters of the alamarBlue reagent (Biosource/Invitrogen) was added to each well with non-diff-MN9D cells and was incubated at 37°C, 5% CO_2 for 4

hrs prior to colorimetric quantification of non-diff-MN9D cellular integrity via determination of alamar-Blue reduction by spectrophotometric absorbance at 570 nm wavelength (blue, oxidized alamarBlue) and 600 nm wavelength (red, reduced alamarBlue) using a Multiskan Ascent absorbance plate reader (Thermo Labsystems). The calculation of percent reduced alamarBlue was determined according to the manufacturer's instructions.

Quantitative Real-Time Polymerase Chain Reaction (Q-RT-PCR) for ER stress markers

Primers (sequences available upon request) were designed using ABI Primer Express software and were purchased from Integrated DNA Technologies (IDT). All primers were validated in species-specific tissue shown to express the gene of interest at high levels according to the SymAtlas of the Genomics Institute of the Novartis Research Foundation (GNF) and were confirmed by Q-RT-PCR to result in a single product. The acidic ribosomal phosphoprotein P0 gene (36B4) was used as the reference gene for each target gene because it was empirically determined by Q-RT-PCR to be unchanged in diff-MN9D cells under conditions known to elicit ER stress in terminally differentiated neurons. Q-RT-PCR was performed as previously described (Frank-Cannon, Tran et al. 2008). Briefly, total RNA was isolated using the RNeasy isolation kit and QIAshredders for homogenization (Qiagen) according to the manufacturer's instructions. The isolated RNA was treated with DNase I (Invitrogen) and reverse transcribed using Superscript II RNase H-reverse transcriptase (Invitrogen). Q-RT-PCR was performed using an ABI Prism 7900 HT Fast Detection System (Applied Biosystems) in a 384-well plate format.

All reactions were performed in duplicate or triplicate. Relative mRNA abundance for each sample was normalized to that of 36B4.

Homogeneous cleaved caspase assay

The Roche Homogeneous Cleaved Caspase Assay was used for the quantitative *in vitro* determination of caspase activity according to the manufacturer's instructions. Briefly, MN9D cells were seeded at a density of 15,000 cells per well in 96 well plates (100 µl CM per well), were incubated overnight and differentiated via complete media change to DM as described above. After 72 hrs differentiation, the diff-MN9D cells were treated via a complete media change with 1X treatments of DMSO vehicle, 25µM C2-DH-cer, or 20 µM C2-cer alone or co-incubated with either 25 µM Z-IETD or 25 µM Z-VAD, in serum free, high glucose (4,500 mg/ml), phenol red-free, Dulbecco's Modified Eagle's Medium (Sigma, D1145) supplemented with 1X N2 supplement and 5mM VPA for 5 hrs. At this point, the Positive Control and R110 rhodamine standards (components of the assay kit) were added immediately prior to addition of the Substrate Stock Solution (100 µl per well, from the assay kit). The plate was incubated for 1 hr at 37°C, 5% CO_2 prior to quantitative fluorimetric measurement of caspase activity (dequenching of rhodamine fluorescence) by excitation at 485 nm and emission at 520 nm on a FLUOstar Omega plate reader (BMG Scientific).

Treatment of differentiated MN9D cells with caspase inhibitors

Diff-MN9D cells in 96-well plates were treated in triplicate or quadruplicate with TNF or C2-cer alone or were co-treated with one of two caspase inhibitors, 25 µM Z-VAD-FMK

(Z-VAD, a pan caspase inhibitor, obtained from Promega), or 25 µM Z-IETD-FMK (Z-IETD, a caspase 8-specific inhibitor, obtained from R&D Systems). The treated diff-MN9D cells were incubated at 37°C, 5% CO_2 with C2-cer for 24 hrs or TNF for 48 hrs prior to determination of overall cell viability via the MTS assay as described above.

Cytofluorometric Analysis of Mitochondrial Membrane Potential Using Tetra Methyl Rhodamine Methyl Ester (TMRM)

Mitochondrial membrane potential in diff-MN9D cells was measured as previously described (Mortiboys and Bandmann 2008). Briefly, MN9D cells were seeded into black-walled, clear-bottomed 24-well plates onto Poly-L-Lysine (PLL) coated (Sigma, P2636, MW=30,000-70,000, 1mg/ml) Assistent glass cover slips (12 mm, No.0, distributed by Carolina Biological Supply) at a density of 35,000 cells per well in 500 µl CM. The MN9D cells were incubated overnight at 37°C, 5% CO_2 and were then differentiated via a complete media change with DM. After 72 hrs in DM, the diff-MN9D cell cultures were treated with C2-cer or DMSO vehicle or TNF or media vehicle via a complete media change with 1X treatment in DM. After incubation with C2-cer for 18 hrs or TNF for 36 hrs, TMRM (Invitrogen, T668, re-suspended in DMSO) was loaded into treated diff-MN9D cells at 150 nM in warm assay buffer (AB, 500 µl per well) which consisted of: NaCl (80 mM), KCl (75 mM), D-glucose (25 mM) and HEPES (25 mM) diluted in sterile H_2O and adjusted to a final pH of 7.4. To control for TMRM background cytofluorescence, carbonyl cyanide 3-chlorophenylhydrazone (CCCP, Sigma, C2759) was used. At the time of incubation with TMRM, 10 µM CCCP (re-suspended in DMSO) was co-added with TMRM in AB to parallel wells of diff-MN9D cells treated with TNF

or C2-cer. TMRM and TMRM/CCCP loaded cells were incubated for 15 minutes at 37°C, 5% CO_2 prior to quantification of TMRM cytofluorescence by excitation at 544 nm wavelength and emission at 590 nm wavelength on a FLUOstar Omega plate reader (BMG Scientific) followed by live cell imaging using an Olympus CK40 inverted microscope.

Statistical Analyses

Statistical analysis was performed using GraphPad Prism5 software (GraphPad Prism, San Diego, CA). Intergroup differences among the means between the various dependent variables were analyzed using one-way ANOVA; when ANOVA indicated significant differences, it was followed by Bonferroni's post-hoc group comparison test. Differences among group means between two independent variables were analyzed by two-way ANOVA, followed by Bonferroni's post-hoc test. Values expressed are the group means $\pm$ S.E.M.

RESULTS

TNF and C2-ceramide induce cytotoxicity in differentiated MN9D cells

Our previous data indicated that dopaminergic neurons are acutely sensitive to TNF *in vitro* and *in vivo* (McCoy, Martinez et al. 2006). To validate that diff-MN9D cells are sensitive to TNF- and C2-ceramide-induced cytotoxicity, we treated diff-MN9D cells with increasing concentrations of TNF and cell permeant C2-ceramide (C2-cer). We observed that diff-MN9D cells are indeed sensitive to TNF and C2-cer in a dose-dependent manner as determined by the MTS assay for total cell viability (**Figure 3.1 a,**

b). Notably, TNF-induced cytotoxicity reached a maximum at 72 hrs post TNF treatment while C2-cer-induced cytotoxicity reached a maximum earlier, at 48 hrs post C2-cer treatment (**Figure 3.1 a, b**). While the faster time-to-peak of C2-cer relative to TNF may be due to the fact that C2-cer is easily cell permeable and does not require ligand-receptor interaction as does TNF, the more rapid kinetic properties of C2-cer-induced cytotoxicity are also consistent with the interpretation that ceramide signaling is downstream of TNFR1 in diff-MN9D cells. As a negative control, C2-dihydroceramide (C2-DH-cer), an analog of C2-ceramide lacking the 4-5 *trans* bond in the sphingosine moiety and is incapable of activating downstream ceramide signaling (Bielawska, Crane et al. 1993; Obeid, Linardic et al. 1993), was used in parallel treatments with C2-cer. Importantly, C2-DH-cer did not adversely affect diff-MN9D viability at any concentration used (**Figure 3.1b**). We previously determined that non-differentiated MN9D (non-diff-MN9D) cells are not sensitive to concentrations of TNF that elicit cytotoxicity in diff-MN9D cells (data not shown). Similarly, non-diff-MN9D cells were not sensitive to concentrations of C2-cer that decreased diff-MN9D cell viability (**Figure 3.1c**).

TNF-induced cytotoxicity is partially ceramide-dependent

Biosynthesis of ceramide occurs via two main pathways: the *de novo* ceramide pathway which involves several enzymatic steps downstream of the initial step of serine and palmitoyl-CoA coalescence and the sphingomyelin recycling pathway, whereby ceramide is produced by hydrolysis of inactive sphingomyelin by sphingomyelinases (Woodcock 2006).To explore the hypothesis that activation of ceramide signaling downstream of TNFR1 evokes cytotoxicity in DA neurons, we pre-treated diff-MN9D

cells with different inhibitors of ceramide for 30 minutes followed by treatment with TNF for 48 hrs. Utilizing the MTS assay to measure total cell viability, we observed that TNF-induced cytotoxicity of diff-MN9D cells is significantly ameliorated by pre-treatment with desipramine, an inhibitor of A-SMase-dependent hydrolysis of sphingomyelin, which catalyzes ceramide production from inactive sphingomyelin pools (**Figure 3.2a**). The inhibitory effect of desipramine was most evident at concentrations of TNF approximating the LC_{50} in diff-MN9D cells at 48 hrs (**Figure 3.2a**). Five μM desipramine was sufficient to ablate the cytotoxic effects of 3 ng/ml TNF and restore viability of diff-MN9D cells in the MTS assay to that of vehicle treated cells (**Figure 3.2a**).

Employing similar methodology, we determined that N-SMase-dependent hydrolysis of sphingomyelin likewise contributes to TNF-induced cytotoxicity in diff-MN9D cells as pretreatment of diff-MN9D cells with 20μM of the N-SMase-specific inhibitor GW4869 attenuated TNF-induced cell death (**Figure 3.2b**). Importantly, inhibition of N-SMase by GW4869 had the greatest effect of preventing diff-MN9D cell death at a concentration of 3 ng/ml TNF (again approximating the LC_{50} for TNF in diff-MN9D cells at 48 hrs) similar to results observed using the A-SMase inhibitor desipramine (**Figure 3.2a**). Together these pharmacological data strongly suggest that TNF-dependent activation of SMases results in SM hydrolysis and ceramide generation which then mediates TNF-dependent cytotoxicity and compromises viability of diff-MN9D cells.

Interestingly, in analogous experiments using pharmacological inhibitors of components of the *de novo* ceramide biosynthesis pathway, we observed that inhibition of the enzyme serine palmitoyltransferase (which is the rate-limiting enzyme in *de novo* ceramide biosynthesis) by myriocin and inhibition of the enzyme ceramide synthase (which converts sphingonine to dihydroceramide) by Fumonisin B1did not mitigate TNF-induced cytotoxicity in diff-MN9D cells (**Figure 3.2 c, d** respectively). These data support the interpretation that *de novo* ceramide biosynthesis is not requisite for TNF-induced cytotoxicity in diff-MN9D cells. Collectively, our data indicate that the cytotoxic effects of TNF in diff-MN9D cells are mediated by SMase hydrolysis of sphingomyelin to form active ceramide, further supporting the interpretation that a signaling pathway of activated ceramide downstream of TNFR1 is intact in diff-MN9D cells.

TNF and C2-ceramide-induced cytotoxicity involves endoplasmic reticulum stress pathways

Endoplasmic reticulum (ER) stress-mediated cell death has been linked to neurodegenerative disease and PD (Lindholm, Wootz et al. 2006; Wang and Sanders 2007). To determine if ER stress pathways contribute to TNF and C2-ceramide induced cytotoxicity in diff-MN9D cells, we used the quantitative real-time polymerase chain reaction (Q-RT-PCR) method to ascertain if TNF or C2-cer treatment of diff-MN9D cells leads to increased mRNA transcripts of key ER stress target genes, namely activating transcription factor 6 (ATF6), Binding Protein (BiP), and C/EBP homologous protein (CHOP). ATF6 is a direct target of the ER stress response (Wang, Cui et al. 2007) and activates transcription of chaperone proteins (Lee, Tirasophon et al. 2002) to facilitate

protein folding and processing capacity. ATF6 also activates ER-associated degradation (ERAD) to promote the degradation of terminally misfolded proteins (Yamamoto, Yoshida et al. 2004). BiP is a chaperone protein important in the cellular ER stress response that binds and stabilizes newly synthesized proteins and assists in preventing aggregation of misfolded substrates (Nishikawa and Mizuno 2001). CHOP (previously cloned as growth-arrest and DNA damage-inducible gene 153 (GADD153) in yeast, is a b-Zip transcription factor with important functions in the ER stress response as two distinct pathways, the ER stress response element (ERSE) and the PERK-ATF4 pathway, converge on the CHOP promoter (Ma, Brewer et al. 2002). Once activated, CHOP has been implicated in the induction of apoptosis (Zinszner, Kuroda et al. 1998)).

TNF has been shown to activate ER stress in a ROS-dependent manner in L929 fibroblast cells (Xue, Piao et al. 2005), and ceramide-mediated ER stress has also been reported in prostate cancer cells (Sauane, Su et al. 2010). Using Q-RT-PCR, we determined that ER stress is a component of TNF-induced cytotoxicity in diff-MN9D cells as evidenced by increased mRNA for ATF6 and BiP (**Figure 3.3 a, b**). TNF treatment did not however, result in increased mRNA expression of CHOP (data not shown). Employing similar methodology, we likewise establish that C2-cer activates the CHOP ER stress pathway (**Figure 3.3 c**), but C2-cer treatment does not induce ATF6 or BiP expression (data not shown). The increased fold-induction of ER stress target genes by TNF and C2-cer was comparable to the fold-induction caused by tunicamycin (**Figure 3.3 a, b, c**), which potently induces ER stress by inhibiting protein glycosylation (Ling,

Li et al. 2009). Interestingly we observe ER stress in TNF and C2-cer treated diff-MN9D cells several hours prior to cell death.

TNF and C2-ceramide compromise mitochondrial membrane potential

Many of the genes associated with PD implicate aberrant mitochondrial function in disease pathogenesis (Lin and Beal 2006) and MPTP and rotenone, chemicals used in animal models of PD, are potent mitochondrial complex I inhibitors (Betarbet, Sherer et al. 2000). Additionally, TNF treatment has been reported to cause a rapid decrease in mitochondrial membrane potential and coincident increase in reactive oxygen species (Ghavami, Eshraghi et al. 2009), and ceramide has been shown to directly affect the mitochondrial electron transport chain (Garcia-Ruiz, Colell et al. 1997).

To further elucidate the mechanisms of TNF and C2-cer-induced cytotoxicity and to determine if TNF/ceramide signaling in diff-MN9D cells impinges on mitochondria, we investigated whether TNF or C2-cer adversely impact mitochondrial membrane potential by evaluating tetramethyl rhodamine methyl ester (TMRM) cytofluorescence. TMRM is a catatonic mitochondrial-selective probe that accumulates in the negatively charged mitochondrial membrane in proportion to mitochondrial membrane potential. To control for TMRM background cytofluorescence, carbonyl cyanide 3-chlorophenylhydrazone (CCCP), a protonophore and uncoupler of oxidative phosphorylation in mitochondria which effectively ablates the charge across the mitochondrial membrane was used in combination with TMRM and parallel to conditions with TMRM alone. Any TMRM signal in TMRM/CCCP conditions can be considered

background, and was used to normalize TMRM cytofluorescence values for each respective TNF or C2-cer condition. Diff-MN9D cells treated with 10 ng/ml TNF for 36 hrs or 15μM C2-cer for 18 hrs exhibited compromised mitochondrial membrane potential as evidence by reduced TMRM cytofluorescence relative to vehicle treated diff-MN9D cells (**Figure 3.4 a-f**), lending support to the interpretation that both TNF and C2-cer adversely affect mitochondrial integrity in diff-MN9D cells.

TNF and C2-ceramide induce caspase activation which is a mechanism of TNF-induced cytotoxic cell death

Numerous reports have linked TNF to caspase activation and apoptosis (reviewed in (Bertazza and Mocellin 2008)). Ceramide has been reported to alter the Bax/Bcl2 ratio, which regulates cytochrome C release from the mitochondria and results in activation of the caspase-9/-3 cascade in C6 glioma cells (Sawada, Nakashima et al. 2000) however direct mechanisms of caspase activation by ceramide in DA neurons have not been well elucidated. To determine if C2-cer treatment activates caspase signaling cascades in diff-MN9D cells, a homogeneous caspase assay was performed. In this assay, caspase activation is quantified by fluorimetric determination of proteolytic cleavage of the assay substrate, resulting in unquenching of a rhodamine signal. Using this assay, we observed that treatment of diff-MN9D cells with 20μM C2-cer for 5 hrs significantly increased caspase activation as demonstrated by a robust augmentation in rhodamine fluorescence compared to rhodamine signal from diff-MN9D cells treated with DMSO vehicle or C2-DH-cer (**Figure 3.5 a**). Notably, co-treatment of diff-MN9D cells with C2-cer and one of two caspase inhibitors, Z-VAD (a pan caspase inhibitor) or Z-IETD (a caspase 8-specific

inhibitor) significantly abated caspase activation in diff-MN9D cells (**Figure 3.5 a**). As caspase cleavage and activation was equivalently mitigated by Z-VAD and Z-IETD, these data imply that, under these experimental conditions, caspase 8 is the predominant caspase species down-stream of ceramide in diff-MN9D cells.

To evaluate the extent to which caspase activation contributes to cytotoxic cell death in response to TNF or C2-ceramide, diff-MN9D cells were treated with TNF or C2-cer alone for 48 or 24 hrs, respectively, or were co-incubated with 25 μM Z-VAD or 25 μM Z-IETD in combination with TNF or C2-cer for the same duration. Total cell viability was then measured using the MTS assay. In the case of TNF, co-treatment with either 25 μM Z-VAD or 25 μM Z-IETD completely inhibited TNF-induced cytotoxic diff-MN9D death at all concentrations of TNF examined (**Figure 3.5 c**), demonstrating that caspase activation is obligate for TNF-induced cytotoxic cell death in terminally differentiated MN9D cells. However, in the case of C2-cer-treated diff-MN9D cells, neither Z-VAD nor Z-IETD was sufficient to attenuate C2-cer-induced cytotoxic cell death (**Figure 3.5 b**). Although C2-cer treatment of diff-MN9D cells induces caspase cleavage (**Figure 3.5 a**), caspase signaling does not seem to be required for C2-cer-induced cell death under the experimental conditions employed here (**Figure 3.5 b**).

DISCUSSION

Our data indicate that TNF-induced cytotoxicity in diff-MN9D cells is partially ceramide-dependent, involves SMase hydrolysis of inactive sphingomyelin into active ceramide, but does not require *de novo* ceramide synthesis (**Figure 3.2**). The SMase

catabolic pathway for ceramide formation is rapidly and transiently activated by diverse endogenous and exogenous stimuli, and A-SMase and N-SMase activation of ceramide occurs within seconds to minutes compared to *de novo* biosynthesis of ceramide, which predominantly accounts for delayed and sustained ceramide production (Wiegmann, Schutze et al. 1994). SMase-generated ceramide is therefore considered to be the major pathway for ceramide formation in early signal transduction (Jana, Hogan et al. 2009). Our findings that inhibition of SMases (but not inhibition of de novo ceramide synthesis) attenuated TNF-dependent cytotoxicity are consistent with a biochemical pathway that involves rapid and early activation of membrane-bound SMases upon binding of TNF ligand to its plasma membrane receptor TNFR1. Importantly, both SMase forms (acidic and neutral) are capable of hydrolyzing ceramide from inactive sphingomyelin within neurons (de Chaves, Bussiere et al. 2001) and it has been suggested that different SMase pathways generate different pools of activated ceramide within the same neurons in response to similar and divergent stimuli (Yu, Nikolova-Karakashian et al. 2000), likely in concert with cell and context-dependent signaling cofactors.

Our data demonstrate that ER stress is a mechanism employed by TNF and ceramide that results in cytotoxicity in diff-MN9D cells (**Figure 3.3**). TNF and ceramide have been shown to impinge on ER stress mechanisms in non-neuronal cells types (Xue, Piao et al. 2005; Sauane, Su et al. 2010) and ER stress has been implicated as a potentially important pathway in PD pathogenesis (Yamamuro, Yoshioka et al. 2006), being coupled to the cell death program in DA cells in response to the toxin paraquat (Chinta, Rane et al. 2008); however it is not fully clear if ER stress is a cause, result, or

epiphenomenon in PD. Here we show for the first time, that inflammatory signaling through TNF and ceramide induces ER stress in DA neuron-like cells. Interestingly, there was divergence in the ER stress target genes that were activated in diff-MN9D cells in response to TNF (**figure 3.3 a, b**) versus C2-cer (**figure 3.3 c**) treatment (and data not shown). This effect could be due to preferential activation of certain ER stress pathways in response to TNF signaling through TNFR1-stimulated ceramide generation by SMase versus exogenous C2-cer, or it could be due to temporal regulation of the ER stress response that was difficult to dissect under the current experimental conditions.

Our data also indicate that another mechanism of TNF and C2-cer-induced cytotoxicity in diff-MN9D cells is compromised mitochondrial membrane potential (**Figure 3.4**). Compromised mitochondrial function has been strongly implicated in PD pathophysiology (Lin and Beal 2006) but to our knowledge compromised mitochondrial membrane potential in response to inflammatory stimuli (in this case TNF and C2-cer) has never been demonstrated in DA cells or DA neurons. In NGF-differentiated PC12 cells, ceramide signaling has been shown to increase mitochondrial free calcium levels and to induce ultrastructural alterations (Muriel, Lambeng et al. 2000). Furthermore, ceramide-induced increases in mitochondrial free calcium were subsequently shown to originate in the ER in a ROS-independent fashion (Darios, Lambeng et al. 2003). Future studies should examine if disrupted intracellular or mitochondrial Ca^{2+} homeostasis plays a causative or synergistic role in TNF or ceramide-induced compromise of mitochondrial membrane potential to elucidate the relative impact of TNF-induced ceramide signaling on mitochondrial function and integrity in DA neurons.

Our data further demonstrate that both TNF and C2-cer elicit caspase activation; however pharmacological caspase inhibition was sufficient to block TNF-induced cytotoxic death but insufficient to block C2-cer-induced cytotoxic death in diff-MN9D cells (**Figure 3.5**). Interestingly, caspase 8, which is an initiator caspase, seems to be the pivotal caspase that mediates downstream caspase-dependent cell death of diff-MN9D cells in response to TNF as the caspase-8 specific inhibitor Z-IETD attenuated TNF-induced cell death equivalently to the pan caspase inhibitor Z-VAD (**Figure 3.5**). Short-term C2-cer treatment (for 5 hrs) did induce caspase cleavage and activation (**Figure 3.5 a**) but neither Z-VAD nor Z-IETD was sufficient to ameliorate C2-cer-induced cytotoxic death in diff-MN9D cells after treatment with C2-cer for 24 hrs (**Figure 3.5 b**).

This divergence in the overall requirement for caspase signaling in TNF- versus C2-cer-dependent cytotoxicity in diff-MN9D cells could be due to several factors. The simplest explanation may be that TNF signaling generates ceramide in a physiological range which acts in concert with other TNF receptor-mediated signaling events to trigger downstream caspase-dependent apoptotic processes whereas addition of exogenous C2-cer (at concentrations that may surpass a physiological range) artificially bypasses TNF receptor-mediated events and exerts toxic effects by targeting other organelles in addition to mitochondria. In support of this interpretation, Rotolo and colleagues observed that Jurkat T cells require A-SMase translocation to plasma membrane lipid microdomains to elicit localized ceramide production and eventual apoptotic cell death (Rotolo, Zhang et al. 2005). Interestingly, Rotolo et al. observed that A-SMase translocation occurred via

two distinct mechanisms: a caspase-dependent mechanism utilized by FasL, and a previously unrecognized caspase-independent mechanism utilized by short wave ultraviolet irradiation (UV-C). Rotolo and colleagues determined that the caspase-independent mechanism of A-SMase translocation led to Type II cell death of Jurkat cells and that UV-C treatment of Jurkat cells activates the sphingomyelin pathway independent of caspase 8 or in the presence of a pan caspase inhibitor. In this study, the authors note that while A-SMase is not a direct target of caspase 8, surface translocation of A-SMase activated by FasL or other TNF superfamily ligands requires minimal caspase 8 and FADD activation (~2% activation is sufficient). Importantly, we infer that caspase 8 is initially activated in diff-MN9D cells after 5 hrs of treatment with 20 μM C2-cer (**Figure 3.5 a**) and is likewise activated in diff-MN9D cells in response to TNF treatment (**Figure 3.5 c**). However, in the case of diff-MN9D cells, perhaps exogenous addition of C2-ceramide bypasses the step of A-SMase translocation to lipid microdomains in the plasma membrane as well as the concomitant activation of caspase cascades from the signaling complex assembled in microdomains at the cell membrane that otherwise occurs in response to TNFR1 activation.

Alternatively, it is possible that C2-cer initially induces caspase 8 activation, but downstream executioner caspase cascades are not subsequently activated robustly or long enough to elicit caspase-dependent apoptotic cell death. Additionally, Grullich and colleagues (Grullich, Sullards et al. 2000) report that in the context of cytokine-induced ceramide formation, generation of ceramide is initiator caspase-dependent and occurs prior to commitment to the effector phase of apoptosis. It was previously known that the

cytokine CD95 induced apoptotic cell death by two distinct mechanisms: so-called Type I cells respond to cytokine stimulation with robust activation of initiator caspase signaling and induce apoptosis via a hierarchal caspase cascade independent of mitochondrial membrane permeability transition and release of mitochondrial apoptogenic factors (i.e. intrinsic apoptosis), in contrast to Type II cells in which effector caspase activation occurs downstream of mitochondrial dysfunction in a fashion that is augmented by ceramide analogs but inhibited by Bcl-2 (i.e. extrinsic apoptosis) (Scaffidi, Schmitz et al. 1999). This mechanism implies a model whereby other TNF superfamily cytokines may induce signaling similar to CD95 and the sensitivity of Type II cells to ceramide would likely occur under conditions where initiator caspase activation is limiting (Grullich, Sullards et al. 2000).

Additionally, it is possible that exogenous addition of ceramide is sufficient to elicit caspase independent cell death via release of mitochondrial apoptogenic factors, but that engagement of TNFR1 leads to SMase-dependent production of ceramide and caspase-dependent cell death of diff-MN9D cells. Lastly, Deerberg and colleagues report that there is a combined requirement of both the ER and mitochondria in the induction of signaling pathways of ceramide-mediated caspase-independent programmed cell death in Jurkat cells (Deerberg, Sosna et al. 2009) and a similar mechanism may be employed in C2-ceramide treated diff-MN9D cells.

Collectively, our data support a model whereby TNF concentrations in the range that elicit half-maximal cytotoxicity and correspond to low TNF receptor 1 (TNFR1)

occupancy activate SMase leading to downstream ceramide signaling and metabolism, thereby inducing ER stress and compromising mitochondrial membrane potential, to culminate in caspase-dependent cytotoxic cell death of DA neurons (**Figure 3.6**). Interestingly, ceramide metabolism has recently received attention as an emerging pathway involved in Lewy body disease (Mata, Samii et al. 2008). PD is considered to be a Lewy body disorder and Lewy body formation, which is caused by the intraneuronal aggregation and clustering of α-synuclein and ubiquitin proteins, is the histopathophysiological hallmark of PD. Some of the genes known to be involved in the genetics of Lewy body disease or heritable PD share in common the fact that they impinge on ceramide metabolism (Bras, Singleton et al. 2008). For example, heterozygous loss-of-function mutations of the glucocerebrosidase (GBA) locus have recently been shown to be a potent risk factor for PD (Aharon-Peretz, Rosenbaum et al. 2004; Bras, Paisan-Ruiz et al. 2009). GBA catalyzes the dissolution of glucocerebrosidase to ceramide and glucose. The lysosomal storage disorder Gaucher's disease (GD) arises from homozygous mutations in GBA, leading to extreme lysosomal accumulation of GBA substrates and onset of GD symptoms (Fuller, Lovejoy et al. 2005). Interestingly however, GBA substrates do not significantly accumulate in the lysosomes of patients with heterozygous GBA mutations, lending support to the hypothesis that generally disrupted ceramide metabolism, as opposed to specific loss of GBA function, may be an initiating factor in PD (Bras, Singleton et al. 2008).

Notably, desipramine, an inhibitor of A-SMase, is a tricyclic antidepressant that functions to inhibit A-SMase by inducing specific and rapid intracellular degradation of

A-SMase and concomitant abolishment of enzymatic activity (Hurwitz, Ferlinz et al. 1994). The actions of desipramine as an antidepressant seems to be independent of its effects on A-SMase, but desipramine has been used in clinical trials to treat depression in PD patients (Devos, Dujardin et al. 2008). These trials were very short-lived however, and the effect of desipramine on ceramide signaling was not evaluated as an outcome. Our data and the data of other groups associating ceramide biology and metabolism with PD warrant future studies examining the potential neuroprotective effects of inhibition of A-SMase or N-SMase in animal models of PD.

FIGURES

Figure 3.1

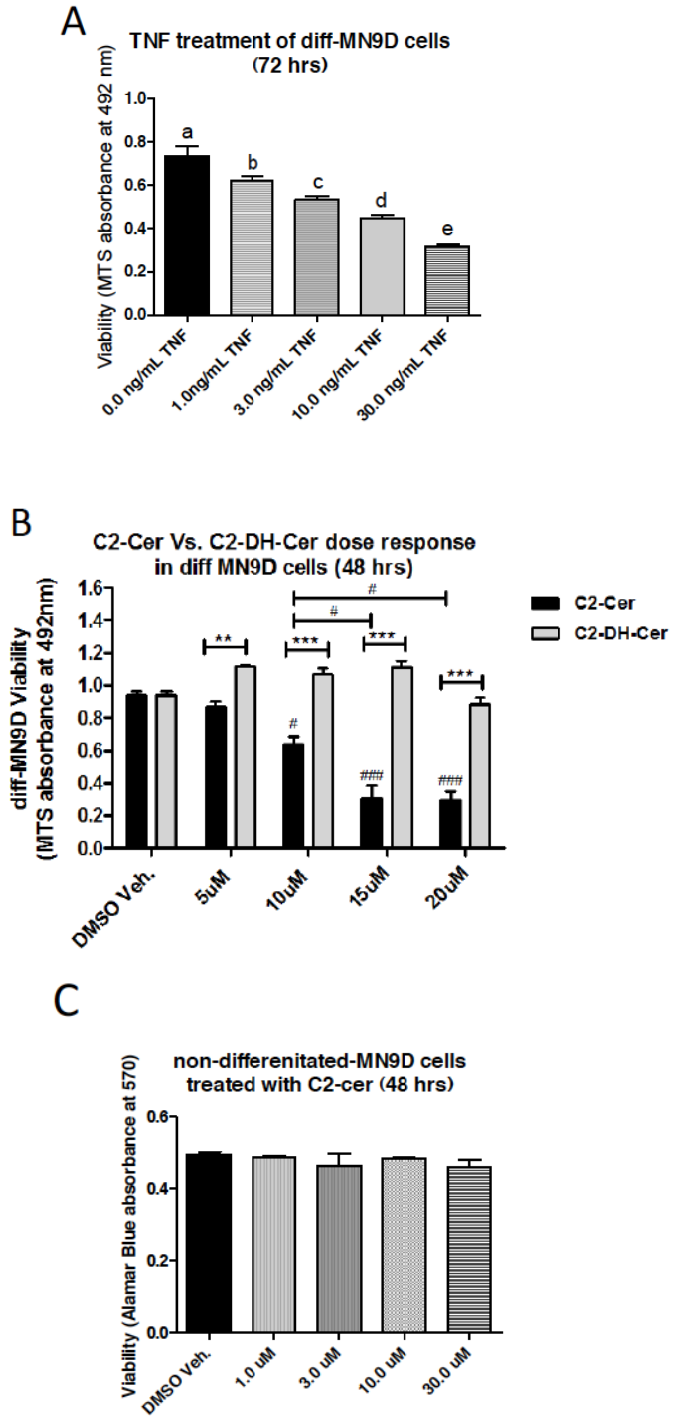

Figure 3.1. TNF and C2-ceramide induce cytotoxic cell death of diff-MN9D cells (but not non-diff-MN9D cells) in a dose dependent manner.

(a) Dose-dependent cytotoxic cell death in diff-MN9D cells treated with TNF for 72 hrs. Stats: One-way ANOVA, Bonferroni's post-hoc. Each letter represents statistical difference relative to any different letter ($p<0.05$). (b) Dose-dependent C2-ceramide-induced cytotoxic death in diff-MN9D cells. Cells were treated with ceramide (C2-cer), or with equal concentrations of C2-dihydroceramide (C2-DH-cer) as a negative control. Stats: Two-way ANOVA, Bonferroni's post-hoc test for comparing C2-cer conditions to C2-DH-cer conditions. **$p<0.01$, ***$p<0.001$. One-way ANOVA to test for dose-dependent cell death in C2-cer conditions, # $p<0.05$, ###$p<0.001$ relative to DMSO vehicle or different C2-cer conditions as indicated. (c) Non-diff-MN9D cells are not sensitive to C2-cer-induced cell death as determined by the alamarBlue assay. Stats: One-way ANOVA, Bonferroni's post-hoc test; no significance. (a-c) All values represent group means +/- SEM, N=3-4.

Figure 3.2

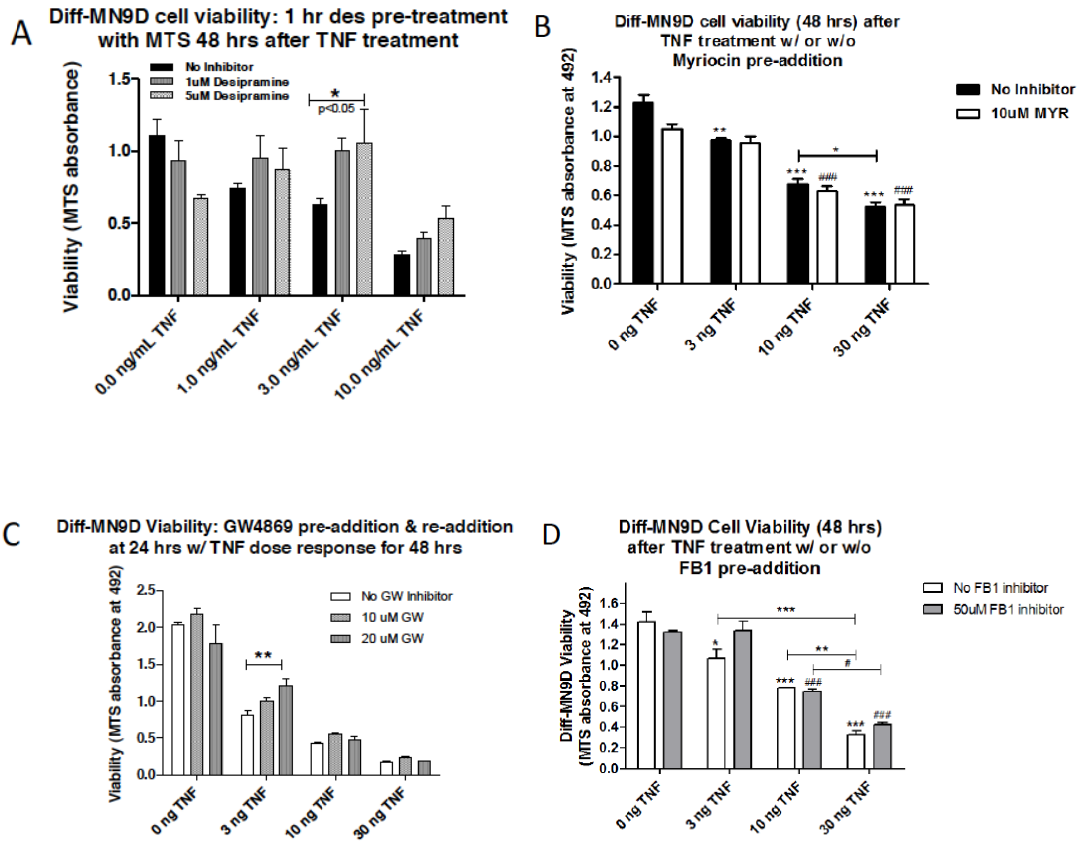
A
Diff-MN9D cell viability: 1 hr des pre-treatment with MTS 48 hrs after TNF treatment
No Inhibitor
1uM Desipramine
5uM Desipramine
p<0.05
Viability (MTS absorbance)
0.0 ng/mL TNF
1.0 ng/mL TNF
3.0 ng/mL TNF
10.0 ng/mL TNF
B
Diff-MN9D cell viability (48 hrs) after TNF treatment w/ or w/o Myriocin pre-addition
Viability (MTS absorbance at 492)
No Inhibitor
10uM MYR
0 ng TNF
3 ng TNF
10 ng TNF
30 ng TNF
C
Diff-MN9D Viability: GW4869 pre-addition & re-addition at 24 hrs w/ TNF dose response for 48 hrs
Viability (MTS absorbance at 492)
No GW Inhibitor
10 uM GW
20 uM GW
0 ng TNF
3 ng TNF
10 ng TNF
30 ng TNF
D
Diff-MN9D Cell Viability (48 hrs) after TNF treatment w/ or w/o FB1 pre-addition
Diff-MN9D Viability (MTS absorbance at 492)
No FB1 inhibitor
50uM FB1 inhibitor
0 ng TNF
3 ng TNF
10 ng TNF
30 ng TNF

Figure 3.2. TNF-induced cytotoxicity is partially ceramide-dependent, requiring ceramide formatin by sphingomyelinase hydrolysis of sphingomyelin but not *de novo* ceramide biosynthesis.

(a) TNF-induced cytoxic cell death is dependent on A-SMase hydrolysis of sphingomyelin. Desipramine significantly inhibited cytotoxic cell death induced by 3 ng/ml TNF. (c) TNF-induced cell death is partially dependent o on N-SMase hydrolysis of sphingomyeline. Diff-MN9D cells were pre-treated with GW4869 followed by TNF treatment. GW4869 partially attenuated TNF-induced cytotoxic death after 48 hrs, especially at 3ng/mL TNF. (b, d) TNF-induced death of diff-MN9D cells does not require *de novo* biosynthesis of ceramide. Neither myriocin (c, an inhibitor for serine palmitoyltransferase) nor fumonisin B1 (d, an inhibitor of ceramide synthase) had any affect onTNF-induced cell death in diff-MN9D cells. Stats: Two-way ANOVA, Bonferroni's post-hoc test to compare inhibitor conditions to TNF or C2-cer alone (no significance); One-way ANOVA, Bonferroni's post-hoc test to compare extent of dose-dependent cell death in response to increasing concentrations of TNF or C2-cer (no significance). (a-d) All values represent group means +/- SEM, N=3-4.

Figure 3.3

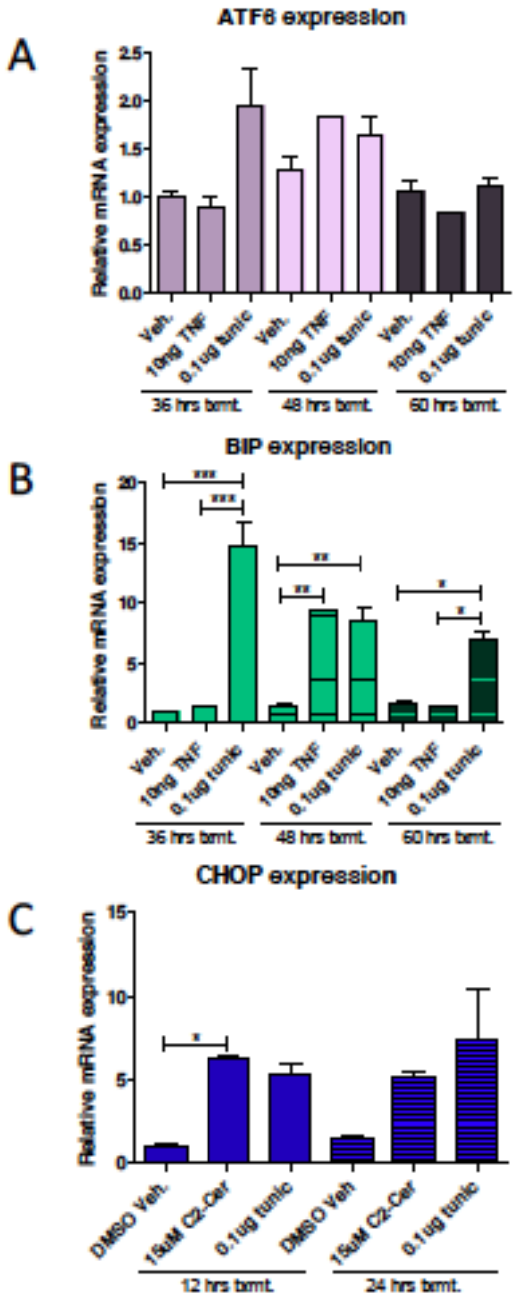
A
ATF6 expression
Relative mRNA expression
2.5
2.0
1.5
1.0
0.5
0.0
Veh.
10ng TNF
0.1ug tunic
Veh.
10ng TNF
0.1ug tunic
Veh.
10ng TNF
0.1ug tunic
36 hrs bmt.
48 hrs bmt.
60 hrs bmt.
B
BIP expression
Relative mRNA expression
20
15
10
5
0
***
***
**
**
*
*
Veh.
10ng TNF
0.1ug tunic
Veh.
10ng TNF
0.1ug tunic
Veh.
10ng TNF
0.1ug tunic
36 hrs bmt.
48 hrs bmt.
60 hrs bmt.
C
CHOP expression
Relative mRNA expression
15
10
5
0
*
DMSO Veh.
15uM C2-Cer
0.1ug tunic
DMSO Veh
15uM C2-Cer
0.1ug tunic
12 hrs bmt.
24 hrs bmt.

Figure 3.3. TNF and C2-ceramide-induced cytotoxicity involve ER stress pathways

Treatment of diff-MN9D cells with 10ng/ml TNF induced mRNA expression of BiP after 48 hrs treatment with TNF (b) but did not induce ATF6 or CHOP under similar conditions (a, data not shown). C2-cer treatment of diff-MN9D cells likewise induced ER stress by inducing CHOP mRNA after 12 hrs treatment with 15ul C2-cer, but had no effect on ATF-6 or BiP (data not shown). TNF and C2-cer induced ER stress was at time points prior to peak cell death and induced ER stress to levels comparable to tunicamyacin (tunic, a-c). Stats: One-way ANOVA, Bonferroni's post-hoc test. *$p<0.05$, **$p<0.01$, ***$p<0.001$, all relative to Veh or DMSO Veh at each timepoint. (a-c) All values represent group means +/- SEM, N=3.

Figure 3.4

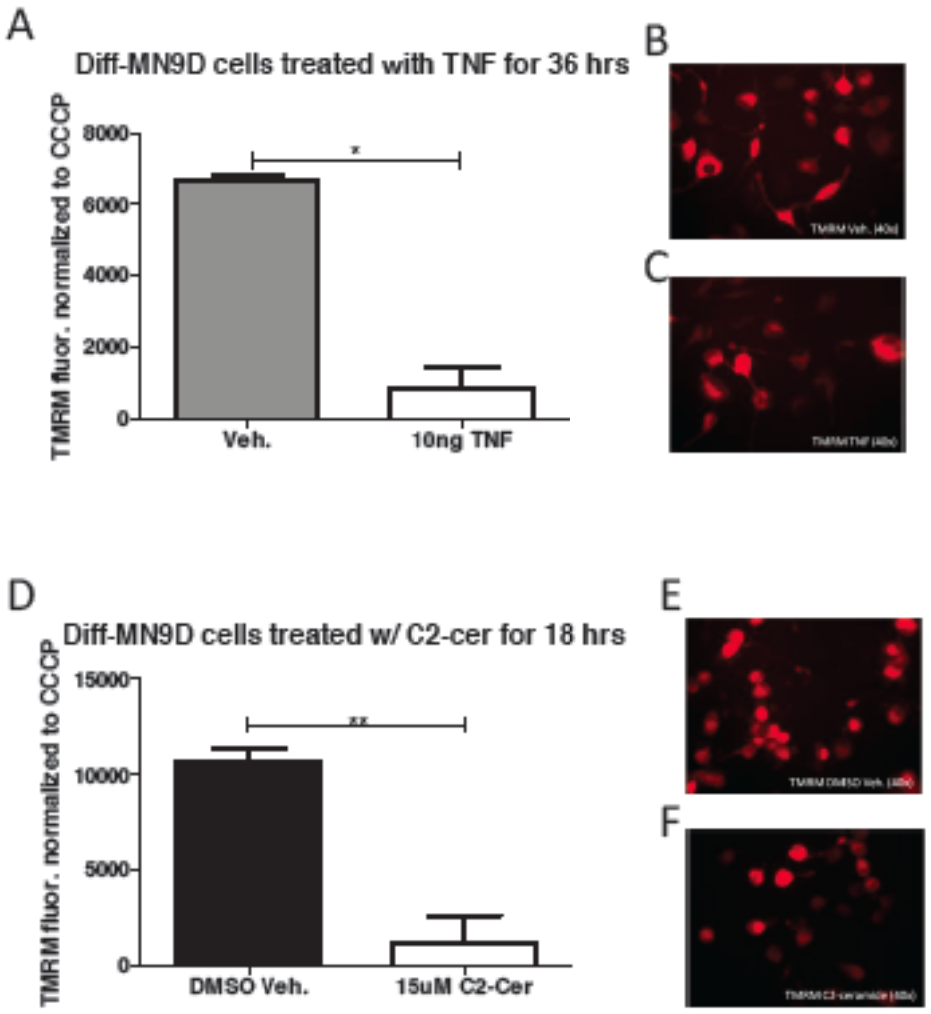
A
Diff-MN9D cells treated with TNF for 36 hrs
TMRM fluor. normalized to CCCP
8000
6000
4000
2000
0
*
Veh.
10ng TNF
B
C
D
Diff-MN9D cells treated w/ C2-cer for 18 hrs
TMRM fluor. normalized to CCCP
15000
10000
5000
0
**
DMSO Veh.
15uM C2-Cer
E
F

Figure 3.4. TNF and C2-ceramide compromise mitochondrial membrane in diff-MN9D cells hours before cell death occurs.

The TMRM assay was used to evaluate the effect of TNF or C2-cer treatment on mitochondrial membrane potential in diff-MN9D cells. Low TMRM/rhodamine fluorescence indicates loss of mitochondria membrane potential. TMRM cytofluorescence was normalized to CCCP + Veh or CCCP + TNF, as CCCP uncouples mitochondrial membranes. (a) Treatment of diff-MN9D cells with 10ng/ml TNF for 36 hrs significantly compromised mitochondria membrane potential in diff-MN9D cells as evidenced by less TMRM cytofluorescence relative to Vehicle (Veh.). Reprsentative 40x live-cell images of TMRM/rhodamine cytofluorescence in Veh. (b) or TNF (c) treated diff-MN9D cells. Treatment of diff-MN9D cells for 18 hrs with 15uM C2-cer also comprised mitochondrial membrane potential (d). Reprsentative live-cell images (at 40x) of DMSO (e) or C2-cer (f) treated diff-MN9D cells. Stats: One-way ANOVA, Bonferroni's post-hoc *$p<0.05$, **$p<0.01$. (a, d) All values represent group means +/- SEM, N=3.

Figure 3.5

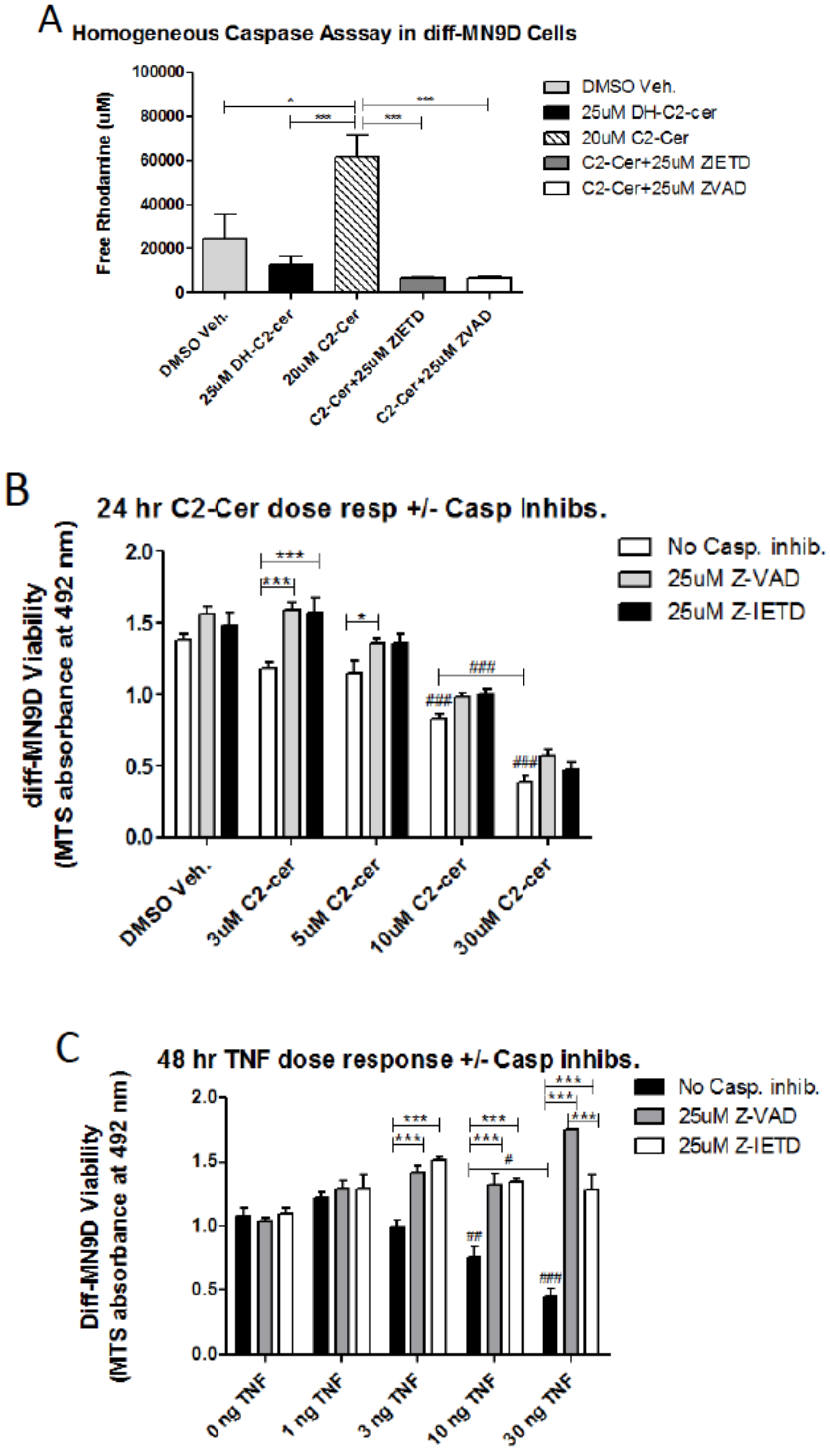
A
Homogeneous Caspase Asssay in diff-MN9D Cells
Free Rhodamine (uM)
100000
80000
60000
40000
20000
0
DMSO Veh.
25uM DH-C2-cer
20uM C2-Cer
C2-Cer+25uM ZIETD
C2-Cer+25uM ZVAD
B
24 hr C2-Cer dose resp +/- Casp Inhibs.
diff-MN9D Viability
(MTS absorbance at 492 nm)
2.0
1.5
1.0
0.5
0.0
No Casp. inhib.
25uM Z-VAD
25uM Z-IETD
DMSO Veh.
3uM C2-cer
5uM C2-cer
10uM C2-cer
30uM C2-cer
C
48 hr TNF dose response +/- Casp inhibs.
Diff-MN9D Viability
(MTS absorbance at 492 nm)
No Casp. inhib.
25uM Z-VAD
25uM Z-IETD
0 ng TNF
1 ng TNF
3 ng TNF
10 ng TNF
30 ng TNF

Figure 3.5. TNF and C2-ceramide treatment of differentiated MN9D cells induces caspase activation, which is a mechanism of cytotoxic cell death in response to TNF.

(a) Homogeneous caspase assay in diff-MN9D cells. Cells were treated with C2-cer alone or in combination with Z-VAD or Z-IETD or with DMSO or C2-DH-cer controls for 5 hrs. C2-cer significantly activated caspases. All values represent SEM (N=3-4) and were calculated from a standard curve. Stats: One-way ANOVA, Bonferroni's post-hoc test. *$p<0.05$, ***$p<0.001$. (b) C2-cer induced death of diff-MN9D cells is not caspase dependent. Co-treatment of C2-cer + Z-VAD or C2-cer + Z-IETD was insufficient to attenuate TNF-induced death of diff-MN9D cells. Stats: One-way ANOVA, Bonferroni's post-hoc test (for C2-cer-induced death, no caspase inhibition conditions), ###$p<0.001$. Two-way ANOVA, Bonferroni's post-hoc test (for comparing C2-cer no caspase inhibition conditions to C2-cer + Z-VAD or C2-cer + Z-IETD at each C2-cer concentration), *$p<0.05$, ***$p<0.001$. (c) TNF-induced death of diff-MN9D cells is caspase-dependent. Co-treatment of TNF + Z-VAD or TNF + Z-IETD completely blocked TNF-induced cell death in diff-MN9D cells. Stats: Two-Way ANOVA, Bonferoni's post-hoc test to compare inhibitor conditions to TNF or C2-cer alone conditions. *$p<0.05$, ***$p<0.001$. One-way ANOVA, Bonferroni's post-hoc test to compare the effect of increased TNF or C2-cer dose on diff-MN9D viability in the MTS assay, # $p<0.05$, ## $p<0.01$, ### $p<0.001$. (a-c) All values represent group means +/- SEM, N=3-4.

Figure 3.6

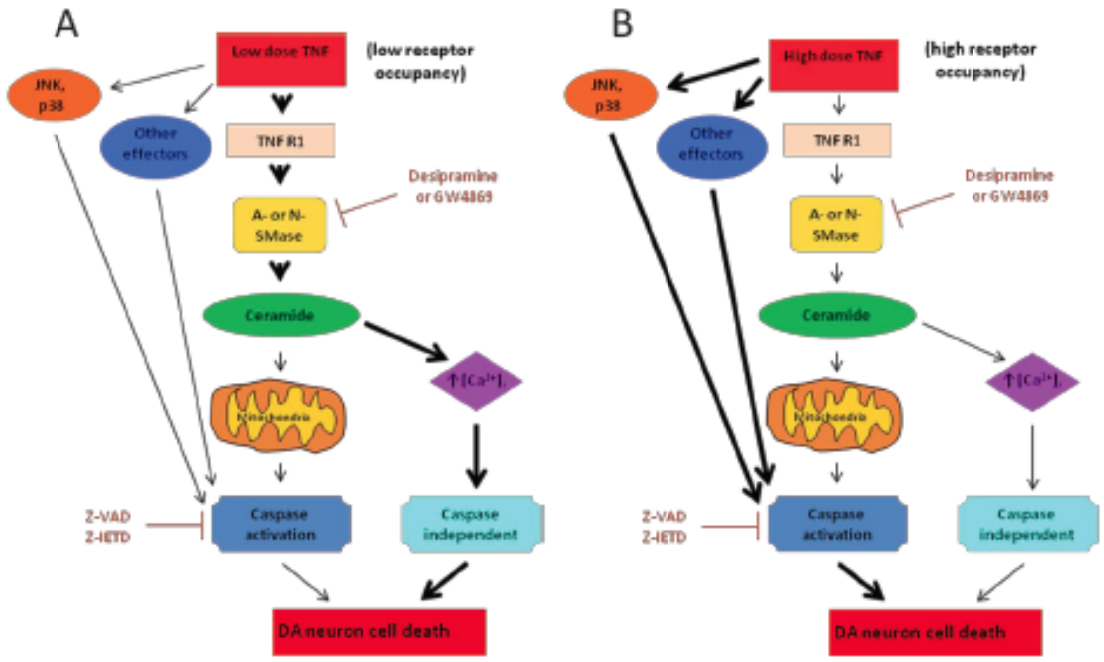
A
Low dose TNF
(low receptor occupancy)
JNK, p38
Other effectors
TNFR1
Desipramine or GW4869
A- or N-SMase
Ceramide
↑[Ca2+]
Mitochondria
Z-VAD
Z-IETD
Caspase activation
Caspase independent
DA neuron cell death
B
High dose TNF
(high receptor occupancy)
JNK, p38
Other effectors
TNFR1
Desipramine or GW4869
A- or N-SMase
Ceramide
↑[Ca2+]
Mitochondria
Z-VAD
Z-IETD
Caspase activation
Caspase independent
DA neuron cell death

Figure 3.6 Schematic for TNF and C2-ceramide induced cytotoxicity in DA neurons.

Under conditions of low-dose TNF/low TNFR1 occupancy, TNF signaling activates SMase enzymes to generate ceramide by hydrolysis of inactive sphingomyelin, leading to caspase dependent cell death. Under conditions of high TNF/high TNFR1 ocupancy, ceramide inhibition no longer attenuates TNF-induced cytotoxic cell death, likely due to signaling through alternate down-stream mediators. All concentrations of TNF tested induced apoptotic cell death that could be blocked equivalently by Z-VAD (a pan caspase inhibitor) or by Z-IETD (a caspase-8 specific inhibitor). C2-cer-induced cell death is not ameliorated by either caspase inhibitor used.

REFERENCES

Aharon-Peretz, J., H. Rosenbaum, et al. (2004). "Mutations in the glucocerebrosidase gene and Parkinson's disease in Ashkenazi Jews." N Engl J Med 351(19): 1972-1977.

Bertazza, L. and S. Mocellin (2008). "Tumor necrosis factor (TNF) biology and cell death." Front Biosci 13: 2736-2743.

Betarbet, R., T. B. Sherer, et al. (2000). "Chronic systemic pesticide exposure reproduces features of Parkinson's disease." Nat Neurosci 3(12): 1301-1306.

Bielawska, A., H. M. Crane, et al. (1993). "Selectivity of ceramide-mediated biology. Lack of activity of erythro-dihydroceramide." J Biol Chem 268(35): 26226-26232.

Bras, J., C. Paisan-Ruiz, et al. (2009). "Complete screening for glucocerebrosidase mutations in Parkinson disease patients from Portugal." Neurobiol Aging 30(9): 1515-1517.

Bras, J., A. Singleton, et al. (2008). "Emerging pathways in genetic Parkinson's disease: Potential role of ceramide metabolism in Lewy body disease." FEBS J 275(23): 5767-5773.

Brugg, B., P. P. Michel, et al. (1996). "Ceramide induces apoptosis in cultured mesencephalic neurons." J Neurochem 66(2): 733-739.

Carvey, P. M., E. Y. Chen, et al. (2005). "Intra-parenchymal injection of tumor necrosis factor-alpha and interleukin 1-beta produces dopamine neuron loss in the rat." J Neural Transm 112(5): 601-612.

Chinta, S. J., A. Rane, et al. (2008). "Coupling endoplasmic reticulum stress to the cell death program in dopaminergic cells: effect of paraquat." Neuromolecular Med 10(4): 333-342.

Choi, H. K., L. Won, et al. (1992). "Specific modulation of dopamine expression in neuronal hybrid cells by primary cells from different brain regions." Proc Natl Acad Sci U S A 89(19): 8943-8947.

Darios, F., N. Lambeng, et al. (2003). "Ceramide increases mitochondrial free calcium levels via caspase 8 and Bid: role in initiation of cell death." J Neurochem 84(4): 643-654.

de Chaves, E. P., M. Bussiere, et al. (2001). "Ceramide inhibits axonal growth and nerve growth factor uptake without compromising the viability of sympathetic neurons." J Biol Chem 276(39): 36207-36214.

Deerberg, A., J. Sosna, et al. (2009). "Differential protection by wildtype vs. organelle-specific Bcl-2 suggests a combined requirement of both the ER and mitochondria in ceramide-mediated caspase-independent programmed cell death." Radiat Oncol 4: 41.

Devos, D., K. Dujardin, et al. (2008). "Comparison of desipramine and citalopram treatments for depression in Parkinson's disease: a double-blind, randomized, placebo-controlled study." Mov Disord 23(6): 850-857.

Fuller, M., M. Lovejoy, et al. (2005). "Immunoquantification of beta-glucosidase: diagnosis and prediction of severity in Gaucher disease." Clin Chem 51(11): 2200-2202.

Garcia-Ruiz, C., A. Colell, et al. (1997). "Direct effect of ceramide on the mitochondrial electron transport chain leads to generation of reactive oxygen species. Role of mitochondrial glutathione." J Biol Chem 272(17): 11369-11377.

Ghavami, S., M. Eshraghi, et al. (2009). "Role of BNIP3 in TNF-induced cell death--TNF upregulates BNIP3 expression." Biochim Biophys Acta 1793(3): 546-560.

Goni, F. M. and A. Alonso (2006). "Biophysics of sphingolipids I. Membrane properties of sphingosine, ceramides and other simple sphingolipids." Biochim Biophys Acta 1758(12): 1902-1921.

Grell, M. (1995). "Tumor necrosis factor (TNF) receptors in cellular signaling of soluble and membrane-expressed TNF." J Inflamm 47(1-2): 8-17.

Grell, M., H. Wajant, et al. (1998). "The type 1 receptor (CD120a) is the high-affinity receptor for soluble tumor necrosis factor." Proc Natl Acad Sci U S A 95(2): 570-575.

Grullich, C., M. C. Sullards, et al. (2000). "CD95(Fas/APO-1) signals ceramide generation independent of the effector stage of apoptosis." J Biol Chem 275(12): 8650-8656.

Hunot, S. and E. C. Hirsch (2003). "Neuroinflammatory processes in Parkinson's disease." Ann Neurol 53 Suppl 3: S49-58; discussion S58-60.

Hunot, S., M. Vila, et al. (2004). "JNK-mediated induction of cyclooxygenase 2 is required for neurodegeneration in a mouse model of Parkinson's disease." Proc Natl Acad Sci U S A 101(2): 665-670.

Hurwitz, R., K. Ferlinz, et al. (1994). "The tricyclic antidepressant desipramine causes proteolytic degradation of lysosomal sphingomyelinase in human fibroblasts." Biol Chem Hoppe Seyler 375(7): 447-450.

Jana, A., E. L. Hogan, et al. (2009). "Ceramide and neurodegeneration: susceptibility of neurons and oligodendrocytes to cell damage and death." J Neurol Sci 278(1-2): 5-15.

Kolesnick, R. (1994). "Signal transduction through the sphingomyelin pathway." Mol Chem Neuropathol 21(2-3): 287-297.

Kolesnick, R. and D. W. Golde (1994). "The sphingomyelin pathway in tumor necrosis factor and interleukin-1 signaling." Cell 77(3): 325-328.

Kolesnick, R. N. and M. Kronke (1998). "Regulation of ceramide production and apoptosis." Annu Rev Physiol 60: 643-665.

Kurrasch, D. M., J. Huang, et al. (2004). "Quantitative real-time polymerase chain reaction measurement of regulators of G-protein signaling mRNA levels in mouse tissues." Methods Enzymol 389: 3-15.

Lee, K., W. Tirasophon, et al. (2002). "IRE1-mediated unconventional mRNA splicing and S2P-mediated ATF6 cleavage merge to regulate XBP1 in signaling the unfolded protein response." Genes Dev 16(4): 452-466.

Lin, M. T. and M. F. Beal (2006). "Mitochondrial dysfunction and oxidative stress in neurodegenerative diseases." Nature 443(7113): 787-795.

Lindholm, D., H. Wootz, et al. (2006). "ER stress and neurodegenerative diseases." Cell Death Differ 13(3): 385-392.

Ling, Y. H., T. Li, et al. (2009). "Activation of ER stress and inhibition of EGFR N-glycosylation by tunicamycin enhances susceptibility of human non-small cell lung cancer cells to erlotinib." Cancer Chemother Pharmacol 64(3): 539-548.

Luberto, C., D. F. Hassler, et al. (2002). "Inhibition of tumor necrosis factor-induced cell death in MCF7 by a novel inhibitor of neutral sphingomyelinase." J Biol Chem 277(43): 41128-41139.

Ma, Y., J. W. Brewer, et al. (2002). "Two distinct stress signaling pathways converge upon the CHOP promoter during the mammalian unfolded protein response." J Mol Biol 318(5): 1351-1365.

MacEwan, D. J. (2002). "TNF receptor subtype signalling: differences and cellular consequences." Cell Signal 14(6): 477-492.

Mata, I. F., A. Samii, et al. (2008). "Glucocerebrosidase gene mutations: a risk factor for Lewy body disorders." Arch Neurol 65(3): 379-382.

McCoy, M. K., T. N. Martinez, et al. (2006). "Blocking soluble tumor necrosis factor signaling with dominant-negative tumor necrosis factor inhibitor attenuates loss of dopaminergic neurons in models of Parkinson's disease." J Neurosci 26(37): 9365-9375.

McGeer, P. L., S. Itagaki, et al. (1988). "Rate of cell death in parkinsonism indicates active neuropathological process." Ann Neurol 24(4): 574-576.

McGeer, P. L., S. Itagaki, et al. (1988). "Reactive microglia are positive for HLA-DR in the substantia nigra of Parkinson's and Alzheimer's disease brains." Neurology 38(8): 1285-1291.

McGuire, S. O., Z. D. Ling, et al. (2001). "Tumor necrosis factor alpha is toxic to embryonic mesencephalic dopamine neurons." Exp Neurol 169(2): 219-230.

Mortiboys, H. and Bandmann, O. (2008). Measuring Mitochondrial Membrane Potential using the FLUOstar Omega Microplate Reader. Univ. of Sheffield. UK. BMG Biotech Application Notes.

Muriel, M. P., N. Lambeng, et al. (2000). "Mitochondrial free calcium levels (Rhod-2 fluorescence) and ultrastructural alterations in neuronally differentiated PC12 cells during ceramide-dependent cell death." J Comp Neurol 426(2): 297-315.

Nagatsu, T., M. Mogi, et al. (2000). "Changes in cytokines and neurotrophins in Parkinson's disease." J Neural Transm Suppl(60): 277-290.

Nishikawa, A. and S. Mizuno (2001). "The efficiency of N-linked glycosylation of bovine DNase I depends on the Asn-Xaa-Ser/Thr sequence and the tissue of origin." Biochem J 355(Pt 1): 245-248.

Obeid, L. M., C. M. Linardic, et al. (1993). "Programmed cell death induced by ceramide." Science 259(5102): 1769-1771.

Rotolo, J. A., J. Zhang, et al. (2005). "Caspase-dependent and -independent activation of acid sphingomyelinase signaling." J Biol Chem 280(28): 26425-26434.

Sauane, M., Z. Z. Su, et al. (2010). "Ceramide plays a prominent role in MDA-7/IL-24-induced cancer-specific apoptosis." J Cell Physiol 222(3): 546-555.

Sawada, M., S. Nakashima, et al. (2000). "Ordering of ceramide formation, caspase activation, and Bax/Bcl-2 expression during etoposide-induced apoptosis in C6 glioma cells." Cell Death Differ 7(9): 761-772.

Scaffidi, C., I. Schmitz, et al. (1999). "Differential modulation of apoptosis sensitivity in CD95 type I and type II cells." J Biol Chem 274(32): 22532-22538.

Tang, L., R. D. Todd, et al. (1994). "Pharmacological and functional characterization of D2, D3 and D4 dopamine receptors in fibroblast and dopaminergic cell lines." J Pharmacol Exp Ther 268(1): 495-502.

Tansey, M. G., T. C. Frank-Cannon, et al. (2008). "Neuroinflammation in Parkinson's disease: is there sufficient evidence for mechanism-based interventional therapy?" Front Biosci 13: 709-717.

Tartaglia, L. A., M. Rothe, et al. (1993). "Tumor necrosis factor's cytotoxic activity is signaled by the p55 TNF receptor." Cell 73(2): 213-216.

Thomas, B. (2009). "Parkinson's disease: from molecular pathways in disease to therapeutic approaches." Antioxid Redox Signal 11(9): 2077-2082.

Wahner, A. D., J. S. Sinsheimer, et al. (2007). "Inflammatory cytokine gene polymorphisms and increased risk of Parkinson disease." Arch Neurol 64(6): 836-840.

Wang, P. X. and P. W. Sanders (2007). "Immunoglobulin light chains generate hydrogen peroxide." J Am Soc Nephrol 18(4): 1239-1245.

Wang, Z., M. Cui, et al. (2007). "Angiopoietin-1 protects H9c2 cells from H2O2-induced apoptosis through AKT signaling." Biochem Biophys Res Commun 359(3): 685-690.

Wiegmann, K., S. Schutze, et al. (1994). "Functional dichotomy of neutral and acidic sphingomyelinases in tumor necrosis factor signaling." Cell 78(6): 1005-1015.

Willaime, S., P. Vanhoutte, et al. (2001). "Ceramide-induced apoptosis in cortical neurons is mediated by an increase in p38 phosphorylation and not by the decrease in ERK phosphorylation." Eur J Neurosci 13(11): 2037-2046.

Woodcock, J. (2006). "Sphingosine and ceramide signalling in apoptosis." IUBMB Life 58(8): 462-466.

Xue, X., J. H. Piao, et al. (2005). "Tumor necrosis factor alpha (TNFalpha) induces the unfolded protein response (UPR) in a reactive oxygen species (ROS)-dependent fashion, and the UPR counteracts ROS accumulation by TNFalpha." J Biol Chem 280(40): 33917-33925.

Yamamoto, K., H. Yoshida, et al. (2004). "Differential contributions of ATF6 and XBP1 to the activation of endoplasmic reticulum stress-responsive cis-acting elements ERSE, UPRE and ERSE-II." J Biochem 136(3): 343-350.

Yamamuro, A., Y. Yoshioka, et al. (2006). "Involvement of endoplasmic reticulum stress on the cell death induced by 6-hydroxydopamine in human neuroblastoma SH-SY5Y cells." Neurochem Res 31(5): 657-664.

Yu, Z. F., M. Nikolova-Karakashian, et al. (2000). "Pivotal role for acidic sphingomyelinase in cerebral ischemia-induced ceramide and cytokine production, and neuronal apoptosis." J Mol Neurosci 15(2): 85-97.

Zinszner, H., M. Kuroda, et al. (1998). "CHOP is implicated in programmed cell death in response to impaired function of the endoplasmic reticulum." Genes Dev 12(7): 982-995.

CHAPTER FOUR

Conclusions and Future Directions

CONCLUSIONS

At the time when I began this body of work, a role for inflammation as a potentially modifying environmental factor in Parkinson's disease was becoming more appreciated and evidence was emerging that supported a plausible role for inflammation in PD onset and progression. The rat LPS model of PD had recently been developed and in conjunction with the hard work of Melissa McCoy and others in our lab, we showed that blockade of soluble TNF signaling with novel dominant-negative inhibitors attenuated dopaminergic neuron cell loss in *vitro* and *in vivo*. Importantly, we demonstrated that solTNF inhibition significantly ameliorated dopaminergic cytotoxicity in two different rodent models of PD, an emerging inflammatory model (LPS) and a classic, oxidative neurotoxin model (6-OHDA) thereby cogently supporting a role for inflammation in general and TNF specifically as conserved mechanisms of neurotoxicity in PD onset and progression (Chapter 2; (McCoy, Martinez et al. 2006)).

However, at the onset of undertaking this study, it was not known which of the many signaling factors downstream of TNF was mediating the neuroinflammatory events we observed in our experiments. TNF activates numerous downstream effectors; I hypothesized that TNF-mediated cytotoxicity in DA neurons is ceramide-dependent. Ceramide is a sphingolipid that mimics the action of TNF in many cell types and is implicated in inflammation and programmed cell death, but has not been well studied in the context of dopaminergic neurons. The data in this dissertation situate ceramide

downstream of the cytotoxic actions of TNF in the murine MN9D dopamine cell line as evidenced by significant attenuation of TNF-induced cytotoxic cell death by pharmacologic inhibition of ceramide in TNF treated cell cultures.

Within cells, ceramide is formed via two major pathways: the *de novo* pathway of ceramide biosynthesis and a ceramide recycling pathway whereby hydrolysis of inactive sphingomyelin into active ceramide is accomplished by sphingomyelinase enzymes. Specifically, by pre-treating differentiated MN9D (diff-MN9D) cells with pharmacological inhibitors for sphingomyelinase, and with specific inhibitors for enzymes that function in the *de novo* ceramide pathway, then treating the same cells with exogenous recombinant mouse TNF protein, I show that sphingomyelinase hydrolysis of ceramide is requisite in TNF-induced cell death but that *de novo* biosynthesis of ceramide is not required. Evidence supporting this conclusion is that pre-treatment of diff-MN9D cells with desipramine or GW4869, inhibitors of acid or neutral sphingomyelinase respectively, attenuated cytotoxic cell death of TNF-treated diff-MN9D cells whereas pre-treatment with myriocin or fumonisin B1, inhibitors for serine palmitoyltransferase (the rate-limiting step in *de novo* ceramide biosynthesis) or ceramide synthase respectively, had no impact on TNF-induced cell death.

Additionally, using exogenously added cell permeant C2-ceramide (C2-cer) and recombinant mouse TNF protein, I show that ER stress is a mechanism of TNF/C2-cer induced cytotoxicity as evidenced by elevated mRNA levels of key mediators of ER stress, namely ATF6, BiP and CHOP. Importantly, TNF and C2-cer induced ER stress

occurred several hours before TNF/C2-cer induced cell death as measured by the MTS assay for cell viability. ER stress has been determined to be an important pathway in PD (Yamamuro, Yoshioka et al. 2006), but it is not fully clear if ER stress is a cause, result, or epiphenomenon in PD.

To further elucidate the mechanisms of TNF and C2-cer-induced cytotoxicity and to determine if TNF/ceramide signaling in diff-MN9D cells impinges on mitochondria, we used TMRM cytofluorescence to visualize mitochondrial membrane potential in TNF, C2-cer and vehicle treated diff-MN9D cells. Using the TMRM assay, we determined that TNF compromised mitochondrial membrane potential after 36 hours of treatment and C2-cer induced compromised mitochondrial membrane potential after 18 hours treatment as evidenced by reduced TMRM cytofluorescence relative to control/vehicle conditions. Importantly, the observed changes in mitochondrial membrane potential occurred after an approximately similar duration of TNF/C2-cer treatment that induced ER stress, indicating that two distinct but potentially crosstalking pathways implicated in PD pathogenesis, namely ER stress and mitochondrial dysregulation, are involved in TNF and C2-cer induced cytotoxicity in a dopamine cell line.

Moreover, my data also show that TNF and C2-cer induce caspase cleavage and activation, and that caspase signaling is a mechanism of TNF-induced cytotoxic cell death. Interestingly, under the experimental conditions used, while C2-cer treatment induced caspase cleavage that was detectable in the homogeneous caspase assay, caspase signaling is not required to elicit C2-cer dependent cytotoxic death in diff-MN9D cells, as

neither a pan-caspase inhibitor (Z-VAD) nor a caspase 8-specific inhibitor (Z-IETD) were sufficient to attenuate C2-cer induced death of diff-MN9D cells in the MTS assay. Notably, both Z-VAD and Z-IETD prevented TNF-induced cell death of diff-MN9D cells in the MTS assay demonstrating that caspase activation is obligate for TNF-induced cytotoxic cell death in terminally differentiated MN9D cells.

The divergence in the overall outcome of caspase signaling in TNF versus C2-cer treated diff-MN9D cells could be due to several factors. First, it is possible that C2-cer causes early caspase 8 activity (caspase 8 is an initiator caspase) but that downstream caspase activity is not robust or sustained enough to induce caspase-mediated cell death in C2-cer treated diff-MN9D cells, but TNF-induced caspase activity is sufficient to elicit caspase-dependent cell death. Second, it is possible that TNF signaling through TNFR1 activates A-SMase translocation to lipid microdomains in caspase-dependent manner where it assembles into signaling complexes with other signaling effectors, similar to A-SMase induced signaling observed by Rotolo and colleagues (Rotolo, Zhang et al. 2005). Perhaps exogenously added cell permeant C2-cer bypasses this step of A-SMase translocation to lipid microdomains in the plasma membrane as well as the concomitant activation of caspase cascades from the membrane assembled signaling complex that otherwise occurs in response to TNFR1 activation. Third, it is possible that exogenous addition of C2-ceramide is sufficient to elicit caspase independent cell death via release of mitochondrial apoptogenic factors, but that engagement of TNFR1 leads to SMase-dependent production of ceramide and caspase-dependent cell death of diff-MN9D cells.

Collectively, my data support a model whereby low-dose TNF and concomitant low TNF receptor 1 occupancy activate SMase leading to downstream ceramide signaling and metabolism, which induces ER stress and compromised mitochondrial membrane potential, culminating in caspase-dependent cytotoxic cell death of DA neurons (Chapter 3). My data indicate that inflammatory signaling alone is sufficient to induce adverse effects in dopamine cells in a manner that is consistent with well established pathogenic pathways in PD, and provide rationale for future studies designed to inhibit sphingomyelinase in *in vivo* models of PD.

Notably desipramine, a specific inhibitor of A-SMase, is an FDA approved tricyclic antidepressant that easily crosses the BBB. Desipramine's function as an antidepressant is independent of its inhibition of A-SMase. Desipramine has been studied in clinical trials to treat depression in PD patients. These trials were very short-term however, and perturbation of ceramide biology by desipramine was not a measured outcome. Our data and the data of other groups associating ceramide biology and metabolism with PD, coupled with the fact that desipramine is a federal drug association (FDA) approved drug with known pharmacokinetics warrant future trials in PD patients designed to examine the effect of A-SMase inhibition *in vivo*.

FUTURE DIRECTIONS

Based on the data that I have generated and a review of relevant literature, I propose numerous future experiments to further elucidate the role of TNF/ceramide signaling in the cytotoxic death of dopaminergic neurons. The results of these proposed studies may

contribute to the body of work from our laboratory and data from other groups that support targeting of inflammatory pathways as a potential therapy for Parkinson's disease.

Why are non-diff-MN9D cells recalcitrant to TNF/C2-ceramide?

To directly follow up on the data generated in this body of work, I would like to determine why non-diff-MN9D cells are recalcitrant to TNF and C2-ceramide. One possibility for this observation is that MN9D cells are more sensitive to TNF and C2-cer when they are terminally differentiated. To test this possibility, Q-RT-PCR can be used to determine if the mRNA expression profile of key determinants of sensitivity to TNF (i.e. TNFR1/2, A-and N-SMase etc.,) is divergent in diff-MN9D cells versus non-diff-MN9D cells. Also, it is possible that factors in serum provide neuronal protection from inflammatory triggers. Serum can be added back to diff-MN9D cells at the time of TNF/C2-cer treatment. Close observation of morphology and proliferative state would help determine if re-addition of serum affords protection by de-differentiating the MN9D cells.

Determine whether ceramide accumulation or ceramide metabolism is mediating cell death downstream of TNF/sphingomyelinase signaling

SMase-generated ceramide can occur on the order of minutes to hours, and has been identified as the pathway of ceramide generation downstream of TNF in our experiments. It would be of extreme interest to do a short term time course of TNF treatment in diff-MN9D cells and then measure ceramide levels to determine if there is transient

accumulation of ceramide shortly after a TNF stimulus. It is possible that TNF induces modest but physiologically relevant increases in ceramide, so it may be difficult to measure appreciable changes in ceramide levels.

As a corollary to measurements of TNF-induced increases in ceramide, it would likewise be of great interest to examine the role of ceramide metabolism in DA neurons. Because ceramide accumulation can be harmful, cellular levels of ceramide are very tightly regulated, and ceramide can be rapidly metabolized into numerous other sphingolipid moieties, including gangliosides. Therefore, it is possible that in our studies, TNFR1 signaling activates SMase hydrolysis of sphingomyelin to transiently increase ceramide levels; ceramide is then rapidly converted to gangliosides that then mediate the observable effects of TNF-induced cytotoxicity. There are two candidate gangliosides in the ceramide metabolism pathway that could be measured by a MS/MS lipidomics approach, namely GM1 and GD3. GM1 is highly abundant in neuronal membranes and has been shown to accumulate at the mitochondria-associated ER membrane and to link ER stress to Ca^{2+}-dependent mitochondrial apoptosis in neurons (Sano, Annunziata et al. 2009). Additionally, A-SMase generated ceramide has been shown to contribute to TNF-mediated apoptosis through GD3 formation (Colell, Morales et al. 2002).

Exploring the effects of TNF/C2-ceramide on mitochondrial dynamics

Mitochondrial dynamics play a crucial role in PD models and pathways as well as in our studies, which indicate that TNF and C2-cer impinge on mitochondria function in diff-MN9D cells. It is of interest to determine if and to what extent the observed decrease in

mitochondrial potential in response to TNF is ceramide-dependent. These experiments are in progress. Additionally it would be interesting to use cyclosporine A in the TMRM assay in TNF-treated diff-MN9D cells to determine if inhibition of the mitochondrial permeability transition pore blocks TNF (or C2-cer) induced changes in mitochondrial membrane potential.

Furthermore, it would be interesting to determine if TNF/ceramide play a role in mitochondrial fission/fusion. Mitochondrial fusion can be a cellular response to stress, and if sustained, is detrimental to mitochondrial and cellular function, while mitochondrial fission promotes segregation of terminally dysfunctional mitochondria. Mitochondrial fission thus allows other cellular pathways to compensate and potentially overcome the mitochondrial insult, by degradation of the affected mitochondria by the ALS system, and effectively "buying time" so to speak for mitochondrial biogenesis. Overall mitochondrial homeostasis is maintained when mitochondrial fission and fusion are in balance. It would be interesting to determine if TNF/C2-cer promote mitochondrial fusion either directly or indirectly, possibly through negative regulation of PINK1 or parkin which have been linked to mitochondrial fission (Whitworth and Pallanck 2009). Moreover, since both parkin and PINK1 play roles in mitochondrial dynamics, it would be interesting to determine if TNF/C2-cer diminish expression or alter mitochondrial localization of parkin/PINK.

Elucidating the contribution of ER stress in TNF/C2-ceramide-induced cytotoxicity

ER stress has been identified as an important pathway in PD but whether it is a cause of or effect of pathogenesis is uncertain. To clarify the role of ER stress in TNF/C2-cer mediated cytotoxicity, it is of interest to determine what extent of TNF-mediated ER stress is ceramide dependent in diff-MN9D cells. These experiments are currently underway by treating diff-MN9D cells with TNF and using pharmacological inhibitors for SMase.

Additionally, to determine if ER stress is causal or collateral in TNF/C2-cer induced cell death, salubrinal can be used in combination with TNF/C2-cer. Salubrinal is an inhibitor of phosphatase activity responsible for dephosphorylating Po4eIF2α (eIF2α down-regulates protein synthesis in the UPR) and in turn blocks ER stress-induced cell death (Boyce, Bryant et al. 2005). If ER stress is coupled to cell death, then salubrinal would be expected to attenuate cell death in response to TNF/C2-cer. Similarly, levels of caspase 12, an ER resident caspase that mediates ER stress-induced cell death can be measured (by Western blot) or inhibited (by specific pharmacological inhibitors) to further clarify to what extent ER stress is coupled to cell death in response to TNF/C2-cer.

Exploring intracellular calcium homeostasis in response to TNF/C2-ceramide

In this study, we first determined that TNF-induced cytotoxicity is partially ceramide-dependent. We next sought to explore TNF and ceramide-mediated mechanisms of cytotoxicity that had been observed in other cell systems to determine if similar TNF/ceramide signaling is intact in DA neurons/diff-MN9D cells. Along this line, one

pathway that should be further examined is intracellular calcium homeostasis. Ceramide has been shown to elicit robust increases in intracellular calcium (Kobrinsky, Spielman et al. 1999), and increases in intracellular calcium have been linked to ER stress, mitochondrial dysregulation and induction of apoptotic cell death. Therefore, in our experiments, TNF/C2-cer could elicit early increases in intracellular calcium that surpasses the buffering capacity of the cell and lead to the cytotoxic effects we observe (i.e., ER stress, compromised mitochondrial membrane potential and caspase activation). We have performed pilot studies examining TNF and C2-ceramide induced changes in intracellular calcium. TNF and C2-cer do seem to increase intracellular calcium, and pretreatment with the cell permeant calcium chelator BAPTA-AM significantly attenuated C2-cer induced diff-MN9D cell death in the MTS assay (data not shown). These experiments should be repeated however, and could be complimented by the use of pharmacological agents for different aspects of intracellular calcium biology. For example ionomycin, which facilitates movement of calcium across membranes, can be used to "dump" calcium stores, allowing for determination of total intracellular calcium when such experiments are preformed in calcium free buffer. Additionally, inhibitors for the IP3 receptor, the ryanodine receptor or the mitochondrial uniporter could be used to determine the intracellular source of TNF/C2-cer induced increases in calcium.

Determine if ceramide inhibits PI3K/AKT/PTEN pro-survival signaling in DA neurons

Arboleda and colleagues have demonstrated that ceramide can exert cytotoxicity by inhibition of the PI3K/AKT/PTEN pro-survival pathway (Arboleda, Morales et al. 2009). Specifically, ceramide causes the re-distribution of PTEN (phosphatase and homolog of

tensin) to the cell membrane (Goswami, Singh et al. 2005). PTEN is the main negative regulator of PI3K/AKT. Over-expression of PI3K inhibits ceramide-induced apoptosis of CAD cells (human derived CNS catecholinergic cells that express dopamine) (Goswami, Singh et al. 2005). Interestingly, by inducing the redistribution of PTEN, ceramide may indirectly affect the function of PINK1 (PTEN induced kinase 1). Thus experiments aimed at determining the ceramide-induced changes in the amount/localization of PTEN, PINK1, and PI3K/AKT would show that, in addition to its role in ER stress and mitochondrial dysregulation, ceramide may play an important role in DA neurotoxicity by inhibition of pro-survival pathways as well.

Does ceramide induce down-regulation of parkin levels?

Unschuld and colleagues have studied parkin function in ceramide treated PC-12 cells and reported parkin over-expression is protective from ceramide induced cytotoxicity but that the mechanism of parkin's protection was not likely from its E3-ligse activity but rather stemmed from parkin's direct or indirect modulation of gene expression (Unschuld, Dachsel et al. 2006). The work of Thi Tran in our lab has shown that parkin is down-regulated at the mRNA and protein level in microglia and macrophages in response to inflammatory stimuli (TNF and LPS). Additionally, LPS (like TNF) has been shown to increase ceramide levels (MacKichan and DeFranco 1999). It would be of interest to determine if ceramide treatment elicits a downregulation of parkin expression in neurons as well as in microglia/macrophages.

Recapitulation of TNF-dependent ceramide signaling in primary neuronal cultures

In order to elucidate the direct effect of TNF on DA neurons, I have used a reductionist system of homogeneous neuronal cell cultures as a DA neuron model system in which to study the mechanisms of TNF signaling. These studies have demonstrated that ceramide is a major downstream mediator of TNF induced cytotoxic signaling in diff-MN9D cells. It is important to recapitulate the TNF and C2-ceramide-induced effects that we have observed in diff-MN9D cells in more physiologically relevant model systems, beginning with primary cultures of mesencephalon (MES). Questions that should be addressed in these experiments include: In mixed neuron/glia MES cultures, how does the presence of glia affect C2-ceramide-induced cytotoxicity of TH neurons? Do glial cells exert a protective effect or do they respond to ceramide by engaging in feed-forward cytokine/chemokine production? If the glia are found to render TH neurons less sensitive to C2-cer than diff-MN9D cells are, it is possible that such a result could be an artifact. Because C2-cer is cell permeable, glial cells in mixed MES cultures could act as a sink for the C2-cer. (As an aside, I have previously determined that murine SS01 astrocytes and BV2 microglia cells are not sensitive to the doses of C2-cer that elicit cytotoxic cell death of diff-MN9D cells (data not shown in this document). Of course, neuron enriched primary cultures should also be used to validate the results of TNF/C2-cer treatment observed in diff-MN9D cells.

In vivo *inhibition of A-SMase in rodent models of Parkinson's disease*

I have already performed a proof-of-principle study in which rats unilaterally lesioned with 6-OHDA or saline were administered desipramine (an inhibitor of A-SMase) or saline via daily intraperitoneal injections. The measurable outcomes of this study were

behavior and evaluation of total TH and NeuN positive neurons in the SNpc as determined by stereology. This stereological analysis for this study is still ongoing. The behavior results were difficult to interpret, as there was much variability among animals in the same treatment group. Going forward, this study should be expanded and repeated. In addition to desipramine, another tricyclic antidepressant should be used as a control. Importantly, desipramine is the only tricyclic antidepressant that has an effect on SMase/ceramide biology. If the results of this proposed study indicate that desipramine can attenuate 6-OHDA-induced DA neuron loss *in vivo* they would provide compelling rationale to begin clinical trials using desipramine in PD patients, and could thus provide a new therapeutic treatment for Parkinson's disease.

REFERENCES

Arboleda, G., L. C. Morales, et al. (2009). "Regulation of ceramide-induced neuronal death: cell metabolism meets neurodegeneration." Brain Res Rev **59**(2): 333-346.

Boyce, M., K. F. Bryant, et al. (2005). "A selective inhibitor of eIF2alpha dephosphorylation protects cells from ER stress." Science **307**(5711): 935-939.

Colell, A., A. Morales, et al. (2002). "Ceramide generated by acidic sphingomyelinase contributes to tumor necrosis factor-alpha-mediated apoptosis in human colon HT-29 cells through glycosphingolipids formation. Possible role of ganglioside GD3." FEBS Lett **526**(1-3): 135-141.

Goswami, R., D. Singh, et al. (2005). "Ceramide regulation of the tumor suppressor phosphatase PTEN in rafts isolated from neurotumor cell lines." J Neurosci Res **81**(4): 541-550.

Kobrinsky, E., A. I. Spielman, et al. (1999). "Ceramide triggers intracellular calcium release via the IP(3) receptor in Xenopus laevis oocytes." Am J Physiol **277**(4 Pt 1): C665-672.

MacKichan, M. L. and A. L. DeFranco (1999). "Role of ceramide in lipopolysaccharide (LPS)-induced signaling. LPS increases ceramide rather than acting as a structural homolog." J Biol Chem **274**(3): 1767-1775.

McCoy, M. K., T. N. Martinez, et al. (2006). "Blocking soluble tumor necrosis factor signaling with dominant-negative tumor necrosis factor inhibitor attenuates loss of dopaminergic neurons in models of Parkinson's disease." J Neurosci **26**(37): 9365-9375.

Rotolo, J. A., J. Zhang, et al. (2005). "Caspase-dependent and -independent activation of acid sphingomyelinase signaling." J Biol Chem **280**(28): 26425-26434.

Sano, R., I. Annunziata, et al. (2009). "GM1-ganglioside accumulation at the mitochondria-associated ER membranes links ER stress to Ca(2+)-dependent mitochondrial apoptosis." Mol Cell **36**(3): 500-511.

Unschuld, P. G., J. Dachsel, et al. (2006). "Parkin modulates gene expression in control and ceramide-treated PC12 cells." Mol Biol Rep **33**(1): 13-32.

Whitworth, A. J. and L. J. Pallanck (2009). "The PINK1/Parkin pathway: a mitochondrial quality control system?" J Bioenerg Biomembr **41**(6): 499-503.

Yamamuro, A., Y. Yoshioka, et al. (2006). "Involvement of endoplasmic reticulum stress on the cell death induced by 6-hydroxydopamine in human neuroblastoma SH-SY5Y cells." Neurochem Res **31**(5): 657-664.

APPENDIX A

AUTOLOGOUS TRANSPLANTS OF ADIPOSE-DERIVED ADULT STROMAL (ADAS) CELLS AFFORD DOPAMINERGIC NEUROPROTECTION IN A MODEL OF PARKINSON'S DISEASE

The contents of this appendix were previously published:

McCoy, M. K*., Martinez, T. N.*, Ruhn, K. A., Wrage, P. C., Keefer, E. W., Botterman, B. R., Tansey, K. E., Tansey, M. G., 2008. Autologous transplants of Adipose-Derived Adult Stromal (ADAS) cells afford dopaminergic neuroprotection in a model of Parkinson's disease. Exp Neurol. 210**,** 14-29.

(*equal contribution).

ABSTRACT

Adult adipose contains stromal progenitor cells with neurogenic potential. However, the stability of neuronal phenotypes adopted by Adipose-Derived Adult Stromal (ADAS) cells and whether terminal neuronal differentiation is required for their consideration as alternatives in cell replacement strategies to treat neurological disorders are largely unknown. We investigated whether *in vitro* neural induction of ADAS cells determined their ability to neuroprotect or restore function in a lesioned dopaminergic pathway. *In vitro*-expanded naïve or differentiated ADAS cells were autologously transplanted into substantia nigra 1-week after an intrastriatal 6-hydroxydopamine injection. Neurochemical and behavioral measures demonstrated neuroprotective effects of both ADAS grafts against 6-hydroxydopamine-induced dopaminergic neuron death, suggesting that pre-transplantation differentiation of the cells does not determine their ability to survive or neuroprotect *in vivo*. Therefore, we investigated whether equivalent

protection by naïve and neurally-induced ADAS grafts resulted from robust *in situ* differentiation of both graft types into dopaminergic fates. Immunohistological analyses revealed that ADAS cells did not adopt dopaminergic cell fates *in situ*, consistent with the limited ability of these cells to undergo terminal differentiation into electrically active neurons *in vitro.* Moreover, re-exposure of neurally-differentiated ADAS cells to serum-containing medium *in vitro* confirmed ADAS cell phenotypic instability (plasticity). Lastly, given that gene expression analyses of *in vitro*-expanded ADAS cells revealed that both naïve and differentiated ADAS cells express potent dopaminergic survival factors, ADAS transplants may have exerted neuroprotective effects by production of trophic factors at the lesion site. ADAS cells may be ideal for *ex vivo* gene transfer therapies in Parkinson's disease treatment.

INTRODUCTION

Because central nervous system tissue has limited capacity for intrinsic repair after injury, cell replacement strategies represent an attractive approach for neurorestorative medicine (Weissman, 2000). Endogenous neural stem cells within certain regions of the adult brain can be proliferated *in vitro* (Gage, 2000; Gage et al., 1995). However, regulation of their growth and proliferation potential *in vivo* remains a major problem (Belmadani et al., 2006; Conti et al., 2006; Hermann et al., 2004b; Miller, 2006). Similarly, widespread use of fetal tissue or embryonic stem cells in cell replacement therapies has been limited by histocompatibility issues, availability, and ethical concerns prompting the search for alternative cell sources (Frankel, 2000; Sonntag and Sanchez-

Pernaute, 2006). Of particular interest are other adult tissues with progenitor populations that could be easily harvested, expanded, and used in autologous transplantation strategies to protect vulnerable neuronal populations and/or to accelerate repair after neural injury or neurodegeneration without the need for immunosuppression. Subpopulations of cells residing within adult liver (Alison and Sarraf, 1998), intestine (Potten, 1998), skin/hair-follicles (Amoh et al., 2005; Fernandes et al., 2004), and bone marrow (Jiang et al., 2002a; Jiang et al., 2002b) express neuroectodermal or neural crest cell markers *in vitro* and/or *in vivo*. Similarly, adult bone marrow-derived mesodermal stromal cells (MSC) display neurogenic properties (Bonilla et al., 2005; Bossolasco et al., 2005; Dezawa et al., 2004; Hermann et al., 2004a; Hermann et al., 2006; Jiang et al., 2002a; Jiang et al., 2002b; Woodbury et al., 2002; Woodbury et al., 2000) including the ability to fire action potentials and respond to neurotransmitters, including GABA, glycine, and glutamate (Wislet-Gendebien et al., 2005).

In recent years, adult adipose was shown by several laboratories (reviewed in (Schaffler and Buchler, 2007) to be a source of multipotent cells from which to derive progenitors such as chondrocytes, adipocytes, osteoblasts, and myocytes for tissue engineering and repair of mesodermal or mesenchymal-derived tissues (Tholpady et al., 2003; Zuk et al., 2002; Zuk et al., 2001) while others reported adipose may also have sub-populations of cells with neurogenic potential *in vitro* (Ashjian et al., 2003; Fujimura et al., 2005; Kang et al., 2004; Ning et al., 2006; Safford et al., 2002; Safford et al., 2004). The term Adipose-Derived Adult Stem (ADAS) cells was the original term used to refer to these cells on the basis of their potential for multi-lineage specification (Safford et al.,

2002). However, strict criteria for ‘stemness’ has not been met conclusively (Easterday et al., 2003; Lakshmipathy and Verfaillie, 2005; Weissman et al., 2001). Therefore, the preferred term for these cells, and the one which we use in our study, is Adipose-Derived Adult Stromal (ADAS) cells (Safford et al., 2004). Despite significant progress in characterization of cell surface markers for ADAS cells (Guilak et al., 2006; Izadpanah et al., 2006), therapeutic benefit derived from transplantation of ADAS cells has yet to be demonstrated in animal models of neurodegeneration.

The primary goal of these studies was to investigate the extent to which autologous grafts of naïve or neurally-induced rat ADAS cells protect, repair, or restore function of the nigrostriatal pathway in a neurotoxin model of PD. Neurochemical and behavioral measures confirmed the neuroprotective effects of both kinds of autologous ADAS cell grafts against 6-OHDA-induced dopaminergic neuron death. On the basis of neurohistological, cell biological, electrophysiological, and gene expression studies, we concluded that the mechanism by which ADAS cell grafts contributed to improved nigrostriatal function does not involve stable differentiation of ADAS cells into functional dopaminergic neurons. Our findings suggest that modulation of the oxidative stress-induced neuroinflammatory environment in the lesioned substantia nigra and/or ADAS-derived production of growth factors known to promote dopaminergic survival and neuroprotection at the lesion site may have contributed to the therapeutic effects of ADAS cell transplants.

MATERIALS AND METHODS

Materials

Animals

All animal procedures were approved by the Institutional Care and Use Committee at UT Southwestern. Animals were housed in a climate controlled facility staffed with certified veterinarians.

Real-time Quantitative PCR .and RT-PCR Primers

Rat primers sequences are as follows:

Cyclophilin forward: 5'-CCC TGA AGG ATG TGA TCA TTG-3'

Cyclophilin reverse: 5'-GGA AAA GGG TTT CTC CAC TT-3'

Nestin forward: 5'-CAA GTG CCC CCG GTA CTG-3'

Nestin reverse: 5'-TCA GCA AAC CCA TCA GAT TCC-3'

GFAP forward: 5'-TGG CCA CCA GTA ACA TGC A-3'

GFAP reverse: 5'-CAA ACT TGG ACC GAT ACC ACT CT-3'

NeuroD forward: 5'-CCC AGA GGC AGC CAA GTC-3'

NeuroD reverse: 5'-AGC CTT TAG TAA AAC AAT TGA ATG TCT AG-3'

S100beta forward: 5'-ATC AAC AAC GAG CTC TCT CAC TTC-3'

S100beta reverse: 5'-CAC TTC CTG CTC TTT GAT TTC CT-3'

Tuj-1/β-tubulin III forward: 5'-GAG GCC TCC TCT CAC AAG TAT GT-3'

Tuj-1/β-tubulin III reverse: 5'-ACG CTG TCC ATG GTT CCA-3'

VE cadherin forward: 5'-CAC GAC AAT ACC GCC AAC A-3'

VE cadherin reverse: 5’-AAC TTG GTA TGC TCC CGA TTA AA-3’

Persephin forward: 5’-GAC CTG GAA GCC CCA TCA- 3’

Persephin reverse: 5’-GCC GGC ACA AAC CAG GTA- 3’

Artemin forward: 5’-TTG GAG AC CTA CTG CAT TGT C- 3’

Artemin reverse: 5’-CAG CTA GGG TTG GCC ACA AG- 3’

Neurturin forward: 5’-CAG CGG AGG CGC GTG CGC AGA GA -3’

Neurturin reverse: 5’- CGG CTG TGC ACG TCC AGG AAG GA-3’

α-actin forward: 5’-TGT AAG GCG GGC TTT GCT-3’

α-actin reverse: 5’-CCC ACG ATG GAT GGG AAA -3’

Tyrosine hydroxylase forward: 5’-TGT TGG CTG ACC GCA CAT T- 3’

Tyrosine hydroxylase reverse: 5’-GCC CCC AGA GAT GCA AGT C- 3’

Nerve growth factor forward: 5’-CTC TGA GGT GCA TAG CGT AAT GTC- 3’

Nerve growth factor reverse: 5’-AAA ACG CTG TGA GAG TGT AGA AC- 3’

Neuron Specific Enolase forward: 5’-GCT TTG CCC CCA ATA TCC T-3’

Neuron Specific Enolase reverse 5’-CCT TGT CAA TGG CTT CCT TCA-3’

Choline acetyltransferase forward: 5’-AGC CAA TCG CTG GTA TGA CA-3’

Choline acetyltransferase reverse: 5’-CAC CGC AGG TGC CAT CT-3’

Smooth muscle alpha actin forward: 5’-TGT AAG GCG GGC TTT GCT- 3’

Smooth muscle alpha actin reverse: 5’-CCC ACG ATG GAT GGG AAA-3’

Platelet derived growth factor forward: 5’-AAT GAC CAC GGC GAT GAG A- 3’

Platelet derived growth factor reverse: 5’-TCT TCC AGT GTT TCC AGC AGC- 3’

Ciliary neurotrophic factor forward: 5’ -CTG GCT AGC AAG GAA GAT TCG- 3’

Ciliary neurotrophic factor reverse: 5’-CAG GCC CTG ATG TTT TAC ATA AGA -3’

Brain-derived neurotrophic factor forward: 5'-CGC ACC TCT TTA GGC ATC CT -3'

Brain-derived neurotrophic factor reverse: 5'-TCC CGG ATG AAA GTC ACT -3'

Vascular endothelial growth factor forward: 5'-AAC GAA AGC CGA AGA AAT CC- 3'

Vascular endothelial growth factor reverse: 5'-CGC TCT GAA CAA GGC TCA CA- 3'

Glial-derived neurotrophic factor forward: 5'-CTC CAA TAT GCC CGA AGA TTA TC- 3'

Glial-derived neurotrophic factor reverse: 5'-AGT CTT TTG ATG GTG GCT TGA A -3'

METHODS

Survival surgeries to harvest adipose tissue

For survival surgeries, adult female Sprague-Dawley rats (200-225g) were anesthetized with 2% halothane and a 0.75cm^2 portion of the interscapular fat pad was excised during a survival surgery when a unilateral striatal 6-hydroxydopamine injection was performed. The adipose tissue was rinsed in cold sterile PBS (Ca/Mg Free, Invitrogen Inc., Carlsbad, CA) and incubated for 1 hr in Dulbecco's Modified Eagle's Medium (DMEM, Invitrogen) supplemented with 10% FBS (Atlanta Biologicals, Lawrenceville, GA) and antibiotic/antimycotic (Invitrogen) prior to dissociation. Fat pads were mechanically triturated then enzymatically digested in collagenase (Invitrogen) for 1 hr at 37 degrees C followed by mechanical dissociation to yield a stromal cell suspension which was collected by centrifugation (x1000g). The cell pellet was resuspended in DMEM

supplemented with 10% FBS (D10 medium) and plated (Day 0, P0) onto 35mm tissue culture-treated dishes.

Expansion and neural induction of ADAS cells for immunocytochemical analyses

Non-adherent cells in P0 cultures were removed 24h post-plating in order to expand the small number of adherent stromal cells (< 10% of total cells plated) by serial passage. Media was replenished every 3 days and cultures were serially passaged at 75% confluence at a 1:4 ratio. Differentiation of cultures (P2 to P4) consisted of pre-induction of cultures plated in D10 with 10ng/ml EGF (R&D Systems, Minneapolis, MN) and 20ng/ml FGF-2 (R&D) for 2 to 3 days prior to a 4-day exposure to either of the following: Neural Differentiation Medium [NDM: D10, 120uM indomethacin (Sigma-Aldrich, St. Louis, MO), 3ug/mL insulin (Sigma-Aldrich), 300uM isobutyl-methylxanthine (Sigma-Aldrich)] or N2-supplemented/VPA [N2/VPA: DMEM, N2 supplement (Invitrogen), 0.5mM valproic acid (Sigma-Aldrich)] to induce gradual neuronal differentiation and outgrowth of processes. Alternatively, differentiation was achieved by pre-induction of cultures grown in D10 by exposure to 10ng/ml EGF + 20ng/ml FGF-2 (E/F) in NS-A Proliferation medium (Stem Cell Technologies, Vancouver, BC) for 3 days followed by 4-day differentiation in NS-A Differentiation supplement (Stem Cell Technologies). Where indicated, specific differentiation factors [1uM all-trans retinoic acid, 1-10uM forskolin, 10-50ng/ml Glial cell-derived neurotrophic factor (GDNF) or 10ng/ml Brain-Derived Neurotrophic Factor (BDNF)] were used to investigate their effects on process outgrowth of ADAS cells.

Immunocytochemical detection of neural and glial markers

Cells in culture were fixed in 4% paraformaldehyde (PFA) for 20 minutes prior to blocking/permeabilization for immunocytochemistry with antibodies to Nestin (BD Pharmingen, San Diego, CA), vimentin (Chemicon, Temecula, CA), Fibronectin (Sigma-Aldrich), Neuron Specific Enolase (Polysciences Inc., Warrington, PA), VE cadherin (Santa Cruz Biotechnology, Santa Cruz, CA), Neuro D (Santa Cruz), Tubulin beta III/Tuj1 (Covance, Princeton, NJ), MAP2b (Chemicon), NeuN (Chemicon), Gamma-Amino Butyric Acid or GABA (Chemicon), TrkB (Chemicon), Choline Acetyl Transferase or ChAT (Chemicon), tyrosine hydroxylase or TH (Chemicon), smooth muscle actin or SMA (Sigma-Aldrich), CD11b or OX-42 (Santa Cruz), Glial Fibrillary Acidic Protein or GFAP (Chemicon), oligodendrocyte marker O4 (R&D), the Schwann cell marker S100β (Sigma-Aldrich), low-affinity neurotrophic factor receptor p75NTR (Chemicon), and myelin basic protein or MBP (Chemicon). Detection of desired antigens was achieved through use of the appropriate secondary antibody conjugated to Alexa-488 or Alexa-594 diluted 1:1000 (Invitrogen). IgG or IgM control sera were used at the same concentration as the corresponding primary antibodies to establish the specificity of staining. Total cell nuclei were visualized with the nuclear dye Hoechst 33258 (bis-benzimide). A CoolSnap ES (monochrome) camera mounted on an upright Olympus BX61 or an inverted Olympus CK40 fluorescence scope and MetaMorph software were used for image capture and analyses.

Survival surgeries for fat pad harvest and intrastriatal 6-OHDA injection

6-OHDA lesions were performed as described previously (McCoy et al., 2006). Briefly, young adult female Harlan Sprague Dawley SASCO rats (200-225g) (n= 4 or 5 per group) were anesthetized with halothane (2%) and placed in a stereotaxic head-holder frame with the incisor bar set at -2.5 mm as per the rat stereotaxic atlas (Paxinos, 1998). Burr holes were drilled at stereotaxic coordinates (AP): -1.2mm from bregma, mediolateral in right hemisphere (ML): -3.9mm; and dorsoventral (DV): -5mm below surface of dura) (Paxinos et al., 1985) to perform unilateral injection of 20μg 6-OHDA (4μL of 5μg/μL in ascorbic acid, Sigma-Aldrich) at a rate of 1μL/min into the striatum with a 5uL Hamilton micro syringe and a 30 gauge needle. Fat pads from the interscapular region were also harvested from all experimental animals at this time (including rats that were to receive a sham-transplant) for *in vitro* expansion of ADAS to passage 2 (P2) as described above. This unilateral intrastriatal 6-OHDA injection was chosen to induce a moderate retrograde lesion in the nigrostriatal pathway resulting in the loss of approximately 65-70% of TH-positive somata in the SNpc three weeks after the lesion (Kirik et al., 1998; McCoy et al., 2006). Seven days after 6-OHDA lesion, drug-induced rotational behavior testing was conducted to establish a baseline for locomotor behavior just prior to cell transplantation.

Rotational behavior analyses

The extent of the retrograde nigrostriatal lesion was physiologically characterized using amphetamine-induced rotational behavior testing (Ungerstedt and Arbuthnott, 1970). Animals received 2.5mg/kg D-amphetamine (Sigma, St. Louis) i.p. and were subsequently placed in a glass cylinder (diameter 24.5cm) to monitor rotational

asymmetry for 20 min. Drug-induced rotational behavior was measured prior to the transplant (one week post 6-OHDA injection) as well as at 1, 2, and 3 weeks post-transplantation to assess effects of the ADAS grafts. Rotation towards the lesion (ipsilateral) was scored as positive and net rotational asymmetry score was expressed as full body turns.

Stereotaxic transplantation of MTR-labeled ADAS grafts

One week after intrastriatal 6-OHDA or saline injection and fat pad harvesting, cell transplants were performed. On the day of transplantation, passage 2 ADAS were labeled with 95-100% efficiency with the fixable mitochondrial dye CMH_2Xros MitoTracker Red (MTR) which fluoresces in a membrane potential-dependent manner (Poot et al., 1996). After MTR loading, the cells were rinsed and resuspended at a density of 4 x 10^6 per mL in order to deliver approximately 40,000 cells (4ul of 10,000/ul) per animal into the substantia nigra in the hemisphere ipsilateral to the 6-OHDA- or saline-injected striatum via stereotaxic injection using a 10ul Hamilton microsyringe with a 30 gauge needle at rate of 1uL/min via automated infusion pump using the following stereotaxic coordinates: AP -5.3mm, ML -2.4mm, DV -6.0mm below surface of dura; incisor bar at -2.5mm. Lesioned rats received E/F treated naïve ADAS (n = 5), NDM differentiated ADAS (n = 5), or saline (n = 4). A control (unlesioned) group of rats (n = 4) was also included.

Perfusion and tissue processing for histology

Animals were deeply anesthetized with Euthasol and intracardially perfused as described previously (Kirik et al., 1998; McCoy et al., 2006) four weeks after autologous

transplantation (i.e. five weeks post lesion). Brains were then removed from the skull and post-fixed for 24 h in the same PFA solution, cryoprotected in 20% sucrose in PBS for 18-24 hr, and frozen by embedding in Tissue-tek cooled by a dry-ice/isopentane solution. Coronal sections (30µm-thickness) were cut through the striatum and substantia nigra pars compacta (SNpc) on a Leica CM1850 cryostat and mounted on glass slides (SuperFrost Plus, Fisher) for immunohistological analyses and stereological estimate of DA neuron number in SNpc.

Immunohistochemistry of brain sections

Processing of brain sections was done as described previously (Kirik et al., 1998; McCoy et al., 2006). IgG or IgM sera were used at the same concentration as the corresponding primary antibodies to confirm the specificity of staining.

Stereological nigral DA neuron counts

StereoInvestigator analyses software (Micro Bright Field Inc., Williston, VT) was used to perform unbiased stereological counts of TH-immunoreactive (TH-IR) cell bodies in the SNpc using the optical fractionator method (West et al., 1991) as described previously (Kirik et al., 1998; McCoy et al., 2006). The boundary of SNpc was outlined under magnification of the 4X objective as defined according to previous anatomical demarcation in the rat (German and Manaye, 1993). For analysis, the treatment of the various brain sections was blinded to the observer. Cells were counted with a 60X oil immersion objective (1.3 NA) using an Olympus BX61 microscope. Serial sections through the extent of SNpc (from AP:-3.3mm to -5.3mm behind bregma) were cut on a

Leica cryostat and placed 4 per slide (cut thickness of 30μm and mounted thickness of 22 μm) for systematic analysis of randomly placed counting frames (size 50 x 50μm) on a counting grid (size of 160μm x 120μm) and sampled using an 18μm optical dissector with 2μm upper and lower guard zones. Every other slide was stained for TH/NeuN and the intervening slide was analyzed for MitoTracker Red fluorescence. A dopaminergic neuron was defined as a TH immunoreactive cell body with a clearly visible TH-negative nucleus. An ADAS cell was defined as a MTR-positive cell. The reason for assessing *in vivo* differentiation of ADAS post transplantation was to determine if MitoTracker Red-positive cells also co-expressed a particular cell fate marker (i.e. tyrosine hydroxylase for differentiation into dopaminergic cell fate).

Quantification of striatal TH-fiber density

Striatal optical density (OD) of TH immunostaining, determined by digital image analysis on Image Pro Plus 5.1, was used as an index of striatal density of TH innervation; densitometric measurements have been shown to provide valid relative indices of extent of fiber innervation on the same brain section of an animal receiving a unilateral 6-OHDA lesion (Burke et al., 1990). ODs were measured to estimate dopaminergic fiber innervation into the striatum. The density readings of TH-immunoreactivity in the striatum on both hemispheres of each animal were corrected for nonspecific background density, as measured on sections stained with non-immune IgG serum. Striatal images taken under a 4x objective converted to gray scale were then delineated and the intensity of staining was thus assessed for the entire striatal region (boundaries according to the rat stereotaxic atlas) of the four sections sampled for the ipsilateral and for the contralateral

striatum, subsequently averaged for each animal to obtain average optical density (AOD). The data are expressed as percent fiber density of the ipsilateral (experimental) side relative to the contralateral (control) side. Values expressed are group means $\pm$ S.D. Values were compared by one-way ANOVA followed by Tukey-Kramer HSD post-hoc test. Groups with different letters are significantly different at $p<0.05$.

Quantification of microglial burden

To estimate the microglial burden in the SNpc, optical density of the OX-42 immunoreactivity in the SNpc was obtained by digital image analysis using the Image-Pro Plus 5.1. The density readings were corrected for nonspecific background density as measured on sections stained with non-immune IgG serum. SNpc images taken under a 4x objective converted to gray scale were then delineated and the intensity of staining was thus assessed for the entire SNpc region (boundaries according to the rat stereotaxic atlas) of the six sections sampled throughout the extent of SNpc, subsequently averaged for each animal. The data was expressed as integrated optical density (IOD). All data are expressed as mean ± S.E.M. Inter-group differences between the various dependent variables were assessed using one-way ANOVA, followed by the Tukey's post hoc multiple comparisons test. Data obtained were analyzed by GraphPad statistic software; $p < 0.05$ were considered significant.

Assessment of Phenotypic Stability of ADAS cells in vitro

Cells were proliferated in base media (D10) to passage 2 or 3 followed by supplementation with 10ng/mL EGF and 20ng/mL FGF-2 (E/F) for 2-3 days.

Differentiation was induced by mitogen withdrawal and exposure to the indicated medium formulations (NDM or N2/VPA). Following a period of 7 days of differentiation, the cells were returned to D10 medium for 24 or 48 hrs prior to harvesting for marker analyses by immunocytochemistry. A qualitative survey of immunoreactivity for each protein marker was performed at high (40X) and low (10X) magnification and scores between 1 and 4 were given based on fluorescence intensity and fraction of total cells expressing that particular marker according to the following scale: 4 = intense immunoreactivity in many (> 50 %) of the cells, 3 = strong staining in ~ 50% of the cells, 2 = detectable staining in less than 50% of the cells, 1 = detectable staining in a small fraction (< 10%) of the cells, 0 = no detectable immunoreactivity.

Real-time Quantitative PCR

Quantitative real-time PCR was performed as previously described (Kurrasch et al., 2004). Briefly, total RNA was isolated with RNAStat60 (Tel-Test Inc., Friendswood, TX) from cultured cells or rat tissues, treated with DNase I, and reverse transcribed using Superscript II RNase H- reverse transcriptase (Invitrogen). Quantitative real-time PCR was performed using an ABI Prism 7900HT Detection System (Applied Biosystems, Foster City, CA). Each reaction was performed in 384-well plate format in a volume of 10ul that contained 3.5ng cDNA, 7ul SYBR green PCR Master Mix, and 200nM of each PCR primer. All reactions were performed in duplicate. Relative mRNA abundance for each sample were normalized to those of cyclophilin.

RT-PCR

Total RNA was isolated with RNA STAT60 from cultured cells or rat brain, treated with DNase I, and reverse transcribed using Superscript II RNase H- reverse transcriptase. Each PCR reaction was performed in a reaction volume of 10uL that contained 5uL GoTaq green (Sigma-Aldrich), 180nM of each PCR primer, and cDNA was added at 20, 4.0, or 0.8pg per reaction. The reaction conditions were as follows: initial denaturation at 95 ºC for 5 min and 3 cycles of amplification (95 ºC for 30 s, 60 ºC for 30 s and72 ºC for 60 s), followed by 35 cycles of amplification (94 ºC for 30 s, 57 ºC for 60s and 72 ºC for 60 s), followed by a final extension step for 10 min at 72 ºC. The PCR reaction products were separated by electrophoresis in a 2.0% agarose gel and stained with ethidium bromide. Relative mRNA abundance for each sample was determined by normalizing the optical density of NTN to that of alpha actin. Total optical densities were quantified using ChemiImager software (Alpha Innotech , San Leandro, CA).

Multi-Electrode Arrays (MEAs)

ADAS cells were passaged to P2 plated into D10 on poly-D-lysine coated multielectrode arrays to record any spontaneous or evoked neural network activity as described previously (Keefer et al., 2001; Mistry et al., 2002). Cells were proliferated in D10 supplemented with 10ng/mL EGF and 20ng/mL FGF-2 for 2 days then differentiated by mitogen withdrawal and exposure to the indicated differentiation conditions (NDM or N2/VPA) for 5 days. Application of the excitatory neurotransmitter glutamate (5μM), the GABA A receptor antagonist bicuculline (20μM), or trains of electrical stimulation (0.75 V biphasic pulses, trains of 10 pulses repeated 5 times with 30 seconds between pulse trains) were performed to evoke neural network activity.

Statistical Analyses

Intergroup differences among the means between the various dependent variables were analyzed using one-way ANOVA. When ANOVA showed significant differences, comparisons between means were tested by Tukey's multiple-comparison post hoc test (Graph Pad Prism, San Diego, CA). Values expressed are the group means $\pm$ S.E.M or group means $\pm$ S.D. as indicated. Groups represented by histogram bars labeled with different letters are significantly different at $p < 0.05$. Groups with asterisks (*) are significantly different from sham-transplanted group at $p < 0.05$.

RESULTS

Morphological differentiation and expression of neuro-glial markers in naïve and differentiated ADAS cells *in vitro.*

The initial selection of the adipose stromal cell population at P0 was accomplished by retaining a relatively small fraction of adherent cells (<10%) and discarding non-adherent cells 24 hrs after plating. In agreement with previous reports, we were able to grow and expand flat and fibroblast-like adipose-derived adult stromal (ADAS) *in vitro* with high efficiency for a number of passages (~P15). Pre-exposure to a mitogenic cocktail consisting of EGF/FGF-2 promoted expansion of a spindle-shaped putative progenitor pool within the heterogenous stromal cell population. To induce differentiation, the mitogenic cocktail was withdrawn and cells were exposed to serum-containing Neural Differentiation Medium (NDM) or to the histone deacetylase inhibitor valproic acid

(VPA) in N2-supplemented serum free medium. The latter was chosen because exposure to VPA/N2 *in vitro* has been shown to induce neuronal differentiation of adult hippocampal neural progenitors via expression of the neurogenic basic helix-loop-helix transcription factor NeuroD (Hsieh et al., 2004). Under these treatment conditions, a large fraction (>50% of total cells) of the cells in ADAS cultures pre-induced with EGF/FGF-2 for 24 hrs displayed bipolar and multipolar morphologies with extensive process outgrowth (Figures A.1 and A.7) appearing by 12 hrs compared to cells not pre-induced with the mitogenic cocktail (5% of total cells) in agreement with morphological differentiation described by others (Ashjian et al., 2003; Safford et al., 2004).

Prior to embarking on transplantation studies, we first established the extent to which the morphological differentiation of ADAS cells into neuron-like cells was coincident with expression of cellular markers of differentiation. Two-day treatment with EGF/FGF-2 induced expression of markers characteristic of early neural progenitors (including nestin, vimentin, and glial fibrillary acidic protein) in a significant fraction of the cells (Table A.1). Molecular markers denoting early commitment to neuronal fates such as β-tubulin III/Tuj1 and neuron specific enolase (NSE) were detectable in a significant fraction of cells only after exposure to NDM or N2/VPA (Figure 1, Table A.1, Figure A.2). Molecular markers of mature neurons, including neuronal N antigen (NeuN), microtubule-associated protein-2 (MAP2), TrkB, tyrosine hydroxylase (TH), choline acetyltransferase (ChAT), and gamma amino butyric acid (GABA) were detected with low frequency in a small population of the cells treated with either differentiation medium and supplemented with factors such as brain-derived neurotrophic factor

(BDNF) or glial-derived neurotrophic factor (GDNF) and did not increase further with additional time (7-10 days) in culture (Figure A.2). Lastly, expression of Smooth Muscle Actin (SMA) and the endothelial cell marker VE cadherin was detectable in a subpopulation of the cells after proliferation in EGF/FGF-2 and after NDM treatment (Table A.1, Figure A.2). As indicated in Table A.1, mRNA expression of several of these protein markers was confirmed by real-time quantitative PCR analysis (data not shown). These findings are in agreement with reports made for adipose-derived stromal cells from humans, rodents, and non-human primates (Ashjian et al., 2003; Fujimura et al., 2005; Ning et al., 2006; Romanov et al., 2005; Safford et al., 2002; Safford et al., 2004; Zuk et al., 2002).

Autologous ADAS cell grafts attenuate 6-OHDA-induced nigrostriatal pathway degeneration and behavioral deficits.

Given that ADAS cells can be coaxed to display morphological, molecular, and cellular markers characteristic of neuroblasts in response to two different neuritizing cocktails, the critical question is whether neural induction of ADAS *in vitro* prior to transplantation is required to derive therapeutic benefit from autologous ADAS grafts in a rat model of Parkinson's disease. To ensure that ADAS cells could be tracked after autologous transplantation to assess ADAS engraftment and neuronal differentiation in brain sections upon completion of the study, we conducted pilot experiments to select a stable cell labeling method that did not compromise cell viability. ADAS cells were harvested from adult rats, expanded *in vitro* to passage 2 with EGF/FGF-2, and pre-labeled with the

fixable mitochondrial-specific probe CMX-H2 MitoTracker Red (MTR) before prior to transplantation. We found that ADAS transplants were able to survive, engraft, and retain MTR fluorescence in unlesioned animals for at least three weeks (Figure A.3). Importantly, because MTR fluorescence in cells requires an intact mitochondrial membrane potential, this cell labeling method enabled us to track and identify *in situ* only those cells which were viable and healthy. Labeling of ADAS cells with a lentivirus encoding Green Fluorescent Protein (GFP) confirmed these findings but was not chosen for these studies to avoid the potential toxicity of GFP overexpression. In addition, GFP fluorescence does not depend on the viability of the cells and could have confounded interpretation of survival and engraftment studies.

Next, we investigated the ability of autologous ADAS cell transplants to protect, repair or restore function in a model of PD. We chose a model in which there is progressive degeneration of the nigrostriatal pathway for at least three weeks following a neurotoxic injury induced by striatal injection of 6-OHDA (Kirik et al., 1998). Autologous transplants of naïve or differentiated (NDM-treated) ADAS cells were injected into the rostral midbrain one week after striatal 6-OHDA admistration while the lesion was still progressing. The extent of the nigrostriatal lesion was evaluated prior to transplantation and weekly thereafter using a standard amphetamine-induced rotational behavior test. Quantitative stereological analyses of TH-positive neuron number in SNpc indicated that the group of 6-OHDA-lesioned rats that received nigral ADAS grafts displayed significantly reduced loss of TH-immunoreactive neurons on the lesioned side 4 weeks post-transplantation compared to sham-transplanted 6-OHDA lesioned rats

(Figure A.4 a and b, Table A.2)**.** In addition, quantification of TH-positive fiber density in the striatum indicated that ADAS cell transplants spared striatal terminals; specifically, 6-OHDA-lesioned/sham transplanted animals displayed 35% of control versus 65-72% of control in 6-OHDA-lesioned/ADAS-transplanted animals (Figure A.4 c). It is difficult to ascertain with certainty whether the increased TH-immunoreactivity in the ADAS cell-transplanted animals reflects true sparing of terminals, re-growth, and/or attenuated down-regulation of TH expression induced by 6-OHDA neurotoxicity, but we speculate it may be a combination of all three processes. Importantly, neurohistological protection by ADAS cell transplants was accompanied by improvement in locomotor deficits. Behavioral analyses indicated that 6-OHDA-lesioned rats that received naïve or differentiated ADAS cell transplants displayed significantly attenuated amphetamine-induced rotational behavior compared to sham-transplanted rats that received no ADAS cells (Figure A.5), suggesting that ADAS grafts prevented the progressive retrograde degeneration of the nigrostriatal pathway and contributed to striatal dopamine preservation. To our knowledge, this is the first demonstration that autologous transplantation of ADAS cells provides robust protection to rostral midbrain dopaminergic neurons against oxidative neurotoxins independent of the pre-differentiation status of the cells. Similar neuroprotective effects of ADAS cells have been reported in stroke and spinal cord injury models using rat, non-human primate, and human adipose-derived adult stromal cell populations (Kang et al., 2003b; Kang et al., 2006; Tansey, 2005).

ADAS cells survive after transplantation but do not differentiate into dopaminergic neurons.

The equivalent degree of nigral dopaminergic neuron protection achieved by transplantation of either naïve or NDM differentiated ADAS into hemi-parkinsonian rats suggested that the pre-transplantation differentiation status of the cells did not determine their ability to survive or neuroprotect *in vivo* after transplantation. This observation led us to hypothesize that either both types of grafts had undergone robust differentiation into dopaminergic fates *in vivo* and partially replaced the lost nigral dopaminergic neurons; or alternatively, that the neurally induced ADAS cells failed to maintain the neural phenotypes *in vivo* but afforded neuroprotection to the same extent as the naïve ADAS cells, implying that a mechanism other than cell replacement had contributed to functional recovery in the hemi-parkinsonian rats. To distinguish between these two mutually exclusive possibilities, we performed immunohistological analyses of midbrain sections. Four weeks after transplantation, examination of brain cryosections revealed the presence of MTR-labeled ADAS cells in close proximity to TH-positive neurons in substantia nigra; however, co-expression of TH (or any other neural markers) and MTR was not detected (Figure A.6 a-c). On the basis of these findings we concluded that neuroprotection by ADAS cells was achieved without them adopting dopaminergic neuron fates *in vivo.*

ADAS cell transplants attenuate microglial activation in SNpc of 6-OHDA-lesioned animals.

Because neuroinflammation has been implicated in the progressive degeneration of the nigrostriatal pathway in humans and in experimental models of PD (reviewed in (Hald and Lotharius, 2005; Hunot and Hirsch, 2003; Whitton, 2007) and previous work from our laboratory implicated microglial-derived soluble TNF as a critical mediator of nigral dopaminergic neuron loss induced by 6-OHDA (McCoy et al., 2006), we aimed to determine whether ADAS cell transplants had a modulatory effect on the neuroinflammatory reaction in the nigrostriatal pathway following a 6-OHDA lesion. Immunohistological analyses of the microglial activation markers OX-42 and F4/80 in SNpc of unlesioned, 6-OHDA-lesioned/sham-transplanted, and 6-OHDA-lesioned ADAS cell-transplanted animals indicated attenuation of the neuroinflammatory response 4 weeks post-transplant in animals that received the ADAS cell transplants compared to lesioned animals that received a sham-transplant (Figure A.6 d). Specifically, quantification of microglial burden in SNpc indicated a reduction in microglial burden of 45% (Figure A.6 e). Although not direct proof that ADAS cells produced anti-inflammatory mediators in the nigral environment, these data raise the interesting possibility that ADAS cell-derived molecular mediators may have the capacity to influence microglial activity at a site of injury.

Phenotypic stability, cell cycle exit, and terminal differentiation of ADAS cells *in vitro*.

The lack of detectable differentiation of ADAS into DA neurons after transplantation left us to consider the alternative hypothesis that ADAS cell differentiation induced *in vitro* was short-lived *in vivo* and both naïve and NDM-treated cell types afforded neuroprotection through a mechanism unrelated to their ability to adopt neuronal fates. We sought empirical support for this hypothesis by investigating the relative stability of the *in vitro* differentiated ADAS phenotypes after re-exposure to serum-containing medium. We monitored P2 and P3 cultures for changes in expression of the early neural progenitor marker nestin and the nuclear proliferation marker Ki67 in ADAS cell cultures grown in serum-containing medium D10, in response to mitogens (EGF and FGF-2), after 4- or 7-day neural induction in NDM, and following re-exposure to D10 for 1 or 2 days. Expression of the nuclear proliferation antigen Ki67 (Figure A.7 a and b) and nestin (Figure A.7 c) increased upon stimulation with mitogens, decreased after 4 days in differentiation media, and continued to decline by 7 days in the same; while expression of the neuronal commitment marker Tuj-1 (Figure A.7 d) was increased in a small fraction of the cells in response to mitogens, peaked in differentiation media after 4 days (see also Table A.1) and remained highly expressed at 7 days**.** However, re-exposure of differentiated cultures to serum-containing medium induced a second wave of proliferation evidenced by Ki67 (Figure A.7 a and b) and nestin (Figure A.7 c) re-emergence in the cultures; concomitantly, Tuj-1 expression (Figure A.7 d) began to decline immediately to levels below those observed after 7 days in NDM. Taken together,

these findings indicate that the *in vitro* differentiated ADAS cell phenotypes induced by the neuritizing cocktails NDM are relatively unstable. Mechanistically, this plasticity is consistent with the possibility that NDM-treated ADAS cells lost their neurally-induced phenotypes *in situ* after transplantation. To extend and confirm the observations that neurally induced ADAS cells do not display characteristics of terminally differentiated neurons, we exposed ADAS cell cultures to a 4-day treatment of VPA-supplemented N2 serum-free medium, conditions previously reported to induce terminal differentiation of neural stem cells (Hsieh et al., 2004). Consistent with results obtained after exposure to NDM, ADAS did not become terminally differentiated into mature neurons after exposure to N2/VPA as evidenced by persistent expression of the transcription factor NeuroD (Figure A.8, top panel) which is present in neuroblasts during the early stages of neural lineage commitment (Amrein et al., 2004; Katayama et al., 1997). Moreover, exposure to NDM induced outgrowth of processes in a subpopulation of the cells in the culture; yet these cells continued to express Ki67 (Figure A.8, white ovals) much like cells treated with the mitogenic cocktail EGF/FGF-2 in D10**.** In fact, proliferation arrest in NDM-treated cultures was not evident in morphologically differentiated cells until supplementation with agents that induce rapid and robust differentiation of neuroblasts into mature neurons (i.e., all-trans retinoic acid and forskolin); under these conditions, only flat fibroblast-like undifferentiated cells without processes continued to cycle (Figure A.8, white rectangles). Together with results from experiments addressing phenotypic stability, these findings suggest that neural induction of ADAS cells *in vitro* prior to transplantation does not induce terminal differentiation of ADAS into mature neurons. Given that morphological and molecular differentiation status of ADAS cells is

determined by the strength and duration of the differentiation signal, supraphysiological stimuli may be required for ADAS to undergo terminal differentiation and cell cycle exit.

ADAS cell cultures do not display spontaneous or evoked electrical activity *in vitro.*

Next, we investigated the extent to which morphological differentiation of ADAS cells correlated with functional differentiation of ADAS cells into mature neurons. Upon elevation of extracellular potassium to 20mM, a subset of morphologically differentiated ADAS cells responded to depolarizing stimuli by increasing intracellular free calcium concentrations as measured by increasing fluorescence intensity of the calcium indicator fluo-4 (data not shown), consistent with published reports that ADAS obtained from human processed lipo-aspirates express a delayed-rectifier type K+ current expressed during early neuronal development (Ashjian et al., 2003). However, attempts to measure spontaneous or evoked action potentials via intracellular recordings were unsuccessful. Likewise, attempts to measure spontaneous neural network activity from ADAS cells grown on multi-electrode arrays (MEAs) or evoked activity in response to glutamate (5 μM), the GABA A receptor antagonist bicuculline (20 μM), or trains of electrical stimulation (0.75 V biphasic pulses, trains of 10 pulses repeated 5 times with 30 seconds between pulse trains) in NDM or N2/VPA-treated cells were also unsuccessful (data not shown) despite their differentiated morphology (i.e., extended processes) (Figure A.9). Taken together, our findings indicate that terminal differentiation of ADAS cells into electrically mature neurons does not occur *in vitro* under the conditions tested. In this respect, our results are similar to those reported for multipotent skin-derived progenitor

(SKP) cells which express neuro-glial markers but fail to progress from neuroblast to neuron-like stages *in vitro* (Fernandes et al., 2006), possibly due to lack of electrical stimulation (Waragai et al., 2006) or other critical signaling cues which may be possible *in vivo* through interactions with endogenous cell populations.

ADAS cells express neurotrophic factors that protect dopaminergic neurons and promote their survival.

We hypothesized that one mechanism by which transplanted ADAS grafts could contribute to attenuated DA neuron loss after toxin-induced death without undergoing terminal differentiation into DA neurons might be through production of trophic factors at the site of injury that can protect DA neurons and promote their survival and/or differentiation of endogenous progenitor populations into dopaminergic neurons. On the basis of previous work (Milbrandt et al., 1998), we determined that the most likely candidates to examine would be the glial-derived neurotrophic factor (GDNF) family ligands (GFLs), brain-derived neurotrophic factor (BDNF), and nerve growth factor (NGF) because multiple *in vitro* and *in vivo* studies have demonstrated their ability to protect dopaminergic neurons and/or help repair a damaged nigrostriatal pathway. To test this idea, we performed real-time quantitative PCR analysis (or RT-PCR in the case on NTN) of ADAS cells proliferated *in vitro* in the presence of EGF/FGF-2 for the exact amount of time as cells used in transplantation studies. We found that ADAS cells express high levels of mRNA for BDNF, GNDF, and NGF relative to the levels normally detected in rat brain (Figure A.10). All of these factors exert potent trophic and

neuroprotective effects on nigral dopaminergic neurons (Hyman et al., 1991; Lin et al., 1993; Stromberg et al., 1985)**.** Levels of these neuroprotective growth factors were generally highest in EGF/FGF-2 expanded cultures. These *in vitro* findings suggest one possible mechanism by which autologous ADAS cell transplants might have mediated neuroprotection.

DISCUSSION

Several studies to date have reported that Adipose-Derived Adult Stromal (ADAS) cells from rats (Ning et al., 2006; Tholpady et al., 2003; Yang et al., 2004), mice (Fujimura et al., 2005; Safford et al., 2002), rhesus monkeys (Kang et al., 2004), and humans (Ashjian et al., 2003; Fujimura et al., 2005; Kang et al., 2003a; Safford et al., 2002; Zuk et al., 2002) can be coaxed to differentiate into neuron-like morphologies and to express neuro-glial markers *in vitro*. Importantly, our study is the first to demonstrate that *in vitro* neural induction and stable terminal differentiation of ADAS cells into functionally mature neurons *in vivo* are not necessary for ADAS cells to exert neuroprotective effects in models of neurological injury and thus be considered viable tissue sources to treat neurodegenerative diseases. It was somewhat surprising that the neuroprotective effects achieved in our studies were derived from transplantation of a small number of naïve or neurally-induced ADAS cells (~40,000). However, neuroprotective effects in hemi-parkinsonian rats have also been reported with small numbers of bone marrow-derived stromal (BMSC) (Aggarwal et al., 2006; Dezawa et al., 2004; Hellmann et al., 2006). We have not transplanted 6-OHDA-lesioned animals with ADAS cells at any other time-

point during the lesion; but we predict that if ADAS cells can survive in the hostile oxidative and neuroinflammatory environment of the SNpc during the first week after a striatal 6-OHDA injection, they are likely to survive at a later date. Future experiments will investigate whether delayed transplantation of ADAS cells affords similar neuroprotective effects.

Ideally, viable sources for cell replacement therapies in neurological disease would limit the magnitude of injury or degeneration or their sequelae, replace lost neurotransmitters, secrete neurotrophic factors or neuromodulatory substances to promote proliferation and survival of endogenous precursors, or promote restoration of function in neural circuits. Successful outcomes of neural stem cell grafts in restoration of function after 6-OHDA-induced nigrostriatal degeneration has been attributed to a combination of neural differentiation and trophic factor production (Yasuhara et al., 2006) in large part based on the observation that a large fraction of adult neural stem cells within transplanted grafts retain detectable nestin expression and never fully mature post-transplantation. Likewise, the *in vivo* neuroprotective effects of other cell types with demonstrated *in vitro* multi-lineage potential, including mesenchymal stem cells (MSC) (Scuteri et al., 2006), umbilical cord matrix stem cells (Weiss et al., 2006), and bone marrow derived stromal cells (BMSCs) (Carvey et al., 2005; Garcia et al., 2004; Ye et al., 2005), has been shown to be mediated in part through a mechanism of trophic support.

ADAS cells may have afforded neurohistological protection and ameliorated functional deficits induced by the striatal 6-OHDA lesion through multiple mechanisms.

Our findings from *in vitro* studies on neurotrophic factor gene expression suggest that one likely mechanism by which both kinds of ADAS cell grafts may have contributed to neuroprotection or attenuated dopaminergic dysfunction and neuronal loss in the 6-OHDA rat model is through production of neurotrophic factors at the lesion site. Consistent with this idea, NGF has been shown to promote survival of fetal ventral mesencephalic cells and rescue dopaminergic neurons (Chaturvedi et al., 2006; Kavanagh et al., 2006) and its mRNA expression in neurally-induced and naïve ADAS cells was approximately 2- and 30-fold, respectively that of total brain. Secretion of BDNF by engineered fibroblasts transplanted into the striatum has been shown to attenuate loss of dopaminergic neuron cell bodies within the SN pars compacta induced by striatal 6-OHDA injection (Levivier et al., 1995). Notably, ADAS cells expressed this and other potent dopaminergic survival factor *in vitro*. Specifically, BDNF and GDNF expression in ADAS cells was 2- to 4-fold that of total brain; we posit that secretion of these potent trophic factors *in situ* may have contributed to protection of vulnerable DA neurons. Similarly, BMSCs engineered with Neurturin were reported to reduce striatal dopamine deficiency and rotational behavior without significantly affecting 6-OHDA-induced TH-neuron loss (Ye et al., 2007). In the future, it may in fact be possible to augment the neuroprotective effects of ADAS grafts in the nigrostriatal pathway even further by engineering them to secrete more of these factors. In support of this idea, human ADAS grafts transduced with an adenovirus encoding BDNF improved functional deficits in a model of stroke (Kang et al., 2003b). Other mechanisms that have been proposed to explain the neurorestorative properties of ADAS cells in other studies include stimulation of migration and proliferation of endogenous neural precursor populations to the lesion

site and production of pro-angiogenic factors including VEGF, hepatocyte growth factor, or TGFβ (Rehman et al., 2004).

In summary, non-engineered ADAS cells may never replace neural stem cells or embryonic cells as a source of multipotent neural progeny for cell replacement therapies to treat CNS diseases. Nevertheless, the discovery that a stromal cell population residing in adult adipose, a tissue of mesodermal origin that is readily accessible and easy to harvest, displays molecular properties of neural progenitor cells *in vitro* and neuroprotective properties *in vivo* has important basic science and clinical implications. Critical advances in the field of neurorestorative medicine may soon be possible due to the identification of adult adipose as a novel non-immunogenic and easy-to-harvest tissue source that contains large numbers of cells with neuroprotective properties towards dopaminergic neurons that can be expanded *in vitro* for autologous transplantation. In addition to the inherent non-immunogenic properties of autologous ADAS grafts and their demonstrated neuroprotective capacity, we predict that the latter could be enhanced further by genetic engineering with GFLs. Alternatively, engineering of ADAS cells with neuroimmune modulatory peptides may also warrant investigation in pre-clinical models of PD in light of the overwhelming amount of recent evidence implicating neuroinflammatory processes in the progressive degeneration of the nigrostriatal pathway and development of PD in humans (reviewed in (Tansey et al., 2007; Whitton, 2007).

FIGURES AND TABLES

Figure A.1

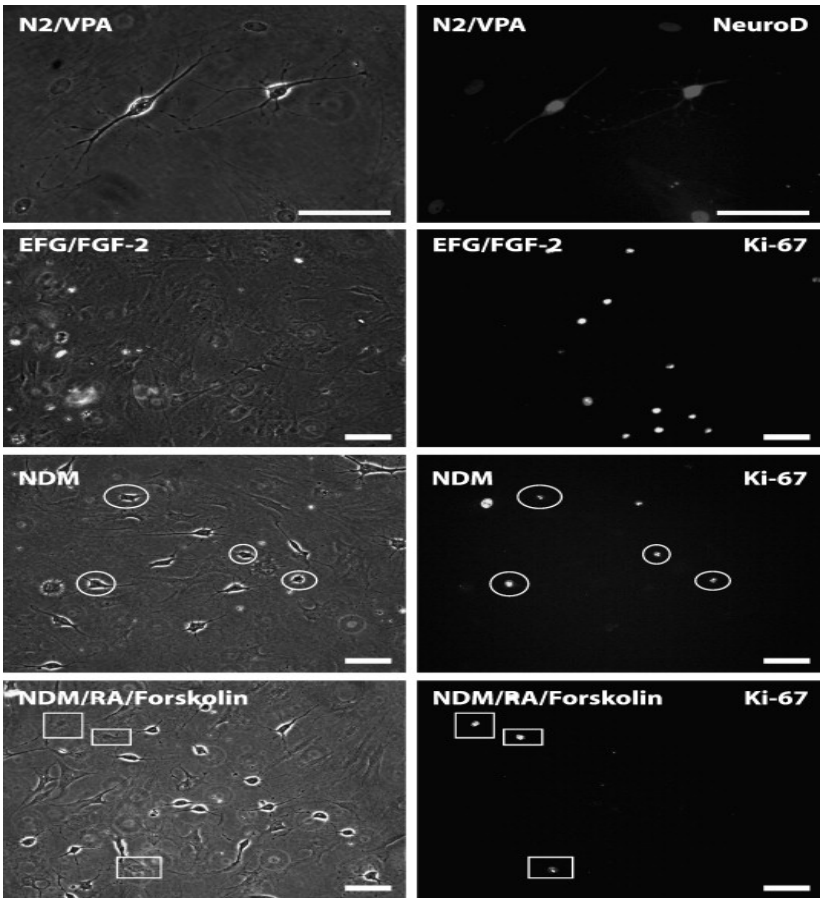

Figure A.1. Immunocytochemical analyses of cellular marker expression in naïve and differentiated rat ADAS cells.

Representative examples of passage 3 naïve and differentiated ADAS cells immunostained for specific neural cell markers (See Materials and Methods). Treatments were as follows: EGF/FGF-2 for 2 days; NDM: 2 days in EGF/FGF-2 plus 4 days in NDM; N2/VPA: 2 days in EGF/FGF-2 plus 4 days in N2 supplement + 0.5mM VPA; 10ng/mL GDNF. Data shown are representative of six independent experiments. Scale bar = 50 um.

Table A.1

Markers	D10 Medium	D10→ EGF/FGF-2 2d	D10→ EGF/FGF-2 → NDM 4d	D10→ EGF/FGF-2 → N2/VPA 4d	NSA Prolif→ NSA Differentiation 4d
Fibronectin	+++	+++	++	++	++
Vimentin	+	++	++	+	++
Nestin*	+	++	+	+	+
VE Cadherin*	-	+	++	++	+
Neuro D*	-	+/-	++	+++	+
Tuj1*	-	+/-	++	++	++
NSE*	-	-	++	++	++
NeuN	-	-	+/-	+/-	++
MAP2b	-	-	+/-	+/-	++
GABA	-	-	+	+/-	+/-
ChAT*	-	-	+/-	+/-	+/-
TH*	-	-	+/-	+/-	+/-
GFAP*	-	+	+/-	+/-	+
S100β*	-	+/-	+/-	+/-	+/-
O4	-	+/-	+/-	+/-	+/-
SMA*	++	++	+/-	+/-	++
TrkB	-	-	+	+	+
OX-42	-	+/-	-	-	-
p75NTR	-	+/-	-	-	+/-
MBP	-	-	-	-	-

Table A.1. Summary of Immunocytochemical analyses of cell marker expression in naive (undifferentiated) and differentiated ADAS cells

* denotes that mRNA confirmed by real time QPCR. Studies were performed on ADAS cells at passages 2 through 4.

+++	= robust expression in >50% of the cells
++	= strong expression in ~ 50% of the cells
+	= detectable expression in < 50% of the cells
+/-	= detectable expression in small percentage (<10%) of the cells
-	= no detectable expression

Figure A.2

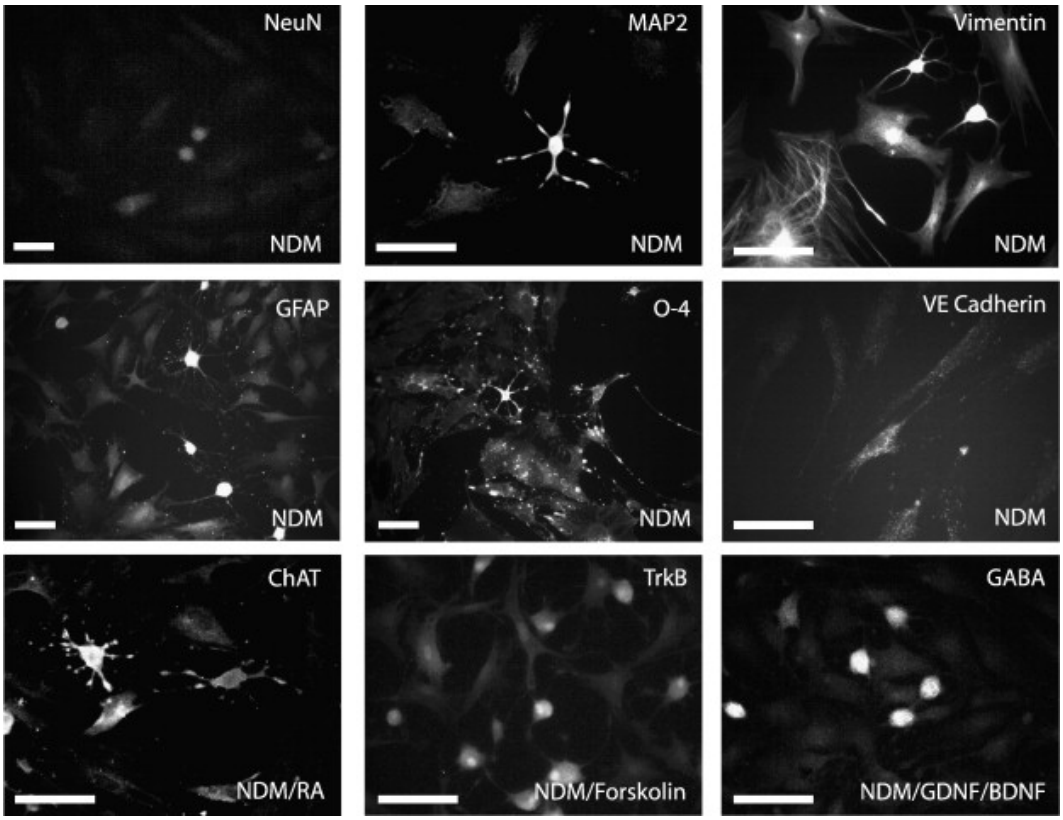
NeuN
NDM
MAP2
NDM
Vimentin
NDM
GFAP
NDM
O-4
NDM
VE Cadherin
NDM
ChAT
NDM/RA
TrkB
NDM/Forskolin
GABA
NDM/GDNF/BDNF

Figure A.2. Immunocytochemical analyses of cellular marker expression in naïve and differentiated rat ADAS cells at passage 4.

Representative examples of naïve and differentiated ADAS cells immunostained for specific neural, glial, and endothelial cell markers (See Materials and Methods). Treatments were as follows: EGF/FGF-2 for 2 days; NDM: 2 days in EGF/FGF-2 plus 4 days in NDM; N2/VPA: 2 days in EGF/FGF-2 plus 4 days in N2 supplement + 0.5mM VPA; 1uM RA (retinoid acid); 10um Forskolin; 10ng/mL GDNF; 10ng/mL BDNF. Data shown are from one of six independent experiments. Scale bars = 50 um.

Figure A.3

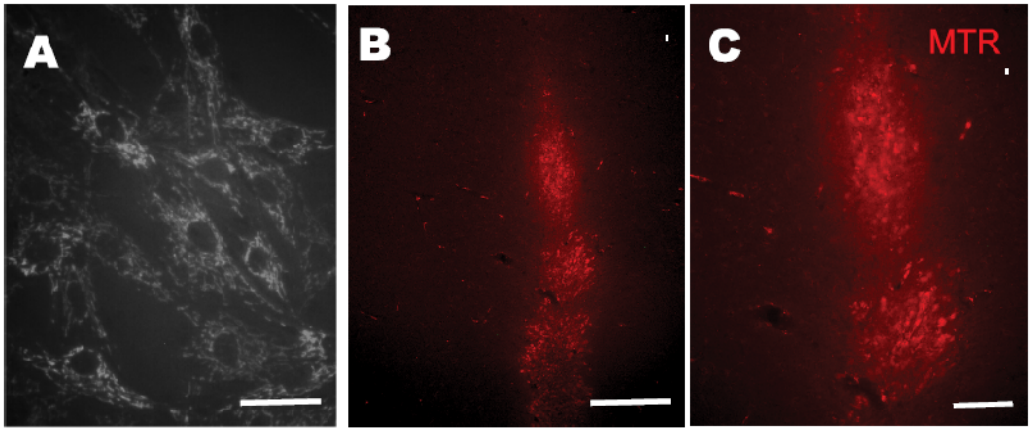

Figure A.3. Mitotracker labeled ADAS cells are detectable in unlesioned rat brain

MitoTracker Red-labeled ADAS cells *in vitro*, scale bar =50uM (a). MitoTracker-Red-labeled ADAS cells (MTR) transplanted into unlesioned rat midbrain are detectable three weeks after transplantation (b,c) (b, scale bar = 400um, c, scale bar = 200uM).

Figure A.4

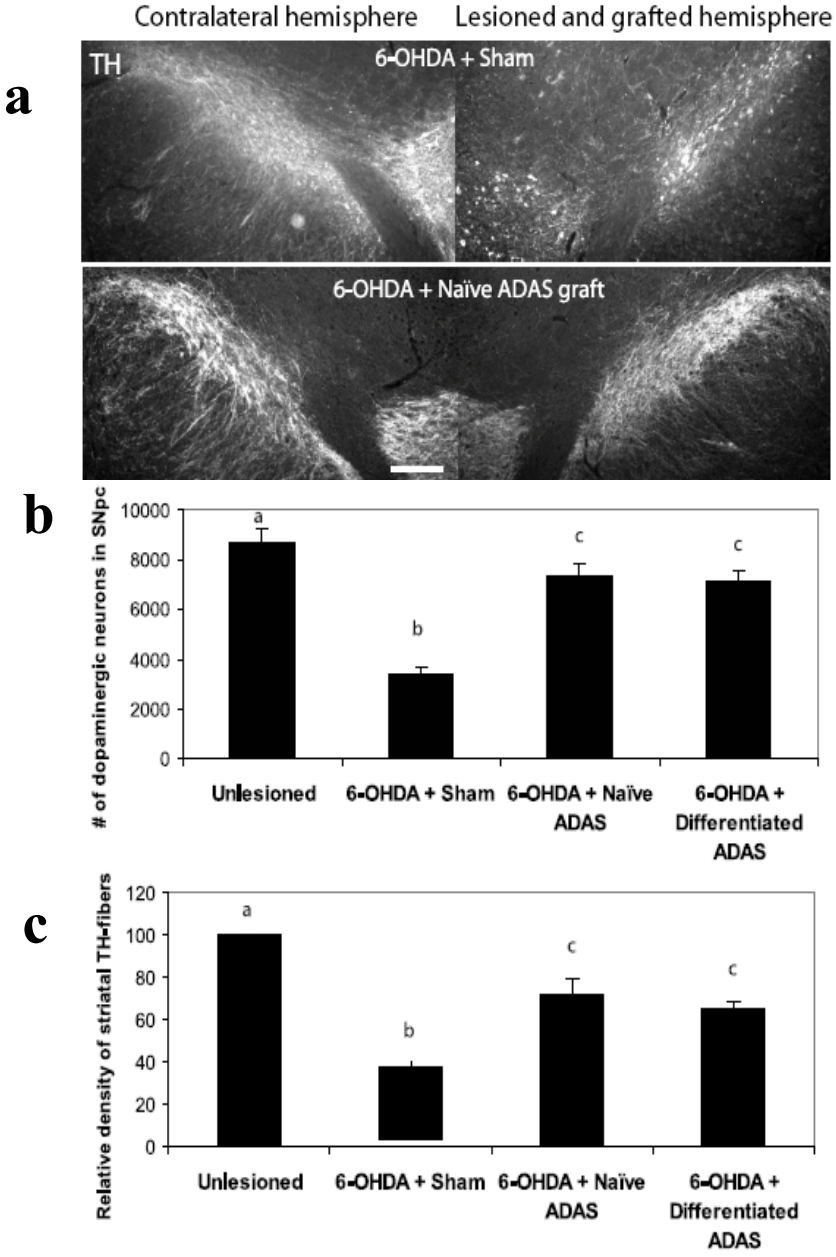
Contralateral hemisphere
Lesioned and grafted hemisphere
a
TH
6-OHDA + Sham
6-OHDA + Naïve ADAS graft
b
# of dopaminergic neurons in SNpc
10000
8000
6000
4000
2000
0
a
b
c
c
Unlesioned
6-OHDA + Sham
6-OHDA + Naïve ADAS
6-OHDA + Differentiated ADAS
c
Relative density of striatal TH-fibers
120
100
80
60
40
20
0
a
b
c
c
Unlesioned
6-OHDA + Sham
6-OHDA + Naïve ADAS
6-OHDA + Differentiated ADAS

Figure A.4. ADAS cell transplants attenuated loss of nigral and striatal tyrosine hydroxylase immunoreactivity in 6-OHDA lesioned rats.

Comparison of midbrain dopaminergic (tyrosine hydroxylase-positive) cell bodies and fiber immunoreactivity at 4 weeks post-lesion in control (unlesioned, n = 4), 6-OHDA-lesioned (n = 4), 6-OHDA-lesioned with sham (n = 4) transplant, 6-OHDA-lesioned with passage 2 naïve ADAS cells transplant (n = 5), or passage 2 differentiated ADAS cells transplant (n = 5). (a) Representative rostral midbrain sections from 6-OHDA/Sham and 6-OHDA/naïve ADAS transplanted rats were stained with an antibody against tyrosine hydroxylase (TH). The 6-OHDA-lesioned hemisphere in the sham-transplanted rat displayed significant loss of TH-immunoreactivity in SNpc relative to the contralateral (unlesioned) side whereas 6-OHDA-lesioned hemisphere of rat that also received a naïve ADAS cell transplant displayed significant sparing of TH-positive cell bodies and fibers. Scale bar = 400 um. (b) Stereological estimates of nigral DA neuron number, and (c) relative density of striatal TH-positive fibers confirm the neuroprotective effects of the autologous grafts of naïve and differentiated ADAS cells against 6-OHDA-induced loss of nigral TH-positive dopaminergic neurons (see Materials and Methods). Values expressed for neuron number and striatal density are group means $\pm$ S.D. Values were compared by one-way ANOVA followed by Tukey-Kramer HSD post-hoc test. Groups with different letters are significantly different at $p<0.05$.

Figure A.5

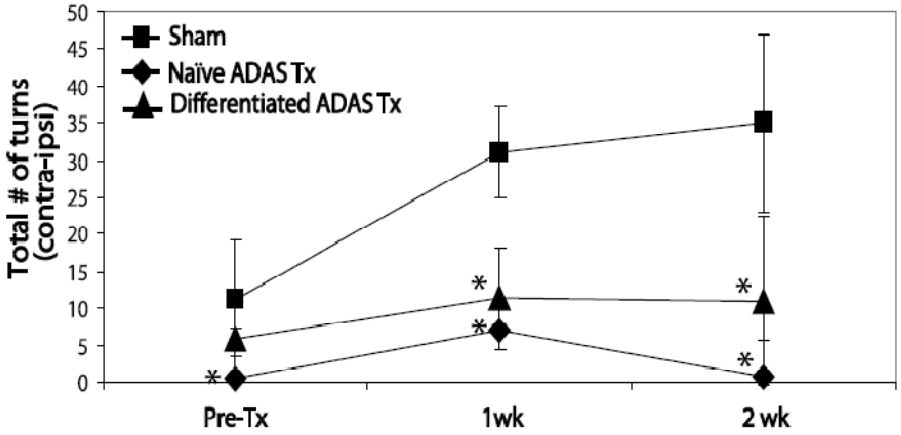
Sham
Naïve ADAS Tx
Differentiated ADAS Tx
Total # of turns (contra-ipsi)
50
45
40
35
30
25
20
15
10
5
0
Pre-Tx
1wk
2 wk
*
*
*
*

Figure A.5. ADAS cell transplants attenuated rotational behavior in 6-OHDA lesioned rats.

Rotational behavior was monitored for 20 minutes after amphetamine administration at 2.5 mg/kg i.p. (see Materials and Methods) as an indirect measure of striatal dopamine depletion induced by 6-OHDA. 6-OHDA-lesioned rats that received passage 2 naïve ADAS cells (black diamonds, n = 5) or NDM-treated ADAS cells (black triangles, n = 5) displayed attenuated amphetamine-induced rotational behavior compared to 6-OHDA-lesioned sham-transplanted (black squares, n = 4) rats. Values expressed are the group means $\pm$ S.D. Values were compared by one-way ANOVA followed by Tukey-Kramer HSD post-hoc test. Groups marked with an asterisk (*) are significantly different from sham at $p < 0.05$.

Table A.2

Stereological estimate of TH-positive neurons in SNpc one month post-transplantation

Group	Right SNpc (ipsilateral)	Left SNpc (contralateral)
Unlesioned (n = 4)	**8664 ± 587**	**8829 ± 1073**
6-OHDA + Sham (n = 4)	**3361 ± 300**	**9002 ± 660**
6-OHDA + Naïve ADAS (n = 5)	**7335 ± 539**	**8488 ± 520**
6-OHDA + Differentiated ADAS (n = 5)	**7109 ± 449**	**9115 ± 547**

Figure A. 6

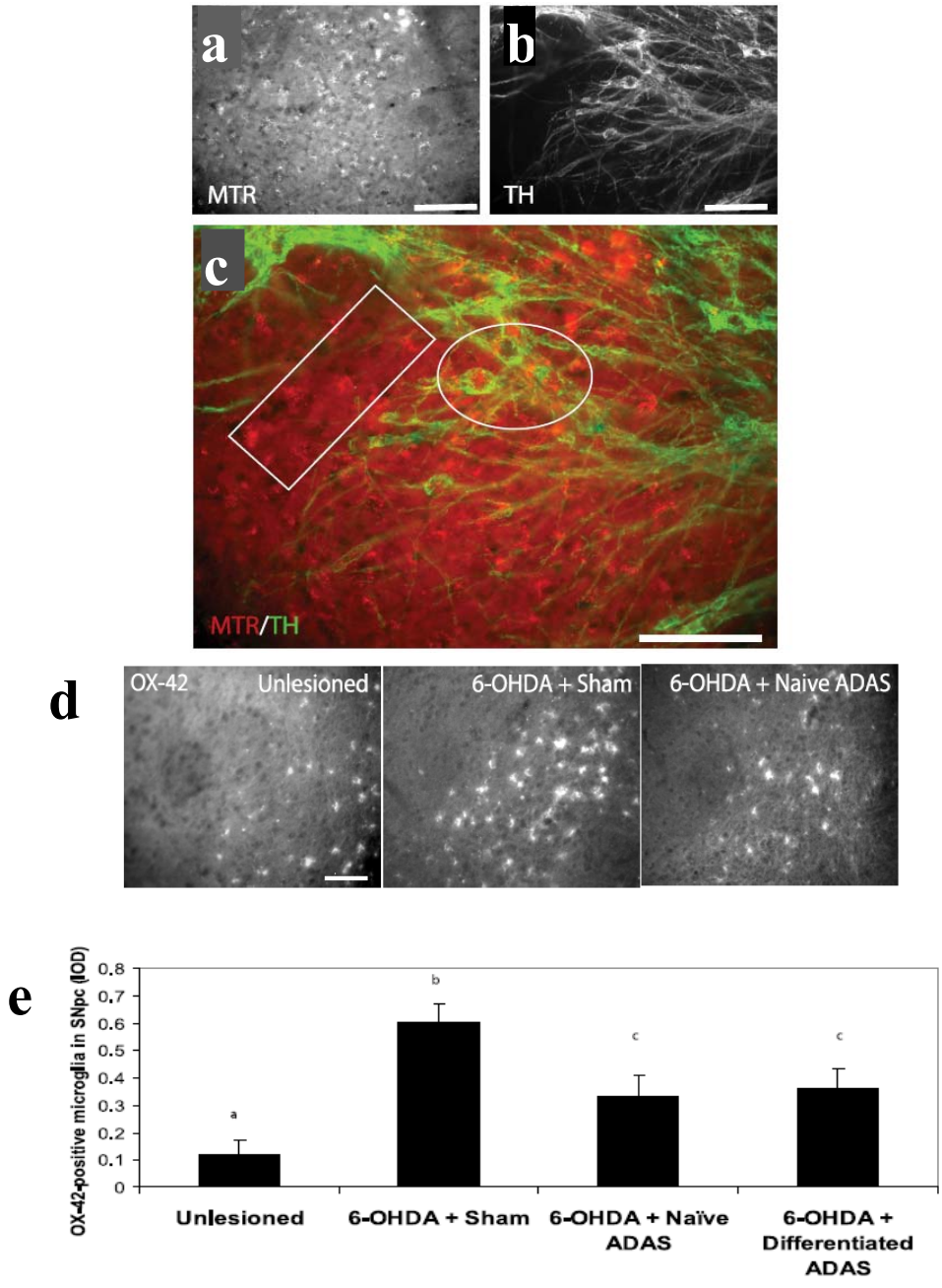
a
MTR
b
TH
c
MTR/TH
d
OX-42
Unlesioned
6-OHDA + Sham
6-OHDA + Naive ADAS
e
OX-42-positive microglia in SNpc (IOD)
0.8
0.7
0.6
0.5
0.4
0.3
0.2
0.1
0
a
b
c
c
Unlesioned
6-OHDA + Sham
6-OHDA + Naïve ADAS
6-OHDA + Differentiated ADAS

Figure A.6. Transplanted ADAS cells engraft in 6-OHDA lesioned brains and attenuate microglial activation.

(a) Mitotracker labeled ADAS cells in midbrain sections of rats lesioned with the oxidative neurotoxin 6-hyroxydopamine (see Materials and Methods). (b) Expression of the dopaminergic marker TH is not detectable in ADAS cells after transplantation. (c) In merged images, the white box indicates a region with singly labeled (MTR-positive) ADAS cells and the white oval indicates a region where MTR-labeled ADAS cells (red) were in close proximity to TH-positive (green) neuron cell bodies. (d) Representative images of OX-42-positive microglial staining in SNpc of unlesioned, 6-OHDA-lesioned/sham-transplanted, and 6-OHDA-lesioned naïve ADAS cell-transplanted animals reveal attenuation of neuroinflammatory response in animals that received the ADAS cell transplants compared to lesioned animals that received a sham-transplant. (e) Quantification of microglial burden in SNpc, IOD = integrated optical density (see Materials and Methods). Values are means $\pm$ S.E.M . Values were compared by one-way ANOVA followed by Tukey-Kramer HSD post-hoc test. Groups with different letters are significantly different at $p<0.05$. Scale bars=200 um.

Figure A.7

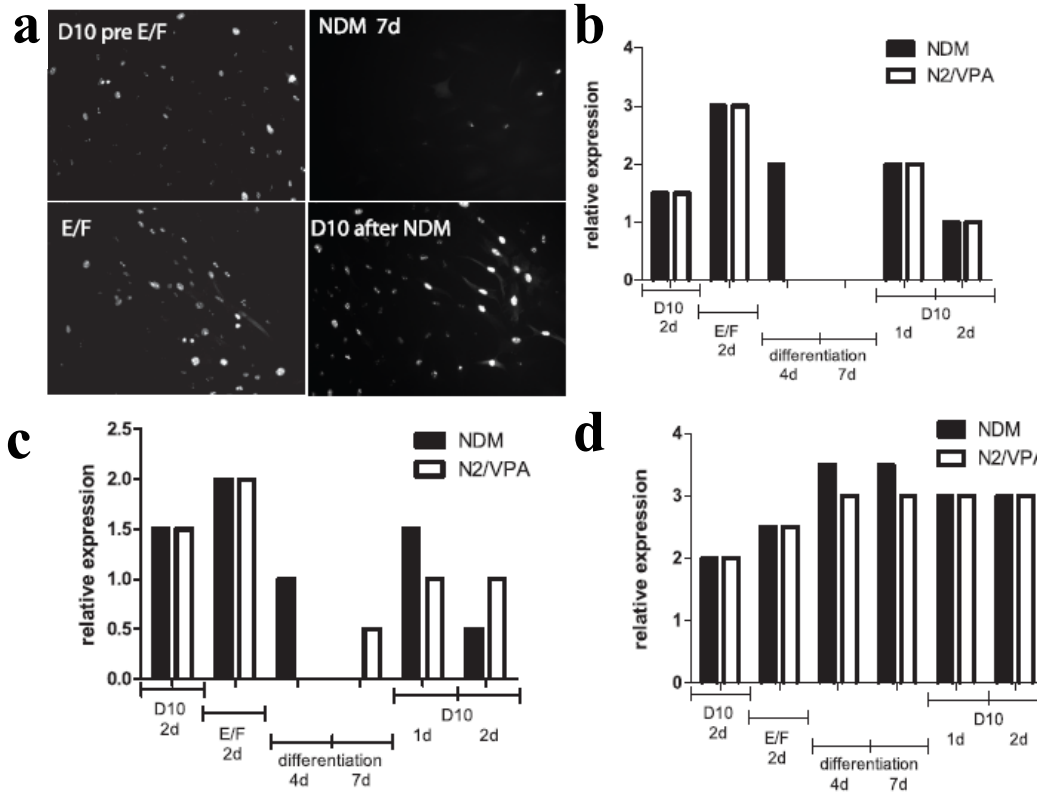
a
D10 pre E/F
NDM 7d
E/F
D10 after NDM
b
NDM
N2/VPA
relative expression
D10 2d
E/F 2d
differentiation 4d 7d
D10 1d 2d
c
NDM
N2/VPA
relative expression
D10 2d
E/F 2d
differentiation 4d 7d
D10 1d 2d
d
NDM
N2/VPA
relative expression
D10 2d
E/F 2d
differentiation 4d 7d
D10 1d 2d

Figure A.7. Stability of differentiated phenotypes of ADAS cells *in vitro*.

A survey of immunoreactivity for each protein marker was performed after the indicated treatment conditions leading up to, during, and following differentiation with NDM (black bars) or N2/VPA exposure (white bars) at high (40x objective) and low (10x objective) magnification. Scores between 1 and 4 were assigned by investigators blinded to the treatment based on fluorescence intensity and fraction of total cells expressing that particular marker according to the following scale: 4 = intense immunoreactivity in many (> 50 %) of the cells, 3 = strong staining in approximately 50% of the cells, 2 = detectable staining in less than 50% of the cells, 1 = detectable staining in a small fraction (< 10%) of the cells, 0 = no detectable immunoreactivity (Panels b, c, d). Independent of which differentiation medium was used (NDM (black bars) or N2/VPA (white bars), See Materials and Methods), results were similar for each of the different markers. (a) Nuclear proliferation antigen Ki-67 expression (immunofluorescence) in ADAS cells under the conditions indicated. (b) Relative expression of Ki-67 in ADAS cell culture under the conditions indicated, (c) Relative expression of nestin in ADAS cell culture under the conditions indicated. (d) Relative expression of Tuj-1 in ADAS cell culture under the conditions indicated. Data shown are representative of two independent experiments.

Figure A.8

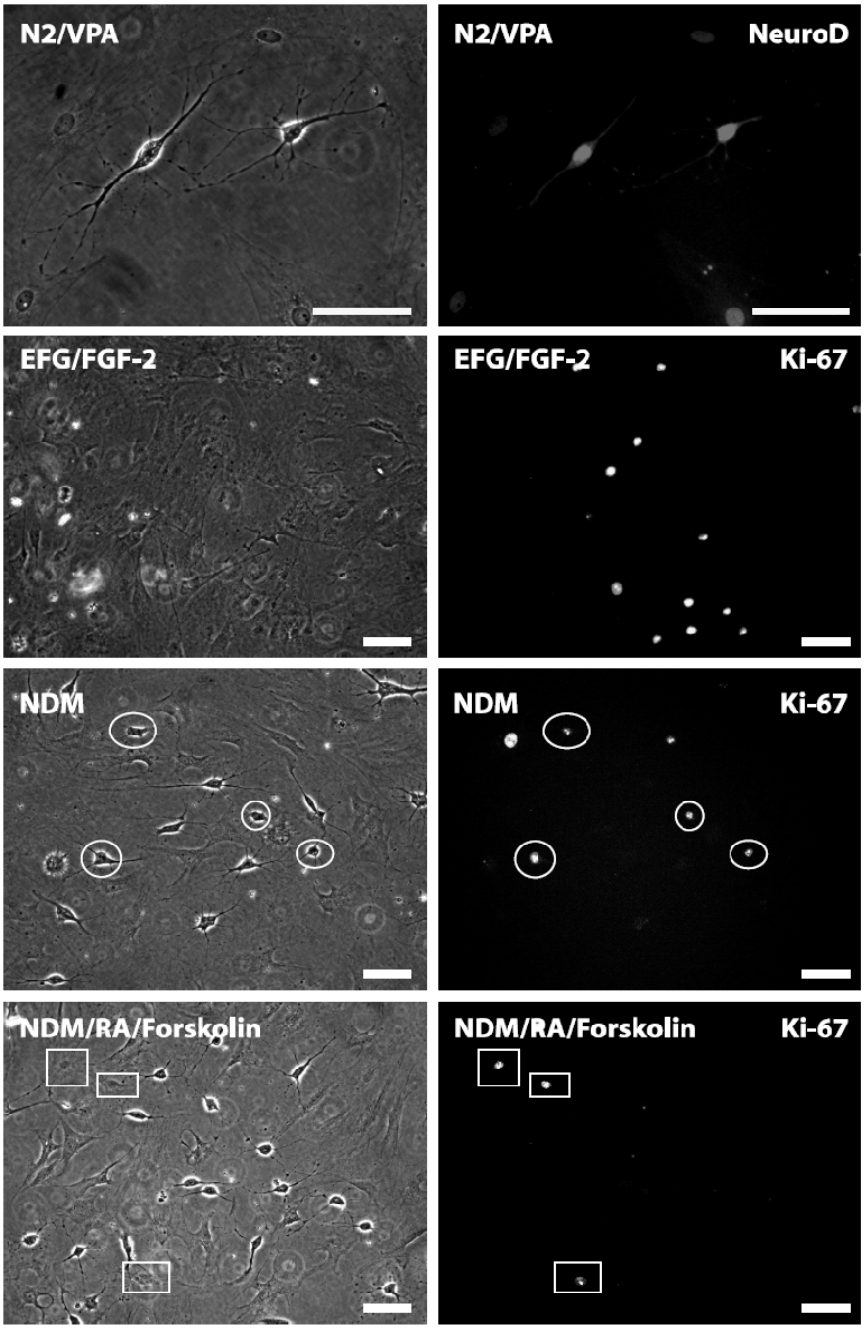
N2/VPA
N2/VPA
NeuroD
EFG/FGF-2
EFG/FGF-2
Ki-67
NDM
NDM
Ki-67
NDM/RA/Forskolin
NDM/RA/Forskolin
Ki-67

Figure A.8. Cell cycle arrest and terminal differentiation of morphologically differentiated ADAS cells requires exposure to retinoid acid and forskolin.

N2/VPA-treated ADAS cell cultures (passage 3) were immunostained with an antibody against NeuroD. Persistent expression of Neuro D was detectable in both undifferentiated (flatter) and in morphologically differentiated ADAS cells. Expression of nuclear proliferation antigen Ki-67 was detectable in subpopulations of ADAS cells growing in EGF/FGF-2 and in some morphologically differentiated ADAS cells exposed to NDM (white ovals). Cell cycle arrest was achieved in morphologically differentiated cells only after supplementation of NDM with RA and forskolin, as evidenced by presence of Ki67 only in non-differentiated cells (white rectangles). Treatments were as follows: EGF/FGF-2 2 days, NDM: 2 days EGF/FGF-2 plus 4 days NDM; N2/VPA: 2 days EGF/FGF-2 plus 2 days N2/VPA; NDM/RA/Forskolin: 2 days EGF/FGF-2 plus 4 days NDM + 1uM RA/10uM Forskolin. Data shown are representative of three independent experiments. Scale bar = 50 um.

Figure A.9

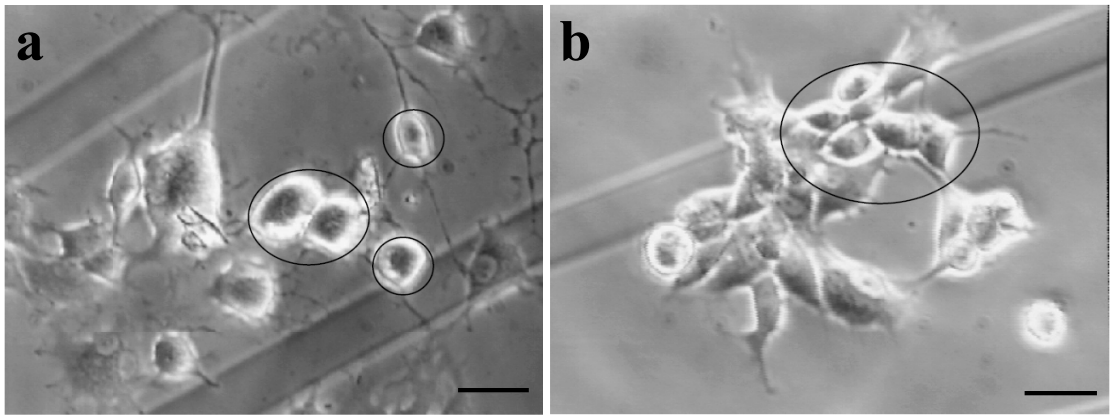

Figure A.9. ADAS cells did not display spontaneous or evoked electrical activity on multi-electrode arrays (MEAs).

ADAS cells (passages 2 through 4) were plated into D10 on poly-D-lysine coated MEAs to record spontaneous and evoked neural network activity as described previously (MEA recordings were performed by Edward Keefer). Cells were proliferated in D10 supplemented with 10ng/mL EGF and 20ng/mL FGF-2. (a) 2 days in EGF/FGF-2 plus 4 days in N2 supplement + 0.5mM VPA. (b) 2 days in EGF/FGF-2 plus 4 days in NDM supplemented with 1uM retinoid acid, and 1uM Forskolin 5uM. No basal or evoked activity was measured despite the presence of cells with extensive process outgrowth.

Figure A.10

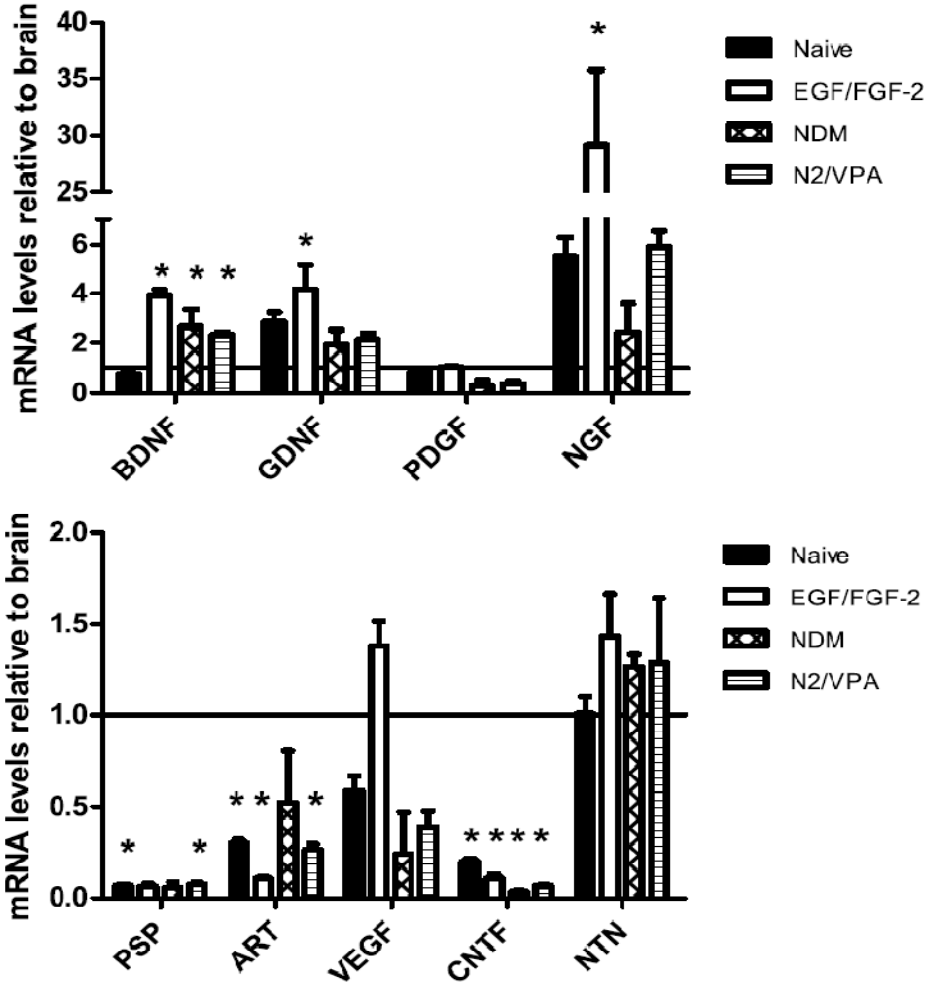
mRNA levels relative to brain
40
35
30
25
6
4
2
0
BDNF
GDNF
PDGF
NGF
Naive
EGF/FGF-2
NDM
N2/VPA
mRNA levels relative to brain
2.0
1.5
1.0
0.5
0.0
PSP
ART
VEGF
CNTF
NTN
Naive
EGF/FGF-2
NDM
N2/VPA

Figure A.10. ADAS cells express potent dopaminergic survival factors *in vitro*.

To investigate the growth factor expression profile of the cells relative to total brain levels just prior to transplantation, ADAS cells were plated and treated as follows at passage 2 or 3 prior to harvesting for real-time quantitative PCR analysis or in the case of neurturin, for semi-quantitave RT-PCR analysis (see Materials and Methods). (a) Expression of BDNF, GDNF, and NGF by ADAS was found to be higher than brain levels. (b) Expression of NTN and VEGF by ADAS was found to be equivalent to that in total brain; while expression of ART and CNTF was below that of total brain and PSP was undetectable. Cells were grown in D10, grown in D10 then proliferated for 2 days in D10 supplemented with 10ng/mL EGF and 20ng/mL FGF-2, or grown in D10, proliferated in EGF/FGF-2, and exposed to NDM or N2/VPA for 2 days. Differences in expression of mRNAs between rat brain and ADAS cultures were analyzed by single factor ANOVA followed by Tukey's post hoc test (GraphPad). Values expressed are means +/- SEM normalized to rat brain (indicated by a solid horizontal line). Genes with asterisks (*) are significantly different from brain at the level of $p<0.05$). Each condition was plated in triplicate. Differences between each group and whole brain were analyzed by single factor ANOVA followed by Tukey's HSD post-hoc test (GraphPad). Values expressed are mean mRNA levels relative to brain levels +/- SEM. Bars marked with an asterisk (*) significant at the level $p < 0.05$).

ACKNOWLEDGEMENTS

We would like to thank John Hong for technical help with immunocytochemistry, Christine Smith for help with surgery and animal care, and members of the Tansey labs for helpful discussions. We would also like to thank Dr. Don Cooper in the Department of Psychiatry for access to his StereoInvestigator system.

REFERENCES

Aggarwal, B. B., Shishodia, S., Takada, Y., Jackson-Bernitsas, D., Ahn, K. S., Sethi, G., Ichikawa, H., 2006. TNF blockade: an inflammatory issue. Ernst Schering Res Found Workshop. 161-86.

Alison, M., Sarraf, C., 1998. Hepatic stem cells. J Hepatol. 29**,** 676-82.

Amoh, Y., Li, L., Katsuoka, K., Penman, S., Hoffman, R. M., 2005. Multipotent nestin-positive, keratin-negative hair-follicle bulge stem cells can form neurons. Proc Natl Acad Sci U S A. 102**,** 5530-4.

Amrein, I., Slomianka, L., Poletaeva, II, Bologova, N. V., Lipp, H. P., 2004. Marked species and age-dependent differences in cell proliferation and neurogenesis in the hippocampus of wild-living rodents. Hippocampus. 14**,** 1000-10.

Ashjian, P. H., Elbarbary, A. S., Edmonds, B., DeUgarte, D., Zhu, M., Zuk, P. A., Lorenz, H. P., Benhaim, P., Hedrick, M. H., 2003. In vitro differentiation of human processed lipoaspirate cells into early neural progenitors. Plast Reconstr Surg. 111**,** 1922-31.

Belmadani, A., Tran, P. B., Ren, D., Miller, R. J., 2006. Chemokines regulate the migration of neural progenitors to sites of neuroinflammation. J Neurosci. 26**,** 3182-91.

Bonilla, S., Silva, A., Valdes, L., Geijo, E., Garcia-Verdugo, J. M., Martinez, S., 2005. Functional neural stem cells derived from adult bone marrow. Neuroscience. 133**,** 85-95.

Bossolasco, P., Cova, L., Calzarossa, C., Rimoldi, S. G., Borsotti, C., Deliliers, G. L., Silani, V., Soligo, D., Polli, E., 2005. Neuro-glial differentiation of human bone marrow stem cells in vitro. Exp Neurol. 193**,** 312-25.

Burke, R. E., Cadet, J. L., Kent, J. D., Karanas, A. L., Jackson-Lewis, V., 1990. An assessment of the validity of densitometric measures of striatal tyrosine hydroxylase-positive fibers: relationship to apomorphine-induced rotations in 6-hydroxydopamine lesioned rats. J Neurosci Methods. 35**,** 63-73.

Carvey, P. M., Chen, E. Y., Lipton, J. W., Tong, C. W., Chang, Q. A., Ling, Z. D., 2005. Intra-parenchymal injection of tumor necrosis factor-alpha and interleukin 1-beta produces dopamine neuron loss in the rat. J Neural Transm. 112**,** 601-12.

Chaturvedi, R. K., Shukla, S., Seth, K., Agrawal, A. K., 2006. Nerve growth factor increases survival of dopaminergic graft, rescue nigral dopaminergic neurons and restores functional deficits in rat model of Parkinson's disease. Neurosci Lett. 398**,** 44-9.

Conti, L., Reitano, E., Cattaneo, E., 2006. Neural stem cell systems: diversities and properties after transplantation in animal models of diseases. Brain Pathol. 16**,** 143-54.

Dezawa, M., Kanno, H., Hoshino, M., Cho, H., Matsumoto, N., Itokazu, Y., Tajima, N., Yamada, H., Sawada, H., Ishikawa, H., Mimura, T., Kitada, M., Suzuki, Y., Ide, C., 2004. Specific induction of neuronal cells from bone marrow stromal cells and application for autologous transplantation. J. Clin. Invest. 113**,** 1701-1710.

Easterday, M. C., Dougherty, J. D., Jackson, R. L., Ou, J., Nakano, I., Paucar, A. A., Roobini, B., Dianati, M., Irvin, D. K., Weissman, I. L., Terskikh, A. V., Geschwind, D. H., Kornblum, H. I., 2003. Neural progenitor genes. Germinal zone expression and analysis of genetic overlap in stem cell populations. Dev Biol. 264**,** 309-22.

Fernandes, K. J., Kobayashi, N. R., Gallagher, C. J., Barnabe-Heider, F., Aumont, A., Kaplan, D. R., Miller, F. D., 2006. Analysis of the neurogenic potential of multipotent skin-derived precursors. Exp Neurol. 201**,** 32-48.

Fernandes, K. J., McKenzie, I. A., Mill, P., Smith, K. M., Akhavan, M., Barnabe-Heider, F., Biernaskie, J., Junek, A., Kobayashi, N. R., Toma, J. G., Kaplan, D. R., Labosky, P. A., Rafuse, V., Hui, C. C., Miller, F. D., 2004. A dermal niche for multipotent adult skin-derived precursor cells. Nat Cell Biol. 6**,** 1082-93.

Frankel, M. S., 2000. In search of stem cell policy. Science. 287**,** 1397.

Fujimura, J., Ogawa, R., Mizuno, H., Fukunaga, Y., Suzuki, H., 2005. Neural differentiation of adipose-derived stem cells isolated from GFP transgenic mice. Biochem Biophys Res Commun. 333**,** 116-21.

Gage, F. H., 2000. Mammalian neural stem cells. Science. 287**,** 1433-8.

Gage, F. H., Ray, J., Fisher, L. J., 1995. Isolation, characterization, and use of stem cells from the CNS. Annu Rev Neurosci. 18**,** 159-92.

Garcia, R., Aguiar, J., Alberti, E., de la Cuetara, K., Pavon, N., 2004. Bone marrow stromal cells produce nerve growth factor and glial cell line-derived neurotrophic factors. Biochem Biophys Res Commun. 316**,** 753-4.

German, D. C., Manaye, K. F., 1993. Midbrain dopaminergic neurons (nuclei A8, A9, and A10): three-dimensional reconstruction in the rat. J Comp Neurol. 331**,** 297-309.

Guilak, F., Lott, K. E., Awad, H. A., Cao, Q., Hicok, K. C., Fermor, B., Gimble, J. M., 2006. Clonal analysis of the differentiation potential of human adipose-derived adult stem cells. J Cell Physiol. 206**,** 229-37.

Hald, A., Lotharius, J., 2005. Oxidative stress and inflammation in Parkinson's disease: is there a causal link? Exp Neurol. 193**,** 279-90.

Hellmann, M. A., Panet, H., Barhum, Y., Melamed, E., Offen, D., 2006. Increased survival and migration of engrafted mesenchymal bone marrow stem cells in 6-hydroxydopamine-lesioned rodents. Neurosci Lett. 395**,** 124-8.

Hermann, A., Gastl, R., Liebau, S., Popa, M. O., Fiedler, J., Boehm, B. O., Maisel, M., Lerche, H., Schwarz, J., Brenner, R., Storch, A., 2004a. Efficient generation of neural stem cell-like cells from adult human bone marrow stromal cells. J Cell Sci. 117**,** 4411-22.

Hermann, A., Gerlach, M., Schwarz, J., Storch, A., 2004b. Neurorestoration in Parkinson's disease by cell replacement and endogenous regeneration. Expert Opin Biol Ther. 4**,** 131-43.

Hermann, A., Maisel, M., Storch, A., 2006. Epigenetic conversion of human adult bone mesodermal stromal cells into neuroectodermal cell types for replacement therapy of neurodegenerative disorders. Expert Opin Biol Ther. 6**,** 653-70.

Hsieh, J., Nakashima, K., Kuwabara, T., Mejia, E., Gage, F. H., 2004. Histone deacetylase inhibition-mediated neuronal differentiation of multipotent adult neural progenitor cells. Proc Natl Acad Sci U S A. 101**,** 16659-64.

Hunot, S., Hirsch, E. C., 2003. Neuroinflammatory processes in Parkinson's disease. Ann Neurol. 53 Suppl 3**,** S49-58; discussion S58-60.

Hyman, C., Hofer, M., Barde, Y. A., Juhasz, M., Yancopoulos, G. D., Squinto, S. P., Lindsay, R. M., 1991. BDNF is a neurotrophic factor for dopaminergic neurons of the substantia nigra. Nature. 350**,** 230-2.

Izadpanah, R., Trygg, C., Patel, B., Kriedt, C., Dufour, J., Gimble, J. M., Bunnell, B. A., 2006. Biologic properties of mesenchymal stem cells derived from bone marrow and adipose tissue. J Cell Biochem. 99**,** 1285-97.

Jiang, Y., Jahagirdar, B. N., Reinhardt, R. L., Schwartz, R. E., Keene, C. D., Ortiz-Gonzalez, X. R., Reyes, M., Lenvik, T., Lund, T., Blackstad, M., Du, J., Aldrich, S., Lisberg, A., Low, W. C., Largaespada, D. A., Verfaillie, C. M., 2002a. Pluripotency of mesenchymal stem cells derived from adult marrow. Nature. 418**,** 41-9.

Jiang, Y., Vaessen, B., Lenvik, T., Blackstad, M., Reyes, M., Verfaillie, C. M., 2002b. Multipotent progenitor cells can be isolated from postnatal murine bone marrow, muscle, and brain. Exp Hematol. 30**,** 896-904.

Kang, S. K., Jun, E. S., Bae, Y. C., Jung, J. S., 2003a. Interactions between human adipose stromal cells and mouse neural stem cells in vitro. Brain Res Dev Brain Res. 145**,** 141-9.

Kang, S. K., Lee, D. H., Bae, Y. C., Kim, H. K., Baik, S. Y., Jung, J. S., 2003b. Improvement of neurological deficits by intracerebral transplantation of human adipose tissue-derived stromal cells after cerebral ischemia in rats. Exp Neurol. 183**,** 355-66.

Kang, S. K., Putnam, L. A., Ylostalo, J., Popescu, I. R., Dufour, J., Belousov, A., Bunnell, B. A., 2004. Neurogenesis of Rhesus adipose stromal cells. J Cell Sci. 117**,** 4289-99.

Kang, S. K., Shin, M. J., Jung, J. S., Kim, Y. G., Kim, C. H., 2006. Autologous adipose tissue-derived stromal cells for treatment of spinal cord injury. Stem Cells Dev. 15**,** 583-94.

Katayama, M., Mizuta, I., Sakoyama, Y., Kohyama-Koganeya, A., Akagawa, K., Uyemura, K., Ishii, K., 1997. Differential expression of neuroD in primary cultures of cerebral cortical neurons. Exp Cell Res. 236**,** 412-7.

Kavanagh, E. T., Loughlin, J. P., Herbert, K. R., Dockery, P., Samali, A., Doyle, K. M., Gorman, A. M., 2006. Functionality of NGF-protected PC12 cells following exposure to 6-hydroxydopamine. Biochem Biophys Res Commun. 351**,** 890-5.

Keefer, E. W., Norton, S. J., Boyle, N. A., Talesa, V., Gross, G. W., 2001. Acute toxicity screening of novel AChE inhibitors using neuronal networks on microelectrode arrays. Neurotoxicology. 22**,** 3-12.

Kirik, D., Rosenblad, C., Bjorklund, A., 1998. Characterization of behavioral and neurodegenerative changes following partial lesions of the nigrostriatal dopamine system induced by intrastriatal 6-hydroxydopamine in the rat. Exp Neurol. 152**,** 259-77.

Kurrasch, D. M., Huang, J., Wilkie, T. M., Repa, J. J., 2004. Quantitative real-time polymerase chain reaction measurement of regulators of G-protein signaling mRNA levels in mouse tissues. Methods Enzymol. 389**,** 3-15.

Lakshmipathy, U., Verfaillie, C., 2005. Stem cell plasticity. Blood Rev. 19**,** 29-38.

Levivier, M., Przedborski, S., Bencsics, C., Kang, U. J., 1995. Intrastriatal implantation of fibroblasts genetically engineered to produce brain-derived neurotrophic factor prevents degeneration of dopaminergic neurons in a rat model of Parkinson's disease. J Neurosci. 15**,** 7810-20.

Lin, L. F., Doherty, D. H., Lile, J. D., Bektesh, S., Collins, F., 1993. GDNF: a glial cell line-derived neurotrophic factor for midbrain dopaminergic neurons. Science. 260**,** 1130-2.

McCoy, M. K., Martinez, T. N., Ruhn, K. A., Szymkowski, D. E., Smith, C. G., Botterman, B. R., Tansey, K. E., Tansey, M. G., 2006. Blocking soluble tumor necrosis factor signaling with dominant-negative tumor necrosis factor inhibitor attenuates loss of dopaminergic neurons in models of Parkinson's disease. J Neurosci. 26**,** 9365-75.

Milbrandt, J., de Sauvage, F. J., Fahrner, T. J., Baloh, R. H., Leitner, M. L., Tansey, M. G., Lampe, P. A., Heuckeroth, R. O., Kotzbauer, P. T., Simburger, K. S., Golden, J. P., Davies, J. A., Vejsada, R., Kato, A. C., Hynes, M., Sherman, D., Nishimura, M., Wang, L. C., Vandlen, R., Moffat, B., Klein, R. D., Poulsen, K., Gray, C., Garces, A., Johnson, E. M., Jr., et al., 1998. Persephin, a novel neurotrophic factor related to GDNF and neurturin. Neuron. 20**,** 245-53.

Miller, R. H., 2006. The promise of stem cells for neural repair. Brain Res. 1091**,** 258-64.

Mistry, S. K., Keefer, E. W., Cunningham, B. A., Edelman, G. M., Crossin, K. L., 2002. Cultured rat hippocampal neural progenitors generate spontaneously active neural networks. Proc Natl Acad Sci U S A. 99**,** 1621-6.

Ning, H., Lin, G., Lue, T. F., Lin, C. S., 2006. Neuron-like differentiation of adipose tissue-derived stromal cells and vascular smooth muscle cells. Differentiation. 74**,** 510-8.

Paxinos, G., Watson, C., Pennisi, M., Topple, A., 1985. Bregma, lambda and the interaural midpoint in stereotaxic surgery with rats of different sex, strain and weight. J Neurosci Methods. 13**,** 139-43.

Paxinos, G. a. W., C., 1998. The rat brain in stereotaxic coordinates. Academic Press.

Poot, M., Zhang, Y. Z., Kramer, J. A., Wells, K. S., Jones, L. J., Hanzel, D. K., Lugade, A. G., Singer, V. L., Haugland, R. P., 1996. Analysis of mitochondrial morphology and function with novel fixable fluorescent stains. J Histochem Cytochem. 44**,** 1363-72.

Potten, C. S., 1998. Stem cells in gastrointestinal epithelium: numbers, characteristics and death. Philos Trans R Soc Lond B Biol Sci. 353**,** 821-30.

Rehman, J., Traktuev, D., Li, J., Merfeld-Clauss, S., Temm-Grove, C. J., Bovenkerk, J. E., Pell, C. L., Johnstone, B. H., Considine, R. V., March, K. L., 2004. Secretion of Angiogenic and Antiapoptotic Factors by Human Adipose Stromal Cells. Circulation. 109**,** 1292-1298.

Romanov, Y. A., Darevskaya, A. N., Merzlikina, N. V., Buravkova, L. B., 2005. Mesenchymal stem cells from human bone marrow and adipose tissue: isolation,

characterization, and differentiation potentialities. Bull Exp Biol Med. 140**,** 138-43.

Safford, K. M., Hicok, K. C., Safford, S. D., Halvorsen, Y. D., Wilkison, W. O., Gimble, J. M., Rice, H. E., 2002. Neurogenic differentiation of murine and human adipose-derived stromal cells. Biochem Biophys Res Commun. 294**,** 371-9.

Safford, K. M., Safford, S. D., Gimble, J. M., Shetty, A. K., Rice, H. E., 2004. Characterization of neuronal/glial differentiation of murine adipose-derived adult stromal cells. Exp Neurol. 187**,** 319-28.

Schaffler, A., Buchler, C., 2007. Concise review: adipose tissue-derived stromal cells--basic and clinical implications for novel cell-based therapies. Stem Cells. 25**,** 818-27.

Scuteri, A., Cassetti, A., Tredici, G., 2006. Adult mesenchymal stem cells rescue dorsal root ganglia neurons from dying. Brain Res. 1116**,** 75-81.

Sonntag, K. C., Sanchez-Pernaute, R., 2006. Tailoring human embryonic stem cells for neurodegenerative disease therapy. Curr Opin Investig Drugs. 7**,** 614-8.

Stromberg, I., Herrera-Marschitz, M., Ungerstedt, U., Ebendal, T., Olson, L., 1985. Chronic implants of chromaffin tissue into the dopamine-denervated striatum. Effects of NGF on graft survival, fiber growth and rotational behavior. Exp Brain Res. 60**,** 335-49.

Tansey, K. E., McCoy, M.K., Martinez, T., Warren, M., Botterman, B.R., Tansey, M.G. , 2005. Adipose Derived Neural Progenitor (ADNP) Cells: A novel source for cell replacement therapy in spinal cord injury. J Neurotrauma. 22**,** 1176.

Tansey, M. G., McCoy, M. K., Frank-Cannon, T. C., 2007. Neuroinflammatory mechanisms in Parkinson's disease: Potential environmental triggers, pathways, and targets for early therapeutic intervention. Experimental Neurology. 208**,** 1-25.

Tholpady, S. S., Katz, A. J., Ogle, R. C., 2003. Mesenchymal stem cells from rat visceral fat exhibit multipotential differentiation in vitro. Anat Rec A Discov Mol Cell Evol Biol. 272**,** 398-402.

Ungerstedt, U., Arbuthnott, G. W., 1970. Quantitative recording of rotational behavior in rats after 6-hydroxy-dopamine lesions of the nigrostriatal dopamine system. Brain Res. 24**,** 485-93.

Waragai, M., Wei, J., Fujita, M., Nakai, M., Ho, G. J., Masliah, E., Akatsu, H., Yamada, T., Hashimoto, M., 2006. Increased level of DJ-1 in the cerebrospinal fluids of sporadic Parkinson's disease. Biochem Biophys Res Commun. 345**,** 967-72.

Weiss, M. L., Medicetty, S., Bledsoe, A. R., Rachakatla, R. S., Choi, M., Merchav, S., Luo, Y., Rao, M. S., Velagaleti, G., Troyer, D., 2006. Human umbilical cord matrix stem cells: preliminary characterization and effect of transplantation in a rodent model of Parkinson's disease. Stem Cells. 24**,** 781-92.

Weissman, I. L., 2000. Translating stem and progenitor cell biology to the clinic: barriers and opportunities. Science. 287**,** 1442-6.

Weissman, I. L., Anderson, D. J., Gage, F., 2001. Stem and progenitor cells: origins, phenotypes, lineage commitments, and transdifferentiations. Annu Rev Cell Dev Biol. 17**,** 387-403.

West, M. J., Slomianka, L., Gundersen, H. J., 1991. Unbiased stereological estimation of the total number of neurons in thesubdivisions of the rat hippocampus using the optical fractionator. Anat Rec. 231**,** 482-97.

Whitton, P. S., 2007. Inflammation as a causative factor in the aetiology of Parkinson's disease. Br J Pharmacol. 150**,** 963-76.

Wislet-Gendebien, S., Hans, G., Leprince, P., Rigo, J. M., Moonen, G., Rogister, B., 2005. Plasticity of cultured mesenchymal stem cells: switch from nestin-positive to excitable neuron-like phenotype. Stem Cells. 23**,** 392-402.

Woodbury, D., Reynolds, K., Black, I. B., 2002. Adult bone marrow stromal stem cells express germline, ectodermal, endodermal, and mesodermal genes prior to neurogenesis. J Neurosci Res. 69**,** 908-17.

Woodbury, D., Schwarz, E. J., Prockop, D. J., Black, I. B., 2000. Adult rat and human bone marrow stromal cells differentiate into neurons. J Neurosci Res. 61**,** 364-70.

Yang, L. Y., Liu, X. M., Sun, B., Hui, G. Z., Fei, J., Guo, L. H., 2004. Adipose tissue-derived stromal cells express neuronal phenotypes. Chin Med J (Engl). 117**,** 425-9.

Yasuhara, T., Matsukawa, N., Hara, K., Yu, G., Xu, L., Maki, M., Kim, S. U., Borlongan, C. V., 2006. Transplantation of human neural stem cells exerts neuroprotection in a rat model of Parkinson's disease. J Neurosci. 26**,** 12497-511.

Ye, M., Chen, S., Wang, X., Qi, C., Lu, G., Liang, L., Xu, J., 2005. Glial cell line-derived neurotrophic factor in bone marrow stromal cells of rat. Neuroreport. 16**,** 581-4.

Ye, M., Wang, X. J., Zhang, Y. H., Lu, G. Q., Liang, L., Xu, J. Y., Chen, S. D., 2007. Transplantation of bone marrow stromal cells containing the neurturin gene in rat model of Parkinson's disease. Brain Res. 1142**,** 206-16.

Zuk, P. A., Zhu, M., Ashjian, P., De Ugarte, D. A., Huang, J. I., Mizuno, H., Alfonso, Z. C., Fraser, J. K., Benhaim, P., Hedrick, M. H., 2002. Human adipose tissue is a source of multipotent stem cells. Mol Biol Cell. 13**,** 4279-95.

Zuk, P. A., Zhu, M., Mizuno, H., Huang, J., Futrell, J. W., Katz, A. J., Benhaim, P., Lorenz, H. P., Hedrick, M. H., 2001. Multilineage cells from human adipose tissue: implications for cell-based therapies. Tissue Eng. 7**,** 211-28.

APPENDIX B

DJ-1-NULL MICE DO NOT DISPLAY INCREASED VULNERABILITY TO INFLAMMATION-RELATED DEGENERATION

The contents of this chapter was submitted as a manuscript for publication to the *Journal of Neuroinflammation.*

Thi Tran[*], Terina N. Martinez[*], Tamy Frank-Cannon[*], Kelly A. Ruhn, Marian Marvin, Bradford Casey, Isaac Treviño, John Hong, Malú G. Tansey, and Matthew S. Goldberg

[*]Equal contribution

Abstract

Background: Complex interactions between genetic susceptibility and environmental factors are thought to underlie the pathogenesis of Parkinson's disease (PD). Although the role of inflammatory processes in modulating risk for development of PD has yet to be fully understood, prospective studies suggest that chronic use of nonsteroidal anti-inflammatory drugs (NSAIDs) reduce the incidence of PD. Loss-of-function mutations in the *DJ-1* gene cause a rare form of familial PD with an autosomal recessive pattern of inheritance; however, *DJ-1-null* mice do not display nigrostriatal pathway degeneration, suggesting that environmental factors may be needed to induce neurodegeneration. Based on recent reports that *DJ-1-null* astrocytes overproduce nitric oxide *in vitro* [2] and work from our group demonstrating that a chronic inflammatory stimulus induce nigral DA neuron loss in *parkin -/-* mice [1], we investigated whether loss of DJ-1 increases vulnerability to inflammation-induced nigral degeneration *in vivo*.

Methods: We exposed young-adult wild type or *DJ-1-null* mice to repeated intraperitoneal injections of low-dose lipopolysaccharide (LPS) or saline vehicle or to

intranasal soluble Tumor Necrosis Factor (TNF). We measured locomotor performance using a variety of behavior tasks and then harvested their brains for molecular analyses of microglial activation and oxidative stress and neurostereological analyses of DA neurons (TH+ cells) and total neurons (NeuN+ cells) in substantia nigra pars compacta (SNpc).

Results: We found that *DJ-1-null* mice displayed enhanced neuroinflammatory responses in the midbrain compared to wild type mice but neither group developed locomotor deficits or nigral degeneration in response to chronic LPS injections or intranasal solTNF. A survey of oxidative stress markers revealed no significant LPS-induced upregulation of Parkin or anti-oxidant gene expression in *DJ-1-null* mice compared to wild type mice.

Conclusions: Our studies indicate that *DJ-1-null* mice do not display increased vulnerability for inflammation-related nigral degeneration. We conclude that either DJ-1 does not have a critical role in protecting DA neurons against inflammation-induced oxidative stress or there is compensatory gene expression in the midbrain of *DJ-1-null* mice which renders them resistant to cytotoxic effects triggered by chronic neuroinflammation.

Background

Over the last decade, a great wealth of new information has emerged to suggest that inflammation-derived oxidative stress and cytokine-dependent neurotoxicity are likely to contribute to nigrostriatal pathway degeneration [3-7], the pathological hallmark of Parkinson's Disease (PD) in humans. Post-mortem analyses of brains from PD patients confirmed the presence of inflammatory mediators in the area of substantia nigra (SN) where maximal destruction of vulnerable melanin-containing dopamine (DA)-producing neurons occurs in PD patients [8-13]. . Signs of inflammation included activated microglia and accumulation of cytokines (including TNF, IL-1β, IL-6, and IFNγ) which exert neurotoxic effects on DA neurons; and SN dopaminergic neurons may be uniquely vulnerable to neuroinflammatory insults that enhance oxidative stress [7]. The higher sensitivity of nigral DA neurons to injury induced by neuroinflammatory mediators may be secondary to reduction of endogenous anti-oxidant capacity (i.e. glutathione depletion). Pharmacologically, chronic infusion of various anti-inflammatory compounds (including COX-2-selective NSAIDs or soluble TNF-selective inhibitors) rescues nigral DA neurons from progressive degeneration and death [14-16]. These findings raise the interesting possibility that environmental triggers initiate cytokine-driven neuroinflammation and contribute to the development of Parkinson's disease in humans.

Monogenic forms of PD have been linked to loss-of-function mutations in a number of genes, giving rise to autosomal recessive parkinsonism [17], including mutations in the E3 ligase Parkin and in DJ-1, a putative redox sensor that associates with chaperones [18] and translocates to mitochondria during conditions of oxidative stress [19-24]. In addition to its proposed role as a redox sensor [25], DJ-1 may also have

important functions as an RNA binding protein chaperone during the unfolded protein response (UPR) to minimize protein misfolding and aggregate formation [26]. Although *DJ-1-null* mice have been reported to be hypersensitive to MPTP [27] and display abnormalities in dopaminergic function when exposed to paraquat [28], these mice do not develop nigrostriatal degeneration [24, 29]. Interestingly, recent *in vitro* studies implicated a role for DJ-1 in astrocytes as an important regulator of nitric oxide production, raising the possibility that exposure to chronic inflammatory stress may induce nigral degeneration in these mice. Therefore, the purpose of our study was to investigate the extent to which loss of DJ-1 increases the vulnerability for inflammation-induced nigrostriatal degeneration *in vivo*. To this end, we investigate the extent to which repeated intraperitoneal injections of low-dose lipopolysaccharide (LPS) or intranasal soluble Tumor Necrosis Factor (TNF) induced locomotor deficits, neuroinflammation, enhanced oxidative stress, or nigral DA neuron loss in *DJ-1-null* or age-matched wild type mice.

Methods

Animals

DJ-1-null mice were generated and characterized as described previously [24]. Prior to these studies, *DJ-1-null* mice were bred onto a C57BL/6 background and back-crossed for over ten generations. All mice were housed in a pathogen-free, climate controlled facility in the Animal Resources Center at The University of Texas Southwestern Medical Center at Dallas and given food and water *ad libitum*. All animal studies were reviewed and approved by the Institutional Animal Care and Use Committee at The University of Texas Southwestern Medical Center at Dallas in accordance with the National Institutes of Health Guide for the Care and Use of Laboratory Animals.

Systemic LPS administration

The regimen of LPS injections was chosen based on previous work from our group which demonstrated this dose and frequency of LPS delivered i.p. triggered a neuroinflammatory response in the midbrain and elicited nigral DA neuron loss in Parkin-null mice [30]. Young adult (6-13 week old *DJ-1-null* mice on a C57BL/6 background and wild type littermate mice were given either 7.5×10^5 EU/kg lipopolysaccharide (LPS) from *Escherichia coli* O111:B4 (Sigma-Aldrich, Saint Louis, MO, USA) or 0.9 % sodium chloride (vehicle control, Braun Medical, Inc, Irvine, CA, USA) injections intraperitoneally (i.p.) twice a week for 3 months (n=4-7) (**Figure 1)**. An additional group was given systemic LPS or vehicle for 3 months followed by a 3-month wait period during which no additional i.p. injections were administered (n = 3-6 mice

per group). A final group was given systemic LPS or vehicle for 6 months with no wait period (n=3-7 mice per group).Following the last i.p. injection, the animals were divided into two sets and processed for either immunohistochemistry or QPCR (**Figure B.1**).

Intranasal TNF Administration

Murine soluble TNF (1-2 µl) was administered intranasally via an L-20 Pipetteman (Rainin) twice weekly for the time indicated in each set of experiments at one of two doses (T1= 0.5ng) and (T2= 5ng) in WT or *DJ-1-null* mice.

Behavior Testing

For all behavioral tests, mice (n = 8 per group) were evaluated at baseline (before i.p. injections began) and depending on the regimen again at 3 and 6 months after LPS or saline administration.

Open-field. Open-field behavior in a glass container (diameter, 24.5 cm) was recorded for 5 min for evaluation of time spent moving and number of rearing events by an investigator blinded to genotype and treatment history.

Narrow Beam walk. A narrow beam (1.1 cm diameter, 80.6 cm testing length) with a home cage at one end was used. Initial training prior to treatment consisted of 3 sessions of 3 trials per session for 4 consecutive days. Mice received additional training sessions at 3 months and 6 months after the start of treatment regimen consisting of 3 sessions of 3 trials per session on one day. Testing was conducted the day after training and consisted

of one session of 3 trials. Average time to traverse the full length of the beam was determined and used for data analysis.

Accelerating rotarod. A base speed of 20 rpm with an acceleration of 0.2 rpm/second was used on the rotarod (Economex 0207-005 M, Columbus Instruments, Columbus, OH). Mice were trained prior to treatment in 3 sessions of 4 trials each for 4 consecutive days. Mice received additional training sessions at 3 months and 6 months after start of treatment consisting of 3 sessions of 4 trials per session on one day. Testing consisted of one session of 3 trials the day after training was completed. Latency to fall (seconds) was calculated and used for data analysis.

Tissue Harvest

Following the last i.p. injection, mice in the 3-month, 3-month/3-month wait, and 6-month treatment cohort (n = 4 mice per treatment group) were deeply anesthetized with Euthasol then intracardially perfused with 0.1 M phosphate buffered saline (PBS) pH 7.4 supplemented with 0.1 % glucose and 1 U/mL heparin prior to rapid whole brain removal. For quantitative real time polymerase chain reaction (QPCR), brain tissue was microdissected into 4 regions on an ice-cold glass Petri dish: olfactory bulb (OB), cerebellum (CB), ventral midbrain (MB) and cortex (CX) then snap-frozen in liquid nitrogen and stored at -80ºC until processed for RNA extraction. For immunohistochemistry, mice in the 3-month, 3-month/3-month wait, and 6-month treatment cohort (n = 7 – 8 mice per group) were perfused with 0.1M PBS followed by 4 % paraformaldehyde in PBS (pH 7.4). Brains (in the skull) were post-fixed overnight in 4

% PFA. Brains were dissected out then cryoprotected for 24 hr in 20 % sucrose in 0.1 M PBS pH 7.4, embedded in Neg 50 (Richard Allen Scientific, Kalamazoo, MI), and frozen in dry ice-cooled isopentane.

Quantitative Real-time Polymerase Chain Reaction

Total RNA was isolated from tissue samples using Tri Reagent® (Molecular Research Center, Cincinnati, OH, USA), treated with DNAse I (Invitrogen, Carlsbad, CA), and reverse transcribed to obtain cDNA. QPCR was performed using SYBR Green Master Mix (ABI) on an Applied Biosystems Prism 7900HT sequence detection system as described [31]. Primers for each gene (available upon request) were designed using Primer Express Software (PerkinElmer Life Sciences, Wellesley, MA, USA) and validated by analysis of template titration and dissociation curves. Results for QPCR were normalized to the housekeeping gene cyclophilin B and evaluated by comparative C_T method (user bulletin No. 2, PerkinElmer Life Sciences). RNA levels are expressed relative to the wild type saline-injected (vehicle) mice.

Immunohistochemistry

Coronal serial sections (30 μm thickness) were cut on a Leica CM 1850 cryostat and placed on Superfrost/Plus microscope slides (Fisher Scientific). Sections on slides were stored at -80° C until processed for immunohistochemistry.

Brightfield immunohistochemistry. Sections were stained for tyrosine hydroxylase (TH) using published protocols [32, 33]. Sections were permeabilized in 0.3 % TritonX-100 in

PBS pH 7.4. Endogenous peroxidases were quenched with 1 % H_2O_2 and non-specific binding was blocked with 5 % normal serum (goat or horse, Equitech-Bio, Inc., Kerrville, TX). Sections were incubated with primary antibodies against TH (rabbit polyclonal diluted 1:2000, Chemicon International, Temecula, CA, USA), or neuronal nuclear antigen (NeuN) (mouse monoclonal diluted 1:1000, Chemicon) overnight at room temperature followed by biotinylated secondary antibody (goat anti-rabbit or horse anti-mouse rat absorbed, or goat anti-rat IgG diluted 1:400, Vector Laboratories, Burlingame, CA, USA) and NeutrAvidin-HRP (diluted 1:5000, Pierce Biotechnology, Inc., Rockford, IL, USA). The tissue bound peroxidase activity was developed with a 0.024 % diaminobenzadine (DAB, Sigma), 0.006 % H_2O_2 in 0.05 M Tris-HCl buffer pH 7.6 for 20 min with or without nickel intensification. Tissue sections were dehydrated in a graded series of ethanols, immersed in xylene, and coverslipped with Permount (Fisher Scientific).

Fluorescence immunohistochemistry. Brain sections were stained for microglial markers using a standard immunofluorescence protocol [14]. Auto-fluorescence was quenched in 0.2 M glycine in PBS pH 7.4, for 1 hr at room temperature. Sections were then permeabilized in 0.3 % Triton X-100 with 1 % normal goat serum in 20 mM Tris-buffered saline (TBS) pH 7.4. Non-specific binding was blocked with species-appropriate 1% normal serum in TBS. Sections were incubated overnight at 4° C with rat monoclonal antibody made against mouse CD68 (diluted 1:150, Serotec, Raleigh, NC) and rabbit polyclonal anti-TH (diluted 1:250, Chemicon) followed by Alexa-488 goat anti-rabbit (Invitrogen) secondary antibody (Fab) or Alexa-594 goat anti-rat secondary antibody

(each at 1:1000 dilution, Invitrogen) for 4 hr at room temperature. Antibodies were diluted in blocking buffer with 0.1 % Triton X-100. Washes were done in TBS with 0.2 % Triton X-100 (TBST). Following secondary antibody incubations, slides were rinsed briefly with dH_2O, then counterstained with Hoescht 33258 (at 1:20,000, Invitrogen) for 15 min, and coverslipped with aqueous mounting media with anti-fade (Biomeda Corp, Foster City, CA, USA).

Stereological Analysis

The optical fractionator probe of Stereoinvestigator software (MicroBrightField, Inc., Williston, VT, USA) was used to obtain an unbiased estimate of TH-positive and NeuN-positive neurons in the substantia nigra pars compacta (SNpc) and ventral tegmental area (VTA) as per the atlas of Paxinos [34]. Stereologic parameters were as follows: counting frame, 50 μm x 50 μm; optical dissector: 20 μm; grid size, 120 μm x 160 μm. For the population size estimate (number of sections per animal), a target coefficient of error (Gundersen's m = 1) of less than 0.10 was considered acceptable. Neuron counting was performed by two different investigators blinded to treatment history.

Striatal TH fiber density and densitometry

Coronal serial sections (30 μm thickness) were cut between Bregma -1.22 to 1.70 on a Leica CM 1850 cryostat and placed on Superfrost/Plus microscope slides (Fisher Scientific). Tissue sections were immunostained for TH and developed using DAB as described above. Images of striatum (caudate putamen) from 12 tissue sections per animal were taken with a CoolSnap cf digital color camera mounted on a Olympus BX61

microscope. Exposure times were kept constant for all images. TH-positive fiber density was determined using background corrected integrated optical density (IOD) measurements for each section using an Alpha Innotech FluorChem FC2 imaging workstation and software. All sections for each animal were averaged and group means were used to compare between treatment groups.

Striatal DA and metabolites

Levels of striatal DA and its metabolites (DOPAC, HVA and 3-MT) were quantified by HPLC with electrochemical detection. Mice were euthanized by carbon dioxide asphyxiation and the striatum was immediately dissected on an ice-cold glass Petri dish, weighed and stored at -80 until analysis. Frozen brain tissue was sonicated in 49 volume/weight (mg of tissue) of 0.1 M perchloric acid containing 0.2 mM sodium metabisulfite and centrifuged at 20,000 rpm 20 minutes 4°C in a benchtop centrifuge to clear debris. 20 µL of cleared supernatant was injected onto a C18 HPLC column and separated by isocratic elution at a flow rate of 0.6 ml/min with MD-TM mobile phase (ESA Inc, Chelmsford, MA). Neurotransmitter monoamines and metabolites were detected using a BAS electrochemical cell set to a potential of +800 mV and compared to external standards.

Statistics

Multiple-way analysis of variance (ANOVA) with significance level $\alpha = 0.05$ were used as indicated for each set of experimental data. Significant differences between groups were further evaluated using Tukey's HSD post hoc test. Kruskal-Wallis analysis was the

nonparametric statistical test used for testing equality of population medians of integrated optical density measurements of striatal TH fiber density.

Results

DJ-1-null mice exposed to prolonged, serial low-dose systemic LPS do not develop locomotor deficits

To test the hypothesis that DJ-1 regulates vulnerability to inflammation-related nigral degeneration, we exposed wild type and *DJ-1-null* mice to various systemic LPS regimens (**Figure B.1**). A number of behavioral tasks were measured at the time-points indicated to investigate the extent to which the prolonged, serial low-dose systemic LPS regimens induced locomotor alterations and subsequently various cohorts were sacrificed as indicated for gene expression or immunohistological analysis of microdissected brain tissue. To assess fine-motor performance, mice were subjected to the narrow beam-walk test. Our results indicate that *DJ-1-null* mice chronically injected with LPS did not display significantly slower average time-to-cross compared to saline-treated *DJ-1-null* mice or either group of WT mice (**Figure B.2A**). To assess gross locomotion, we measured rotarod performance. No differences were noted on rotarod performance (**Figure B.2B**; $p = 0.19$) or open-field testing (data not shown). Thus, in the present study, prolonged, serial i.p. injections of LPS or saline did not cause gross motor abnormalities.

Chronic low-dose systemic LPS does not promote loss of nigral DA neurons in *DJ-1-null* mice

We measured endpoint immunohistological outcomes for unbiased stereological analyses of DA neuron number and total neuron number by staining midbrain sections with the DA neuron marker TH and the pan-neuronal marker NeuN (**Figure B.3**). Compared to similarly dosed wild type mice, *DJ-1-null* mice that received 3 months of repeated low-dose systemic LPS did not exhibit significant reductions in TH positive or NeuN positive neurons in the SNpc. Similarly, neither *DJ-1-null* mice nor wild type mice that received 3 months of repeated low-dose systemic LPS followed by a 3-month lag period or 6 months of repeated low-dose systemic LPS displayed significant reductions in the number of TH positive or NeuN positive SNpc neurons (**Figure B.3A**). Levels of TH and NeuN positive neurons were also unchanged in the ventral tegmental area (VTA) (**Figure B.3B**).

To investigate whether repeated low-dose systemic LPS affected dopaminergic terminals at the striatum, we stained striatal sections for TH. No decreases in striatal TH fiber immunoreactivity were detectable in brain sections from *DJ-1null* mice treated with low-dose systemic LPS for 3 or 6 months or for 3 months followed by a 3-month lag period (**Figure B.4B**), densitometric analysis of multiple sections indicated the only significant change occurred in *DJ-1-null* exposed to 3-month LPS which displayed an increase in striatal TH-fiber density (**Figure B.4A**). To extend and confirm these findings, we measured the tissue levels of DA and its metabolites in microdissected striatum by HPLC and electrochemical detection. In agreement with the immunohistological results, repeated low-dose i.p. LPS injections caused a detectable increase in striatal DA content in *DJ-1-null* mice exposed to the 3-month regimen; no

changes in DA turnover were observed in any treatment group of either genotype (**Figure B.4C**).

DJ-1-/- and wild type mice display similar neuroinflammatory responses in midbrain in response to low-dose systemic LPS administration

To investigate the possibility that the lack of nigral neuron loss in LPS-treated *DJ-1-null* mice may have been attributed to an attenuated neuroinflammatory response, we used QPCR to measure the relative mRNA expression of TNF and CD45 in midbrain and cortex in the mice from the 6-month treatment groups. We found that the *DJ1-null* mice displayed increased TNF mRNA in response to the LPS challenge in both midbrain and cortex but an attenuated LPS-induced expression of CD45 compared to the wild type mice in midbrain. Together, these data suggest that the repeated low-dose LPS injections triggered similar midbrain neuroinflammatory responses in WT and *DJ-1-null* mice. Based on previous work in which we found that Parkin function may influence neuroinflammatory responses and vulnerability to inflammation-induced degeneration (Frank-Cannon et al., 2008); we measured the levels of Parkin expression in both genotypes. We found no differences in the levels of Parkin expression between genotypes (**Figure B.5A, B**).

DJ-1-null mice do not display basal upregulation of anti-oxidant genes in midbrain or in response to low-dose systemic LPS administration

We next investigated whether the lack of nigral cell loss in *DJ-1-null* mice following repeated, serial systemic low-dose LPS administration might have been

attributed to upregulation of anti-oxidant responses as a consequence of DJ-1 loss. We used QPCR to measure the level of expression of key antioxidant genes implicated in protection of DA neurons in the midbrain of WT or *DJ-1-null* mice that received 3- or 6-month low-dose systemic LPS administration. Based on the current literature, we elected to analyze the transcription factor NF-E2 related factor (Nrf2), which binds to the antioxidant response element (ARE) to induce expression of antioxidant and phase 2 detoxification enzymes, NAD(P)H:quinone oxidoreductase (NQO1), heme-oxygenase-1 (HO-1), inducible nitric oxide synthase (iNOS), superoxide dismutase-1(SOD1), and superoxide dismutase -2 (SOD2). We found no significant upregulation of oxidative stress markers in either genotype or in response to LPS treatment.

Intranasal soluble TNF delivery does not promote nigral DA neuron loss in WT or *DJ-1-null* mice

Because the repeated i.p. LPS injections failed to trigger nigral DA neuron loss in DJ-1-null mice, we tested an additional inflammatory regimen designed to trigger neuroinflammation directly in the olfactory bulb. We delivered rhodamine-labeled human TNF (rh-TNF) intranasally to confirm uptake and transport by nasal epithelia (NE). Immunofluorescence analyses of cryosectioned rostral and caudal tissues revealed detectable uptake and transport of rh-TNF in rostral sections of NE during the early time points. As expected, the distribution of rh-TNF decreased in rostral sections and increased in caudal sections as a function of time (**Supplemental Figure B.S1**). Because TNF can induce cachexia, we investigated the extent to which intranasal TNF (inTNF) administration decreased food and water intake. Murine soluble TNF was administered

intranasally twice weekly at one of two doses (T1= 0.5ng) and (T2= 5ng) for 1-wk (Paradigm 1, P1) or for 2-weeks (Paradigm 2, P2) in WT or *DJ-1-null* mice. Food consumption was monitored for 4-5 wks just prior to and during the inTNF dosing. Results revealed no adverse systemic effects (i.e., loss of appetite or other cachexic effects) (data not shown) after repeated systemic inTNF dosing. Upon confirmation that inTNF uptake and transport did not elicit cachexic effects, we investigated the extent to which inTNF dosing triggered an inflammatory response in the midbrain. We administered three inTNF doses of 0.5 or 5ng TNF followed by a 3-week wait then measured inflammatory gene expression by QPCR. We found that *DJ-1-null* mice displayed increased expression of TNF, CD45 and Cox-1 compared to WT mice, but inTNF exposure did not increase these responses further to any significant extent (data not shown).

Next we investigated whether the enhanced neuroinflammatory gene expression in *DJ-1-null* mice resulted in detectable nigral DA neuron loss. Building on the intranasal dosing paradigm, we subjected older (10-mo old) *DJ-1null* mice and age-matched WT mice to an experimental regimen of inTNF dosing that included several boost doses and a two-month lag time such that mice were on average 13 mos old at the time of sacrifice (**Figure B.7A**). Stereological analyses to determine the extent to which the experimental paradigm induced nigral DA neuron loss revealed no inTNF-induced nigral DA neuron loss in mice of either genotype (**Figure B.7B**). Consistent with immunohistological findings, measurements of striatal DA, DA metabolites and DA turnover (**Figure B.7C**) as well as 5-HT (data not shown) by HPLC and electrochemical detection showed no effects on DA or 5-HT metabolism.

Discussion

Although, *DJ-1-null* mice do not display loss of nigral DA neurons they display deficits in dopaminergic function [24] which are further accentuated when exposed to paraquat [28] and MPTP [27], suggesting a protective role for DJ-1 in mitochondrial function and/or against oxidative stress. In support of this molecular model, DJ-1 has been shown to translocate to mitochondria [21] in response to oxidative stress when key cysteine residues become acidified [19] and to interact with multifunctional regulators of transcription and RNA metabolism in the nucleus [35]. More recently, DJ-1 (but not pathogenic mutants linked to familial parkinsonism) was shown to associate with a number of different RNA targets in cells in an oxidation-dependent fashion, including mitochondrial genes, genes involved in glutathione metabolism, and PTEN/PI3K pathway components [26] which are consistent with studies implicating DJ-1 in malignancies through suppression of PTEN-induced apoptosis and these interactions have been confirmed in human brain [36].

In the last 10 years, a role for DJ-1 in regulation of inflammation-induced oxidative stress was implicated by *in vitro* observations that i.p. LPS can increase DJ-1 expression in peritoneal macrophages robustly in response to NADPH oxidase-derived ROS [37] and that *DJ-1-null* astrocytes overproduced nitric oxide when stimulated with LPS [2]. However, we report here the unexpected finding that *DJ-1-null* mice do not display increased vulnerability to inflammation-induced nigral degeneration when exposed to repeated i.p. LPS injections or direct intranasal delivery of soluble TNF. We speculate that compensatory gene expression in mitochondrial enzymes in *DJ-1-null* mice [38] may be one possible explanation for their apparent resistance to inflammation-

induced loss of nigral DA neurons *in vivo*. Alternatively, it is possible that a longer lag-time between the delivery of the inflammatory stimuli and the endpoint of the study (greater than 3 months) might be required to uncover increased vulnerability to inflammation-induced degeneration.

Previous work from our group demonstrated that the same serial regimen of low-dose intraperitoneal (i.p.) LPS injections used in these studies triggered a modest neuroinflammatory response in the central nervous system (CNS) in anatomical regions that show early involvement in PD (olfactory bulb and midbrain) and not in areas that are unaffected in the early stages of the disease. In addition, *Parkin-null* mice displayed increased vulnerability to inflammation-induced degeneration of nigral DA neurons when exposed to the same repeated i.p. LPS regimen used in these studies [1]. Importantly, these findings indicate that Parkin loss increased vulnerability to inflammation-related neurodegeneration [1] in contrast to their lack of increased susceptibility to oxidative neurotoxins such as MPTP, 6-OHDA and methamphetamine [39-41]. Based on these findings, we conclude that Parkin and DJ-1 have non-overlapping roles in protecting the nigrostriatal pathway against a variety of specific neurotoxic stresses.

FIGURES

Figure B.1

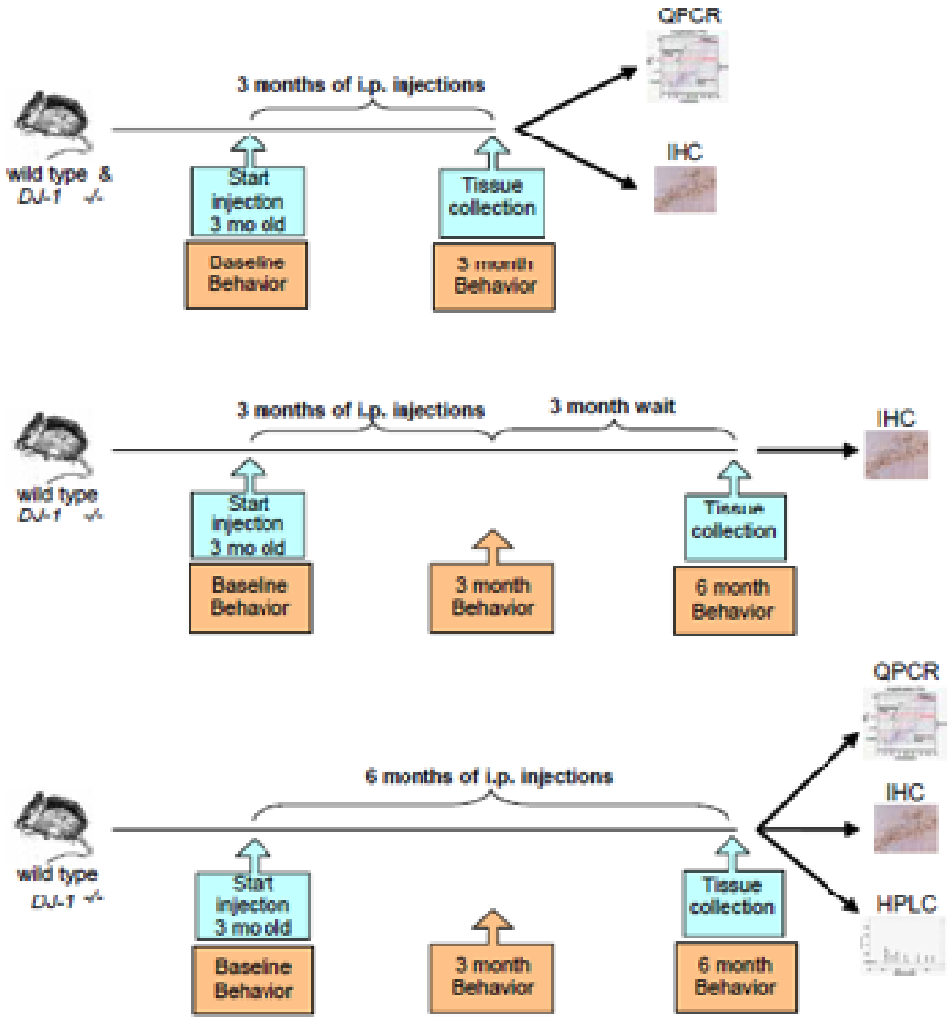

Figure B.1. Schematic of systemic LPS administration regimens and measurable outcomes.

Wild type and DJ-1-/- mice were given low-dose LPS or an equivalent volume of saline vehicle twice a week intraperitoneally for the indicated times. Locomotor behavior was evaluated before and during the course of treatment. Groups of animals were sacrificed as indicated for biochemical and immunohistological analyses. IHC, Immunohistochemistry.

Figure B.2

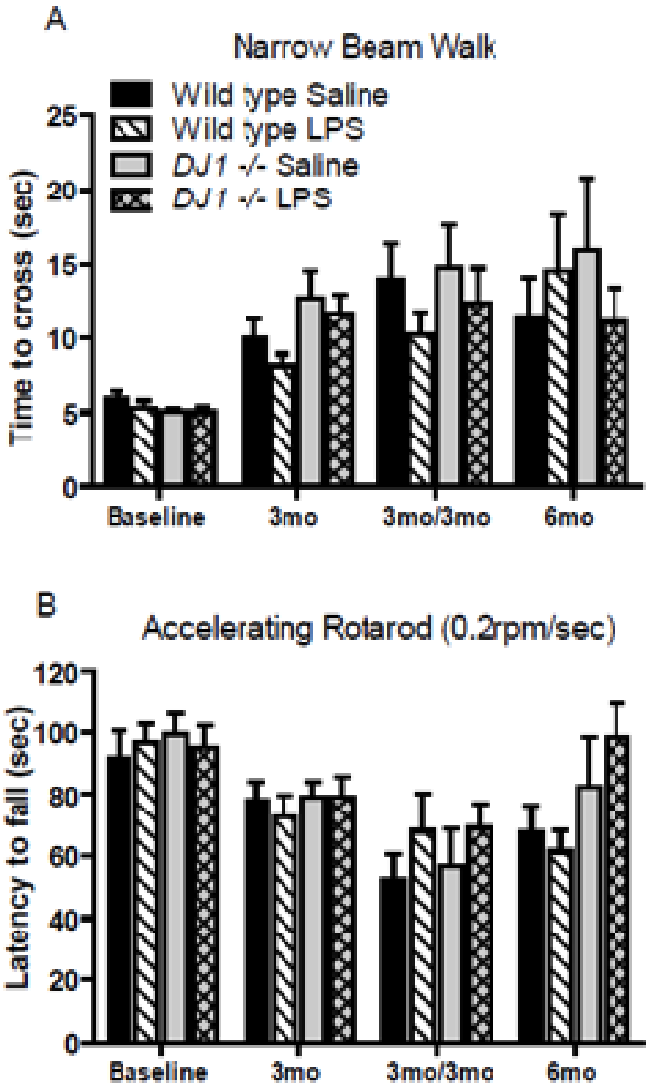
A
Narrow Beam Walk
Wild type Saline
Wild type LPS
DJ1 -/- Saline
DJ1 -/- LPS
Time to cross (sec)
25
20
15
10
5
0
Baseline
3mo
3mo/3mo
6mo
B
Accelerating Rotarod (0.2rpm/sec)
Latency to fall (sec)
120
100
80
60
40
20
0
Baseline
3mo
3mo/3mo
6mo

Figure B.2. Fine-locomotor deficits in *DJ-1*$^{-/-}$ mice exposed to prolonged, serial lowdose systemic LPS.

(a) No significant differences were detected between genotypes or treatment groups on accelerating rotarod, suggesting no general malaise. Bars represent mean $\pm$ SEM; n=8 per group. (b) *DJ-1*$^{-/-}$ mice display significantly prolonged time to cross on narrow beam walk after LPS treatment regimens. Asterisks indicate significant differences compared with saline-treated wild type and LPS-treated wild type group, whereas double asterisks indicate difference from all other groups. The triangle indicates a significant difference compared with LPS-treated wild type animals only.

Figure B.3

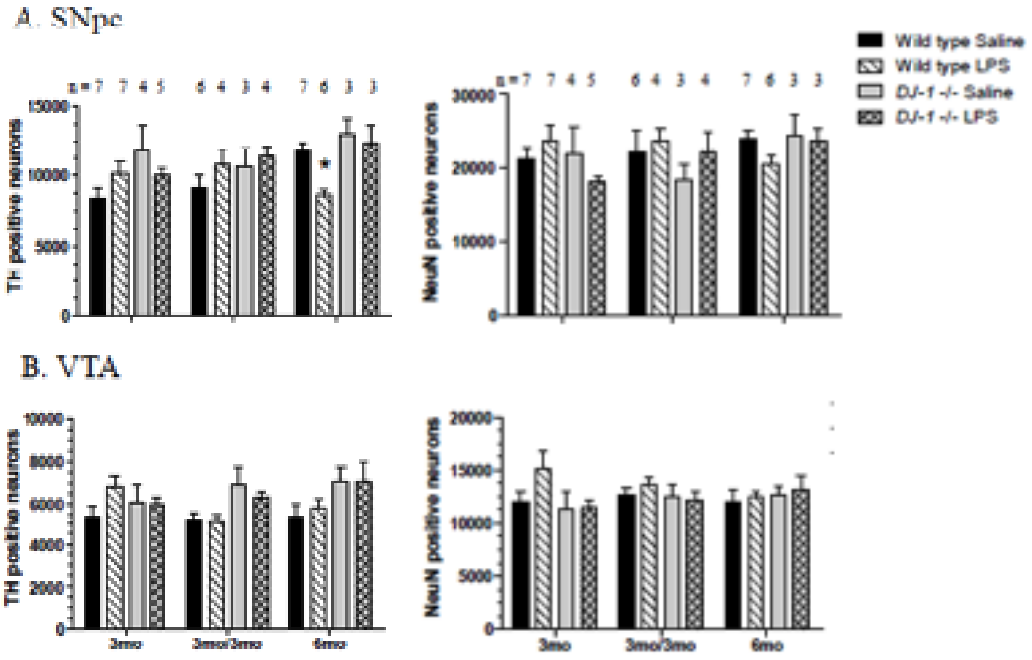
A. SNpc
B. VTA
Wild type Saline
Wild type LPS
DJ-1 -/- Saline
DJ-1 -/- LPS
TH+ positive neurons
NeuN positive neurons
TH positive neurons
n=7 7 4 5 6 4 3 4 7 6 3 3
3mo
3mo/3mo
6mo

Figure B.3. *DJ-1*$^{-/-}$ mice do not display increased vulnerability to nigral DA neuron loss induced by repeated low-dose systemic LPS compared to wild type mice.

Unbiased stereological analysis indicates that *DJ-1*$^{-/-}$ mice exposed to 3 months of low-dose systemic LPS followed by a 3 month wait or mice exposed to 6 months of low-dose systemic LPS do not display a significant reduction of TH or NeuN immunopositive neurons in the SNpc. Error bars represent SEM, and the number of mice in each group is denoted in parentheses (n). Asterisks indicate significant differences compared with wild type, saline-treated animals by three-way ANOVA followed by Tukey's HSD post hoc test at $p < 0.05$.

Figure B.4

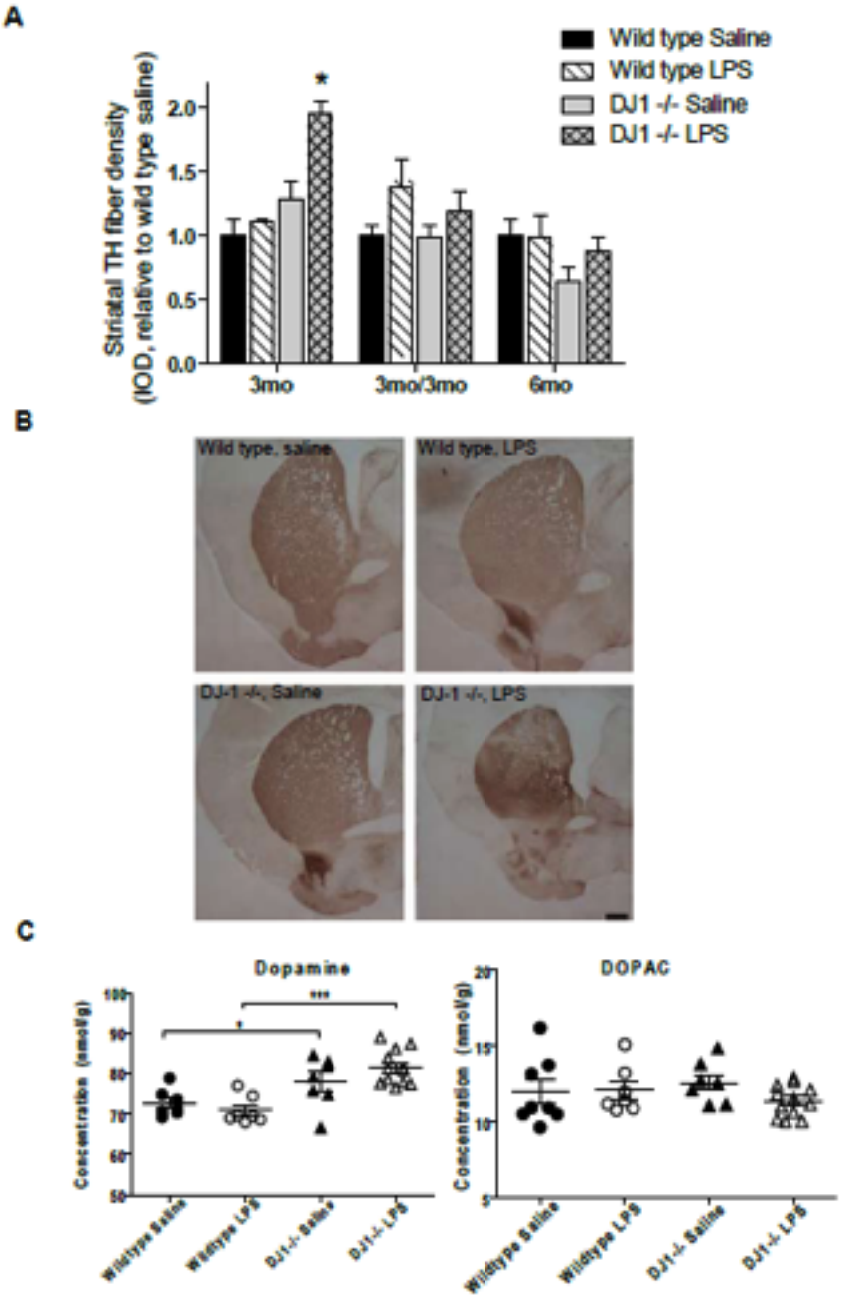
A
Wild type Saline
Wild type LPS
DJ1 -/- Saline
DJ1 -/- LPS
Striatal TH fiber density
(IOD, relative to wild type saline)
2.0
1.5
1.0
0.5
0.0
*
3mo
3mo/3mo
6mo
B
Wild type, saline
Wild type, LPS
DJ-1 -/-, Saline
DJ-1 -/-, LPS
C
Dopamine
DOPAC
Concentration (nmol/g)
***
*
Wildtype Saline
Wildtype LPS
DJ1-/- Saline
DJ1-/- LPS

Figure B.4. Repeated low-dose intraperitoneal LPS injections does not cause loss of striatal TH-immunopositive terminals or DA depletion in *DJ-1-null* or wild type mice.

(a) Densitometric analysis of striatal TH fiber density (see Materials and Methods) indicates no significant differences between genotypes or treatment groups. Bars represent mean $\pm$ SEM; n = 7-12 animals per group. (b) Representative striatal sections stained for TH from mice in the 6 month treatment groups. (c) Striatal levels of DA and its metabolite DOPAC were measured by HPLC and electrochemical detection.

Figure B.5

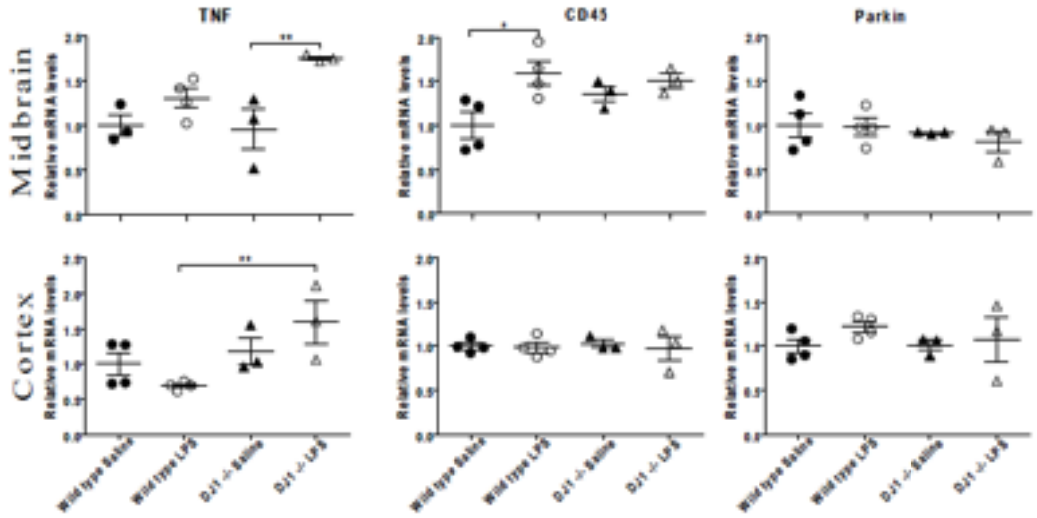
TNF
CD45
Parkin
Midbrain
Cortex
Relative mRNA levels
Wild type Saline
Wild type LPS
DJ1 -/- Saline
DJ1 -/- LPS

Figure B.5. *DJ-1-null* and wild type mice display similar neuroinflammatory responses after repeated low-dose systemic LPS administration.

Real-time QPCR analyses of microdissected midbrain tissue measured expression levels of neuroinflammation markers TNF and CD45 by QPCR in the ventral midbrain and cortex of mice treated with low-dose systemic LPS for 6 months. Parkin mRNA was also measured and found to be similar in both genotypes. Asterisks indicate significant difference wild typeas indicated. Bars represent mean $\pm$ SEM; n = 3– 4 animals per group. Two-way ANOVA was performed with Bonferroni's post hoc at $*p < 0.05$, $**p<0.01$.

Figure B.6

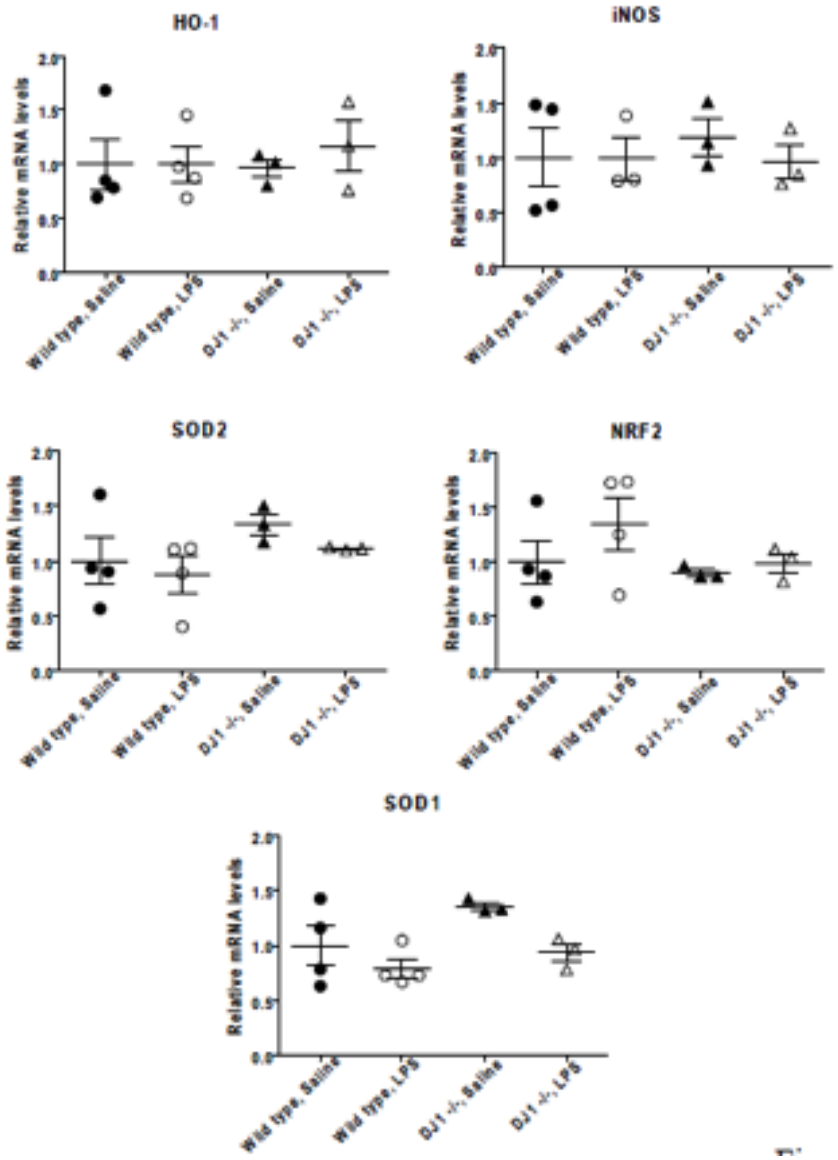
HO-1
iNOS
SOD2
NRF2
SOD1
Relative mRNA levels
2.0
1.5
1.0
0.5
0.0
Wild type, Saline
Wild type, LPS
DJ1 -/-, Saline
DJ1 -/-, LPS

Figure B.6. Oxidative stress responses to prolonged, serial administration of low-dose systemic LPS are similar in *DJ-1-null* and wild type mice.

Real-time QPCR analyses of microdissected midbrain tissue measured expression levels of Nrf2, HO-1, NQO1, iNOS, SOD1, and SOD2.

Figure B.7

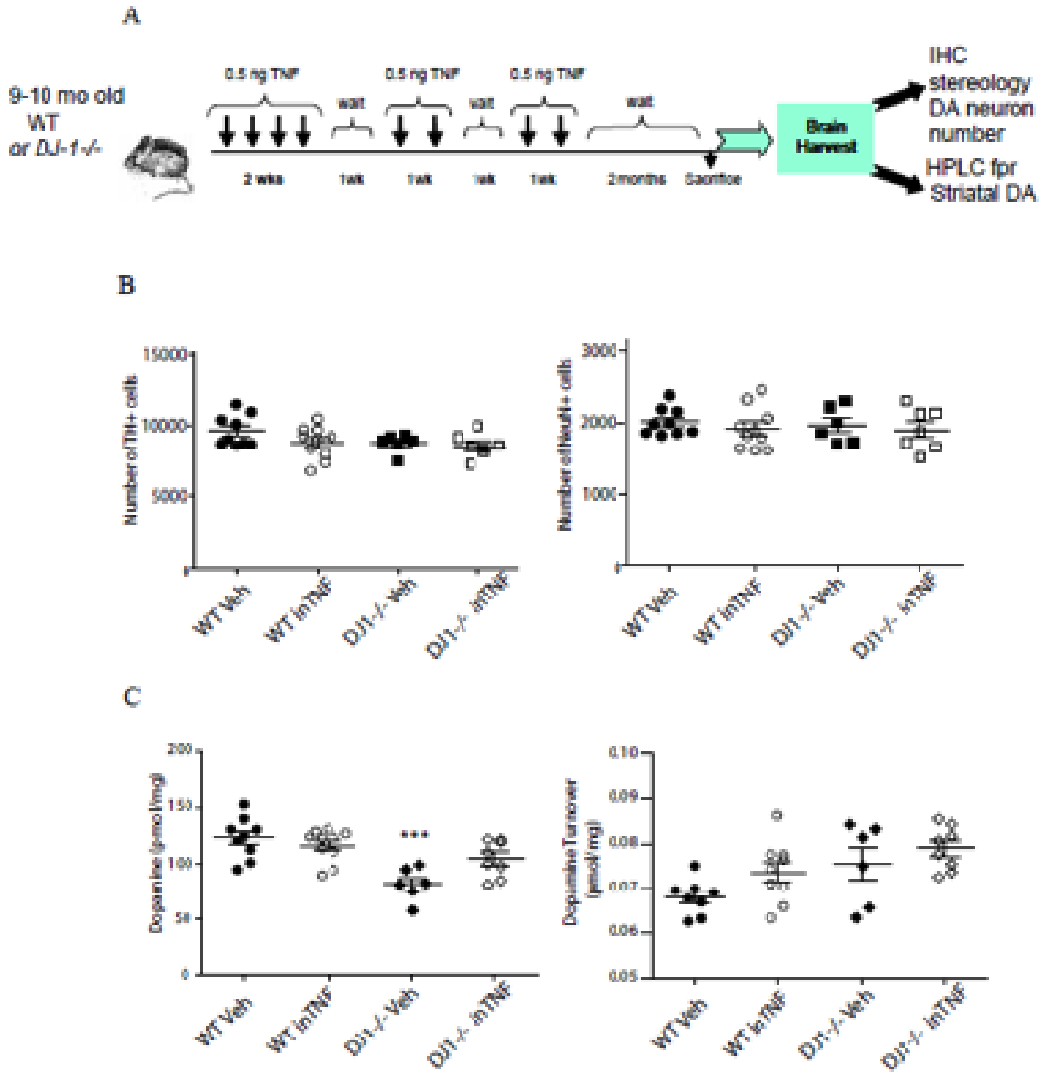
A
9-10 mo old
WT
or DJ-1-/-
0.5 ng TNF
0.5 ng TNF
0.5 ng TNF
wait
wait
wait
2 wks
1wk
1wk
1wk
1wk
2 months
Sacrifice
Brain Harvest
IHC
stereology
DA neuron
number
HPLC for
Striatal DA
B
Number of TH+ cells
15000
10000
5000
0
WT Veh
WT inTNF
DJ1-/- Veh
DJ1-/- inTNF
Number of Nissl+ cells
3000
2000
1000
0
WT Veh
WT inTNF
DJ1-/- Veh
DJ1-/- inTNF
C
Dopamine (pmol/mg)
200
150
100
50
0
***
WT Veh
WT inTNF
DJ1-/- Veh
DJ1-/- inTNF
Dopamine Turnover (pmol/mg)
0.10
0.09
0.08
0.07
0.06
0.05
WT Veh
WT inTNF
DJ1-/- Veh
DJ1-/- inTNF

Figure B.7. Schematic of intranasal TNF (inTNF) dosing paradigm in *DJ-1-null* and wild type mice and effects on nigral DA neuron number and striatal DA.

(a) Schematic of experimental design. Wild type and *DJ-1-null* mice were given soluble murine TNF at the indicated concentrations or an equivalent volume of saline vehicle intranasally for the indicated times. Groups of mice were sacrificed as indicated for biochemical (striatal DA measurements by HPLC) and immunohistological analyses (unbiased stereological estimate of nigral DA neuron number). (b) Unbiased stereological analysis indicates that *DJ-1*$^{-/-}$ mice exposed to inTNF do not display a significant reduction of TH or NeuN immunopositive neurons in the SNpc. Error bars represent SEM, n=6-10 animals per group. Two-way ANOVA indicated no significant differences. (c) Striatal dopamine (DA) and DA metabolites were measured by HPLC and electrochemical detection. Error bars represent SEM, n=6-10 animals per group. Two-way ANOVA, Bonferroni's post hoc ***$p<0.001$.

Supplementary Figure B.S1

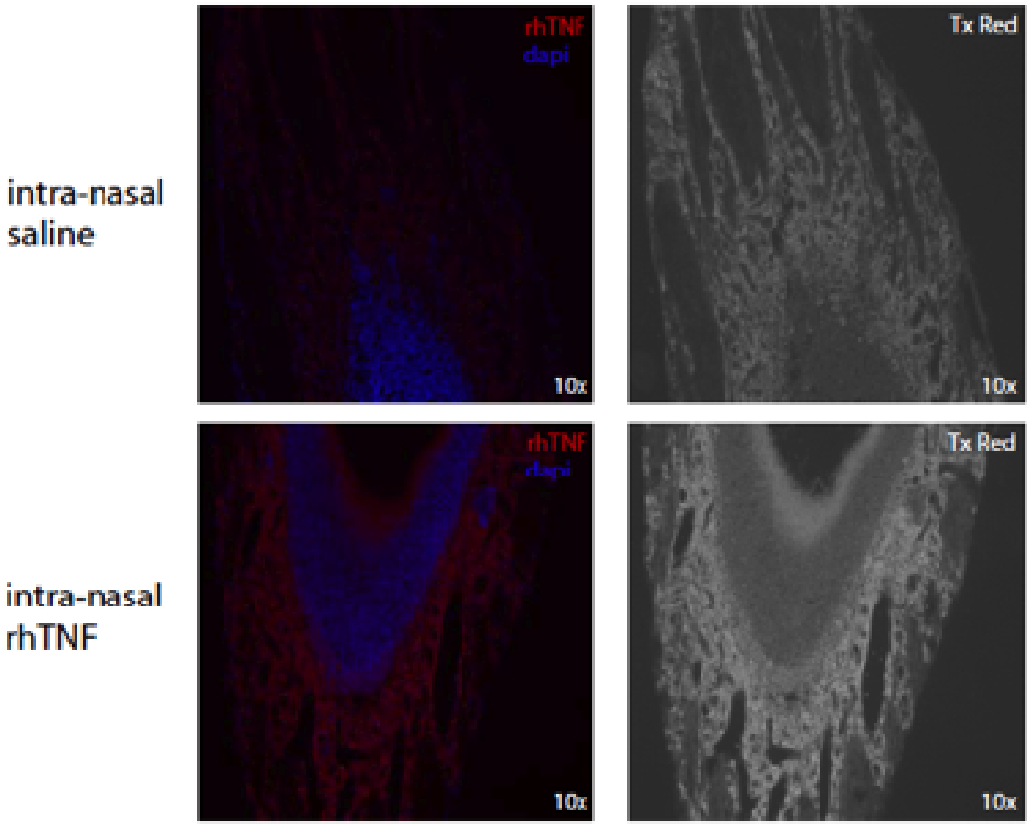

Supplementary Figure B.S1. Uptake and transport of rhodamine labeled hTNF into mouse nasal epithelial cells.

Rhodamine-labeled TNF (Rh-TNF) was used to confirm uptake and transport of intranasally administered soluble TNF in nasal epithelia (NE) by immunofluorescence analyses of cryosectioned rostral and caudal tissues. Rhodamine-TNF fluorescence indicated detectable uptake and transport in rostral sections of NE by 12 hrs post administration.

Acknowledgements

We thank M.K. McCoy and F.E. McAlpine for assistance with behavior studies, T. Bottiglieri and G. Kramer for assistance with HPLC, C. Lemere for advice on intranasal regimen, A.S. Harms for assistance with RNA processing, and members of the Tansey and Goldberg labs for useful discussions. This work was made possible with funding from The Michael J. Fox Foundation for Parkinson's Research (MGT and MSG) and the National Institutes of Health NINDS 5R01NS049433 (MGT).

References Cited

1. Frank-Cannon, T.C., et al., *Parkin deficiency increases vulnerability to inflammation-related nigral degeneration.* J Neurosci, 2008. **28**(43): p. 10825-34.
2. Waak, J., et al., *Regulation of astrocyte inflammatory responses by the Parkinson's disease-associated gene DJ-1.* FASEB J, 2009. **23**(8): p. 2478-89.
3. McGeer, P.L., et al., *Presence of reactive microglia in monkey substantia nigra years after 1-methyl-4-phenyl-1,2,3,6-tetrahydropyridine administration.* Ann Neurol, 2003. **54**(5): p. 599-604.
4. Mrak, R.E. and W.S. Griffin, *Glia and their cytokines in progression of neurodegeneration.* Neurobiol Aging, 2005. **26**(3): p. 349-54.
5. Wersinger, C. and A. Sidhu, *Inflammation and Parkinson's disease.* Curr Drug Targets Inflamm Allergy, 2002. **1**(3): p. 221-42.
6. Zhang, L., V.L. Dawson, and T.M. Dawson, *Role of nitric oxide in Parkinson's disease.* Pharmacol Ther, 2006. **109**(1-2): p. 33-41.
7. Tansey, M.G., M.K. McCoy, and T.C. Frank-Cannon, *Neuroinflammatory mechanisms in Parkinson's disease: potential environmental triggers, pathways, and targets for early therapeutic intervention.* Exp Neurol, 2007. **208**(1): p. 1-25.
8. McGeer, P.L., et al., *Reactive microglia are positive for HLA-DR in the substantia nigra of Parkinson's and Alzheimer's disease brains.* Neurology, 1988. **38**(8): p. 1285-91.
9. Cassarino, D.S., et al., *Interaction among mitochondria, mitogen-activated protein kinases, and nuclear factor-kappaB in cellular models of Parkinson's disease.* J Neurochem, 2000. **74**(4): p. 1384-92.
10. Banati, R.B., S.E. Daniel, and S.B. Blunt, *Glial pathology but absence of apoptotic nigral neurons in long-standing Parkinson's disease.* Mov Disord, 1998. **13**(2): p. 221-7.
11. Hunot, S., et al., *FcepsilonRII/CD23 is expressed in Parkinson's disease and induces, in vitro, production of nitric oxide and tumor necrosis factor-alpha in glial cells.* J Neurosci, 1999. **19**(9): p. 3440-7.
12. Pavese, N., et al., *Microglial activation correlates with severity in Huntington disease: a clinical and PET study.* Neurology, 2006. **66**(11): p. 1638-43.
13. Whitton, P.S., *Inflammation as a causative factor in the aetiology of Parkinson's disease.* Br J Pharmacol, 2007. **150**(8): p. 963-76.
14. McCoy, M.K., et al., *Blocking soluble tumor necrosis factor signaling with dominant-negative tumor necrosis factor inhibitor attenuates loss of dopaminergic neurons in models of Parkinson's disease.* J Neurosci, 2006. **26**(37): p. 9365-75.
15. McCoy, M.K., et al., *Intranigral lentiviral delivery of dominant-negative TNF attenuates neurodegeneration and behavioral deficits in hemiparkinsonian rats.* Mol Ther, 2008. **16**(9): p. 1572-9.
16. Sanchez-Pernaute, R., et al., *Selective COX-2 inhibition prevents progressive dopamine neuron degeneration in a rat model of Parkinson's disease.* J Neuroinflammation, 2004. **1**(1): p. 6.

17. Farrer, M.J., *Genetics of Parkinson disease: paradigm shifts and future prospects.* Nat Rev Genet, 2006. **7**(4): p. 306-18.
18. Li, H.M., et al., *Association of DJ-1 with chaperones and enhanced association and colocalization with mitochondrial Hsp70 by oxidative stress.* Free Radic Res, 2005. **39**(10): p. 1091-9.
19. Canet-Aviles, R.M., et al., *The Parkinson's disease protein DJ-1 is neuroprotective due to cysteine-sulfinic acid-driven mitochondrial localization.* Proc Natl Acad Sci U S A, 2004. **101**(24): p. 9103-8.
20. Zhang, J., et al., *Quantitative proteomic analysis of age-related changes in human cerebrospinal fluid.* Neurobiol Aging, 2005. **26**(2): p. 207-27.
21. Zhang, L., et al., *Mitochondrial localization of the Parkinson's disease related protein DJ-1: implications for pathogenesis.* Hum Mol Genet, 2005. **14**(14): p. 2063-73.
22. Bonifati, V., B.A. Oostra, and P. Heutink, *Unraveling the pathogenesis of Parkinson's disease--the contribution of monogenic forms.* Cell Mol Life Sci, 2004. **61**(14): p. 1729-50.
23. Bonifati, V., et al., *Mutations in the DJ-1 gene associated with autosomal recessive early-onset parkinsonism.* Science, 2003. **299**(5604): p. 256-9.
24. Goldberg, M.S., et al., *Nigrostriatal dopaminergic deficits and hypokinesia caused by inactivation of the familial Parkinsonism-linked gene DJ-1.* Neuron, 2005. **45**(4): p. 489-96.
25. Shen, J. and M.R. Cookson, *Mitochondria and dopamine: new insights into recessive parkinsonism.* Neuron, 2004. **43**(3): p. 301-4.
26. van der Brug, M.P., et al., *RNA binding activity of the recessive parkinsonism protein DJ-1 supports involvement in multiple cellular pathways.* Proc Natl Acad Sci U S A, 2008. **105**(29): p. 10244-9.
27. Kim, R.H., et al., *Hypersensitivity of DJ-1-deficient mice to 1-methyl-4-phenyl-1,2,3,6-tetrahydropyrindine (MPTP) and oxidative stress.* Proc Natl Acad Sci U S A, 2005. **102**(14): p. 5215-20.
28. Yang, W., et al., *Paraquat induces dopaminergic dysfunction and proteasome impairment in DJ-1-deficient mice.* Hum Mol Genet, 2007. **16**(23): p. 2900-10.
29. Yamaguchi, H. and J. Shen, *Absence of dopaminergic neuronal degeneration and oxidative damage in aged DJ-1-deficient mice.* Mol Neurodegener, 2007. **2**: p. 10.
30. Frank-Cannon, T.C., Tran, T., Ruhn, K.A., Martinez, T.N., Hong, J., Marvin, M., Hartley, M., Treviño, I., O'Brien, D.E, Casey, B. Goldberg, M.S., Tansey, M.G., *Parkin deficiency increases vulnerabiity to inflammation-related nigral degeneration* J Neurosci, 2008. **28**(43).
31. Kurrasch, D.M., et al., *Quantitative real-time PCR measurement of regulators of G-protein signaling (RGS) mRNA levels in mouse tissues.* Methods in Enzymology, 2004. **389**: p. 3-15.
32. Frank, T.C., et al., *Fluoro-jade identification of cerebellar granule cell and purkinje cell death in the alpha1A calcium ion channel mutant mouse, leaner.* Neuroscience, 2003. **118**(3): p. 667-80.

33. Abbott, L.C. and D.M. Jacobowitz, *Development of calretinin-immunoreactive unipolar brush-like cells and an afferent pathway to the embryonic and early postnatal mouse cerebellum.* Anat Embryol (Berl), 1995. **191**(6): p. 541-59.
34. Paxinos, G., Franklin, K.B.J., *The Mouse Brain in Stereotaxic Coordinates*. 2nd Edition ed. 2001, San Diego, CA: Academic Press.
35. Xu, J., et al., *The Parkinson's disease-associated DJ-1 protein is a transcriptional co-activator that protects against neuronal apoptosis.* Hum Mol Genet, 2005. **14**(9): p. 1231-41.
36. Blackinton, J., et al., *Post-transcriptional regulation of mRNA associated with DJ-1 in sporadic Parkinson disease.* Neurosci Lett, 2009. **452**(1): p. 8-11.
37. Mitsumoto, A. and Y. Nakagawa, *DJ-1 is an indicator for endogenous reactive oxygen species elicited by endotoxin.* Free Radical Research, 2001. **35**: p. 885-893.
38. Pham, T.T., et al., *DJ-1-deficient mice show less TH-positive neurons in the ventral tegmental area and exhibit non-motoric behavioural impairments.* Genes Brain Behav, 2009.
39. Perez, F.A., W.R. Curtis, and R.D. Palmiter, *Parkin-deficient mice are not more sensitive to 6-hydroxydopamine or methamphetamine neurotoxicity.* BMC Neurosci, 2005. **6**: p. 71.
40. Thomas, B., et al., *MPTP and DSP-4 susceptibility of substantia nigra and locus coeruleus catecholaminergic neurons in mice is independent of parkin activity.* Neurobiol Dis, 2007. **26**(2): p. 312-22.
41. Zhu, X.R., et al., *Non-motor behavioural impairments in parkin-deficient mice.* Eur J Neurosci, 2007. **26**(7): p. 1902-11.